Environmental Influences on Synthetic and Biogenic Calcium Carbonate in Aragonite-Calcite Sea Conditions

Caroline E. Miller

BA (Hons) Glasgow Caledonian University, 2005
BSc (Hons) University of Glasgow, 2011
MSc (Merit) University of Stirling, 2012

Submitted in fulfilment of the requirement for the
Degree of Doctor of Philosophy

School of Geographical and Earth Sciences
College of Science and Engineering
University of Glasgow

January 2018

Dedication

This thesis is dedicated in loving memory of two inspiring women who were gone before completion of this thesis:

My amazing Gran, Kathleen Margaret

November 1920- January 2016

A lady from another era who taught me the true meaning of being strong and what it truly means to be a fighter until the very end. The centre of my world and my best friend. I might have made an excuse to come cook your dinner so often, but I think you always knew it was a good excuse for us to chat and put the world to rights. Your support was invaluable even if at times you were heartbroken on my behalf with what I was going through. You always took so much interest in how I was getting on completing my thesis. It's completed now. I hope you would be as proud as when I became your 'Nurse of People' to become as you put it, your 'Doc of Rock'.

Louise

July 1984- February 2016

LouLou, your mind was too troubled for this world yet you have touched so many with your bubbly, caring and absolutely bonkers nature! The true meaning of an Angel, always caring for everyone in your presence whether at work or not. Always with that massive smile that lit up every room or that cheeky laugh that carried so far. If only you had known how many of us were there to turn to. You are sorely missed; your memory will stay with us forever.

'This world was never meant for one as
beautiful as you'

Don McLean - 'Vincent (Starry, Starry Night)

Abstract

Ocean chemistry has oscillated throughout Earth history to favour the dominant non-biogenic polymorph of calcium carbonate ($CaCO_3$) to be either calcite or aragonite (Sandberg, 1983). Throughout the Phanerozoic these oscillations have occurred to facilitate aragonite-dominant conditions three times and calcite-dominant conditions twice. These aragonite-calcite seas conditions have previously been viewed as a global phenomenon where conditions fluctuate over time, but not in space, and represent the main environmental context in which the evolution of $CaCO_3$ biomineralisation has occurred (Stanley & Hardie, 1998). $CaCO_3$ is one of the most widely distributed minerals in the marine environment, occurring throughout geological history, both biogenically and non-biogenically (Lowenstam & Weiner, 1989). Marine non-biogenic precipitates are commonly found as carbonate ooids, sedimentary cements and muds (Nichols, 2009). Biogenic $CaCO_3$ is formed via biomineralisation in calcifying organisms (Lowenstam & Weiner, 1989; Allemand et al., 2004), and is much more abundant than the non-biogenic forms. Although $CaCO_3$ is abundant, it only accounts for a small proportion of the global carbon budget. Biogenic $CaCO_3$ is representative of a larger proportion of the global carbon budget than non-biogenically formed $CaCO_3$ (Berelson et al., 2007).

The main driving force controlling the precipitation of $CaCO_3$ polymorphs is the Mg:Ca molar ratio of seawater (Morse et al., 2007). However, other parameters such as temperature (Burton & Walter, 1984; Morse et al, 1997; Balthasar & Cusack, 2015), pCO_2 (Lee & Morse, 2010), and SO_4 (Morse et al., 2007) are also known to influence $CaCO_3$ polymorph formation but are often overlooked in the context of aragonite-calcite seas. Fluctuations in these parameters of Mg:Ca ratio, SO_4^{2+} and pCO_2 of seawater have been suggested to cause shifts in original composition of non-biogenic marine carbonates, and in turn viewed as the main driving mechanisms facilitating the switch between aragonite and calcite dominance (Morse et al., 1997; Lee & Morse, 2010; Bots et al., 2011). Specifically the influence of temperature is important because it is likely to result in aragonite-calcite sea conditions to vary spatially (Balthasar & Cusack, 2015). Today marine temperatures are changing across the latitudes due to environmental factors. Global CO_2 levels have increased significantly since industrialisation (Doney et al., 2009), with 33%

entering the oceans and reducing pH (Raven et al., 2005) accelerating climate change (IPCC, 2013) and influencing marine calcification (Fitzer et al., 2014a; 2015b; Bach, 2015; Zhao et al., 2017). Strong links between the carbon cycle and climate change observed in the rock record give evidence that environmental changes such as pCO_2 and global warming have impacts on calcification and marine biota (Hönish et al., 2012).

The first objective was to determine the influence of Mg:Ca ratio, temperature and water movement on the first-formed precipitates of non-biogenic $CaCO_3$ precipitation yielded via a continuous addition technique experiments (Chapter 3). $CaCO_3$ precipitation was induced by continuously adding bicarbonate to a bulk solution of known Mg:Ca ratio (1,2 or 3), and fixed salinity of 35 (practical salinity scale), at 20°C and 30°C in still conditions, and then repeated with the solution being shaken at 80rpm mimicking more natural marine conditions. The mineralogy and crystal morphology of precipitates was determined using Raman Spectroscopy and Scanning Electron Microscopy. Results in Chapter 3 indicated that polymorphs co-precipitate, with the ratio of aragonite to calcite increasing with increased Mg:Ca ratio and elevated temperature. The main difference between still and shaken conditions was that overall, more crystals of aragonite compared to calcite precipitate in shaking conditions. The crystal size is less influenced in aragonite, but calcite crystals were smaller. These results contradict current views on aragonite-calcite seas as spatially homogenous ocean states need to be re-examined to include the effect of temperature on the spatial distribution of $CaCO_3$ polymorphs. Examining polymorph growth under these experimental constraints allows us to gain a better understanding of how temperature and Mg:Ca together control non-biogenic aragonite and calcite precipitation providing a more realistic environmental framework in which to evaluate the evolution of biomineralisation.

To further this work, the same continuous addition technique was used with the presence of sulphate in the mother solution (Chapter 4). Sulphate being the 4th most common marine ion (Halvey et al., 2012) and known to have an influence on mineralogy (Kontrec et al., 2004). The presence of sulphate increase the aragonite to calcite proportion formed compared to sulphate-free conditions (Chapter 4). Elevated temperature with sulphate further increased the proportion of aragonite to calcite facilitated (Chapter 4). In the presence of sulphate the main difference between sulphate-free environments and

those with sulphate environments was: in still conditions the presence of sulphate increased the crystal number more than the crystal size at 20°C; at 30°C or in shaken conditions the presence of sulphate increased the crystal size of aragonite to calcite much more than it had influence on the crystal number. Non-biogenically the influence of sulphate lowered the threshold of Mg:Ca ratio that the switch between calcite and aragonite would be facilitated at (Bots et al., 2011). This would have implications for marine calcification as pure calcite seas would become very rare and imply that organisms would be forming calcified hard parts out with the supported mineralogies.

Biogenic application of these results is complex however as organisms often have the ability to select aragonite as their main polymorph for their own functional requirements (Weiner & Dove, 2003). The growth parameters of non-biogenic polymorph formations grown from artificial seawater can be used to understand how organism control can influence the polymorph formation under similar conditions (Kawano et al., 2009). Assessing the elemental composition of mussel shells grown under know conditions of temperature and pCO_2 allowed the environmental influences on mineralogy be assessed under possible the projected changes in climate forecast to occur by 2100 by IPCC (2013).

Prior to this research, no study had used *Mytilus edulis* shell elemental composition to test the influence of aragonite-calcite sea conditions on mineralogy. This research compiles a detailed source of information on the constraints from environmental sources such as temperature and pCO_2, on the elemental concentrations within shell formation and what potential changes could occur in response to a changing marine environment (Chapter 5). Here elevated temperature significantly increased the concentration of magnesium in calcite, but did not influence the magnesium concentration of aragonite unless combined with elevated pCO_2. The concentrations of sulphur in calcite were significantly decreased at elevated pCO_2 or combined increased temperature and pCO_2 as concentrations of sodium were found to be increased under these conditions. In aragonite the concentrations of both sulphur and sodium were significantly different under all scenarios. Strontium did not yield any significant results in this research in either calcite or aragonite. Results observed indicate that the shell elemental concentrations are influenced differently in aragonite or calcite, and further influenced by environmental conditions based on the original mineralogy. This suggests that physiological mechanisms under the

constraints of increased temperature and pCO_2 can override the seawater chemistry influences of aragonite-calcite seas impacting on mineralogy.

This research allows comparison of how non-biogenic and biogenic $CaCO_3$ formation is influenced by seawater chemistry and environmental parameters to determine the dominant mineralogy. Increased temperature in both formations has shown to increase the impact of magnesium on calcite enabling the facilitation of aragonite. However, magnesium has influence on biogenic aragonite in extreme combined conditions of elevated temperature and pCO_2. This work indicates that $CaCO_3$ formation is complex and requires a multi-variable approach to understanding the mechanisms that facilitate the dominant mineralogy. By including variables such as temperature, this research suggests that aragonite-calcite seas conditions do not facilitate globally homogeneous switches in mineralogy, but the mineralogy is indeed influenced on latitudinal scales by other factors that influence the mechanisms involved.

Contents

Figures

Tables

Acknowledgements

pages xiv-xvi removed due to confidentiality issues

Author's declaration

I declare that this thesis, except where acknowledged to others, represents my own work carried out in the School of Geographical and Earth Sciences, University of Glasgow. The research presented here has not been submitted for any other degree at the University of Glasgow, nor at any other institution. Any published or unpublished work by other authors has been given full acknowledgement in the text.

Caroline E. Miller

1

Introduction

1.1 Marine Calcium Carbonate

Global calcium carbonate ($CaCO_3$) production is estimated to be approximately 3 billion tons per year (Milliman, 1993). $CaCO_3$ minerals are the most widely distributed deposits in the marine environment, forming both non-biogenically and biogenically as the polymorphs of calcite, aragonite and more rarely vaterite, throughout geological history (Sandberg, 1975; Lowenstam & Weiner, 1989). Around 60% of marine $CaCO_3$ is preserved within the rock record, of both non-biogenic and biogenic origins (Milliman, 1993). Being so abundant and widely distributed, the $CaCO_3$ mineral system is of great importance to the Earth system as it links the biosphere, geosphere, and atmosphere.

Although $CaCO_3$ is abundant, it only accounts for a small proportion of the global carbon cycle components. Biogenic $CaCO_3$ is representative of a larger proportion of the global carbon budget than non-biogenic $CaCO_3$ minerals (Berelson et al., 2007). Biogenic $CaCO_3$ however, is closely linked to atmospheric CO_2 cycling as well as individual aspects of the carbon cycle (Milliman, 1993).

Marine non-biogenic precipitates are commonly found as carbonate ooids, sedimentary cements and muds (Nichols, 2009) (Figure 1-1 ***(a-c)*****).** Biogenically, $CaCO_3$ is formed via biomineralisation in calcifying organisms (Lowenstam & Weiner, 1989; Allemand et al., 2004). Biogenic $CaCO_3$ is formed in many organisms including algae, corals, phytoplankton, mussels and sponges **(*see Figure 1-1(d-g)*).**

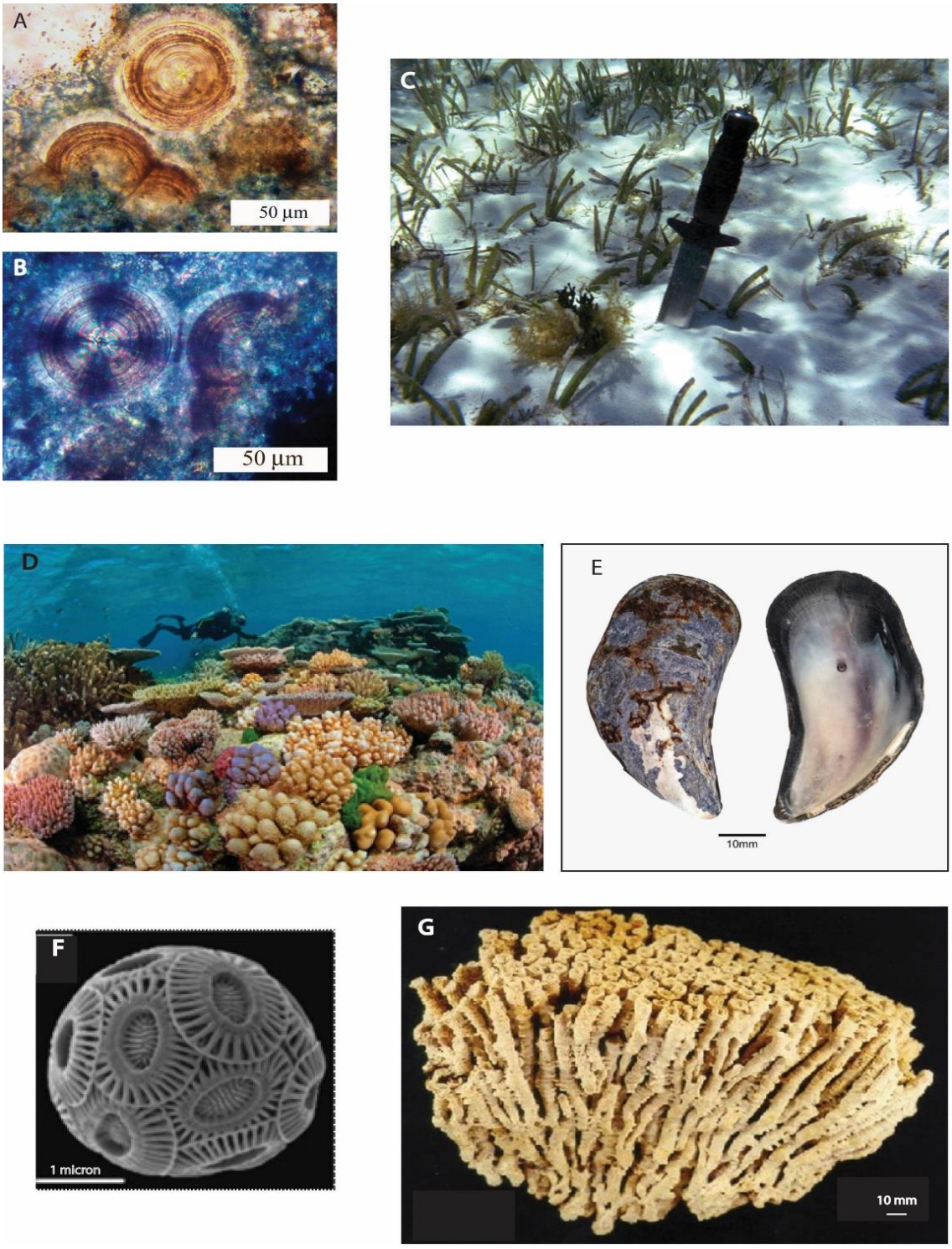

Figure 1-1 Examples of non-biogenic and of biogenic calcium carbonate structures.
A-C – Non-biogenic structures. A - Pleistocene ooids in thin section showing concentric layers (scale = 50 µm). B- Ooids in cross-polar, dark cross markings showing crystallographic alignment (scale = 50 µm). C- Ooid sand example (A,B &C from Colin Braithwaite).
D-G – Biogenic structures. D- Coral reef of the Great Barrier Reef, Australia (Doubilet, 2016). E- Bi-mineralic blue mussel shell *Mytilus edulis* showing both aragonite (pale inner layer) and calcite (blue outer shell) layers (scale = 10mm) (from Les Hill). F – The coccilithophore *Emiliania huxleyi* (scale = 1µm) (Brownlee et al., 2015). G- *Entelophyllum a* Silurian rugose coral in limestone (scale = 10mm) (Kentucky Geological Society, 2012).

1.2 Aragonite-Calcite Seas; the evolution of a hypothesis

1.2.1 Aragonite-Calcite Sea Hypothesis

Sandberg (1983) defined 5 periods of time throughout the Phanerozoic when either calcite or aragonite dominated non-biogenic marine $CaCO_3$ production. There were three periods when aragonite dominated and two when calcite was the most abundant polymorph produced non-biogenically (Sandberg, 1983). These oscillations between aragonite-facilitating and calcite-facilitating periods ***(Figure 1-2)*** are widely referred to as 'aragonite-calcite seas' (e.g. Hardie, 1996; Stanley & Hardie, 1998). The aragonite-calcite sea hypothesis suggests that fluctuations in seawater chemistry caused the switch between the dominance of either aragonite or calcite, over timescales of 10s to 100s of Mya (Sandberg, 1983; Stanley & Hardie, 1998) and these fluctuations occur over time and space (Balthasar & Cusack, 2015).

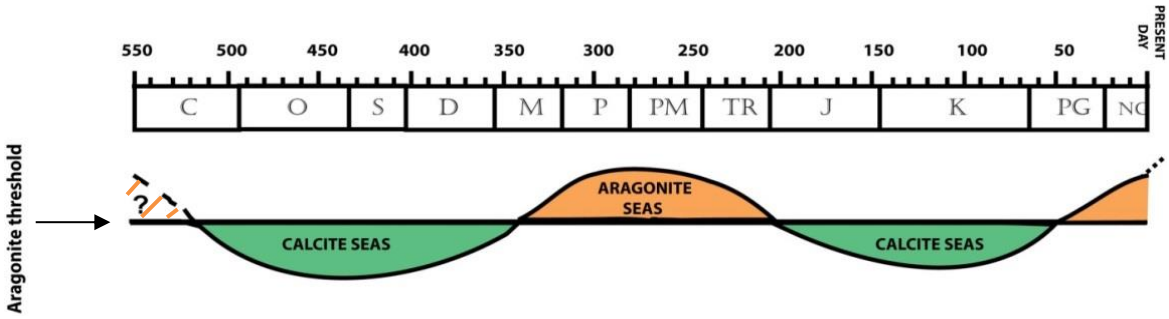

Figure 1-2 Oscillations of non-skeletal carbonate mineralogy throughout the Phanerozoic. Oscillations occur around an aragonite threshold below which aragonite growth is inhibited, and above which aragonite precipitation is facilitated. This pattern was based on the primary mineralogy of ooids and marine cements (Adapted from Sandberg, 1983).

As will be explained, aragonite-calcite sea oscillations are supported by evidence from the original mineralogy of ooids (Sandberg, 1975; 1983), marine evaporite deposits (Hardie, 1996), from the original seawater composition as deduced from fluid inclusions in marine deposits (Horita et al., 2002; Lowenstein et al., 2001; 2003; Timofeeff et al., 2006; Coggon et al., 2010) and from echinoderm skeletons (Dickson, 2002; 2004). Furthermore, various studies suggest that fluctuations in aragonite-calcite sea conditions have influenced the evolution of calcifying organisms (Harper et al., 1997; Stanley & Hardie, 1998; Porter, 2010) although, this does not appear to work as a general rule (Kiessling et al., 2008).

The drivers of Phanerozoic aragonite-calcite sea oscillations that are discussed in the literature are the ratio of marine Mg:Ca concentrations (Sandberg, 1975; Hardie, 1996; Morse et al., 2007) and pCO_2 (Sandberg, 1983; Lee & Morse, 2010). The Mg:Ca ratio of seawater is viewed as the main driver of the switch between aragonite or calcite dominance (Sandberg, 1975; Hardie, 1996; Morse et al., 2007). It is widely assumed that a critical threshold at Mg:Ca ratio of 2 indicates the boundary between calcite (below 2) and aragonite formation (above 2) (Folk, 1974; Hardie, 1996). This Mg:Ca ratio of 2 has been used as a guide to define the boundary between 'aragonite seas' and 'calcite seas' (Sandberg, 1975; Hardie, 1996). However, in combination with Mg:Ca ratio, other drivers are now also considered an influence on mineralogy such as temperature (Burton & Walter, 1987; Morse et al., 1997; Balthasar & Cusack, 2015), pCO_2 (Sandberg, 1983; Lee & Morse, 2011) and SO_4^{2-} (Bots et al., 2011). More detail on this threshold boundary will be provided in section 1.2.8.

Although aragonite is favoured in the marine realm today, it is calcite that is the thermodynamically most stable form of $CaCO_3$ at the Earth's surface conditions (Albright, 1971; Morse et al., 2007). Understanding the changes in ocean conditions or chemistry that result in these oscillations in dominant polymorph production is important for our understanding of the marine environment and the context in which marine biomineralisation occurs.

1.2.2 Evidence from the Primary Composition of Ooids

Today, the majority of ooids and marine cements which form are aragonitic. Aragonite is not as thermodynamically stable as calcite is and is poorly preserved within the rock record. The consensus at the time of ooid investigation by Sandberg (1975) was that ooids always were of aragonite as a primary mineralogy, like today's are. However, Sandberg (1975) observed that texturally, the calcitic ooids in the rock record that had radial-fibrous texture were of a primary calcite composition, and did not form from diagenesis of aragonitic ooids as originally believed (Sandberg, 1975; 1983; Tucker & Bathurst, 2009). Therefore, this suggested that their original mineralogy was calcite and not aragonite as previously championed and, therefore different from the prevalent mineralogy of modern ooids (Sandberg, 1975). This initial evidence of ancient primary calcite ooids came from two intervals in the Phanerozoic: Oligocene to mid-Jurassic (25-

175Ma) and Late Pennsylvanian (285-305 Ma) to Mid-Cambrian (335-545 Ma) (Sandberg, 1975; Gaffin, 1987), indicating that seawater chemistry had had changed over geological time to favour primary calcite precipitation (calcite seas) (Sandberg, 1975).

In this initial work by Sandberg (1975) hypothesised that the difference between mineralogies of ancient and modern ooids were due to a single shift in seawater chemistry, occurring in the early Cenozoic, altering conditions from calcite-facilitating during the Palaeozoic and Mesozoic to aragonite-facilitating during the Cenozoic, driven by the Mg:Ca ratio of seawater (Sandberg, 1975). The Mg:Ca ratio was specifically championed as Sandberg (1975) suggested that a decrease in calcium concentration could be caused by increases in the abundance of calcite-secreting organisms such as foraminiferans and nanoplankton. Decreasing calcium concentrations increase the Mg:Ca ratio and are represented in ooid mineralogy (Sandberg, 1975).

As mentioned earlier, this interpretation was in agreement with the consensus at the time that abiotic precipitation of aragonite occurs at higher Mg:Ca ratios, while calcite precipitates at lower Mg:Ca ratios (Lippman, 1960; Folk, 1974; Füchbauer & Hardie, 1976; Wilkinson, 1979). Evidence supporting Mg:Ca ratio influencing mineralogy came from the mineralogical changes observed in carbonates in modern salt lakes formed at differing Mg:Ca ratios (Müller et al., 1972), experiments investigating Mg:Ca ratio on non-biogenic $CaCO_3$ precipitation (Füchbauer & Hardie, 1976), fluid inclusion data for palaeo-seawater concentration derived from non-skeletal marine carbonates (Spencer & Hardie, 1990) and mineralogical changes from calcite to aragonite in biogenic skeletal fossils and non-biogenic ooids (Wilkinson, 1979). Each of these studies agreed that changes in seawater chemistry were responsible but suggested the mineralogical change was also driven by CO_2 flux from tectonic movements in the mid-Carboniferous.

1.2.3 pCO_2 as a Driver of Aragonite-Calcite Seas

The initial study by Sandberg (1975) was based on a limited number of geological samples of ooids and the interpretation was contested by Mackenzie & Pigott (1981). Investigation of ooids by Mackenzie & Pigott (1981) suggested that the mineralogical trends observed did match with the observations of Sandberg (1975), however, Mackenzie & Pigott (1981) proposed these were driven by pCO_2 not Mg:Ca ratio. Elevated pCO_2 lowers

how much carbonate ion is dissolved in the ocean impacting of calcification (Given & Wilkinson, 1987). This suggestion that pCO_2 drove the fluctuations changes in ooid mineralogy came from noting that the calcite observed had differing quantities of Mg composition which in turn gave varied solubility as a function of pCO_2 (Mackenzie & Pigott, 1981). They did reinforce that functions of pCO_2 and Mg:Ca ratio do appear to co-exist i.e. increased pCO_2 can result in elevated the Mg:Ca ratio due to atmosphere and ocean system interactions (Mackenzie & Pigott, 1981).

Sandberg (1983) further investigated the mineralogy of ooids and the aragonite-calcite sea hypothesis was developed from evidence that ooids with poorly preserved or recrystallized mineralogy were predominantly preserved in 3 separate intervals: (Holocene – Miocene (0-25 Ma), Mid-Jurassic – Early Permian (175-285 Ma), Mid-Pennsylvanian – Late Mississippian (305-335 Ma) and Early Cambrian to late Precambrian (545-600+ Ma) (Sandberg, 1983; Gaffin, 1987), suggesting that the marine conditions favoured primary aragonite precipitation (aragonite seas). Therefore, Sandberg (1983) championed that the mineralogy of the ooids are driven by fluctuations in the seawater chemistry they form which has occurred 5 times throughout the Phanerozoic (3 periods of aragonite sea periods, 2 periods of calcite sea periods) (Sandberg, 1983), and not from a singular shift in seawater chemistry (Sandberg, 1975). This comprehensive survey of Phanerozoic ooid preservation led Sandberg (1983) to discard a shift in Mg:Ca ratio as the main driver of the oscillations in the primary mineralogy of non-skeletal $CaCO_3$ precipitates, probably due to the absence of a plausible mechanism regulating an oscillation of marine Mg:Ca ratios. Instead, Sandberg (1983) favoured pCO_2 as the best explanation, as the observed aragonite-calcite cyclicity broadly coincides with the tectonic-eustatic-climatic cycles supported by the emplacement of granites (Engel & Engel, 1958), global sea-level (Vail et al., 1977) and icehouse – greenhouse climate (Fischer, 1981, 1983).

1.2.4 Evidence from Evaporite Deposition

A landmark study by Hardie (1996) shifted the focus of explaining aragonite-calcite seas back to the Mg:Ca ratio. In this paper, Hardie (1996) recognised that a secular variation in compositions of evaporite mineral deposition occurred through the Phanerozoic correlated with the timing of aragonite-calcite seas. The deposited $CaCO_3$ mineralogy suggested a co-variance with the Phanerozoic Mg:Ca ratio, e.g. $MgSO_4$

deposition indicating high Mg:Ca ratios (aragonite seas) and KCl deposition indicating low Mg:Ca ratios (calcite seas) (Hardie, 1996). This observation suggests that when aragonite sea intervals occurred there was more Mg available in the seawater, thus also suggesting Mg^{2+} co-varied with aragonite-calcite sea intervals. The non-skeletal limestone and potash mineralogies observed (Hardie, 1996) match well with the Mg:Ca ratios noted to influence mineralogy by Füchtbauer & Hardie (1976), suggesting their precipitation mechanisms are similar.

To explain this co-variance of Mg with aragonite-calcite sea periods, Hardie (1996) suggested that cyclicity in the composition of non-biogenic $CaCO_3$ is controlled by hydrothermal brine flux at mid-ocean ridges (Hardie, 1996). Hydrothermal activity along mid-ocean ridges (MOR) releases Ca^{2+} and K^{+} to the seawater from the rock, whilst Mg^{2+} and SO_4^{2-} are removed from the seawater and incorporated into the rock, altering the Mg:Ca ratio (Hardie, 1996; Stanley & Hardie, 1999). At these MOR hydrothermal diagenesis of newly deposited Ca-rich basalt interacts with seawater to form Mg-rich alteration products such as serpentinite (Bonatti, 1976).

The rate of crust production at the MOR (Spencer & Hardie, 1990) also correlates with aragonite-calcite sea intervals (Hardie, 1996). When spreading rates are higher, the Mg:Ca ratio is decreased, facilitating calcite seas, whereas, lower spreading rates facilitate aragonite seas because the Mg:Ca ratio is increased (Hardie, 1996). Increased spreading rates at MOR lowers the Mg:Ca ratio by increasing the brine flux at the MOR and increasing the $CaCl_2$ component of the brine. This in turn evaporates to form KCl evaporites (Stanley & Hardie, 1999). Therefore, lowered spreading rates increase the Mg:Ca ratio by decreased brine flux influencing the brine to become $MgSO_4$ enriched which evaporates to form $MgSO_4$ evaporites (Baker et al., 1995; Stanley & Hardie, 1999). The spreading rate is also related to sea level, fast spreading resulting in high sea level and low spreading rate resulting in low sea level (Stanley & Hardie, 1999). However, the spreading rate having varied enough to drive seawater chemistry was challenged by Rowley (2004). Here the rate of ridge production was modelled from calculations based on the area/age against the age distribution of oceanic crust today (Rowley, 2004). The findings suggested that the rates of crust production have not changed significantly over geological time (Rowley, 2004). However, reconstructed Cretaceous seafloor spreading rate by Kominz & Scotese (2004)

propose rates of fast ridge spreading that could be a reason for the high pCO_2 and greenhouse climate proposed at this time. Therefore, the realisation that the variation in Mg:Ca ratio co-varies with aragonite-calcite seas and that it can be explained by rates of MOR spreading activity strongly favours the Mg:Ca ratio as being the primary driver of aragonite-calcite seas. In turn, this influences the resultant changes in chemistry that occur through hydrothermal MOR brine flux which determine which evaporite mineralogy occurs (Warren, 2016; ***Figure 1-3***).

The Mg:Ca ratio of seawater initially determines the first step in brine-evolution 'the $CaCO_3$ divide' (Warren, 2016; ***Figure 1-3***). The next stage 'the gypsum divide' evolves either Ca^{2+}-poor, Mg^{2+}-rich brines where no gypsum will form, or Ca^{2+}-rich brines where gypsum will form (Warren, 2016; ***Figure 1-3***). The last stage divides the brines after the precipitation of gypsum, if SO_4^{2-}- rich the brine evolved will be $MgSO_4$ enriched and evaporate to form $MgSO_4$ minerals, if SO_4^{2-}-poor then $CaCl_2$ brine will evolve to evaporate to KCl minerals (Warren, 2016; ***Figure 1-3***).

Two explanations for the oscillations in seawater chemistry related to how these evaporites would be facilitated have been proposed. The first explanation tries to account for evaporites which form at lowered Mg:Ca ratios by dolomitization followed by $CaSO_4$ or $CaSO_4.2H_2O$ (gypsum) precipitation in turn facilitating a change in seawater chemistry (Horita et al., 1991; Horita et al., 1996).

The second suggests that $MgSO_4$-poor evaporites formed at low Mg:Ca ratios (such as KCl or sylvite), have been related to formation of carbonate platforms with high rates of MOR spreading rates, again suggesting a Mg:Ca ratio influence on mineralogy (Holland et al., 1996).

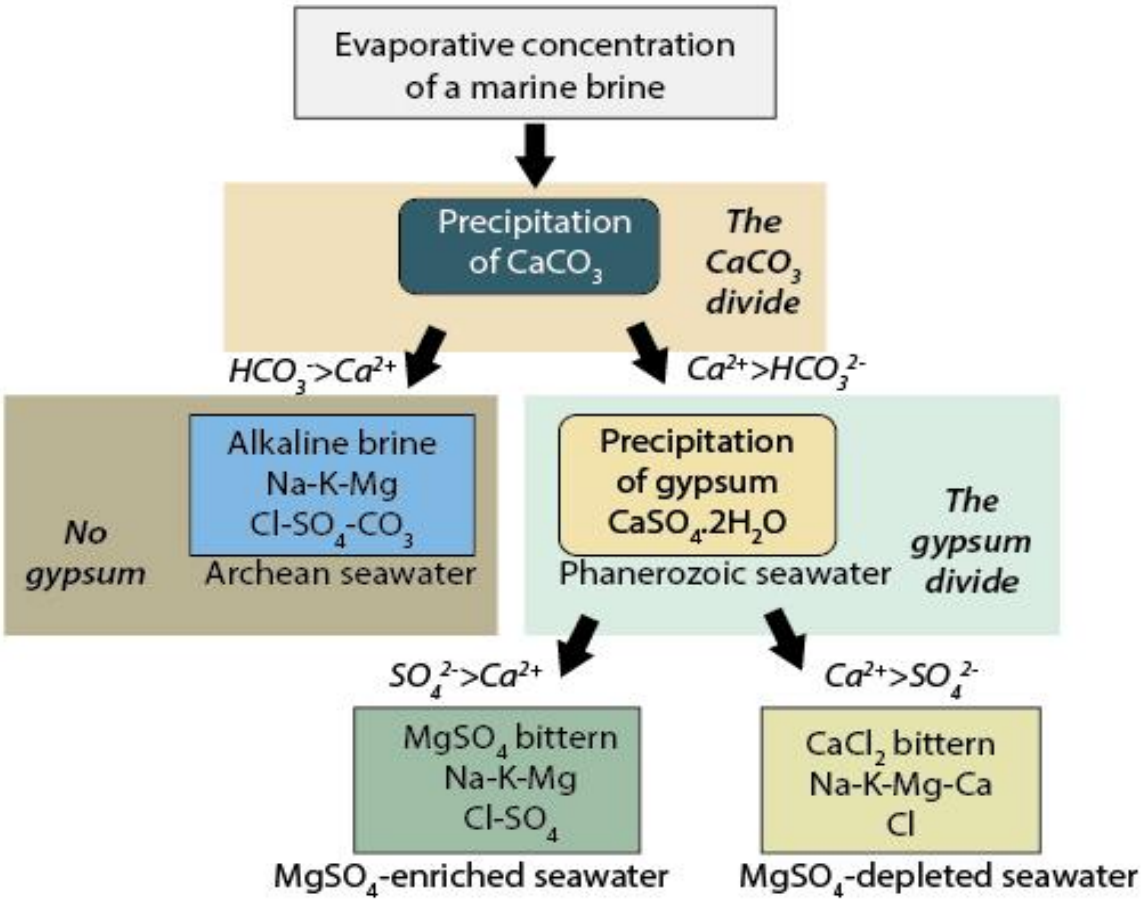

Figure 1-3: Pathways for brine water evolution to form mineralogically different evaporite formations
Indicated are the chemical divides where brine water formations allow for different evaporite formations to occur on evaporation (taken from Warren, 2016, p148).

The Hardie (1996) model's ability to correlate the oscillations in aragonite-calcite sea periods with evaporite mineralogy in the Phanerozoic facilitated by Mg:Ca ratio instead of pCO_2, was due to pCO_2 not influencing the mineralogy of the evaporites (Hardie, 1996). However, the Hardie (1996) model, has been criticised for being based on the work of Spencer & Hardie (1990) who used a lower Ca/Cl and K/Cl and a higher Na/Cl than modern MOR brines (Holland et al., 1996). Therefore, to improve on this Holland et al. (1996) attempted to alter the Hardie (1996) model by adding Mg^{2+} uptake by deep-sea sediments alongside the altered MOR brine, giving lower Ca/Cl and K/Cl with higher Na/Cl than modern MOR brines, which differed from the lower Ca/Cl and K/Cl levels used by Hardie (1996). However, the Holland et al., (1996) results corroborate that secular variation within the MOR and river water ratio influence secular changes within the resultant chemistry of the seawater. Holland et al. (1996) disregarded the suggestion by Hardie (1996) that the

influence of the Mg:Ca ratio was the main driver of calcite and aragonite mineralogy and suggested other parameters such as pCO_2 may be more significant. They based this suggestion on the premise that "nucleation of calcite versus that of aragonite is a fickle function of many environmental parameters" (Holland et al., 1996, p966). Hardie (1998) argues that disregarding the Mg:Ca ratio as the main driver of aragonite-calcite mineralogy based on this premise ignores laboratory results which show the Mg:Ca ratio will determine the $CaCO_3$ mineralogy at given temperature and pressure (Füchtbauer & Hardie, 1976).

Demicco et al. (2005) later expanded the Spencer & Hardie (1990) and Hardie (1996) models to project the chemical reactions that would occur on the MOR. Adding their calculations for river influx and varied rates of alteration of seawater to the original model gained results that were in agreement with the predicted composition of seawater that Spencer & Hardie (1990) had suggested. These results reinforced that seawater is influenced by variation in the rates of interactions occurring at the MOR which add Ca^{2+} and in turn remove K^+ and SO_4^{2-} from seawater influencing chemistry over time. The combined evidence of seawater chemistry oscillations, alongside the evaporite mineralogy of KCl and $MgSO_4$ deposits suggested by the Hardie (1996) model are highly supportive of Mg:Ca ratio being the main driver of seawater chemistry changes.

1.2.5 The Influence of Temperature on $CaCO_3$ Polymorph Formation

Laboratory experiments investigating the influence of combined Mg:Ca ratio and temperature on non-biogenic $CaCO_3$ mineralogy by Morse et al. (1997) were the first to investigate the polymorph precipitation fields under these constraints ***(Figure 1-4).*** Prior to the experiments by Morse et al. (1997), temperature had been suggested to influence crystallisation alongside solution chemistry in laboratory experiments (Burton & Walter, 1987; Morse & Mackenzie, 1990; Burton, 1993; Morse & He, 1993).

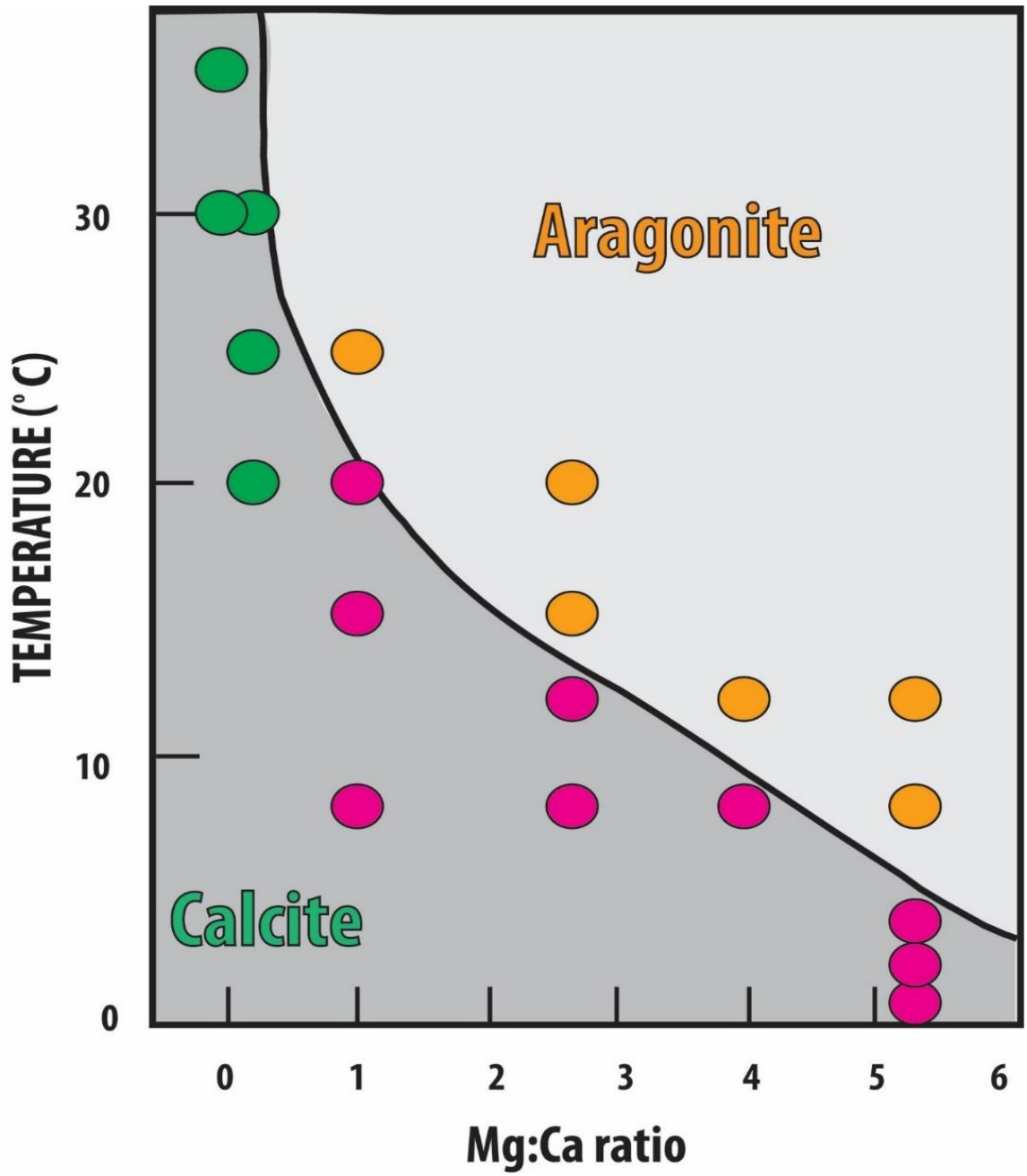

Figure 1-4 Influences of Mg:Ca ratio and temperature on the $CaCO_3$ polymorph precipitating from solution.
Results from degassing $CaCO_3$ precipitation experiments. Coloured points indicate individual experiments with different mineralogical compositions: green- calcite only, orange- aragonite only and pink- calcite with aragonite overgrowths (adapted from Morse et al., 2007).

However, the influence of temperature has often been overlooked in favour of other drivers such as pCO_2 and Mg:Ca ratio. In the marine environment $CaCO_3$ is often segregated by polymorph type depending on the latitude and depth it forms in (Morse et al., 2007). Shallow marine tropical pools are mostly formed of aragonite cements, whereas

colder latitudes and deeper waters are mostly form calcite (Burton & Walter, 1987), indicating the important role of temperature in mineral polymorph formation in the natural environment.

The experiments of Morse et al. (1997) indicated that non-biogenic $CaCO_3$ polymorph formation was indeed influenced by the Mg:Ca ratio, however they noted that aragonite and calcite form as a non-linear function of Mg:Ca ratio together with temperature, in distinct, non-overlapping precipitation fields (Morse et al., 1997). This work suggests that the aragonite-calcite sea hypothesis can no longer be viewed as a phenomenon that is driven by changes in Mg:Ca ratio alone. The findings of Morse et al. (1997) also suggests that temperature influences polymorph formation at a given Mg:Ca ratio. The influence of temperature on polymorph formation is an important consideration in today's changing climate.

1.2.6 Reconstruction of past seawater composition

In order to understand how seawater composition has evolved through the Phanerozoic, marine evaporite fluid inclusions were investigated as a means of directly analysing the original concentrations of Mg^{2+}, Ca^{2+}, Na^{+}, Cl^{-}, K^{+}, and SO_4^{2-} content to reconstruct seawater chemistry. The fluid inclusion archive provides evidence that the seawater chemistry in the Phanerozoic was chemically different to that of today. By using the archives from fluid inclusions has provided evidence that there had been major fluxes in the seawater chemistry throughout the Phanerozoic globally by indicating that only rocks of similar ages had similar seawater chemistry, no matter the geography of their distribution (Lowenstein et al., 2001; Horita et al., 2002).

Results from these analyses suggest a cyclicity in the composition of seawater that links to hydrothermal fluxes at seafloor spreading centres (Lowenstein et al., 2001; Horita et al. 2002; Brennan et al., 2002; Brennan et al., 2004). Evidence from fluid inclusions in Silurian halite suggest that seawater chemistry was different from today (Brennan et al., 2002). Fluid inclusions recorded low Mg^{2+}, Na^{+} and SO_4^{2-} with elevated Ca^{2+} and correlated with KCl evaporite deposition (Brennan et al., 2002). Results led to suggestion that the flux from MOR noted in the fluid inclusion record would be driven by the lowered Mg:Ca ratio (noted to be 1.4) rather than lowered pCO_2 from the Silurian atmosphere giving evidence

for oscillation in seawater chemistry. Brennan et al. (2002) disregarded dolomitization as a possible explanation for the increase in Ca^{2+} observed because the Na^{+} concentrations observed were not consistent with global dolomitization. Brennan et al., (2004) further examined the link between seawater chemistry and calcification by investigating early Cambrian halite fluid inclusions. Here they noted that the fluid inclusion records were almost triple the Ca^{2+} than today's seawater and indicative of the time around the Cambrian explosion (Brennan et al., 2004). In order to have increased Ca^{2+} to this level, MOR rates would be increased, suggesting the increase in Ca^{2+} in brine flux aided the increase in biota occurring at this time. Evidence from trace fossils show the increase in metazoan occurrence matches with the time of increases Ca^{2+} (Knoll & Carroll, 1999). This led Brennan et al., (2004) to suggest a link between MOR, the composition of seawater and bio-calcification as all occur within the timeframe in which biogenic calcification increases. This direct evidence of seawater chemistry recorded within fluid inclusions supports the aragonite-calcite sea hypothesis (Lowenstein et al., 2001; Horita et al., 2002; Brennan et al., 2002; Lowenstein et al., 2003; Brennan et al., 2004; Lowenstein et al., 2005; Timofeeff et al., 2006; Timofeeff et al., 2008).

Whether the archive generated from fluid inclusions is an accurate reflection of Phanerozoic seawater at the time of deposition is still debated (Lowenstein & Timofeeff, 2008; Houston et al., 2011). In order to be sure that records obtained from fluid inclusions are valid a number of steps are undertaken when investigating them. Contested aspects of fluid inclusion analysis come from the possibility that there has been modification of the parent water by either recycling or addition of non-marine water (Lowenstein et al., 2001), although this cannot be totally ruled out, palaeo-environments known to have a great volume of recycling are avoided. Secondly, the possibility that the signal for the concentrations has been obscured by the possibility that dolomitization has occurred which would alter the Ca^{2+} in brine flux available (Timofeeff et al., 2006).

More recently, modelling of fluctuations in seawater chemistry by Ardvison et al. (2006) used the MAGic model (a dynamic elemental cycling model) with input parameters derived from fluid inclusions, isotope analyses and mineralogy records to constrain whether seafloor spreading rates influence the interactions between Earth and ocean. These results show that the uncertainty on the composition of seawater was controlled by

the spread rate at MOR (Ardvison et al., 2006). The results indicated that the influxes of ions to seawater match the Mg:Ca ratio of the bulk seawater acting as a buffer to the seawater-atmosphere system represented in similar ratio changes in pH and pCO_2.

Alongside geochemical modelling of seawater chemistry fluctuations (Wilkinson & Algeo, 1989; Hardie, 1996; Wallmann, 2001) and fluid inclusion archives (Lowenstein et al., 2001; Horita et al., 2002; Brennan et al., 2002; Brennan et al., 2004) another line of evidence that has been considered relevant to aragonite-calcite sea conditions is the geochemistry of echinoderm fossils (Dickson, 2002; Dickson, 2004). The results from Dickson (2002) show Mg:Ca ratios that broadly match with those found in fluid inclusions observed by Lowenstein et al., (2002) whereby Mg:Ca ratios range from ~1.4 in the Cretaceous to ~3.3 in the Triassic, thereby much lower than today Mg:Ca ratio of ~5 (Dickson, 2002). In particular, Dickson (2002) noted an exponential increase in the Mg content in echinoderms at increased temperature. The concentrations of Mg^{2+} noted matched with concentrations in abiotic cements. The Mg^{2+} content exponentially increasing with temperature matches with previous laboratory studies non-biogenic precipitates showing that increased temperature facilitates Mg^{2+} incorporation into calcite (Burton & Walter, 1987; Morse et al. 2007). Echinoderms were previously not investigated as a method for assessing past seawater chemistry as is originally had been presumed that their skeletons were always subjected to alteration (Weber, 1973). However, Dickson (2004) argued that echinoderms that their bulk chemistry is kept, despite alteration, and therefore can be used to record Mg:Ca ratio.

The magnesium content of echinoderms further supports the Mg:Ca ratio as an influencing factor on mineralogy, the shells of echinoderms have recorded seawater chemistry at the time of formation, and therefore any oscillations that occurred (Dickson, 2002; Dickson, 2004). The evidence from Dickson (2002; 2004) echinoderms alongside the analyses of fluid inclusions and geochemical modelling, show that the Phanerozoic seawater chemistry has fluctuated between aragonite and calcite sea periods, matching with the Sandberg (1983) aragonite-calcite sea hypothesis.

1.2.7 The Aragonite-Calcite Sea Hypothesis and biomineralisation

The results from Mg content analyses of echinoderms Dickson (2002; 2004) and those of hyper-calcifying organisms from the Hardie (1996) model alongside fluid inclusion data (Lowenstein et al., 2001; Horita et al., 2003; Brennan et al., 2002; 2004; Timoffeeff et al., 2006; 2008) match with the earlier laboratory experiment findings of Füchtbauer & Hardie (1976), where calcite formed at lower Mg:Ca ratio, and aragonite and high-Mg calcite formed at higher Mg:Ca ratio. The above all correlate with the global seawater oscillations of the Sandberg (1983) hypothesis. Direct transfer of the aragonite-calcite sea hypothesis to biogenic $CaCO_3$ formation is complex, but seawater chemistry has seemed a likely influence biomineralisation. However, this may be an over-simplification to assume that seawater chemistry directly influences biogenic $CaCO_3$ formation.

It has been observed that organisms control their own mineralogy to a large degree (Lorens & Bender, 1977; Lowenstam & Weiner, 1989) and so, biogenic polymorph formation is significantly buffered against surrounding seawater conditions. Lorens & Bender (1977), for example, discovered that *Mytilus edulis* shells have a physiological mechanism which allows controlled uptake and incorporation of magnesium into its forming calcite shell mineralogy. As control over biomineralisation will vary between different organisms this will make it difficult determining an overall relationship that accommodates the aragonite-calcite sea hypothesis on biomineralisation (Stanley et al., 2002). Aragonite-calcite seas conditions control the environment the organism lives within in the context of supplying the ions required for biomineral formation, but organisms generally control how to use this supply. However, a number of studies suggest that this organismal control over biomineralisation can be overprinted by environmental i.e. aragonite-calcite sea conditions.

A landmark study suggesting a link between aragonite-calcite seas and biomineralisation was compiled by Stanley & Hardie (1998). Stanley & Hardie (1998) studied the influence of changes in Mg:Ca ratio on hyper-calcifying organisms; those with massive skeletons, those that form large reefs or those that produce large volumes of sediment. Simple skeletal calcifiers (i.e. reef-builders and hyper-calcifiers) are more susceptible to seawater conditions due to their fast growth to compete for space (Stanley

et al., 2002). By investigating the influence of Mg:Ca ratio on polymorph formation by hyper-calcifying organisms and calcifiers who had a limited control over their mineralogy. Stanley & Hardie (1998) showed that the mineralogy matched with the aragonite-calcite sea hypothesis and with predictions of the thresholds determining calcite and aragonite modelled by Hardie (1996). This work correlated calcitic hyper-calcifiers forming in calcite seas and aragonitic organisms being favoured in aragonite sea conditions. Stanley & Hardie (1998) agreed with the Hardie (1996) model findings, noting that variations within skeletal rocks had mineralogical similarities to non-biogenic ooids and cements from similar geological time, their mineralogy matching with hypothesised aragonite and calcite sea periods, supporting the Sandberg (1983) hypothesis. However, Stanley & Hardie (1998) emphasised that this was true for simple skeletal calcifiers only. The results of this study (Stanley & Hardie, 1998) added further support for the concept that the marine Mg:Ca ratio drives oscillations in $CaCO_3$ polymorph dominance correlating secular changes in Mg:Ca ratio with oscillations in skeletal carbonate mineralogy.

In modern seawater (aragonite sea), most simple calcifying organisms consist of aragonite or high Mg-calcite (Stanley & Hardie, 1998; 1999). The Mg^{2+} content within calcite of skeletal organisms has been observed to decrease at lowered temperature matching the trends observed in non-skeletal laboratory experiments (Füchtbauer & Hardie, 1976). This suggests there may be a linkage to the mechanisms forming $CaCO_3$ both biogenically and non-biogenically. The observation that decreased Mg^{2+} content occurred at lower temperatures was most prominent only in simple calcifiers (Chave, 1954), also suggesting that any lowering of Mg:Ca ratio in seawater could have facilitated these calcifiers to incorporate less Mg^{2+} into their skeletons in palaeo-seawaters with lower Mg:Ca ratios than today (Stanley et al., 2002). The results of Chave (1954) and Stanley & Hardie (1998) together suggest that seawater chemistry does impact on calcification of simple calcifiers.

Around the same time as the Stanley & Hardie (1998) results, investigations to determine if more complex calcifying organisms were influenced by aragonite-calcite seas by Harper et al., (1997) who organised bivalves by family data from previously published work (Taylor et al., 1969; 1973; Carter, 1990; Sepkoski, 1992; Skelton & Breton, 1993) and categorised into new groups based on whether they were entirely aragonitic or had some

calcite contents within their structure. It was observed that entirely aragonitic families of bivalve increased over geological time, but that in periods of calcite seas the diversity of entirely aragonitic families was decreased by ~23% (Harper et al., 1997). Here, it was proposed that a dynamic link between an organism and the seawater chemistry existed (Harper et al., 1997). Harper et al., (1997) suggested that to explain the occurrence of calcite, that extrinsic factors were the key influence on the evolution of calcite in bivalves when advantageous for the organism.

A number of laboratory experiments also support the observed correlation of simple calcifiers with non-skeletal mineralogies in the rock record. Stanley et al., (2002) investigated high-Mg calcite secreting coralline algae of modern seas and how their mineralogy was influenced when grown in artificial seawater of 1, 2.5 and 5.8 Mg:Ca ratios. The Stanley et al. (2002) findings were significant in that they observed the algae produce low-Mg calcite in low Mg:Ca ratio seawater, suggesting that in the past, the currently high Mg-calcite producing coralline algae would have produced low-Mg calcite skeletons facilitated by Mg:Ca ratio. These findings support the suggestion of Hardie (1996) who predicted aragonite and calcite sea periods match with the mineralogy of hyper-calcifying organisms in the rock record.

Sandberg (1975) suggested only one shift between aragonite and calcite sea conditions, facilitated by the calcification of nannoplankton and foraminifera removing Ca^{2+} from seawater and resulting in elevated Mg:Ca ratio and aragonite production. Such high production by these calcifiers removed pCO_2 via respiration and on death results in CO_2 fertilization of the seawater. To further investigate the Sandberg (1975) suggested link between seawater conditions and calcification, high-Mg calcite producing coccolithophores (calcareous nannoplankton) in varied Mg:Ca ratio seawater from 0.5 up to 5.2 were investigated by Stanley et al. (2005). The results indicated that Mg incorporation decreased in seawater with lower Mg:Ca ratios. Further to this, they concluded that the accelerated calcification observed from the Cretaceous was facilitated by the ionic composition of the seawater (calcite sea) allowing the vast chalk deposits to form, and conversely that today's modern ocean prevents these formations due to its ionic composition (Stanley et al., 2005).

Direct influences of aragonite-calcite sea conditions on biomineralisation were investigated by Porter (2007; 2010). Porter (2007) observed that in the 21 taxa studied during the Edicarian and Ordovician, they rarely switched mineralogy once they formed. Porter (2007) argued that the mineralogy of skeletal calcifiers was indirectly influenced by seawater chemistry because precipitating a skeleton not supported by the seawater chemistry was at increased physiological cost to the organism. Porter (2010) expanded the dataset of Porter (2007) to further test their hypothesis on 40 taxa throughout the Phanerozoic to investigate aragonite-calcite sea conditions on the mineralogy when organisms first acquire their $CaCO_3$ skeletons. If seawater chemistry influenced the mineralogy of the first formed skeletons then this would suggest that the mineralogy of biogenically formed $CaCO_3$ could be influenced by aspects similar to non-biogenic $CaCO_3$. Of these, 25 taxa matched the predicted mineralogy from the seawater chemistry (Porter, 2010). Only 2 taxa precipitated mineralogy that was unsupported by the seawater chemistry they formed within and this was not due to aragonite-calcite sea conditions (Porter, 2010). The observations Porter (2010) made indicates that aragonite-calcite seas have strong influence over skeletal mineralogy only on the first appearance of calcification in lineages of organisms, therefore suggesting that new evolutionary constraints appear once a group had adopted a particular mineral composition preventing a mineralogical switch after this time.

Despite the findings of studies such as Stanley & Hardie (1998) indicating that the mineralogy of both biogenic and non-biogenic $CaCO_3$ oscillates throughout the Phanerozoic matching aragonite and calcite sea conditions, there is evidence that within each 'sea' period the $CaCO_3$ mineralogy, never reached 100% calcite or aragonite (Sandberg, 1983; Zhuravlev & Wood, 2009). Further influences alongside the Mg:Ca ratio on the formation of $CaCO_3$ mineralogy may explain these co-occurrences of aragonite and calcite. This certainly has been represented non-biogenically in the experiment results of Balthasar & Cusack (2015), where co-precipitation of aragonite and calcite polymorphs occurred, with pure calcite formation being restricted to experiments without magnesium. This indicates that not all polymorphs formed are in equilibrium with the general environment they form in.

Initial work by Ries (2005) into the influence of Mg:Ca ratio on algae observed that the mineralogy produced is 75% controlled by the organism, but a quarter of the precipitated mineralogy was controlled by the seawater Mg:Ca ratio indicating the organisms control can be overridden. Lowered Mg:Ca ratios decreased the calcification occurring and Ries (2005) suggested that growth of algae consisting of aragonite would be hindered in low Mg:Ca ratio seawaters as this would not support their mineralogy.

The suggestion that taxa do not 'switch' mineralogy after first calcified of Porter (2007) was disputed by Ries (2010). Ries (2010) suggested that the mineralogy of some simple hyper-calcifying aragonite-secreting species do 'switch' to match calcite-sea conditions, whereas more complex calcifiers, such as molluscs, are generally less affected. Porter (2010) had suggested that switches in mineralogy were more costly to the organism than forming mineralogy not supported by the seawater chemistry. Ries (2010) suggested that the faster calcification rate of the hyper-calcifiers observed. Nevertheless, complex calcifying organisms forming shells out of equilibrium with the aragonite-calcite sea state of the seawater do so at greater energetic cost and may be more prone to dissolution (Wood, 2011). Changes to seawater chemistry could therefore impact on organisms unable to evolve to the changing conditions.

Kiessling et al. (2008) statistically tested if the relative abundance of biogenic calcite and aragonite over time is influenced by changes in aragonite-calcite sea conditions and mass extinctions. Kiessling et al. (2008) used the patterns of skeletal mineralogical occurrences from the PaleoReefs and Paleobiology databases. Reviewing the occurrences at the genus level allowed a large-scale data collection to be grouped into 49 time-bins segregated based on the marine invertebrate groups from the Paleobiology database, for the entire Phanerozoic. Their initial study indicated a relationship between the polymorph mineralogy in reef-builders with aragonite-calcite sea conditions (Kiessling et al., 2008). However, when expanding their study from reef-builders only to include all calcifying organisms across Phanerozoic time, the trend where mineralogy followed aragonite-calcite sea periods was not observed showing no indication that skeletal mineralogy correlates with the changes in aragonite-calcite sea conditions. (Kiessling et al., 2008). By using the number of fossil occurrences Kiessling et al. (2008) generated a comparison of aragonite to calcite ratio and noted it increased over time. This suggested that oscillations between

aragonite and calcite sea conditions were not the only influencing factor. Instead of aragonite-calcite sea conditions, Kiessling et al. (2008) proposed that mass extinctions were a major influencing in determining long-term skeletal mineralogy. Furthermore, mass extinction might also explain the proportional increase in the occurrences of aragonite skeletal remains (Kiessling et al., 2008).

Zhuravlev & Wood (2009) also supported the idea that mass extinctions have a great influence on skeletal mineralogy following an investigation using the invertebrate database of Sepkoski (2002) to study evolution of mineralogy throughout the Phanerozoic. Zhuravlev & Wood (2009) observed that non-biogenic $CaCO_3$ mineralogy correlates with periods of icehouse and greenhouse as noted by Fischer (1982) which Sandberg, (1983) previously matched with his aragonite-calcite sea periods. However, Zhuravlev & Wood (2009) show that aragonite increasingly replaced low-Mg calcite after mass extinctions, allowing for biota unsupported by the seawater chemistry to be removed while those which were supported could flourish. Zhuravlev & Wood (2009) suggested that the driver for this was higher pCO_2 and global changes in temperature rather than Mg:Ca ratio. In particular, Zhuravlev & Wood (2009) observed that higher pCO_2 with Mg:Ca ratio <2 precipitated low-Mg calcite, however, lower pCO_2 at Mg:Ca ratios >2 would facilitate aragonite formation. It was suggested that their evidence shows that once a calcifying organism has evolved, their mineralogy does not switch possibly leaving them susceptible to changes in seawater chemistry to the detriment of the organism (Zhuravlev & Wood, 2009).

The findings of both Zhuravlev & Wood (2009) and Kiessling et al. (2008), using information from databases, are in contrast with evidence from growth experiments by Ries (2006), which show that some hyper-calcifying organisms begin to secrete low-Mg calcite when exposed to Mg:Ca ratios <1 instead of high-Mg calcite as they did at Mg:Ca ratio ~5.2. Ries (2009) also noted aragonite producing algae in modern seawater produce 25% calcite skeletons when grown in seawater with Mg:Ca ratios <2, which would be a reflection of Cretaceous calcite sea conditions. Furthermore, Ries (2010) found that when the Mg:Ca ratio favoured the skeletal mineralogy, there was a noted increase in calcification rate. These experimental data suggest that organisms may adapt to aragonite-calcite sea conditions.

However, the influence of aragonite-calcite seas on the majority of biogenic $CaCO_3$ formers remains poorly understood (Stanley, 2008; Balthasar et al., 2011). Influences on the seawater chemistry, such as the presence of organic compounds (DeYoreo & Dove, 2004), can influence mineralogy by manipulating the Mg:Ca ratio at which bivalves make either aragonite or calcite (Falini et al., 1996). Temperature has also shown to influence coral Mg:Ca ratios of their skeletal mineralogy (Reynauld et al., 2007). However, laboratory experiments growing corals at constant temperature remained to show a correlation with Mg^{2+} uptake and increased Mg:Ca ratios of seawater chemistry suggesting any palaeo-temperature reconstructions would need to be corrected for seawater chemistry changes (Mitsuguchi et al., 1996) .

1.2.8 Conflicting Evidence Supporting the Mg:Ca ratio threshold of 2

Constraining the parameters of seawater chemistry influences on $CaCO_3$ has been a point of interest to aid the understanding of how they influence the $CaCO_3$ system amidst changes in global climate today (Pelejero et al., 2010; IPCC, 2013; Fitzer et al., 2014a; 2014c). Fluctuations of the Mg:Ca ratio in Phanerozoic seawater ***(Figure 1-5)*** range from 0.6 in the mid-Cambrian, to approximately 5.2 in the Neogene (Lowenstein et al., 2001; Stanley, 2008). Higher Mg:Ca ratios result in the precipitation of aragonite, and lower ratios in calcite formation. It is widely assumed that a critical threshold at Mg:Ca ratio of 2 indicates the boundary between calcite and aragonite formation (Folk, 1974; Hardie, 1996). This Mg:Ca ratio of 2 has been used as a guide to define the boundary between 'aragonite seas' and 'calcite seas' (Sandberg, 1975; Sandberg, 1985; Hardie, 1996).

However, Füchtbauaer & Hardie (1976) documented that magnesium substitution of calcium in non-skeletal calcite increases with higher Mg:Ca ratio above a Mg:Ca ratio of 2, and a mix of high-Mg calcite (Mg content > 4%) and aragonite forms. At lower Mg:Ca ratio between 1 & 2 high-Mg calcite forms but with no aragonite growth, and below Mg:Ca ratio 1, only low-magnesium calcite forms (Folk, 1974; Sandberg, 1975; Füchtbauer & Hardie, 1980; Lowenstein et al, 2001; Stanley, 2008).

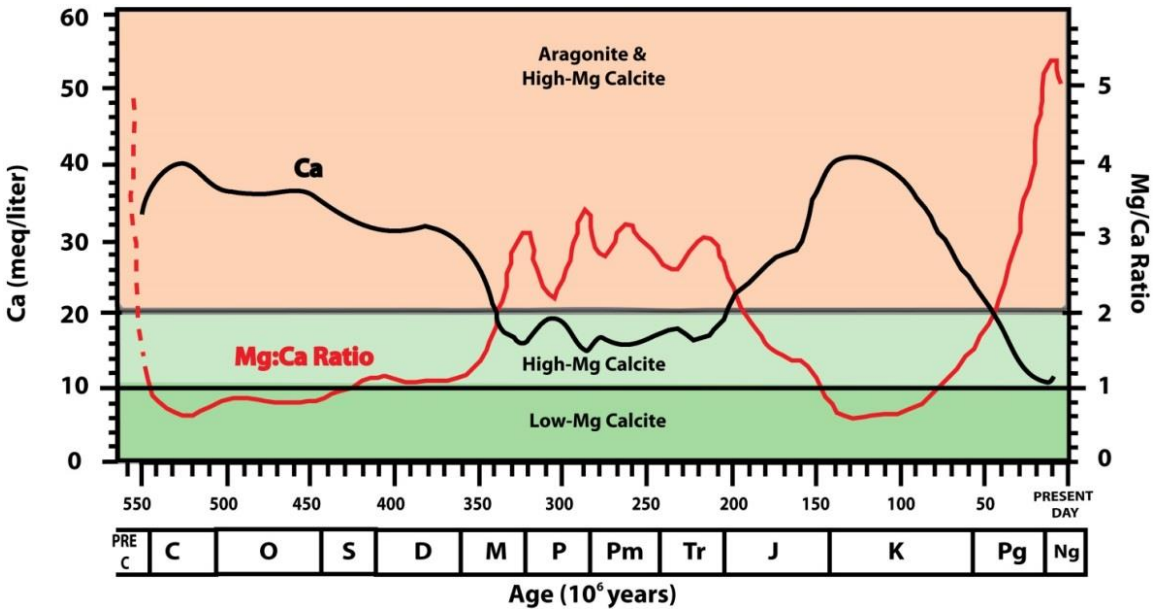

Figure 1-5: Fluctuations of Mg:Ca ratio and calcium concentration throughout the Phanerozoic. The red line shows the Mg:Ca ratio over time. The Mg:Ca ratios of 2 (the critical threshold for the switch between calcite and aragonite) and 1 (the boundary between low and high Mg-calcite) are indicated. Aragonite formation is only considered to occur above a Mg:Ca ratio of 2 (Adapted from Stanley, 2008).

The boundary between calcite and aragonite formation at Mg:Ca ratio 2 has been contested (Lee & Morse, 2010; Bots et al., 2011; Balthasar & Cusack, 2015). In addition to the Mg:Ca ratio, factors such as temperature (section 1.2.5.) and pCO_2 (section 1.2.3.) also influence the proportions of calcium carbonate formed. Bots et al. (2011) demonstrated that sulphate ions (SO_4^{2-}) lowered the Mg:Ca ratio required for calcite dominance, and only in sulphate-free experiments did a pure 100% calcite form. Bots et al. (2011) also showed vaterite to be >50% dominant at lower Mg:Ca ratios. Thus, while Mg:Ca ratio is an important driver in the aragonite-calcite sea hypothesis, temperature, pCO_2 and SO_4^{2-} ion concentration all influence the effect of Mg:Ca ratio on the resultant mineralogy.

The aragonite-calcite sea hypothesis proposes that fluctuations in seawater chemistry influence polymorph formation (Sandberg, 1983), regardless of latitudinal variations such as temperature. Increasing temperature inhibits the growth of calcite and facilitates aragonite (Morse et al., 1997). Lower temperatures reduce Mg^{2+} incorporation into calcite and decrease the abundance of aragonite (Burton & Walter, 1987; Morse et al, 2007). To constrain how the parameters of Mg:Ca ratio and temperature influence non-biogenic $CaCO_3$ polymorph precipitation laboratory experiments based on the work of Morse & He (1993) were carried out by Morse et al. (1997).

The degassing of artificial seawater over 48 hours was used to initiate nucleation of $CaCO_3$ (Morse et al., 1997). Individual experiments constraining the assumed critical threshold of Mg:Ca ratio 2, were sparse in Morse et al. (1997) (see also Section 1.2.5. ***Figure 1-4***). Further, although the experiments by Morse et al. (1997) resulted in two distinct precipitation fields, one for aragonite and one for calcite, calcite with aragonite overgrowths (pink circles in ***Figure 1-4***) occurred in some experiments. These aragonite overgrowths on calcite were interpreted as initial calcite precipitates and thus as representative of the calcite precipitation field. Due to the experiment set-up, the solution's Mg:Ca ratio increases by removal of Ca^{2+} as $CaCO_3$ forms, thus, facilitating aragonite overgrowths on the initial calcite precipitate at a later stage in the experiments. No co-precipitation was reported by Morse et al. (1997) between aragonite and calcite polymorphs. In a study of instantaneous nucleation from supersaturated solutions on degassing, De Choudens-Sánchez & González (2009) gained similar results whereby the degassed solution increased in Mg:Ca ratio over time due to the removal Ca^{2+} by precipitates. This study also showed calcite to be favoured at low Mg:Ca ratios with less aragonite forming and at increased Mg:Ca ratios aragonite would be favoured (De Choudens-Sánchez & González). The trend for lowering the rate of calcite growth but having little influence over aragonite at higher Mg:Ca ratios has been suggested to be due to the influence of Mg^{2+} influencing mineralogy (Davis et al., 2000; Jiménez-López et al., 2004; Morse et al., 2007).

Further work to constrain the influence on $CaCO_3$ precipitates at Mg:Ca ratio 2 was required, and since has been investigated further by Balthasar & Cusack (2015). Balthasar & Cusack (2015) used Morse et al. (1997)'s technique with the adaption that they quantified the first-formed precipitates which limited the possibility of the solution chemistry to change during the experiments. Balthasar & Cusack (2015) presented the precipitation fields of aragonite and calcite, but show a 'grey' area in which aragonite and calcite precipitate together (***Figure 1-6***) with no clear-cut boundary as originally proposed by Morse et al. (1997).

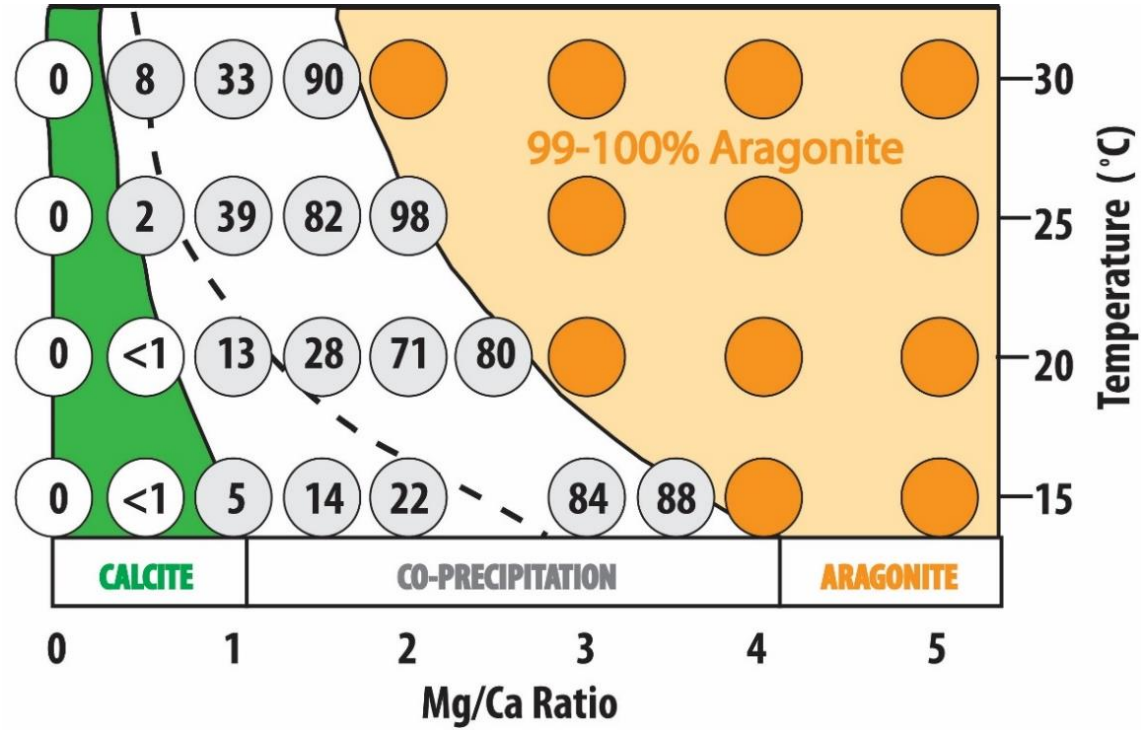

Figure 1-6 Proportions of aragonite precipitates as a function of Mg:Ca ratio and temperature from de-gassing precipitation experiments (Adapted from Balthasar & Cusack, 2015). Orange = 99-100% aragonite; Green = 99-100% calcite. Numerical values indicate the ratio of aragonite to calcite as a volumetric proportion (mole % of aragonite) for a given Mg:Ca ratio and temperature. The dashed line indicates the threshold between aragonite and calcite by Morse et al. (1997). White area with grey circles represents Mg:Ca ratio and temperature conditions during which aragonite and calcite co-precipitate.

The non-linear relationship from the combined effect of Mg:Ca ratio and temperature on $CaCO_3$ mineralogy defined in the work of Morse et al. (1997), and the fact that both parameters influence $CaCO_3$ polymorph formation suggests that the original views of aragonite-calcite seas as spatially homogeneous are incorrect because the temperature of the oceans varies in space (Balthasar et al., 2011). This is especially important in order to understand the non-biogenic mechanisms of polymorph growth. Instead, Balthasar & Cusack (2015) propose that $CaCO_3$ polymorph ratios gradually become more aragonitic at increased Mg:Ca ratios and temperatures, suggesting that a purely calcite sea scenario would have been extremely rare.

This emphasises that aragonite–calcite sea theory should not be viewed as a spatially homogeneous switch between dominant aragonite or calcite precipitation that is controlled by the Mg:Ca ratio alone. Instead, the influence of temperature differentiates $CaCO_3$ polymorph formation on a spatial level. Each of these studies has demonstrated

how the Mg:Ca ratio is a main driver of $CaCO_3$ polymorph formation and thus of aragonite-calcite seas. Emphasis has been placed on understanding aragonite-calcite seas as resulting from multiple influences acting together on the subsequent $CaCO_3$ mineralogy. The work of Balthasar & Cusack (2015) illustrates that increases in temperature would increase the proportion of non-biogenic aragonite precipitated and therefore in turn could influence biomineralising organisms.

1.2.9 The Influence of pCO_2 and Alkalinity on Polymorph Formation

pCO_2 is a strong influencer of the $CaCO_3$ system (Lee & Morse, 2010). Strong links between the carbon cycle and climate change have been observed in the rock record where major environmental change such as raised pCO_2, global warming and ocean acidification (OA) impacts on biota and calcification (Hönisch et al., 2012). Currently the increase in pCO_2 has been absorbed into the ocean resulting in decreased oceanic pH and altering the saturation state with respect to $CaCO_3$ (Hönisch et al., 2012). This in turn will influence subsequent calcification. Supersaturated seawater with respect to $CaCO_3$ will have higher pH and higher alkalinity than normal seawater (Pytkowicz, 1973) which will influences the polymorph which will precipitate (Berner, 1975).

Specifically, the saturation state of seawater is altered by changes in carbonate chemistry. The rate of CO_2 release influences CO_3^{2-} chemistry and therefore is linked to long-term terrestrial weathering releasing CO_2 to the atmosphere (pCO_2). It is important to monitor because the saturation state with respect to $CaCO_3$ because decreases in carbonate availability can hamper calcification. Ongoing investigations into environmental change have shown that sea ice melt into the ocean can reduce saturation state of $CaCO_3$ by decreasing the CO_3^{2-} (Chierici & Fransson, 2009) which could be influential in future calcification if predicated global temperature increases continue as projected by IPCC, (2013).

Increased pCO_2 was suggested by Wilkinson & Given (1986) facilitate calcite due to decreased CO_3^{2-} concentration. Aragonite, however, is facilitated when CO_3^{2-} concentration is higher such as occur in environments where fast degassing of CO_2 to the atmosphere favours quick precipitation (Given & Wlkinson, 1985). However, geochemical

modelling more recently has shown that it is possible for increased alkalinity to prevent the precipitation of calcite despite raised pCO_2 (Arvidson et al., 2006).

pCO_2 does not directly impact on total alkalinity even with CO_2 absorption from the atmosphere into the ocean, or on its release to the atmosphere (Zeebe & Wolf-Gladrow, 2001). However, pCO_2 does impact on oceanic pH, which in turn is related to alkalinity, making the measurement of alkalinity important as it allows the strength of the bases within seawater to be determined, whereas pH will only measure the concentration of the H^+ ions (Hach, 2010). Total alkalinity of seawater is a measurement of combined carbonate speciation's in seawater which is defined the moles of H^+ (acid proton donors) equal to the excess of bases (the proton acceptors i.e. HCO_3^-) in 1 kg of seawater (Dickson, 1981; Zeebe & Wolf-Gladrow, 2001) influencing $CaCO_3$ polymorph precipitation, both non-biogenically and biogenically. Total alkalinity of seawater is influenced by salinity (Chierici & Fransson, 2009) as this alters the variation in charges between the cations and anions (Zeebe & Wolf-Gladrow, 2001). Total alkalinity can also be influenced by calcifying organisms as the uptake of Ca^{2+} into the mineralogy decreases the concentration of Ca^{2+} available within the seawater which in turn decreases total alkalinity (Zeebe & Wolf-Gladrow, 2001). Seawater alkalinity allows quantification of the ability of the seawater to buffer against acidification by uptake of H^+ ions and combining them to a base.

Alkalinity as a parameter for forming non-biogenic aragonite or calcite, was not considered until the laboratory experiments of Lee & Morse (2010). Lee & Morse (2010) indicated that the pCO_2 level influences the $CaCO_3$ polymorph, when held at reasonable alkalinity (~10mM or less). Lower pCO_2 will raise the CO_3^- concentration increase the pH (Wilkinson & Given, 1986) and in turn increase the saturation state of seawater (Zeebe & Wolf-Gladrow, 2001). Highly supersaturated seawater with a high Mg^{2+} content was found to facilitate calcite formation because it overcame the inhibiting effect Mg^{2+} normally has on calcite growth (Fernández-Diaz et al., 1996). De Choudens-Sánchez & González (2009) determined that in turn the saturation state with respect to $CaCO_3$ alongside the Mg:Ca ratio influence calcite and aragonite precipitation fields, again noting that to facilitate calcite a higher saturation is required as Mg:Ca ratio is increased.

To understand how Mg:Ca ratio and pCO_2 work together to influence $CaCO_3$ mineralogy, Lee & Morse (2010) carried out $CaCO_3$ precipitation experiments using artificial

seawater under constrained alkalinity and pCO_2. Lee & Morse (2010) noted that alongside Mg:Ca ratio, the influences of alkalinity and pCO_2 alter the Mg:Ca threshold between aragonite and calcite. In particular, at alkalinity of 10 mM, Mg:Ca ratio of 1.2 and pCO_2 above 2500 µatm, pure aragonite is formed (Lee & Morse, 2010) such as in the Late Cambrian (Berner, 2006). When pCO_2 is below this value, calcite with aragonite overgrowths formed (Lee & Morse, 2010). The relationship was less clear with altered alkalinity at a Mg:Ca ratio of 1.2. Lee & Morse (2010) also observed that varying the alkalinity was more likely to produce aragonite at Mg:Ca ratio 1.7 and lower alkalinity (<~11) but calcite would be facilitated at a higher alkalinity (>~18). Therefore, this suggests that when considering the Mg:Ca threshold influence on $CaCO_3$ mineralogy, alkalinity and pCO_2 need to also be taken into consideration (Lee & More, 2010). This is contrary to modelling (MAGic model) that indicated when pH is held higher, calcite precipitation is hindered if alkalinity is elevated (Ardvison et al., 2006).

This is important when considering the $CaCO_3$ saturation state of seawater as higher saturated solutions will be linked to lower pCO_2 and therefore higher pH, and this could facilitate the growth of aragonite at the expense of calcite. Laboratory experiments investigating $CaCO_3$ under varying levels of super-saturation further support a link with the mineralogy, facilitated by kinetics of growth (de Choudens-Sanchez & Gonzalez 2009). Specifically, higher super-saturations at increased Mg:Ca ratios can facilitate calcite of larger size due to rates of growth increasing compared to those of aragonite (de Choudens-Sanchez & Gonzalez 2009).

The importance of accounting for pCO_2 may be indicated when considering the timeframes for each aragonite-sea period as these could be significantly underestimated because the pCO_2 has been significantly higher in the past, particularly during intervals considered calcite seas (e.g. Zhuravlev & Wood, 2009). Today, the influences of pCO_2 and temperature on $CaCO_3$ polymorph growth are important when considering the effect of OA on biomineralisation, as both influence the $CaCO_3$ mineralogy both individually, and combined. Temperature also has been shown to elevate the pCO_2 concentration that is required for non-biogenic nucleation of $CaCO_3$ to occur (Morse & He, 1993). Therefore, application to biogenic $CaCO_3$ formation also needs to be considered. The mechanisms of OA on $CaCO_3$ will be discussed later in section 1.3.5.

1.2.10 The Influence of Sulphate on $CaCO_3$ Polymorph Formation

Another influencing factor which has been considered in the context of aragonite-calcite seas is the influence of sulphate. Sodium sulphate is the second most common water-soluble mineral in nature after NaCl and therefore is present in natural seawater influencing $CaCO_3$ polymorphs precipitated from seawater (Vavouraki et al., 2008; Garett, 2011). $CaCO_3$ growth is influenced by various ions within the seawater (Mg^{2+}, Ca^{2+}, S^{2-}, SO_4^{2-}) as aragonite and calcite incorporate the ions into the crystallographic structure (Fernandez-Diaz et al., 2010). Sulphate is one such ion that can alter the crystal lattice structure of the forming $CaCO_3$ crystal (Vavouraki et al., 2008). This is important to consider when investigating $CaCO_3$ precipitation parameters in the context of aragonite-calcite seas, as the concentration of sulphate in marine environments can be extremely high, especially in evaporitic environments (Hanor, 2004).

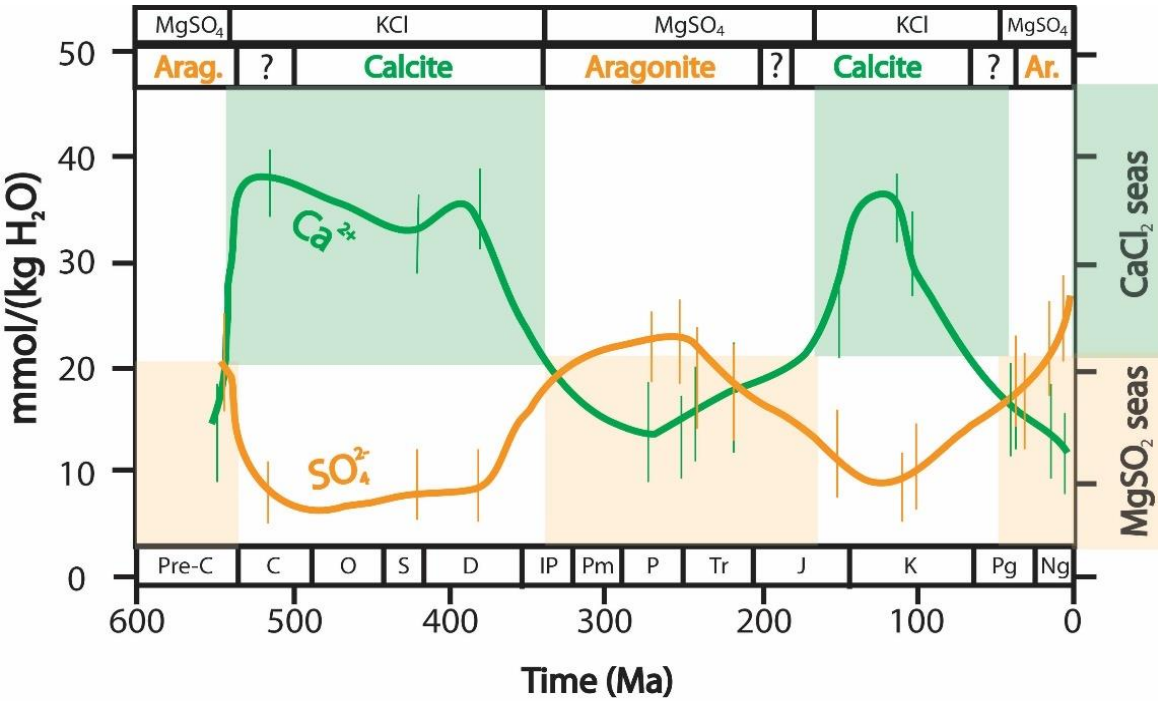

Figure 1-7: Marine concentrations of Ca^{2+} & SO_4^{2-} throughout the Phanerozoic (Figure adapted from Lowenstein et al., 2003).

Figure indicates that the highest concentrations of SO_4^{2-} (orange line) match with decreases in Ca^{2+} (green line) concentration (high Mg:Ca ratio) and $CaCl_2$ seas (aragonite facilitating). Estimates plotted are from marine halite fluid inclusions (mM/kg H_2O). Correlations with the deposition of marine evaporites are indicated along the upper top bar (data from Hardie, 1996) and non-skeletal mineralogy in the lower top bar (data from Sandberg, 1983).

Halite fluid inclusions and basinal brines show that the sulphate concentration in seawater has co-varied with the magnesium concentration throughout the Phanerozoic (Horita et al., 2002; Lowenstein et al, 2003) (see ***Figure 1-7*****).** The marine SO_4^{2-} concentration has fluctuated throughout the Phanerozoic between 5 & 30 mM (Horita et al., 2002; Lowenstein et al., 2003), the higher concentrations of SO_4^{2-} correlate with times of aragonite formation, calcite formation when the SO_4^{2-} concentration is low.

A number of sources of SO_4^{2-} feed the concentration in the ocean. River water flux to the ocean brings SO_4^{2-} from the oxidation of pyrite on weathering (Tostevin et al., 2017). Sulphur is also released by gaseous emissions from volcanism and anthropogenically through the burning of fossil fuels, which in turn will combine with water to form SO_4^{2-} and acid rain (Vavouraki et al., 2008). These main sources of SO_4^{2-} are maintained in seawater from dissolution of marine evaporites (gypsum, $CaSO_4.2H_2O$ and anhydrite $CaSO_4$) and sulphide oxidation of sediments (Vavouraki et al., 2008).

The influence of sulphate on $CaCO_3$ mineralogy in the context of the aragonite-calcite seas hypothesis had mainly been overlooked before the work of Bots et al (2011). Bots et al. (2011) presented the influence of sulphate on $CaCO_3$ mineralogy at differing Mg:Ca ratios and demonstrated that the critical Mg:Ca threshold for the switch in which $CaCO_3$ polymorph dominates appears to be significantly lower under the influence of SO_4^{2-} than any previous estimates (Horita et al., 2002; Lowenstein et al., 2003). Bots et al. (2011) also indicate that Mg:Ca ratio and SO_4^{2-} presence are mutually dependent. Their study suggested that the possibility of having a 100% pure calcite sea would only occur at very low Mg:Ca ratios (<0.15 when 3mM [SO_4^{2-}] present), which is unrealistic. This Mg:Ca threshold is much lower than modelled thresholds based of fluid inclusions, which were around Mg:Ca ratios of 1.5 (+/- 0.5) (Horita et al., 2002) and also lower than thresholds derived from PHREEQC modelling of marine evaporites which were predicted to switch between KCl to $MgSO_4$ at Mg:Ca ratio 1 with 9mM [SO_4^{2-}] (Lowenstein et al. 2003).

These findings suggest that the aragonite-calcite sea hypothesis needs to also take into consideration the influence of sulphate in the facilitation of the dominant mineralogy (Bots et al., 2011). Bots et al., (2001) suggested that a change in labelling of how the polymorphs were quantified from '100% calcite sea' to 'calcite dominant sea' period was more realistic. The threshold for calcite dominant seas were proposed to be at a Mg:Ca

ratio of 0.3 at 5mM [SO_4^{2-}], lowering the Mg:Ca threshold previously suggested for pure calcite seas. Suggesting the Mg:Ca threshold is lower in the presence of sulphate means aragonite-calcite sea theory over estimates the duration of calcite seas in the past.

Since the aragonite-calcite seas hypothesis was first described, it has morphed over the past few decades to suggest more factors alongside Mg:Ca ratio need to be included as well when evaluating the hypothesis from fossil ooids (Mackenzie & Piggot, 1981; Sandberg, 1983), fluid inclusions (Horita et al., 2001; Lowenstein et al., 2003) and experiments both non-biogenic (Morse et al., 1997; Bots et al., 2011; Balthasar & Cusack, 2015) and biogenically (Ries, 2010) demonstrating that factors such as temperature (Burton & Walter, 1987; Morse et al., 1997; Balthasar & Cusack, 2015), pCO_2 (Lee & Morse, 2010) and SO_4^{2-} (Bots et al., 2011)

1.3 Mechanism of Physical and Chemical Parameters Influencing Aragonite-Calcite Seas

Differences in crystallographic structure between $CaCO_3$ polymorphs gives different chemical and thermodynamic properties (Morse et al., 2007; Sun et al., 2015). Compared to other sedimentary minerals, the carbonate system has structurally simple mineral unit-cells, but complex reactions and behaviours occur in seawater due to these differences in crystallography between aragonite and calcite (Morse et al., 2007).

1.3.1 Solubility of $CaCO_3$

The polymorphs aragonite, calcite and vaterite differ in density: aragonite is most dense (2.947 g/cm^3), followed by calcite (2.715g/cm^3) and vaterite (2.645 g/cm^3) (densities available from www.mindat.org). Solubility is another important aspect of $CaCO_3$ polymorph growth or dissolution. Solubility is assessed using the solubility product: the ion concentrations of Ca^{2+} and CO_3^{2-} that can co-exist in solution. Calcite's apparent solubility product or $K_{SP(Ca)}$, for example, is 4.36 (+/- 0.20) x10^{-7} mol^2/kg^2 (at 25^{o}C and Salinity =35, whereas, that of aragonite is much higher at $K_{SP(Arag)}$ 6.65 (+/- 0.12) x10^{-7} mol^2/kg^2 (both from Morse et al., 1980).

1.3.2 Thermodynamic Properties of $CaCO_3$ Polymorphs

With so many factors such as Mg:Ca ratio, temperature, pCO_2 and SO_4^{2-} ion concentration, influencing $CaCO_3$ polymorph formation from seawater, it is important to understand how these factors influence the marine carbonate system. The controls on $CaCO_3$ polymorph formation can partly be explained by the differences in the thermodynamic properties of the polymorphs. The adsorption and incorporation of seawater ions into the forming $CaCO_3$ crystal alters the structure and morphology of the forming polymorphs, ultimately determining which will predominate (Morse et al., 2007). Although calcite is the most stable polymorph at ambient temperature and pressure, modern oceans are predominantly facilitating the precipitation of non-biogenic aragonite in terms of temperature and pressure alone (Albright, 1971) (

Figure 1-8).

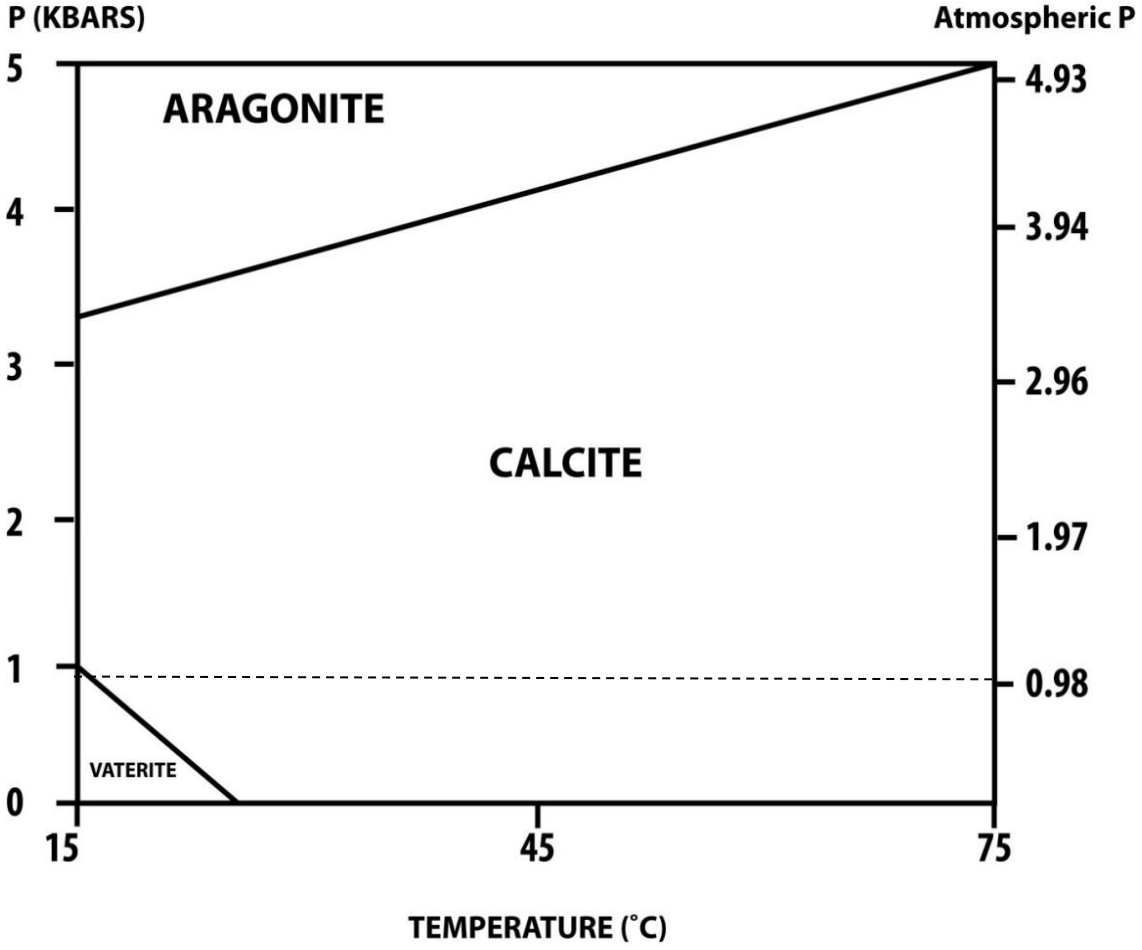

Figure 1-8: Thermodynamic stability fields of $CaCO_3$ polymorphs Adapted from Albright (1971).
The dashed line indicates ambient pressure conditions on the surface of the Earth.

As discussed previously, fluctuations in the Mg:Ca ratio, temperature, pCO_2 and SO_4^{2-} ion concentration have all influence non-biogenic $CaCO_3$ polymorph formation in ways that are relevant to the aragonite-calcite sea theory (Morse et al., 1997; Lee & Morse, 2010; Bots et al., 2011; Balthasar & Cusack, 2015). The question is, how do these factors influence polymorph formation? The following sections consider the mechanisms of influence of each of these four parameters in turn.

1.3.3 The Mechanisms of How Magnesium Influences Polymorph Formation

The Mg:Ca ratio is a driver of aragonite-calcite seas by influencing the polymorphs of $CaCO_3$. This is due to interaction of the ions of Mg^{2+} and Ca^{2+} on the $CaCO_3$-crystal lattice as it forms. On a crystallographic scale, Mg^{2+} can easily incorporate into the calcite crystal lattice via substitution of Ca^{2+}, but this is much rarer with the aragonite crystal lattice (Loste et al., 2003; Kawano et al., 2016). Mg^{2+} absorption is 30 times more likely into calcite than into aragonite (Mucci & Morse, 1985). Mg^{2+} adsorbs to calcite surfaces affecting the surface energy inhibiting the precipitation rate in terms of calcite growth by preventing bonds from forming (Mucci & Morse, 1983; Davis et al., 2000; Morse et al., 2007; Sun et al., 2015). Therefore, higher Mg^{2+} concentrations should result in fewer calcite crystal nucleations, and these should be smaller because growth is inhibited (Sun et al., 2015).

The calcite unit-cell is much larger than that of aragonite because the aragonite lattice is much more densely packed (Morse et al., 2007) (see ***Figure 1-9).*** Calcite lattice structure is layered with the Ca^{2+} being 6-fold co-ordinated with CO_3^- ion layers, which gives a larger unit-cell hexagonal in shape (Markgraf & Reeder, 1985; Morse et al., 2007). However, the smaller aragonite lattice unit-cell occurs because the Ca^{2+} is 9-fold coordinated with CO_3^- allowing denser packing of the unit-cell giving its orthorhombic shape (Morse et al., 2007). It is the morphology of the lattice which allows for substitution of the Ca^{2+} in these $CaCO_3$ polymorphs (***Figure 1-9***). Orthorhombic structures (aragonite) tend to allow ions with radii larger than Ca^{2+} into the lattice structure i.e. Sr^{2+}, whereas hexagonal lattice structures (calcite) are more accommodating to ions with smaller radii such as Mg^{2+} (Morse et al., 2007). It is the differences in the crystal lattice structure which allow Mg^{2+} to influence calcite more so than aragonite (Mucci & More, 1983).

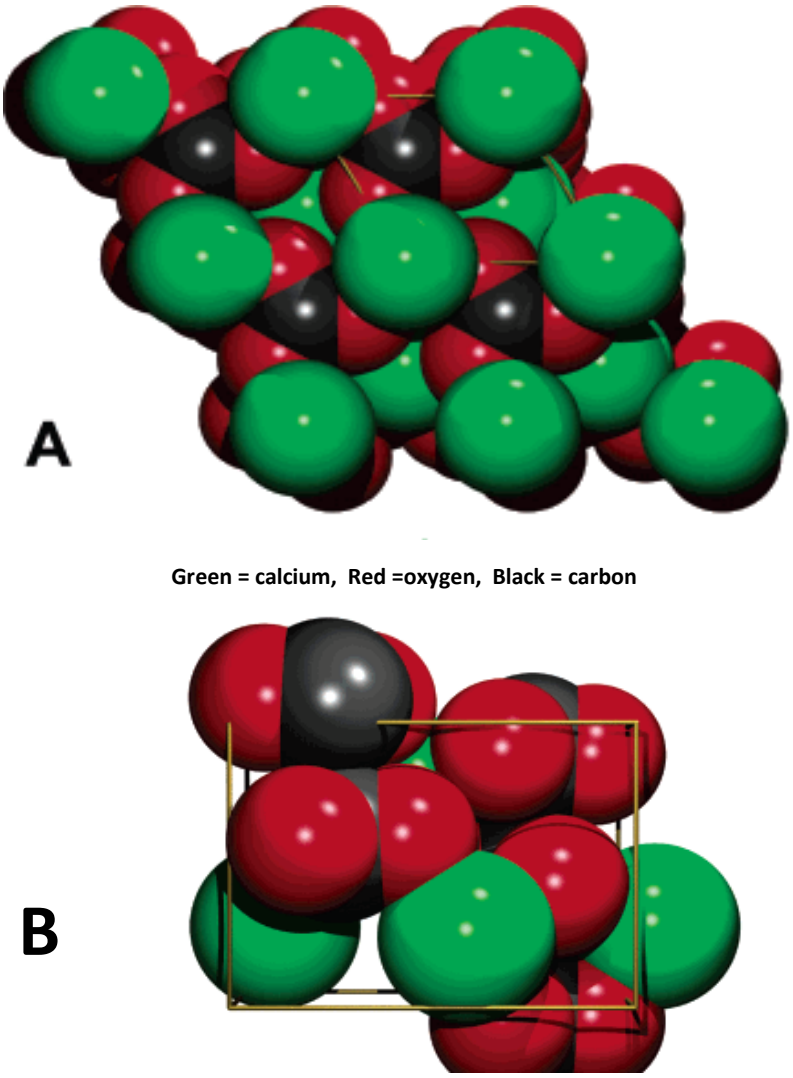

Figure 1-9: The unit-cells of $CaCO_3$ polymorphs (taken from Morse et al., 2007, p 345**). Illustrated are the different arrangements of ions in the $CaCO_3$ polymorph units. (A)- Represents the hexagonal structure of calcite. (B)- Represents the orthorhombic structure of aragonite, the box representing the densely packed atoms.**

Growth of calcite is further influenced by the incorporation of Mg^{2+} because it decreases lattice stability as the ion radius of dehydrated Mg^{2+} is smaller than Ca^{2+} which results in a weaker bond strength between Mg^{2+} and the CO_3^{2-} group (Morse et al., 2007). The presence of Mg^{2+} in the crystal lattice causes disorder and a stress field develops within the lattice (Sun et al., 2015). As a net effect, this increases solubility due to the decreased stability of the bonding (Berner, 1975; Mucci & Morse, 1983). Therefore, higher concentrations of magnesium will not prevent nucleations, but makes them more difficult

to occur by increasing the energy requirements to form attachments. Increased magnesium concentrations will inhibit growth of calcite by increasing its solubility.

Although Mg^{2+} ions have the smallest un-hydrated nucleus, Mg^{2+} ions when hydrated are the largest of all major cations in seawater (Sun et al., 2015). A hydrated Mg^{2+} ion is 400x larger than the dehydrated Mg^{2+} ion (Macguire & Cowan, 2002). This increase in size is due to the attachment of water molecules. While most divalent cations such as Ca^{2+} ions only form a single stable hydration shell, Mg^{2+} forms up to two hydration shells (Jahnen-Dechent & Ketteler, 2012), thus increasing the reactive radius radically compared to Ca^{2+} ions. In crystal growth, ions need to be stripped of their hydration shells before incorporation into the crystal lattice. The energy required for this dehydration is much higher for Mg^{2+} ions than Ca^{2+} ions, thus slowing down crystal growth in the presence of Mg^{2+} (Sun et al., 2015). Hydrated Mg^{2+} ions have slow exchange rates of water molecules from the outer hydration shell (Macguire & Cowan, 2002) and require more energy to form attachments in order to release water molecules to free up bonds. Ultimately, this makes it more difficult for these hydrated ions to form attachment to nucleation surfaces (Sun et al., 2015) due to their large size because the hydrated Mg^{2+} ions prevent the surface processes from forming further bonds (De Yoreo et al., 2009).

1.3.4 The Mechanisms of How Temperature Influences $CaCO_3$ Polymorph Formation

Temperature influences Mg^{2+} incorporation into $CaCO_3$, specifically into calcite. As Mg^{2+} incorporates less into the lattice of aragonite, higher temperatures will inhibit the growth of calcite but not aragonite, resulting in an overall increase in the growth of aragonite (Morse et al., 1997; Balthasar & Cusack, 2015). Although temperature influences $CaCO_3$ mineralogy, it is often overlooked in the literature. Initial investigations into the influence of temperature on the precipitation of calcite overgrowths gave suggestion that increased temperature increased the incorporation of magnesium into the calcite crystal lattice (Katz, 1973; Füchtbauer & Hardie, 1976). Further investigation by Mucci (1987), although presented a correlation for magnesium uptake being increasingly facilitated in calcite at increased temperature, dismissed temperature as a main driver of variation within the mineralogy observed in marine calcite cements.

Specifically, the growth rate of $CaCO_3$ polymorphs has been linked to temperature (Burton & Walter, 1987). When the temperature is increased the growth rate of aragonite increases faster than that of calcite. This is because at higher temperature increases the activity of ions and thus the effect of Mg^{2+}. This link with temperature has allowed the Mg^{2+} content in calcite to be used as a palaeothermometer (Lear et al., 2000; Wasylenki et al., 2005).

1.3.5 The Mechanisms of How pCO_2 Influences $CaCO_3$ Polymorph Formation

Production of calcium carbonate from seawater initiates changes in the aqueous carbonate system due to subsequent dissolution and precipitation pathways (Berger, 1989). The saturation state of seawater is influenced by environmental parameters such as temperature and pCO_2 (Morse et al., 2007; Chierici & Fransson, 2009; Lee & Morse, 2010). It is important to understand this, as previously discussed, pH and alkalinity of seawater have a role in determining the $CaCO_3$ mineralogy forming and can alter saturation state.

To explain how saturation state influences $CaCO_3$ mineralogy in more detail the dissolution and precipitation reactions that occur in carbonate systems can be applied to the three most common $CaCO_3$ polymorph phases (DOE, 1994). $CaCO_3$ mineral solubility is represented as:

$$\mathbf{CaCO_3 \longleftrightarrow Ca^{2+}(aq) + CO_3^{2-}(aq)}$$

Equation 1 (Gattuso & Hansson, 2011)

Equation 1 *:* **Dissolution and precipitation reaction**.

The saturation state (Ω) of the $CaCO_3$ minerals determines whether the mineral has the potential to precipitate or dissolve within the solution. $CaCO_3$ saturation state is a ratio between the observed ions produced to the expected ions produced at equilibrium where Ω=1.

$$\mathbf{\Omega = [Ca^{2+}]_{sw}\,[CO_3^{2-}]_{sw}/K_{sp}}$$

Equation 2 (Gattuso & Hansson, 2011)

Equation 2*:* describes the saturation state of $CaCO_3$

where K_{sp} is the equilibrium constant which defines the solubility of either calcite or aragonite against carbonate i.e.

$$K_{sp} = [Ca^{2+}]_{sat}[CO_3^{2-}]_{sat}$$

Equation 3 (Gattuso & Hansson, 2011)

Equation 3 Equilibrium constant for solubility.

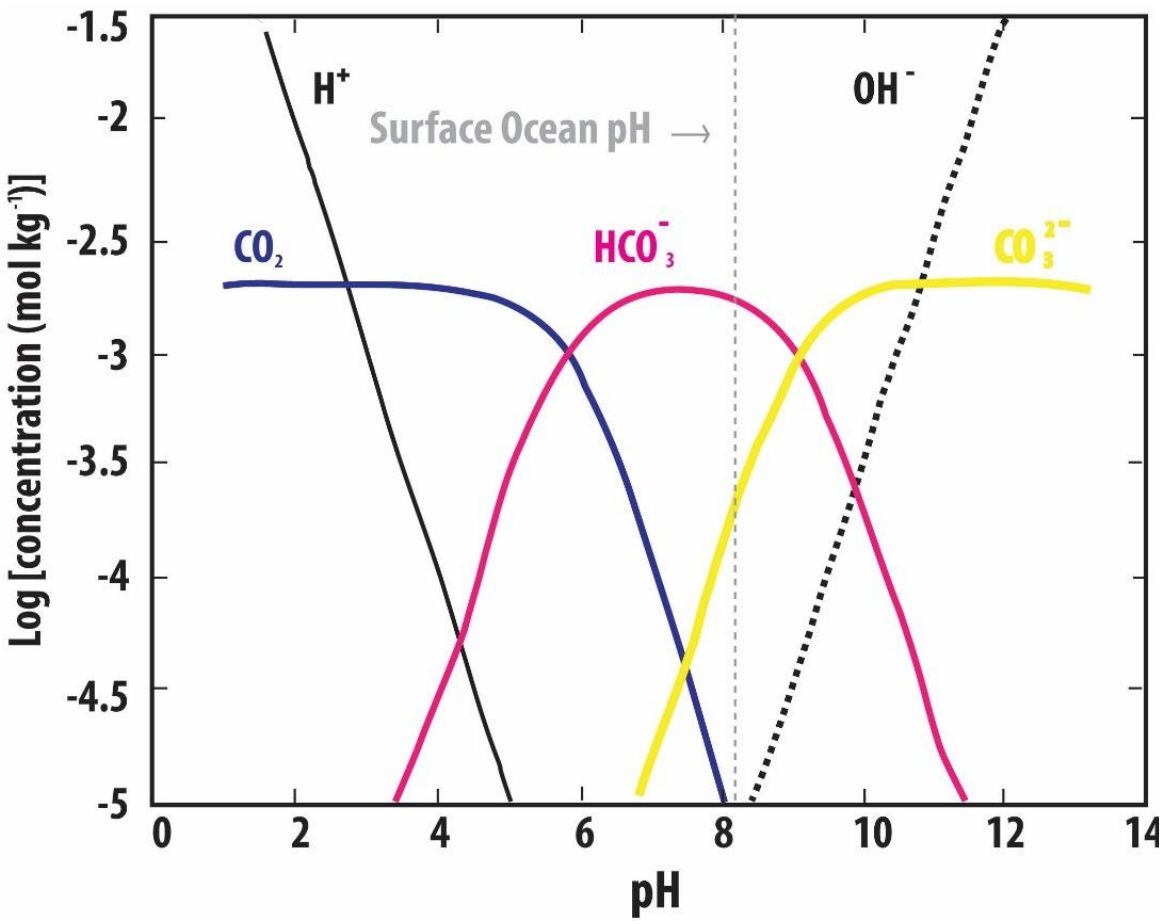

Figure 1-10: The solubility of $CaCO_3$ system.
The pH scale is logarithmic and therefore, a change in pH is represented by a 10-fold change in concentration. By following the pathway to the left indicates the changes in $CaCO_3$ under ocean acidification (OA). The grey dashed line indicates current surface ocean pH. Ocean pH is expected to decrease in forthcoming years due to OA conditions. (Adapted from DOE, 1994).

At Ω>1 seawater is super-saturated which will stimulate inorganic precipitation, at Ω<1 seawater is under-saturated and will advocate inorganic dissolution (Gattusso & Hansson, 2011). Lower temperature will increase the solubility of $CaCO_3$. pCO_2 in turn influences pH and alkalinity and further modifies the carbonate system. Chemical pathways occur when pCO_2 reacts with surficial seawater allowing CO_2 components to combine with

H_2O to form carbonic acid (H_2CO_3). This in turn then breaks up to form bicarbonate (HCO_3) and H^+ ions, and further decreases the saturation state because fewer CO_3 complexes are available **(*Figure 1-10*).**

When pH drops it allows more H^+ ions to become free, in carbonate systems this is through Ca^{2+} combining with HCO_3^- to form $CaCO_3$ and H^+ ions (Pokrovsky, 1998). This is also representative of OA:

i.e. $Ca^{2+} + HCO_3^- \rightarrow CaCO_3 + H^+$

Equation 4 (Pokrovsky, 1998)

Equation 4: showing the chemical pathway to OA

With respect to carbonate minerals, the saturation state of seawater is higher in lower altitudes and shallow marine waters than it is in high altitudes and deep waters (Andersson et al., 2008), therefore suggesting a link between saturation state and OA conditions. Previous work has also linked saturation state to the rate of growth in calcifying marine organisms (Gattuso et al., 1999; Marubini et al., 2003). OA conditions on corals have been investigated due to their influence on biogenic ecosystems and ability to form biodiversity platforms and reefs (Kleypas et al., 1999; Ries et al., 2006; Kleypas et al., 2006; Hoegh-Guldberg et al., 2007; Zhang et al., 2012). OA conditions are of concern to calcifying organism because increases in pCO_2 to oceans ultimately lower the CO_3^{2-} concentration, lowering saturation state favouring with respect to the mineral phases (Mackenzie et al., 1983; Orr et al., 2005; Andersson et al. 2008).

OA is an ever-growing concern for marine life as the increasing uptake of CO_2 in the form of a carbon sink leads to increased acidification and in turn will promote further dissolution of $CaCO_3$. Oceanic pH is decreasing and may come from a number of natural causes such as volcanic activity and from anthropogenic causes (IPCC, 2013). Organisms with $CaCO_3$ consisting of higher Mg^{2+} content are the most soluble (Kuffner et al., 2008) and thus lower saturation states may increase the vulnerability of these organisms to dissolution (Martin et al., 2008). A recent multigenerational study showed that increased temperature and pCO_2 detrimentally impacts on the shell thickness and shape of bivalve shells (Fitzer et al., 2015). Their studies also concluded that the mineralogical organisation under OA conditions was impacted upon causing deformations to crystallography and

resulted in shell softness and loss of control over structures (Fitzer et al., 2014a; 2015a; 2015b). However, their multigenerational study did observe that juvenile shells continued to grow shells in OA conditions if they were from adults already exposed to such scenarios (Fitzer et al., 2014b).

Aragonite-calcite sea conditions previously have been matched with episodes of eustatic-climatic-tectonic change which in turn alter seawater Mg;Ca ratio and pCO_2 and therefore altering the saturation state (Sandberg, 1983; Morse & Mackenzie, 1990; Stanley & Hardie, 1998; Guidry et al., 2007; Andersson et al., 2008). The impact of OA conditions decreasing saturation state and influencing marine calcification have shown similar mineralogical and compositional changes which match with those found within the rock record (Sandberg, 1983; Morse & Mackenzie, 1990; Guidry et al., 2007). Therefore, it has been suggested that if these environmental conditions continue, seawater saturation could facilitate calcite-facilitating sea conditions which in turn could impact greatly on marine calcification (Andersson et al., 2008). Investigation of how these OA conditions do directly impact on the marine calcification therefore may also aid our knowledge into the mechanisms involved in the evolution of biomineralisation within the Phanerozoic.

Alongside the $CaCO_3$ polymorphs of aragonite, calcite and vaterite, various transient phases also exist in biogenic systems (Addadi et al., 2003; Radha et al., 2010). One such phase is the formation of amorphous calcium carbonate (ACC). ACC is one unstable transient phase which has been observed in both non-biogenic and biomineralising environments (Addadi et al., 2003; Radha et al., 2010) and exists as a preparation stage to the formation of crystalline calcite and aragonite (Gong et al., 2012) either by heating or through the presence of water (Radha et al., 2010). ACC has been observed as a precursor in complex $CaCO_3$ calcifying organisms, such as mollusc shells (Weiss et al., 2002). CO_2 can initiate the phase through it reacting with hydrated phases of $CaCO_3$ formation before transforming through a series of processes to dehydrate and form crystalline phases by lowering enthalpy within the $CaCO_3$ system at each stage (Radha et al., 2010).

The ACC phase can be distinguished by the fact it does not diffract x-rays unlike the other crystalline phases (Prenant, 1927 In Addadi et al., 2003). This should be kept in mind when investigating polymorph precipitation parameters because it can precipitate faster than crystalline polymorphs of calcite. Recently ACC has been observed to providing a way

of storing Ca^{2+} and CO_3^{2-} ions until these constituents are needed for rapid mineralisation into the crystalline forms of aragonite and calcite in the calcifying organism (Weiner et al., 2005; Tao et al., 2009). However, the transition between the phases is still not well understood (Fitzer et al., 2014a). The role of ACC is thought to be greater in environments of increased pCO_2 and temperature as the ACC phase is noted to be increasingly present resulting in changes to shell structures and impacting on morbidity of the organisms (Fitzer et al., 2014a; Fitzer et al., 2016). An increase in CO_2 flux to the ocean could increase the occurrence of ACC formation, making calcification less stable and impacting on the stability of the $CaCO_3$ forming from calcifying organisms.

1.3.6 The Mechanisms of How Sulphate Influences $CaCO_3$ Polymorph Formation

SO_4^{2-} influences the polymorph phase formed and its growth (Tang et al., 2012). It does not stop growth of $CaCO_3$ as the SO_4^{2-} ion does not act on the surface processes (Reddy & Nancholas, 1980). The morphology of the calcite crystal lattice distorts when the sulphate concentration increases because SO_4^{2-} ions can substitute for CO_3^{-} ions in calcite, but not in aragonite, and very rarely in vaterite (Kontrec et al., 2004; Bots et al, 2011). This increases the size of the calcite unit-cell due to the shape of the SO_4^{2-} ion (Kontrec et al., 2004) and in turn hinders the growth rate of calcite significantly (Busenberg & Plummer, 1985). The increase in the calcite unit-cell stretches bonds allowing more spaces for Mg^{2+} to fill, and also incorporate Mg^{2+} into the calcite crystal lattice due to their small size (Plummer, 1985), whereas, aragonite and vaterite are affected to a lesser degree (Tang et al., 2012).

The presence of increased concentrations of both SO_4^{2-} and Mg^{2+} together favour the growth of aragonite at the expense of calcite (Burton, 1993). Both ions can incorporate into calcite but do not incorporate easily into aragonite thus altering the thermodynamic properties of the polymorph formed and decreasing calcite precipitation rate (Busenberg & Plummer, 1985). SO_4^{2-} concentrations have shown to fluctuate (Railsback & Anderson, 1987), evidence in evaporite mineralogies deposited throughout the Phanerozoic (Lowenstein et al., 2003). Biomineralisation is viewed as representative of the seawater chemistry at the time of formation, therefore may have influence on the subsequent mineralogy in a similar fashion.

Chemically there are two processes which lead to the formation of the biomineral. The first stage accrues the secreted macromolecules synthesised to form an organic matrix. The second allows transport of required ions to the nucleation site allowing the formation of the biomineral to occur (Allemand et al., 2004). Their formation is influenced by a number of drivers such as Mg:Ca ratio, temperature, SO_4^{2-} and pCO_2 similarly to those formed non-biogenically. The mechanisms behind the incorporation of SO_4^{2-} into $CaCO_3$ from seawater are not greatly understood and often show conflicting results. The influence of Mg^{2+} has been suggested to increase SO_4^{2-} incorporation non-biogenically (Takano, 1985), others have shown SO_4^{2-} influenced a decrease in Mg^{2+} incorporation (Burton & Walter, 1991), whereas Busenberg & Plummer (1985) observed an increase in Mg^{2+} uptake into calcite when SO_4^{2-} was present. However, less is known about SO_4^{2-} incorporation biogenically. Many investigations of SO_4^{2-} in biogenic $CaCO_3$ use sulphur isotope analysis to investigate elemental compositions (Gill et al., 2007; Newton et al., 2011).

1.4 **Research Objectives**

Temperature has long been considered an influencing factor on $CaCO_3$ formation but focus has always been on other drivers such as Mg:Ca ratio (Füchtbauer & Hardie, 1976; 1980; Burton & Walter, 1987; Morse et al., 1997; Balthasar & Cusack, 2015). In order to ensure incorporation of temperature into the traditional aragonite-calcite sea concept, $CaCO_3$ precipitation experiments were carried out to quantify the combined effect of Mg:Ca ratio and temperature at the time of first precipitates under constant addition conditions. This approach strives for a much more realistic environmental framework in which latitudinal variability in $CaCO_3$ precipitation is considered. The influence of Mg:Ca ratio and temperature on $CaCO_3$ formation will be considered in still conditions and then, in order to further mimic natural conditions, shaken conditions will be employed. A second suite of experiments will be considered, using the same technique, with the addition of sulphate in the mother solution, to study how the presence of sulphate influences non-biogenic $CaCO_3$ precipitation alongside the influence of Mg:Ca ratio, temperature and water movement (both still and shaken conditions). By considering $CaCO_3$ with respect to Mg:Ca ratio, temperature, water movement, and sulphate, a more realistic framework will be approached which can be applied to the conditions of the marine realm today.

Finally, acknowledging that the aragonite-calcite seas are the environmental context in which biominerals evolve and grow, the influence of temperature and pCO_2 on magnesium and sulphur incorporation into calcite and aragonite of the modern blue mussel, *Mytilus edulis* will be investigated.

The research objectives for this work were 3 fold:

a. To determine the influence of Mg:Ca ratio and temperature on non-biogenic $CaCO_3$ polymorph formation in still and shaken environments.
b. To determine how sulphate influences non-biogenic $CaCO_3$ growth parameters.
c. To investigate how temperature and pCO_2 influence the incorporation of magnesium and sulphur, in the aragonite and calcite layers of (*Mytilus edulis*) blue mussel shells.

2

Materials and Methodology

This research investigated non-biogenic and biogenic $CaCO_3$ formation in the context of the aragonite-calcite sea hypothesis. The influence of temperature and Mg:Ca ratio on the proportions of non-biogenic aragonite and calcite was investigated through constant addition $CaCO_3$ precipitation experiments. Laboratory experiments in still and shaken conditions were carried out at temperatures of 20°C and 30°C in Mg:Ca ratios of 1, 2 and 3. The shaken laboratory experiments mimicked aspects of natural seawater conditions during ooid growth. Using the same technique, laboratory experiments were repeated in still and shaken conditions at temperatures of 20°C and 30°C in the presence of sulphate in a Mg:Ca ratio 1. Precipitates were quantified for the proportion of aragonite, the number of nucleations and crystal size. To investigate the influence of temperature on Mg and S content of biogenic $CaCO_3$, elemental concentrations were determined in *Mytilus edulis* shells, gifted from a multigenerational study by Fitzer et al. (2014), which had been maintained in a laboratory mesocosm under known environmental conditions of temperature and pCO_2. Energy Dispersive Spectroscopy was employed to determine the elemental concentrations within the shells. The techniques used throughout the thesis are detailed in this chapter along with details of the *M. edulis* sample collections and growth conditions.

2.1 Continuous Addition Experiment Design

To investigate the influence of temperature and Mg:Ca ratio on non-biogenic $CaCO_3$ precipitation, experiments were designed based on previous studies (Tesoriero & Pankow, 1996; Morse et al., 1997; Bots et al., 2011; Balthasar & Cusack, 2015). The aim was to quantify the precipitates of calcite and aragonite in terms of crystal number and size, and

mole percentage to quantify the influence of each parameter of Mg:Ca ratio, temperature and water movement on polymorph formation.

2.1.1 Background and Experimental Scenarios

Previously two separate approaches to $CaCO_3$ precipitation experimentally have been used to study the aragonite-calcite sea hypothesis: continuous addition method and degassing of solution (Füchtbauer & Hardie, 1976; Mucci, 1981; Tesoriero & Pankow, 1996; Morse et al., 1997; Balthasar & Cusack, 2015). Continuous addition methodology uses constant addition of carbonate or bicarbonate ion concentration to slowly increase its concentration, initiating nucleation within the mother solution it is added to. This method allows for a steady pCO_2 level and allows for easy maintenance of pH and estimation of alkalinity. Degassing of solution initiates precipitation as CO_2 escapes from solution, as a result the escape of CO_2 alters the pCO_2, pH and alkalinity throughout the experimental run.

Continuous addition methodology was selected for the purposes of these experiments. This method allows supersaturation of solution to be achieved without a large variation in pCO_2 as observed in degassing experiments whereby pCO_2 is removed initiating supersaturation. Using continuous addition of the bicarbonate volume to dilute the mother solution resulted in the target end concentrations of Mg and Ca to be reached, therefore allowing the study to pin-point the parameters under which precipitates occur. The continuous addition method was adapted from Tesoriero & Pankow (1996) and Bots et al (2011). Tesoriero & Pankow (1996) used continuous addition to study Sr^{2+} uptake in calcite mimicking groundwater $CaCO_3$ precipitation. Tesoriero & Pankow (1996)'s technique used addition of $CaCl_2$ and Na_2CO_3 to a closed container and bubbled it with CO_2, which on degassing this initiated supersaturation through removal of CO_2 resulting in precipitation. This resulted in the solution becoming increasingly supersaturated with respect to calcite (Tesoriero & Pankow, 1996). Bots et al. (2011) adapted this method to add two solutions of $CaCl_2$ with $MgCl_2$ and Na_2CO_3 with Na_2SO_4 of various concentrations together. The $CaCl_2$ and Na_2CO_3 addition initiates precipitation and the $MgCl_2$ and Na_2SO_4 aids to cancel out the dilution of Mg^{2+} and SO_4^{2-}. Glass spheres acted as nucleation surfaces

and allowed analysis the precipitates grown at 21°C. In both methods, an orbital shaker maintained movement of the solutions.

The research presented in this thesis differs from the previous studies of Bots et al. (2011) in that the constant addition design adds sodium bicarbonate ($NaHCO_3$) (220mM) to mother solutions of known Mg:Ca ratio (1, 2 and 3) at either 20°C or 30°C to initiate nucleation of $CaCO_3$ polymorphs. By choosing bicarbonate over carbonate the pH of the solution is held more stable as H^+ ions were already combined to the to CO_3^- ions and CO_2 in solution is not being used in the extra chemistry pathways (See first line of in grey Equation 5 (Arvidson et al., 2006; Bots et al., 2011) of carbonate precipitation and dissolution pathway which is bypassed) influencing pH (Appelo & Postma, 2005) buffering the carbonate chemistry (Arvidson et al., 2006).

$$CO_2 + H_2O \leftrightarrow \ H^+ + HCO_3^-$$

$$CaCO_3 + H^+ \leftrightarrow \ Ca^{2+} + HCO_3^-$$

$$CaCO_3 + CO_2 + H_2O \leftrightarrow \ Ca^{2+} + 2HCO_3^-$$

Equation 5 (Arvidson et al., 2006; Bots et al., 2011)

To minimise the parameters being investigated, simplified continuous addition to solution of only $MgCl_2$, $CaCl_2$ and NaCl was chosen rather than using the approaches of Tesoriero & Pankow (1996) and Bots et al. (2011) whose solution chemistry was more complex. Glass slides were used as a nucleation surface which could be readily removed for analysis of precipitates which differs from Bots et al. (2011)'s glass spheres. The most comparable studies to the present study used degassing of a supersaturated solution of known Mg:Ca ratio to initiate nucleation at a given temperature (Morse et al.,1997; Balthasar & Cusack,2015). The degassing solution's composition changed over time due to removal of more Ca^{2+} than Na^+ ions as the $CaCO_3$ crystals form, altering the Mg:Ca ratio, and influenced Morse et al. (1997)'s precipitates. Using continuous addition, prevents the Mg:Ca ratio from being influenced.

Experiments were carried out at Mg:Ca ratios of 1, 2 and 3 at 20˚C or 30˚C in still conditions, then repeated in shaken conditions to mimic the environment for ooid growth (totalling twelve scenarios). Each experiment was repeated in triplicate. The aim of these

experiments was to investigate how Mg:Ca ratio and temperature influence the non-biogenic $CaCO_3$ polymorphs formed in relation to Phanerozoic seawater composition (natural environment). The chosen Mg:Ca ratios constrain the middle range of Mg:Ca ratios of the Phanerozoic and capture the critical Mg:Ca range of 1.3-2 between which the change between aragonite and calcite dominance is generally assumed (Wilkinson & Algeo, 1989; Hardie, 1996; Lowenstein et al., 2001; Dickson, 2002; 2004; Timofeeff et al., 2008). Using the same constant addition set-up a third suite of experiments were conducted in both still and shaken conditions, in the presence of sulphate at Mg:Ca ratio 1 (totalling 4 scenarios).

Replication of the experiments in the presence of sulphate was chosen because sulphate influences which $CaCO_3$ polymorph will form (Vavouraki et al., 2008; Bots et al., 2011). Previous work suggests that when Mg^{2+} and SO_4^{2-} concentrations are increased they will favour the precipitation of aragonite over calcite (Burton, 1993; Vavouraki et al., 2008). This is because the presence of sulphate influences the polymorph that will form (Bots et al., 2011). Throughout the Phanerozoic the Mg^{2+} and SO_4^{2-} concentrations have co-varied (Horita et al., 2002; Lowenstein, et al., 2003). Sodium sulphate is also the second most common water-soluble mineral in nature after NaCl and therefore is present in natural seawater (Garett, 2011; Vavouraki et al., 2008). Bots et al., (2011) also suggest that the presence of sulphate will lower the Mg:Ca ratio threshold from where calcite dominant seas would form. Sulphate has more influence over calcite than aragonite because the SO_4^{2-} ion can substitute for CO_3^{2-} ions in the calcite crystal lattice (Sun et al., 2015).

Comparing the calcite dominance in the sulphate-free scenarios to scenarios in the presence of sulphate were done with an aim to give a better representation of calcite seas. Calcite dominance was chosen, as suggested by Bots et al., (2011), as this provides a more realistic measure than the measure of pure calcite based on the evidence that each sea period rarely exclusively formed of calcite or aragonite (Zhuruvlev & Wood, 2009). Sulphate experiments were ran at Mg:Ca ratio of 1 only, firstly, to allow comparison to the sulphate-free experiments and secondly, because in the sulphate-free experiments most experiments at Mg:Ca ratio 2 or 3 were already dominated by aragonite formation and therefore, the addition of sulphate would not help or constrain the conditions at which dominance shifts between calcite and aragonite, or give a calcite dominance as suggested by Bots et al., (2011) to represent calcite sea conditions. A Mg:Ca ratio lower than 1 was

not selected because in the sulphate-free experiments at Mg:Ca ratio 1, it was difficult to grow quantifiable crystal precipitates because in many experiment runs an instantaneous precipitation of non-specific, poorly formed crystals occurred and this was increasingly evident in higher temperatures and shaken conditions. Mg:Ca ratio 1 is also in the lower end of the Phanerozoic range of Mg:Ca ratio (Horita et al., 2002).

2.1.2 Continuous Addition Set-Up

$CaCO_3$ precipitation was induced by adding $NaHCO_3$ (Sigma-Aldrich BioXtra 99.5-100.5%) to 100ml of mother solution containing $CaCl_2.6H_20$ (Sigma-Aldrich), $MgCl_2.6H_20$ (Acros organics 99+% ACS reagent), and NaCl (Fisher Scientific, AnalR) for sulphate-free solutions, and addition of Na_2SO_4 (Fisher Scientific) for experiments that included sulphate.

For each experiment, 12 cleaned glass slides were placed in a beaker with 100ml of mother solution. Mother solution of artificial seawater was prepared to ensure reproducible solution chemistry, and minimises biological influence (Kester et al., 1967). AnalR compounds were used throughout, dissolved in MilliQ water to minimise contaminants.

The pump set-up (***Figure 2-1***) consisted of a 10ml syringe attached to rubber tubing primed with 220mM $NaHCO_3$ solution ready to be added to 100ml of mother solution (Ca^{2+} end target concentration 10.2mM/8hrs and Mg^{2+} added accordingly to required Mg:Ca ratio) via a PICO PLUS II ELITE syringe driver (1.25ml/hr, end target concentration 20mM after 8hours) in still and shaken conditions (by orbital shaker) for a total of 6 hours. The top of the beaker was covered with parafilm to prevent contamination by dust particles and evaporation. The rubber tubing was inserted through the centre of the parafilm to administer $NaHCO_3$ solution just above the level of the 100ml of mother solution to prevent precipitation occurring on or within the tubing tip. Still experiments were run separately to the shaken experiments to minimise error from vibrations. The still solution was placed on top shelve of incubator to minimise vibrations from the incubator motor, orbital shaker in base of incubator for shaken conditions due to height constraints. Salinity was adjusted to *S*=35 in mother solution and monitored throughout experiment. pH adjustments made in each experiment maintained solution pH at ~8.2. Crystals precipitated on cleaned glass slides of 1mm thickness on the bottom of the beaker within 100ml of mother solution.

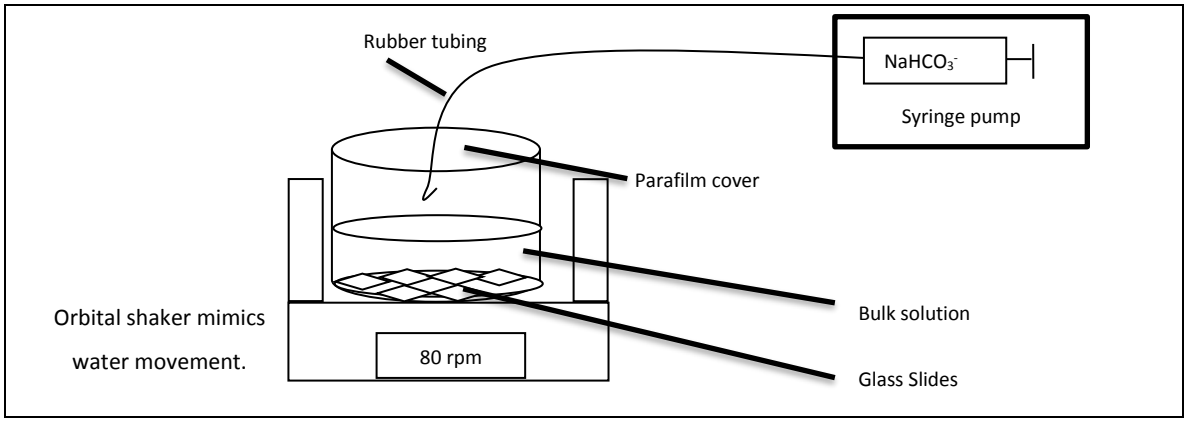

Figure 2-1: Schematic of continuous addition experiment set-up
Set-up used for the method to precipitate $CaCO_3$ crystals and although their removal for analysis, adapted from the method of Bots et al. (2011).

During each experiment, a glass slide was removed every 30 minutes, rinsed with deionised water and oven dried at 40˚C before storing in Sterilin tray wells for subsequent digital imaging. The experimental setup was the same for the experiments mimicking water movement, except that the beaker with 100ml of mother solution was shaken at 80 rpm using a mini-orbital shaker within the incubator.

To ensure that all experiments were conducted under the same constraints, all experiments were run in the same incubator at 20°C or 30°C, and mother solutions were acclimatised in the incubator overnight before each experiment. For still scenarios, all possible movement was minimised (i.e. incubator door opening, movement of beaker to remove samples). The shaken scenarios were run separately to the still experiments so that vibrations from the orbital shaker did not influence results. All experiments were carried out in triplicate.

2.1.2.1 **Mother solutions**

The mother solution was made to a higher concentration than required based on calculation that each 100ml of solution removed is diluted by addition of 10ml of $NaHCO_3$ solution over 8 hours. All experiment concentrations were based on an end-target concentration following this dilution over 8 hours. All mother solutions have an end-target concentration of 10.2mM of Ca^{2+}, which is the average concentration in modern seawater (DOE, 1994). The Mg:Ca ratios of 1, 2 and 3 were reached by adding the

equivalent amount of $MgCl_2.6H_2O$ to the mother solution for sulphate-free experiments. Experiments in the presence of sulphate were carried out at Mg:Ca ratio 1 using the same technique except they had 5mM $NaSO_4$ (end concentration) added to the mother solution. Mother solutions were adjusted with NaCl to a salinity of ***S*** =35 (checked by refractometer) and the pH of the solution was corrected to ~8.2 (representative of pre-industrial seawater) using 0.05M of NaOH. 100ml of the 1000ml mother solution was used for each experiment **(**

Table 2-1***; Table 2-2***). Experiments were stopped after 6 hours because nucleation of the first precipitates had occurred by this point.

Mg/Ca ratio		Mother Solution Composition						Addition Solution	
		$CaCl_2.6H_20$		$MgCl_2.6H_20$		NaCl		$NaHCO_3$	
Target Mg:Ca ratio	Actual Mg/Ca Ratio	Initial concentration (mM)	End Target Final Concentration (mM)	Initial concentration (mM)	End target Final concentration (mM)	Initial Salinity	End Salinity	Initial concentration (mM)	End target Final concentration (mM)
1	0.998-1.002	11.21 – 11.23	10.41-10.43	11.22-11.23	10.44-10.45	35	33-35	221.15	15.34
2	1.99-2.00	11.20-11.24	10.44-10.46	22.43-22.60	20.87-20.89	35	33-35	221.15	15.34
3	2.99-3.00	11.20- 11.22	10.42-10.44	33.60-33.67	31.06-31.32	35	33-35	221.15	15.34

Table 2-1: Mother solution composition for sulphate-free experiments.
Indicated are the actual Mg:Ca ratio, the concentration of the mother solution components and their diluted end target concentration by the end of the 6 hour experiments. The same has been indicated for the addition solution.

Mg/Ca ratio		Mother Solution Composition								Addition Solution	
		Na_2SO_4		$CaCl_2.6H_20$		$MgCl_2.6H_20$		NaCl		$NaHCO_3$	
Aim Mg:Ca ratio	Actual Mg/Ca Ratio	Initial Conc. (mM)	End target Final Conc. (mM)	Initial Conc. (mM)	End target Final Conc. (mM)	Initial Conc. (mM)	End target Final Conc. (mM)	Initial Salinity	End Salinity	Initial Conc. (mM)	End target Final Conc. (mM)
1	0.99-1.00	5.55-5.58	5.16-5.16	11.21 - 11.32	10.42-10.53	11.23-11.25	10.45-10.47	35	33-34	220.14	15.36

Table 2-2: Mother solution composition for experiments with sulphate.
Mother solutions were made in the same way as the sulphate-free solutions but with an added end target 5mM sulphate concentration. Indicated are the actual Mg:Ca ratio, the concentration of mother solution components and their diluted end target concentration by the end of the 6 hour experiments. The same has been indicated for the addition solution.

2.1.3 Protocol for Cleaning Glassware

Crystal precipitates were nucleated on glass sheets of 1mm thickness placed on the bottom of the reaction beaker. These were cut into 13mm square slides using a diamond saw prior to the experiment. The thickness of this glass was selected to prevent slides from moving over each other in shaking conditions.

Prior to experiments slides were cleaned by soaking in a solution of 10% Decon 90 for 48 hours then rinsed in deionised water to remove organic contaminants. Slides were then soaked in 15% HCl for a further 48 hours to ensure residues from Decon 90 solution were removed, rinsed in deionised water and then oven dried at 40 degrees (keeping same surface upwards at all times). All glassware, test tubes and petri dishes were soaked in 10% HCl overnight and thoroughly rinsed with deionised water before use.

2.1.4 Constant Parameters

2.1.4.1 Temperature and Salinity

Temperature was controlled in the laboratory using an incubator. The temperature of artificial seawater was also measured using a handheld temperature probe inbuilt into ISFET pH meter (HACH-LANGE H135 ISFET mini LAB^{TM}, USA). Both the temperature of the incubator and the artificial seawater solution were recorded every 15 minutes.

Salinity was recorded via a portable, handheld refractometer (accurate to +/- 0.10% (1ppt) at 10-30°C) (model RHS – 10/ATC). Salinity was recorded at the start and end of each experiment and also pre- and post-total alkalinity titration.

2.1.4.2 pH

Solution pH was recorded using an ISFET pH meter (HACH-LANGE H135 ISFET mini LAB^{TM}, USA), calibrated using control solutions of pH 4, 7 and 10 on the National Bureau of Standards Scale. The hand-held probe enabled accurate measurement of very small volumes of liquid.

The addition of $NaHCO_3$ held pH more stable than the addition of CO_3^{2-} would have, but the pH still had to be monitored throughout the experiments due to the changing chemistry as nucleation occurred. The pH of solution during each experiment was monitored every 15 minutes and adjusted to ~pH 8.2 with 0.1% & 0.01 % HNO_3 to lower or 0.5M or 0.05M NaOH to raise pH, as in ***(Table 2-3)*** All alterations were based on pH readings acquired in the first experiment ran using a HACH H135 minilab pH and temperature probe with the aim to keep solution pH ~8.2. Alterations were recorded in number of drops of either 0.5M or 0.05M NaOH or 0.1% or 0.01% nitric acid from a 1 ml disposable pipette. All subsequent experiments had pH recorded but use this protocol regardless of pH readings to ensure chemistry pathways were of identical set-up.

Time (min)	Drops of NaOH/HNO_3 added
0 (before bulk solution of 100ml removed from the mother solution)	5 x[0.5M] NaOH, 5x [0.1%] HNO_3, 12 x [0.05M] NaOH 3x [0.01%] HNO_3
15	-
30	2x [0.01%] HNO_3
45	2x [0.1%] HNO_3
60	3x[0.05M] NaOH
75	1x [0.1%] HNO_3
90	-
105	2x [0.5M] NaOH
120	3x [0.01%] HNO_3
150	3x [0.05M] NaOH
195	3x [0.01%] HNO_3
240	2x [0.01%] HNO_3
255	2x [0.01%] HNO_3
300	1x [0.1%] HNO_3
315	1x [0.05M] NaOH
330	1x [0.05M] NaOH

Table 2-3: pH routine used in each constant addition experiment.

2.1.4.3 **Monitoring Total Alkalinity (TA)**

Total alkalinity (TA) is defined as the capacity of a solution to neutralize an acid (i.e. H^+) (Dickson, 1981), and it is measured in the laboratory via a titrimetric method. The species which can influence total alkalinity are the bicarbonate ion, carbonate ion and hydroxide ion (Manahan, 2004). TA is a measurement of the pH buffering capacity of seawater (Manahan, 2004; Li et al., 2013) and is expressed by the pH reaching a specific endpoint (pH 3.9) at which bicarbonate and carbonate species have been converted to CO_2 by addition of acid.

The TA of seawater is important to monitor because it influences polymorph precipitation (Morse & He, 1993; Arvidson, et al., 2006). TA is a crucial measurement in

the analytical assessment of CO_2 cycling in the ocean, because in the natural environment, TA is held almost constant, even when influxes of CO_2 increase the pCO_2 in seawater (Ilyina et al., 2013) because it aids in maintaining the balance of pH. Four measurements can be made on the CO_2 system (alkalinity, total inorganic carbon, CO_2 fugacity and pH). In order to measure TA, two of these four CO_2 system measurements are required (Yao & Byrne, 1998; Li et al., 2013). Modelling data suggest that a total alkalinity of 10mM is a realistic maximum for Phanerozoic seawater (Arvidson et al., 2006), and all experiments were designed to reach an endpoint of ~10mM after 8 hours of addition of $NaHCO_3$. Lee & Morse (2010) also noted that the $CaCO_3$ polymorph precipitate at a given Mg:Ca ratio is dependent on the alkalinity at the time of formation, therefore a consistent TA is required in each experiment for comparability.

The methodology chosen to measure TA in this study was a 2-step method proposed by Dickson (1981) and Yao & Byrne (1998) which is the current method of choice in the literature as it is accurate, precise and fast with minimal cost due to the number of measurements required.

The titration method of Dickson (1981) used potentiometric titration to project TA using non-linear least squares. The facilities to carry out the titration method of Dickson (1981) requires a high-precision titrator, which was unavailable at the time of this study. To account for this, initial titration of the artificial seawater solution was complimented by the modified spectrophotometric of Yao & Byrne (1998). This approach uses spectrophotometer measurements of the acidified seawater sample after the initial titration to allow rapid and accurate TA measurements at beginning and end of experiments.

This approach increases analytical precision and accuracy of the TA calculation and can be achieved within 10-12 minutes (Yao & Byrne, 1998). The closed cell titration vessel allows for volumes as small as 10ml of artificial seawater solution. TA was measured at the beginning and end of two experiments per scenario and measurements were recorded for all Mg:Ca ratios and temperatures (except Mg:Ca ratio 3 at 20 °C where only one experiment could be measured per scenario), at time = 0 following the initial pH adjustment, and at time = 360 minutes. Average TA for each analysis point was gained by taking an

average of at least 2 separate solution experiments. This data was used to calculate the predicted TA at the time of the first crystal precipitations that were large enough to be quantified.

2.1.4.3.1 Titration Procedure for TA (Step 1)

For each titration at the start of an experiment, 10 ml of the mother solution was removed, placed in a 30ml beaker with a magnetic flea and placed within the *Metrohm 848 Titrino Plus Automated Titrator* using the method described by Dickson (1981)**.** The same was repeated at the end of experiment using the final experiment solution. The automated titrator purges the solution of CO_2 **(see *Figure 2-2*)**.

Experiment temperatures set by the incubator and water bath for heating buffer solutions at 20°C or 30°C were corrected in the *Metrohm 848 Titrino Plus Automated Titrator* settings before titration commenced, and then in the calculation software to adapt to required temperature as the standard inbuilt program is set to 25 °C.

The pH probe and was calibrated using Metrohm buffers, and as both are temperature sensitive, the buffers of pH 4, 7, and 9, were required to be heated to within $\pm$0.05°C of the sample temperature (either 20°C or 30°C) via a water bath. The pH probe tip and acid burette administration tip were placed into the sample vessel, ensuring to keep both tips at the same depth in the sample (as this influences accuracy) and the vessel was closed. Use of a closed cell titration vessel allows the assumption that DIC is relatively constant throughout the titration (Riebesell et al., 2010).

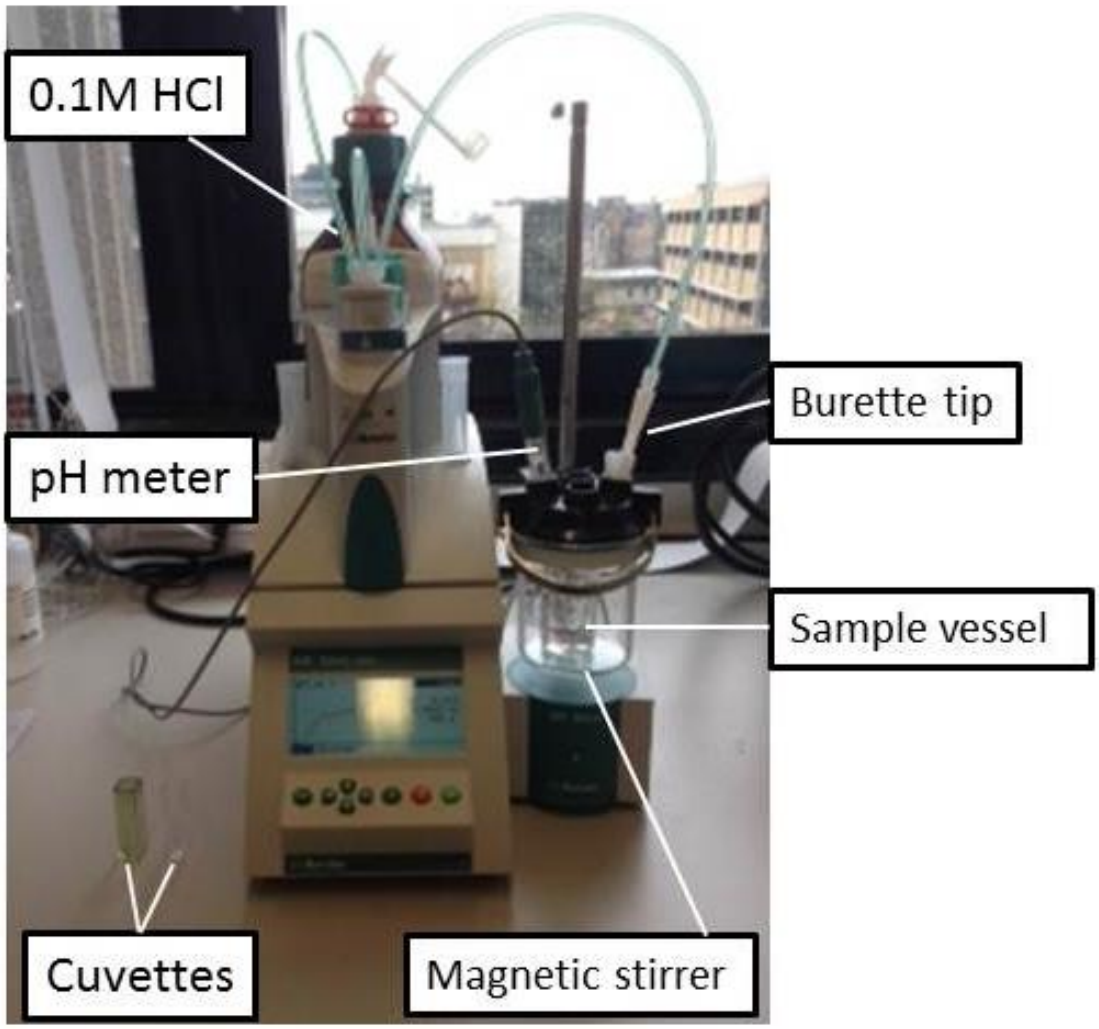

Figure 2-2: Image of titration equipment used for TA analysis.
***Metrohm 848 Titrino Plus Automated Titrator*.**

The sample was automatically titrated in a single influx using HCl 0.1M, until the pH reaches ~3.9 whilst solution is stirred on magnetic stirrer plate. The final solution pH and the volume of acid used to titrate to pH ~3.9 were then recorded. The acidified sample was then removed for spectrophotometric analysis. Salinity of the sample was measured via a portable refractometer pre- and post-titration with aim of keeping close to S=35.

This titration method locates the end point pH for TA by measuring the amount of acid the seawater sample can absorb, this can then be interpreted to define the seawater total alkalinity as the amount of protons than can be accepted by the proton acceptors) to remove CO_2 from the sample (Dickson, 1981), ie TA = $[HCO_3^-]$ +2 $[CO_3^{2-}]$, the '+2' is due to

the fact 2 protons have to be accepted by CO_3^{2-} in order to convert to CO_2 (Wolf-Gladrow et al., 2007).

Data collected from the automated titrator was used to calculate TA using Gran functions (a graphical method using the intersection of linear least square regression lines of acid and base concentrations to estimate the titration end-point (Hansson & Jagner, 1973; Dickson et al., 2007).

2.1.4.3.2 Modified Spectrophotometer Procedure for TA (Step 2)

A *Lange DR 5000™ UV-Vis* laboratory bench-top spectrophotometer (HACH, USA) is used to record the absorbance of the acidified sample. Using the spectrophotometer allows precision to $\pm$ 0.0004 pH units and H^+ concentrations accurate to 1% and allows the dependency of temperature and salinity of the pH measurement to be considered (Yao & Byrne, 1998).

Absorbance at ʎ444 and ʎ616 nm wavelength was measured using a *Lange DR 5000™ UV-Vis* laboratory bench-top spectrophotometer (HACH, USA) and the absorbance value was included in the TA calculation (discussed in following section 2.1.4.3.3.) Using a ratio of the two absorbances allows the pH of solution to be calculated for the given temperature (**pH_T**). The spectrophotometer is calibrated using a sample of natural seawater placed in a clear plastic cuvette. The acidified sample from the titration procedure is poured into a SMART pH cuvette with pre-stained bromocreosol green (Bromocresol green (BCG) SMART cuvette, Ocean Optics) (see ***Figure 2-2)***. BCG acts as an indicator as it has a dissociation constant that can be used to determine the salinity dependence (Breland & Byrne, 1993; Yao & Byrne, 1998). BCG absorbance is also temperature sensitive and therefore aids calculation of **pH_T**.

2.1.4.3.3 Calculating results for TA

Measurements gained from the two-step TA titration procedure were input into a Microsoft Excel spreadsheet based on the least squares calculations and procedures obtained from Dickson (1981) and Yao & Byrne (1998), allowing calculation of TA based on the following 3 equations:

The total alkalinity ($\boldsymbol{A_T}$) of the acidified sample following titration to remove CO_2 is given by the equation below (**Equation** 6; Yao & Byrne, 1998).

$$\boldsymbol{A_T M_{SW} = N_A M_A - [H^+]_{ASW} M_{ASW} - [HI]_{total} \Delta (HI) M_{ASW}}$$

Equation 6 (Breland & Byrne, 1993; Yao & Byrne, 1998)

$\boldsymbol{A_T}$ $\mathbf{M_{SW}}$ is the total alkalinity ($\boldsymbol{A_T}$) in mol kg^{-1} of the seawater sample (Kg) ($\mathbf{M_{SW}}$). This is calculated by taking the acid concentration of known mass $\mathbf{N_A M_A}$ (the mass of acid used in the titration) and subtracting the excess hydrogen concentration $\mathbf{[H^+]_{ASW}}$ (measured by spectrophotometry) and the mass of the acidified seawater derived from $\mathbf{M_{ASW}}$. The equation in grey was not required because no indicator solution is added to the acidified seawater as SMART cuvettes were used instead (Yao & Byrne, 1998). This part of the equation only needs to be considered if using indicator because this would give the full concentration within the indicator of both the pronated and un-protonated forms of seawater (mol kg^{-1}), as well as **the Δ (HI)** (measured by spectrophotometry) which accounts for the $\mathbf{H^+}$ (moles) change either lost or gained by the indicator in the acidified sample relative to the bulk solution. This part of the equation remains as $\mathbf{[H^+]_{ASW}}$ and **Δ (HI)** both measured by spectroscopy were accounted for using the following equations to correct for temperature and salinity: **Equation 7, Equation 8 & Equation 9**.

$$\mathbf{[H^+]_{ASW} = 10^{-pH_T}}$$

Equation 7 (Breland & Byrne, 1993; Yao & Byrne, 1998)

The total excess acid concentration $\mathbf{[H^+]_{ASW}}$ is calculated from the solution $\mathbf{pH_T}$ **(Equation 7)**. Seawater pH has a dependency on temperature and salinity of seawater ($\mathbf{pH_T}$) which is accounted for through use of BCG indicator within the SMART cuvette. $\mathbf{pH_T}$ is thus calculated as follows where $\boldsymbol{s}$ is the final salinity of the solution:

$$\mathbf{pH_T = 4.2699 + 0.002578\,(35-}\boldsymbol{s}\mathbf{) + \log\left((R(25) - 0.00131)/(2.3148 - 0.1299\,R\,(25))\right) - \log(1 - 0.001005\,}\boldsymbol{s}\mathbf{)}$$

Equation 8 (Breland & Byrne, 1993)

where $29 \leq \boldsymbol{s} \geq 37$ and temperature $13°C \leq t \geq 32°C$. The BCG dissociation constant in **Equation 8** is given by (-log K(BCG)= 4.2699 at ***s***=35 and ***t***=25°C and originally was measured on the molar scale (Yao & Byrne, 1998). **R** is the indicator absorbance ratio, with

$$\mathbf{R(25) = R(}t\mathbf{)\ \{1 + 0.00907\ (25 - }t\mathbf{)\}}$$

Equation 9 (Breland & Byrne, 1993)

where ***t*** is the temperature of the solution in which **R(*t*)** is measured and the final term (0.00907 (25-t)) allows addition of the total excess acid concentration $\mathbf{[H^+]_{ASW}}$ in moles per kg of solution, i.e. $\mathbf{pH_T = -log[H^+]_{ASW}}$. The absorbance ratio calculated at 25 °C in **Equation 8** also requires the temperature ***t*** to be set due to the temperature dependency of the BCG absorbance in **Equation 9** with $\mathbf{R(t) = A_{616}/A_{444}}$ (the absorbance levels measured within the spectrophotometer). Using **Equation 8** and **Equation 9,** allows **Equation 6** to be extended into lower temperature determination by calculating the $\mathbf{[H^+]_{ASW}}$, and therefore to calculate TA (Breland & Byrne, 1993; Yao & Byrne, 1998).

2.2 Mineral identification and documentation

Analysis of the precipitates was done via Raman Spectroscopy and Scanning Electron Microscopy which allows the mineralogy of the precipitates to be documented and then quantified via digital analysis using Corel Paint X6 and ImageJ. All samples were imaged at the University of Glasgow Imaging Spectroscopy and Analysis Centre (ISSAC).

The precipitates nucleated on removable glass slides and were analysed for their mineralogy by Raman Spectroscopy using a *Renishaw In-Via Raman Microscope*, which required no sample preparation. Next, to match the mineralogy to crystal morphology, samples were gold-coated and stuck to SEM metal stubs using carbon tape. Crystals were then imaged using a *Zeiss Sigma variable-pressure analytical Scanning Electron Microscope* (SEM). Three minerals were evident: aragonite, calcite ***(Figure 2-5***) and (very rarely) vaterite**.** SEM images were collected and used to quantify polymorph proportions using Corel Paint X6 and ImageJ software packages.

2.2.1 Raman Spectroscopy

For Raman Spectroscopy, the instrument consists of an optical microscope that can document the crystal morphology and Raman Spectroscopy which can fingerprint the mineralogy of the sample and identify the polymorphs (Renishaw, 2016). A laser vibrates the bonds which scatters light at a different frequency from the laser beam. The difference between the frequencies is recorded as a Raman Spectrum which presents the data as an 'intensity-vs-wavelength' shift (Settle, 1997; Bumbrah & Sharma, 2016). It is the vibration of the bonding which is unique to Raman Spectroscopy (Hope et al., 2001). This can be used to identify the specific mineralogical phase of the crystal **(Figure 2-3**).

The Raman shift occurs as the laser beam passes through the crystal lattice vibrating the bonds between the atoms releasing, or scattering, light energy. Thus, it measures the frequency of a molecular bond (B&W Tek, 2016) which is unique for different minerals. Two types of scattered light occur on hitting a sample with the laser beam, elastic scatter of light (where the scattering leaves the sample in the same energy state it arrived in) or inelastic scatter of photons (where the scattering leaves the sample in a different quantum state from which it arrived). The transferred energy released from photons to the molecule hit, correlates to the vibration within that molecule (Verkaaik et al., 2015).

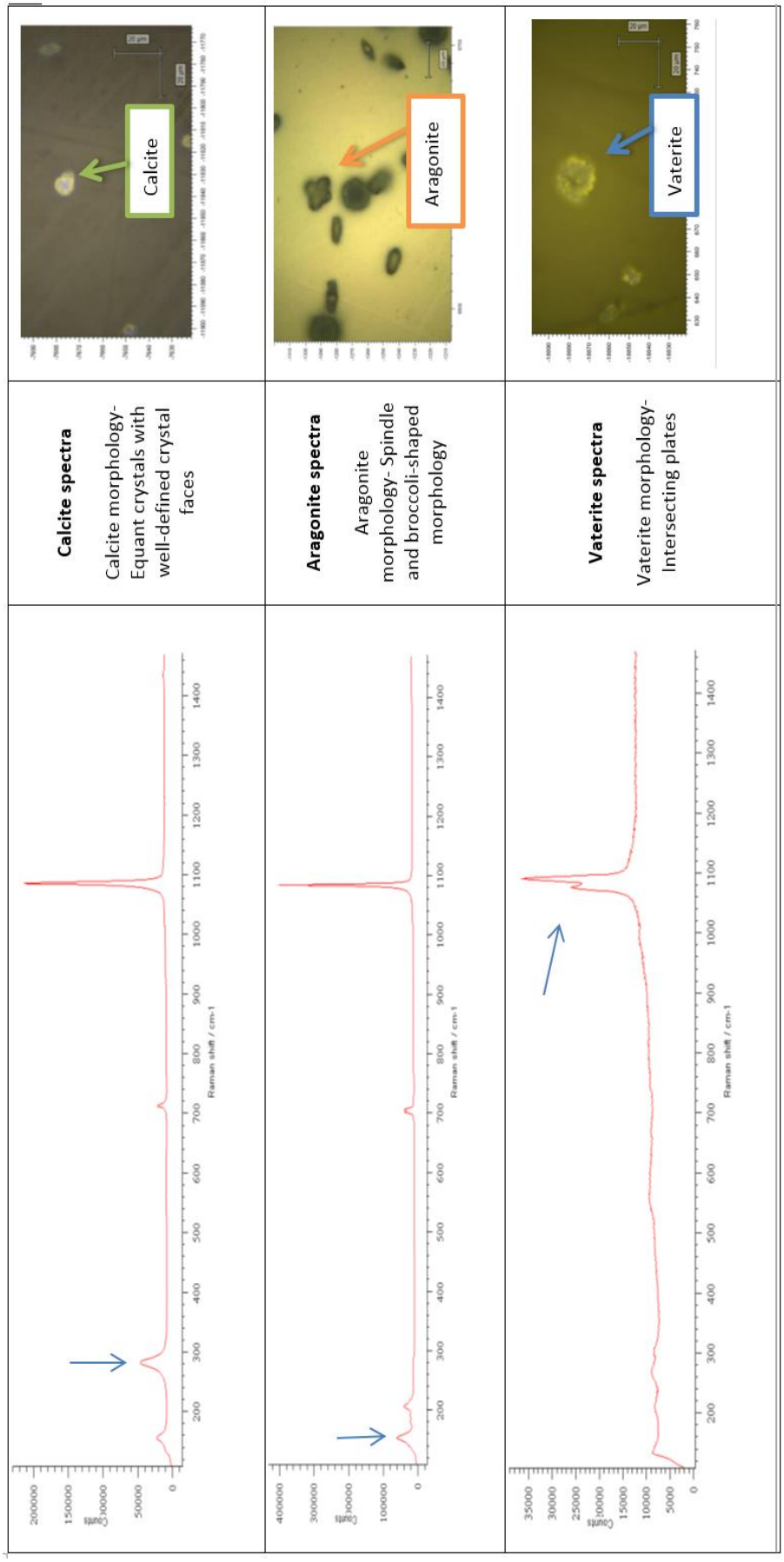

Figure 2-3 Examples of Raman Spectra of $CaCO_3$ polymorphs.
Spectra obtained on crystal mineralogy (left) indicate the different mineralogies of the three $CaCO_3$ polymorphs. Raman analysis allows correlation of types of mineralogy with morphology. The images of each polymorph captured on Raman spectroscopy (right) show vague morphology which can be matched to clearer morphology imaging by use of SEM. Characteristic peaks that characterise the different polymorphs are indicated with blue arrows.

The spectra graphs obtained (see **Figure 2-3**) show the number of wavelengths per $cm^{-1}t$ (x-axis) relative to the laser, and were plotted against the intensity of the scattered light (y-axis) (Renishaw, 2016). Change in band width indicates how strong the bonding is and therefore the crystallinity. Narrower peaks indicate a more crystalline subject **(***Figure 2-4***)**. Lighter atoms with strong bonds will have a high Raman shift and heavier atoms with weak bonds will have a lower Raman shift.

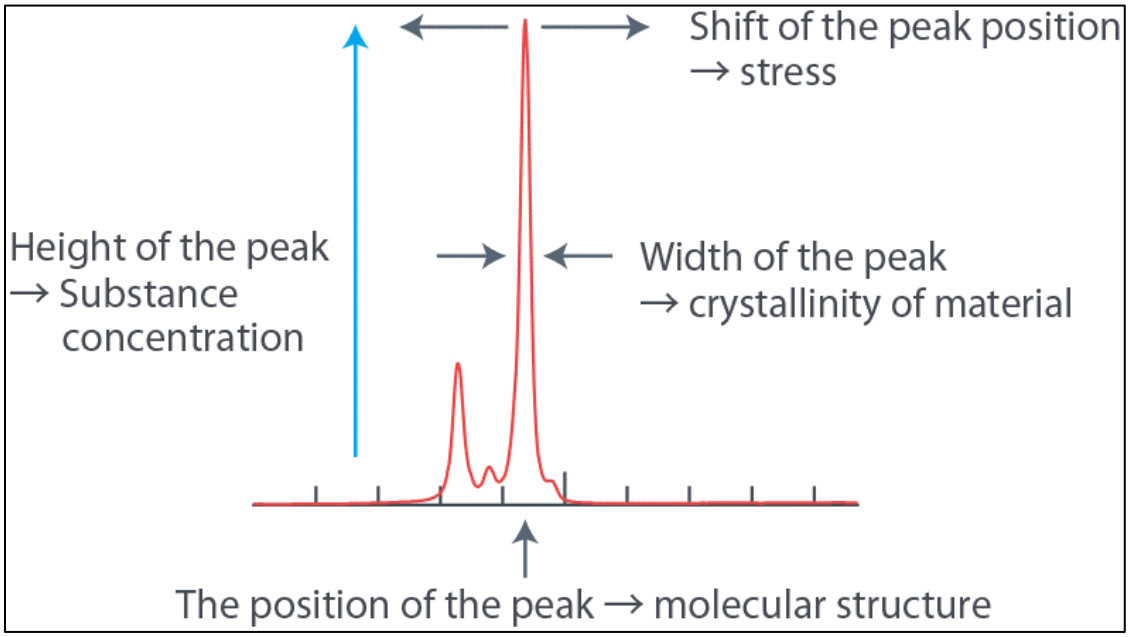

Figure 2-4: Raman Spectroscopy peak (from Nanophoton, 2016). Indicated are the relevant aspects of a Raman spectra peak which define the sample being analysed.

All samples were analysed using a 514nm wavelength laser for 3 seconds with 10 accumulations to generate the Raman shift profile used to identify the polymorphs (Hope et al., 2001).

2.2.2 Scanning Electron Microscopy to quantify $CaCO_3$ polymorphs

Following Raman analyses, the glass slides with $CaCO_3$ precipitates were placed on a SEM sample holder plate, and gold coated for 80 seconds using an Agar Sputter Coater Model 109. Having identified polymorph habit using Raman Spectroscopy (**Figure 2-3**) secondary electron (SE) imaging using a *Carl Zeiss Sigma Variable Pressure Analytical*

Scanning Electron Microscope was used to document the morphology i.e. mineralogy) for each experimental scenario (***Figure 2-5***).

For each experiment, the first-formed $CaCO_3$ precipitates identifiable at 500x magnification, a series of non-overlapping secondary electron SE images were taken along a transect, using an aperture of 30µm, an accelerating voltage of 20kV, and a resolution of 2048x1536. A total of 25-30 non-overlapping images were taken per slide.

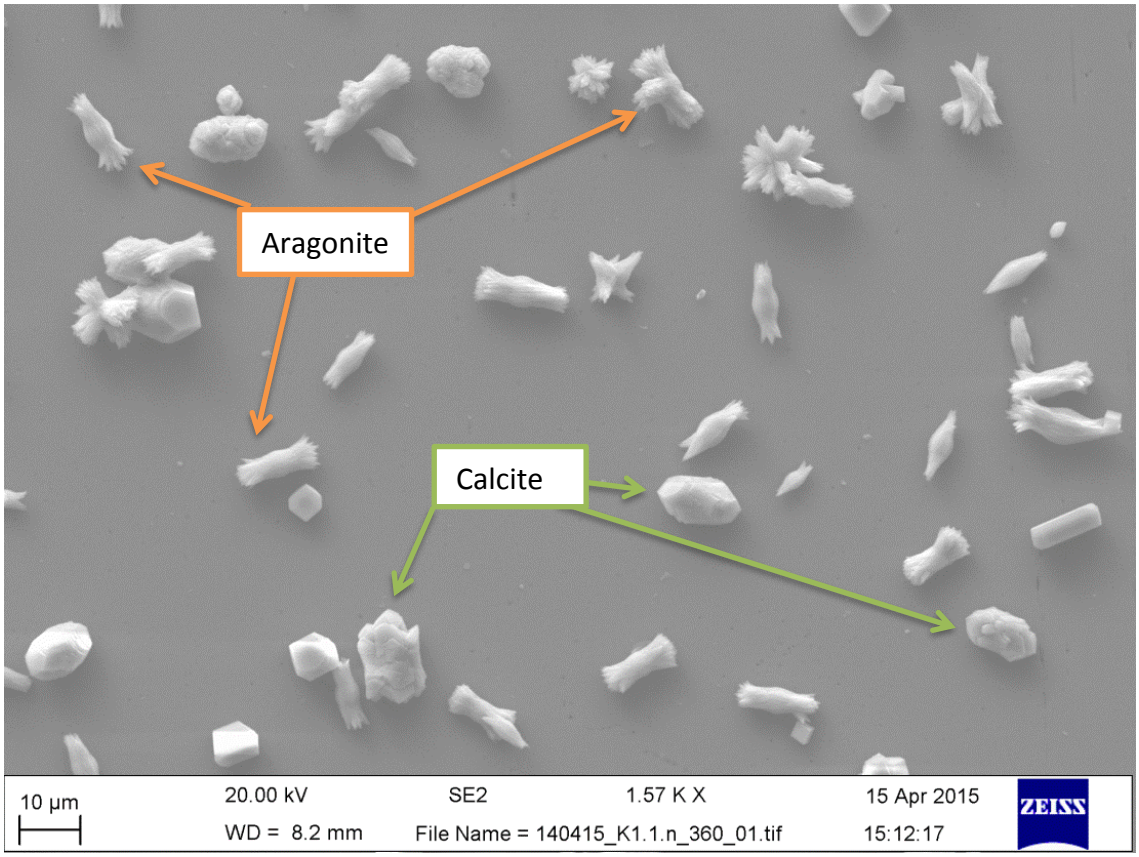

Figure 2-5: Secondary electron SEM image of the morphology of aragonite and calcite Polymorphs of $CaCO_3$.
Calcite has a tabular shape (green arrows) and aragonite crystals have needle or 'broccoli' shape (orange arrows). Image taken from constant addition experiment where precipitates formed with a Mg:Ca ratio of 1 in still conditions at 20°C.

Secondary electron (SE2) imaging occurs following the beam hitting the sample and scattering the electrons in-elastically from the atomic core of the sample. SE electrons are less than 50eV and therefore low energy (those above 50eV are backscatter electrons). In SE2 imaging the inelastic scattering of the electrons may occur not only from the spot of focus, but also from scattering at a distance from the spot focus centre.

2.2.3 Digital Image Processing for Quantification

SEM-based secondary electron images of the first precipitates visible were imported into Corel Photo-Paint X6. The outlines of individual crystals were manually drawn and then converted into separate black and white images for each polymorph using the technique of Balthasar & Cusack (2015). In this way, up to 3 separate black and white images were created from each SEM image: one each for calcite, aragonite and vaterite crystals.

The black and white images of calcite and aragonite were then imported to the ImageJ software package (available from: http://imagej.nih.gov/ij/) which was used to quantify the precipitates in each image by counting the number of black pixels (Rasband, 1997-2012). Each black and white image is analysed for the number of crystals and the area of each crystal. These data were then transferred to Microsoft Excel.

In most experiments, the very first precipitates were too small and undistinguished to be quantified accurately. These were noted forming ~30 minutes before becoming large enough to observe on 500X magnification. Data is presented as an average $CaCO_3$ crystal mole percentage precipitated per 0.22 mm^2 (the area covered in one SEM image).

Individual crystal sizes were calculated as the average volume per crystal (μm^3) and crystal number was calculated as an average per experiment (crystal size and crystal number were both an average from three images per experiment, images chosen as representative of crystal formation that was non-overlapping, with no obvious clusters to prevent bias). To convert ImageJ data into moles a number of steps were used to calculate from the form of pixels into moles.

1. Using the ImageJ measurement tool, the pixel count over a set distance was obtained so the microns per pixel could be determined, I.e.

   Pixel distance = 74 pixels

   Known distance = 20 µm, therefore = 0.27 µm per pixel.

2. Using the returned data for the pixel count per crystal was converted to μm^2

   $(\mu m \text{ per pixel})^2$ x (number of pixels per crystal, e.g. 115)

$(0.27)^2$ x (115) = 8.3835 μm^2

3. To convert from surface area (μm^2) to a volume (μm^3) equations from Balthasar & Cusack (2015) for crystal size were utilized. Equations for the reconstruction of 3D crystal volumes from 2D SEM images were obtained by Balthasar & Cusack (2015) using *Alicona MeX 5.0* computation software (available from www.alicona.co.uk/home/products/mex.html) to obtain regression equations to calculate volume for crystals grown in their degassing experiments (see supplementary data for Balthasar & Cusack, 2015, figure DR4). A separate regression equation was obtained for aragonite and calcite.

Aragonite – 0.1286 x $(\mu m^2)^{1.5204}$

e.g. 0.1286 x $(8.3835)^{1.5204}$ = 3.26 μm^3

Calcite - 0.0982 x $(\mu m^2)^{1.6438}$

e.g. 0.0982 x $(8.3835)^{1.6438}$ = 3.24 μm^3

Equations were not available for vaterite from the Balthasar & Cusack (2015) study. As only one experiment (Mg:Ca ratio 3 at 20°C in shaken conditions) produced vaterite crystals, and only two were evident, this was not deemed large enough to impact on the ratio or aragonite to calcite mole percentage.

4. To convert this data to micrograms from a volume was more complex. Firstly, the density of the crystal was required:

   I.e. molecular mass of aragonite = 2.947 g/cm^3

   First, divide by 100 to convert to $\mu g/mm^3$ = 0.002947 $\mu g/mm^3$
   Next, divide by 1000 to convert to $\mu g/\mu m^3$ = 0.000002947 $\mu g/\mu m^3$
   This value is then used to convert to micrograms by multiplying the μm^3 value from step 3.
   I.e. Aragonite = 3.26 x 0.000002947 $\mu g/\mu m^3$ = 0.0000096 µg

   The same is done, except using the molecular mass for calcite i.e. **calcite** = 2.710 g/cm^3

5. To convert the micrograms (µg) to micromoles (µmol), the micrograms obtained in step 4 are divided by the molar mass of $CaCO_3$

i.e. Aragonite 0.0000096 µg / 100.0869 µg/µmol = 9.60 µmol

The same calculation was repeated for **calcite**.

2.2.4 Statistical Analysis

For each experiment, the SEM-based crystal measurements represent a small proportion of the total number of crystals precipitated and thus only allows an estimate of the total crystal population. Each (i.e. crystals measured from the SEM images) are assumed to be representative of the whole population. Following this assumption, bootstrap statistics were employed to estimate the averages of crystal size and the mole percentage of aragonite. Bootstrapping statistics repeatedly draw as random subsamples from the sample of measured crystals. For each bootstrap cycle, a set of crystal measurements was copied into the subsample at random with the possibility of repeated copies of the same crystal (bootstrapping with replacement). The cycle was repeated until the subsample had the same size as the original sample. In total, each sample was resampled 10, 000 times each time generating a new average which can be plotted into a normal t-distribution curve. The nature of bootstrap sampling distributions allows to estimate the true average of the total population and the relevant 95% confidence interval (Willmott et al., 1985; von Davier, 1997), which are used as error bars for the mole percentage of aragonite and for crystal size. Bootstrapping statistics were performed via the statistical package *R* (*version 3.2.1) (available from* https://www.rstudio.com/) using an R script written by Dr Uwe Balthasar.

A number of assumptions are made before the data can be assessed by bootstrap statistics. All measured crystals were assumed to be representative of the total crystal population, with respect to size, shape and occurrence. By randomly drawing individual crystals from the subset of measured crystals, additional samples can be simulated. The R-script repeats 10,000 bootstraps, each time calculating a new average of crystal size and mole percentage of aragonite which can be plotted within a normal t-distribution curve. The mean of all bootstraps is representative of the average crystal size and aragonite mole

percentage of the total crystal population. The t-distribution of all bootstrap means allows the calculation of the 95% confidence interval (von Davier, 1997).

2.3 Methods To Investigate *Mytilus edulis* Elemental Composition

The blue mussel *Mytilus edulis* (*M. edulis*) occurs within the waters of the Atlantic Ocean coasts and South American coasts (Dalbeck, 2007). *M. edulis* has a high economical value, and is tolerant to many environments (Gossling, 1992). *M. edulis* shells consist of two bi-mineralic valves of aragonite (inner layer) and calcite (outer layer).

2.3.1 *Mytilus edulis* shell collection

Shells from mussels that had been grown in a marine mesocosm facility in the School of Geographical & Earth Sciences of the University of Glasgow (Fitzer et al., 2014a; 2014b; 2014c, 2015, 2016) were gifted for use in this study by Dr Susan Fitzer. One-year-old mussels originating from the same brackish sea-loch, Loch Fyne, Argyll, Scotland (Loch Fyne Oysters Ltd.) were brought to the mesocosm facility in October 2012. *M. edulis* specimens were then transferred and acclimatised to laboratory aquaria over a 2-week timeframe where natural Loch Fyne conditions were mirrored and then slowly altered over a 2-week acclimation period to experimental conditions by Fitzer et al. (2014a) reflecting an ocean acidification (OA) scenario. The mussels were maintained in closely monitored laboratory conditions of temperature (adjusted monthly) and pCO_2. All seawater conditions were tightly controlled to mimic the natural environment of Loch Fyne. The mussels were removed from aquaria after 4 months of growth under known environmental conditions of ambient temperature (*t*) and ambient temperature (+2°C) (*t*+2), with pCO_2 of 380 and 1000 µatm, at a salinity of 32.78 ± 1.42 (380 µatm pCO_2) and 34.18 ± 4.58 (1000 µatm pCO_2) (Fitzer et al., 2014b).

2.3.2 Elemental Analysis

2.3.2.1 Mussel sample preparation for SEM and EDS analyses

Mytilus edulis shells (***Figure 2-6***) were cleansed using a soft toothbrush to remove any residue from the natural environment, including barnacles and seaweed, and rinsed using deionised Milli-Q water before mounting into resin.

For the resin mounting, rubber mounts were coated with a release agent. The resin mixture was made using Epoxy Cure 2 resin (20-3432-032, Buehler) mixed with Epoxy cure hardener 2 (20-3430-064, Buehler) at 4:1 parts resin to hardener for 1 minute. Each shell was placed flat into its own mount with the inner shell surface facing upwards. The resin was poured on top of the shell and allowed to flow around the sides to prevent air bubbles forming. The mounted shell was left for at least 1 day to set firmly before cutting.

Once hardened the mounted shell was removed from the rubber mount and cut down its length 8-10mm from the centre on a slow diamond saw at a rate of 1.7mm/min. A second cut was made cutting precisely through centre of shell.

Figure 2-6: *Mytilus edulis* shells.
1 –Interior of valves of *M. edulis* shell, the darker blue calcite layer and the paler white/pearlescent aragonite layer. 2- Exterior of valves of *M.edulis* shell with organic periostracum. Photo-credit Les Hill.

Each shell cross-section was polished by hand, using a series of grit papers (p320, p800, p1200, p2500, p4000) and the surface was checked at each stage using an optical microscope. The sections were then machine polished following a similar technique to Fitzer et al. (2014a). Firstly, fine polishing cloths of 1µm and 0.3µm Alpha alumina were used for 5 minutes each, and then further polished on colloidal silica for 10 minutes, rinsing with deionised water in an ultrasonic bath between polishes.

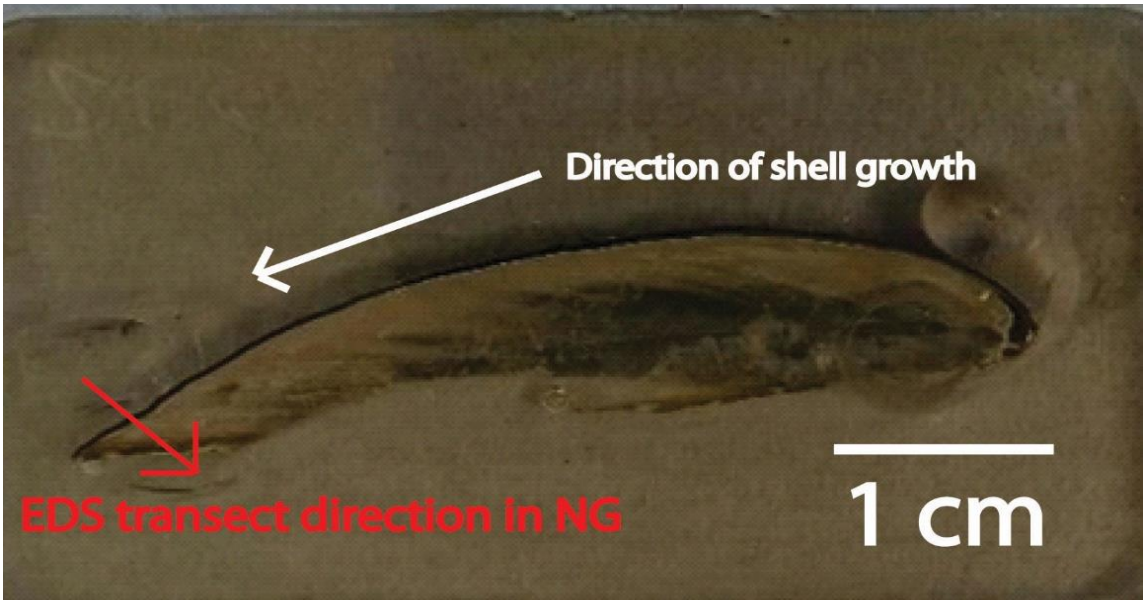

Figure 2-7: OA mussel shell resin section
(Shell 51.B4.38 - representative of pCO_2 380 and ambient (+2°C) temperature). Resin mounted shells were cut into thin, flat cross sections and polished before carbon-coating for EDS analysis. Red arrow represents the direction of analysis of an EDS transect across the new growth (NG) the shell from the outer calcite to inner aragonite layer.

Polished mussel shell sections (***Figure 2-7***) were carbon coated using a Precision Etching-Coating System (*Model 682*) by Gatan Inc. to cover the sample with a uniform 2.5nm thick layer of amorphous carbon before placing on metal mount ready for EDS.

2.3.2.2 **SEM Imaging of *Mytilus edulis***

Each mussel shell was imaged on SEM using Angle-selective Backscatter (AsB) imaging on SEM (***Figure 2-8***). This method was chosen as it allowed representation of the crystallographic topography and aids in qualitative analysis. The beam hits the sample producing backscattered electrons from elastic collision. AsB imaging gives a characteristic greyscale image that represents the atomic number of the sample, higher atomic numbers

are lighter in colour (Catlos, 2017). Backscatter electrons (BSE) are of higher energy than SE, therefore giving a stronger signal than in SE imaging. Images were captured using a 30 µm aperture and 30 kV a working distance of 6-8mm was set to allow the angle of detection to be exploited so electrons would hit the BSE detector.

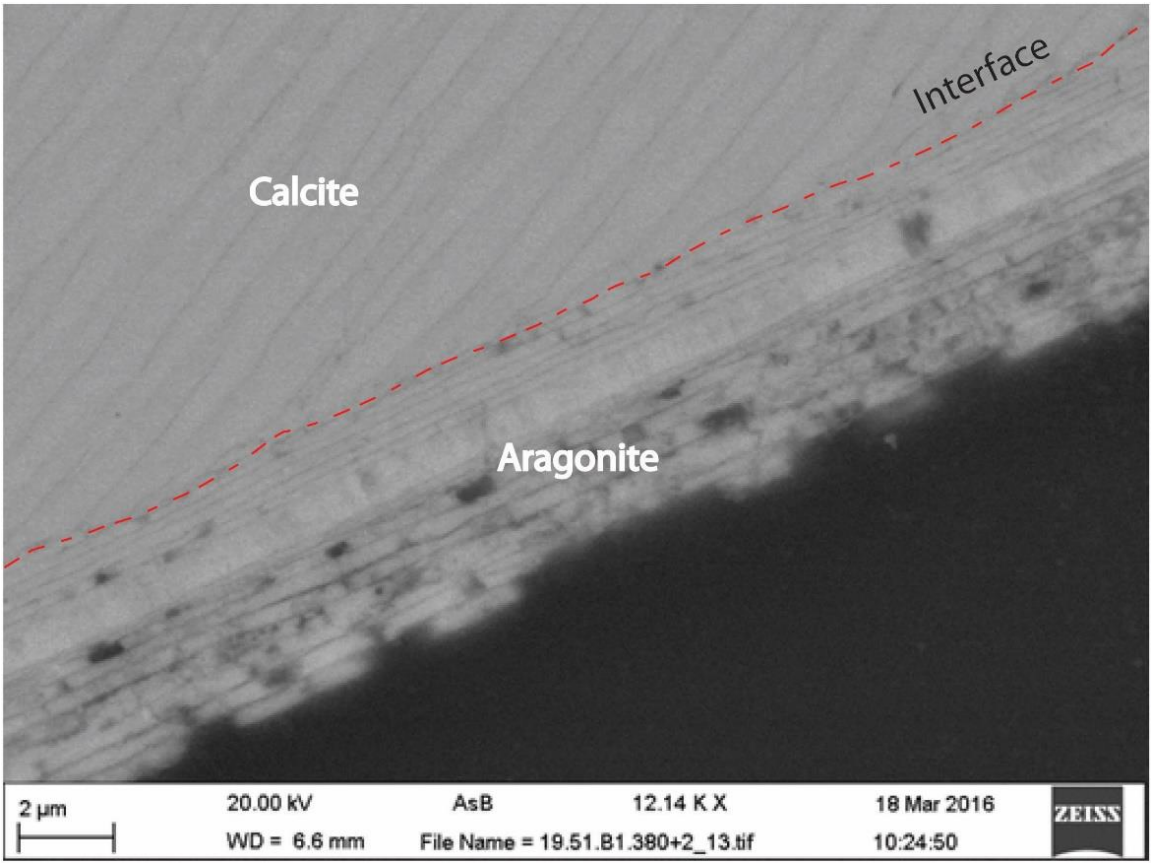

Figure 2-8: Detailed Angle selective backscatter (AsB) image of the aragonite-calcite interface. AsB image allows contrast between the crystallography to be shown in detail. The polymorph outlines for both calcite (upper section) and aragonite (Lower, brickwork pattern) meeting at the interface.

2.3.2.3 **Energy Dispersive X-ray Spectroscopy (EDS)**

Scanning Electron Microscopy Energy dispersive x-ray spectroscopy (EDS) was utilised using a *Carl Zeiss Sigma Variable Pressure Analytical Scanning Electron Microscope* to measure the relative elemental concentrations in the aragonite and calcite layers within the mussel shell.

In EDS, an electron beam is directed at the sample. The interaction of the beam with sample generates x-rays as electrons of inner shells are knocked from their shell and an electron in a higher shell drops down to occupy the gap (***Figure 2-9***). The energy difference

between the two electrons is emitted as x-rays, whose energy is characteristic of each element (Block et al., 1991).

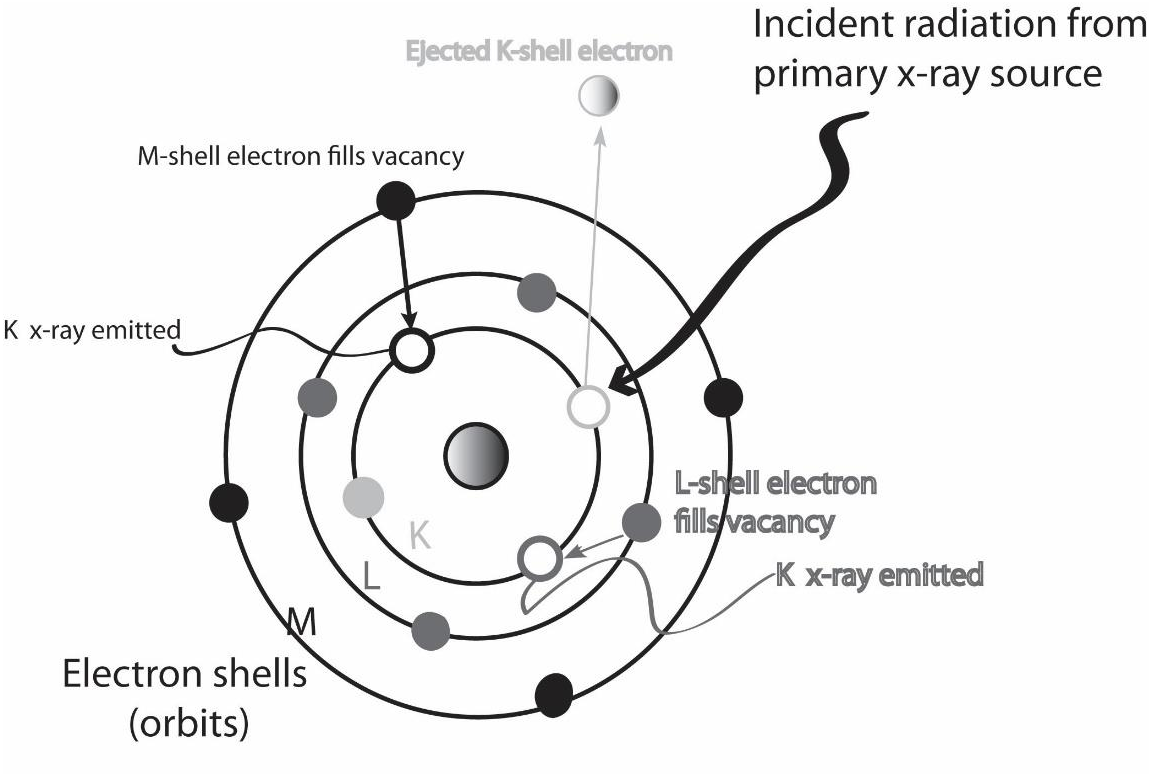

Figure 2-9: Physical principles behind EDS (adapted from Oxford Labs, 2009).

When assessing for S concentrations, SO_4^{2-} will not be measured by EDS and therefore must be considered a possible influence on the other element concentrations although not directly measured. One way to assess this is to consider the Mg/S ratio as Mg content should increase with increased sulphur content, whether this be in S form or SO_4^{2-} form. Non-biogenically, SO_4^{2-} incorporation into calcite is reliant on the SO_4^{2-}/CO_3^{2-} ratio (Busenberg & Plummer, 1985) and in turn this will be influence by changes in pH or alkalinity (Pingitore et al., 1978).

2.3.2.4 Defining old and new growth conditions in OA experiment mussels

Mussel shells for the OA experiments were placed in a calcein dye before being transferred to the lab conditions by Fitzer et al. (2014a). It was intended that the calcein dye act as the marker of the start of the laboratory conditions. Unfortunately, too much time had elapsed since the OA experiments, and so there was no fluorescence to indicate

the start of growth in the experimental conditions. Instead, measurements of growth taken during the initial OA experiments have been used to determine where the old growth stops and new growth begins (see Fitzer et al., 2014a).

The average growth over the 4-month timescale is in **(**

Table 2-4). These growth data allow transects for EDS spectra to be taken within 'new' growth (NG) conditions. Transects were also taken 1cm to 1.5cm from the tip of the shell, ensuring that each transect taken was within 'old' growth (OG) conditions from Loch Fyne natural conditions.

Temp (°C)	pCO_2 (µatm)	Average Shell New Growth mm (±SD)
(ambient) ~7	380	0.66 (0.19)
(ambient +2) ~9	380	0.79 (0.29)
(ambient) ~7	1000	0.70 (0.33)
(ambient +2) ~9	1000	0.50 (0.41)

Table 2-4: Estimates of new growth of shells under 4 months of known experimental conditions.
Each average was calculated using 7-9 mussel shell samples measured at the 4-month timeframe from unpublished data from OA study by Fitzer et al., (2014a; 2014b).

For all examined mussel cross-sections, SEM imaging was done initially to ensure that the calcite-aragonite interface was visible (***Figure 2-8***). Three transects within the OG area were taken close to each other across the full thickness of the shell, across the calcite-aragonite interface representative of natural Loch Fyne conditions. A further 3 transects were taken within the NG area to represent the known lab conditions and the data presented here is from these NG conditions.

2.3.3 Element concentration quantification

INCA software was utilised with aperture of 30 µm at 20 KeV. Two sets of three EDS transects were taken, three transects for the calcite layer and another three transects for the aragonite layer. Initially, three transects for spectral acquisitions were taken over the complete thickness of the shell from the calcite layer, through the aragonite-calcite interface and finishing on the aragonite layer. By guiding a transect line across the entire

thickness of the shell, from the calcite layer to the aragonite layer, spectra of all elements contained within the shell were acquired. Each calcite layer transect comprises 30-42 spot analyses, each spot ~8-14 microns spaced **(*Figure 2-10*).** Aragonite layer transects were much smaller and comprised of 4-24 spot analyses, 1-2 microns spaced.

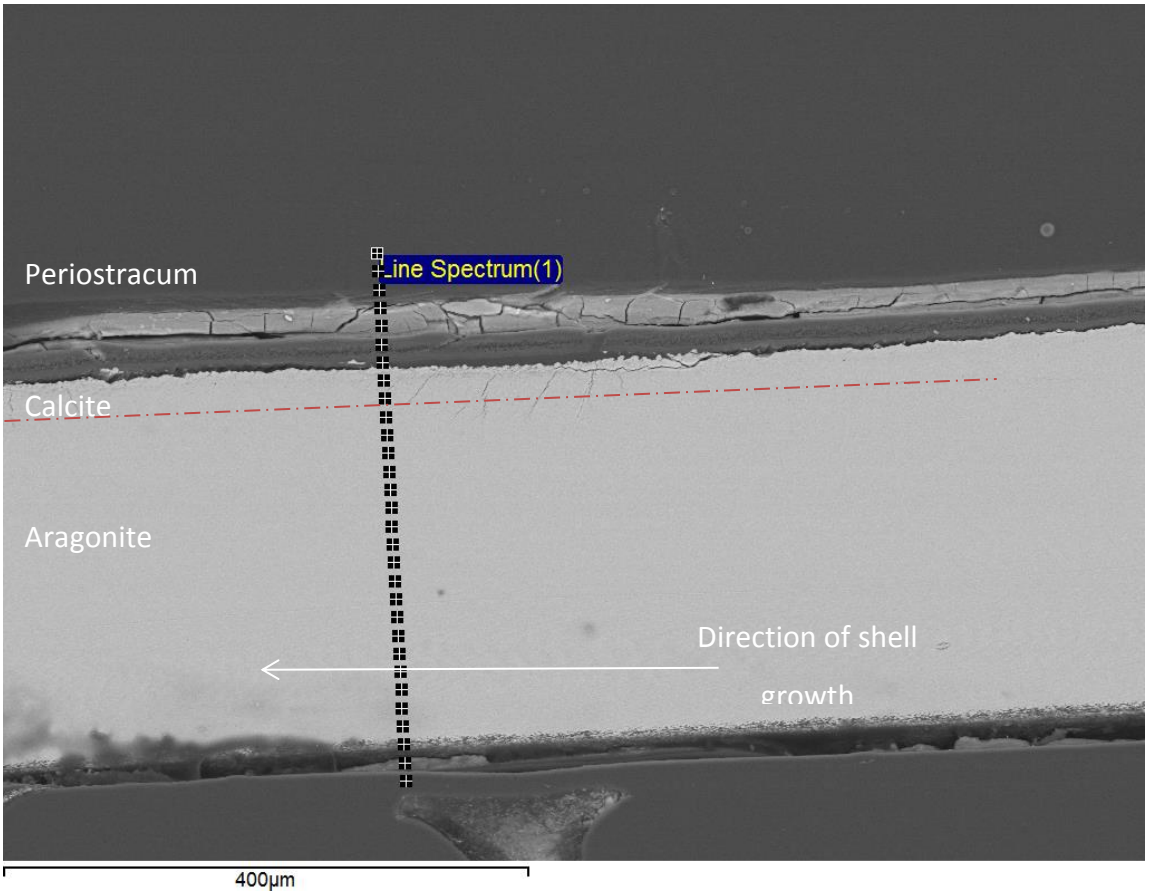

Figure 2-10: Example spectral analysis transect across the calcite-aragonite interface. Example from shell B1 representing a pCO_2 of 380 µatm, ambient temperature OG transect 1.

However, due to the tapered shape of the shell edge this in some instances only gave spectra for the calcite layer. Therefore, these initial transects were used only for their calcite data. Newest aragonite is further back and to gain the element concentrations in the aragonite layer, 'new growth' was sampled at first appearance, again taking three transects across the layer.

2.3.3.1 **Determining EDS Detection Limits**

For both sets of transects spot analyses of resin or periostracum were removed prior to further analysis. For each spot of analysis, concentrations of carbon, oxygen,

calcium, strontium, sulphur, magnesium and sodium were recorded in weight percent (wt%) (***Figure 2-11***). Several steps to exclude concentrations that fell out-with detection were carried out.

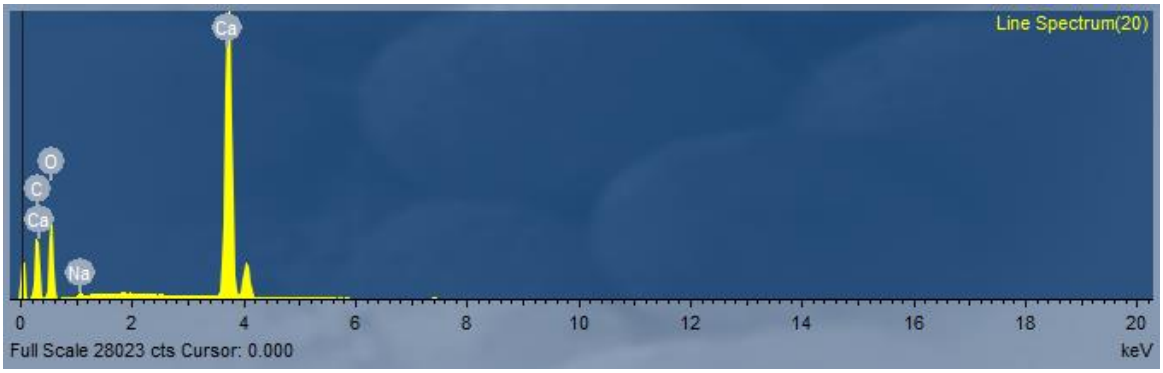

Figure 2-11: Example EDS Spectra
Example spectra from Generic mussel 1 (transect 3). Around 30-42 spectra analyses were completed in this way and the data is exported to excel for quantification.

Firstly, each transect was checked to exclude the periostracum or organic matrix by checking the location of the analysis points on the SEM images. Similarly, each of the 3 transects taken from each shell were compared to each other to ensure all data gained for each element was of the same range. Next, each analysis point was searched for notable concentrations of elements that don't easily fit within calcite or aragonite such as i.e. Ytterbium (found in resin), or beryllium. Such were excluded from further analysis.

Next, each analysis point was checked for unjustifiable element concentrations. If only 1 of the 7 elements measured in that analysis point was deemed an outlier, then the spectra analysis point were kept within the dataset, as the other 6 elements allow the data to be confidently justified as being of importance. If 2 or more of the elements had a discrepancy in the given analysis point, then the entire suite of elements from that one analysis point were removed from the dataset.

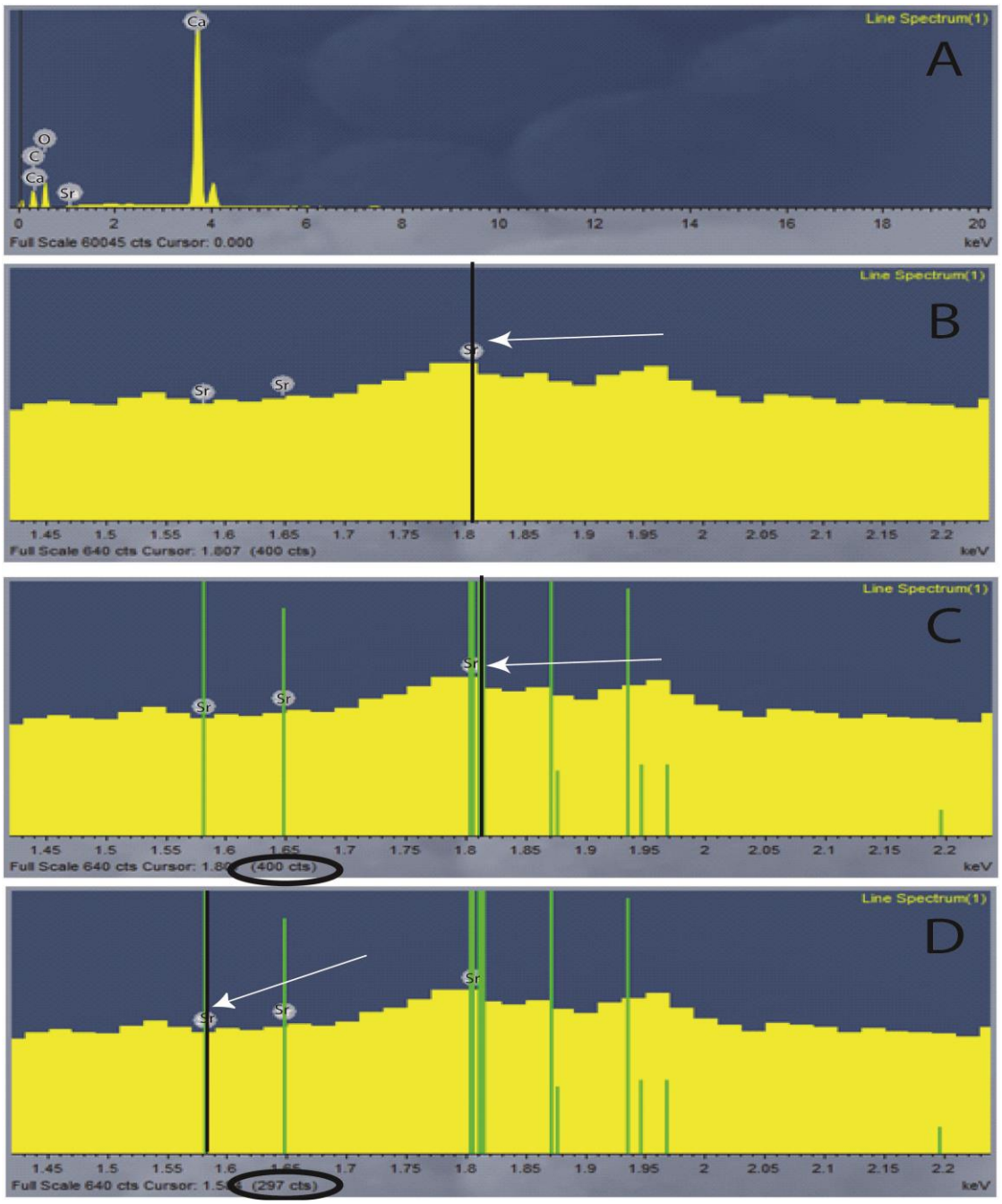

Figure 2-12: Obtaining spectra detection limits
(a) Example of spectra from shell 4.55.B3 (*t*+2, 1000). (b) Sr element selected. (c) Curser markers option selected (visualised by green lines) and curser then placed over the highest peak count and noted ('400 cts' count number indicated by black circle). (d) To exclude the background noise the curser is placed over the lowest peak count and the count number obtained ('297 cts').

Further to this any data points below the EDS detection limits were removed. Manually each element from individual analysis points had the wt% of the maximum and minimum peak count (excluding background noise) measured, before then the difference

between the maximum and minimum peaks calculated. Elements falling within the range between maximum and minimum peaks were kept (*Figure 2-12*).

For example, for each analysis point each element concentration was calculated as follows:

E.g. Wt% C = 19.78 which matches the highest count in energy spectra of C = 4780

Therefore, 19.72% = 4780 counts,

1% = 4780/19.72% = 242.39 counts

The lowest count in energy spectra of C = 92 counts

Therefore, lowest C wt% = 92/(1% of max counts (242.39)) = 0.38 %. Thus, this was indicating that there was a required minimum of 0.38 wt% required to be detected by EDS.

Finally, to remove any remaining analysis points of abnormally high concentration, a comparison to pure inorganic $CaCO_3$ was made. Pure inorganic $CaCO_3$ has concentrations of C = 12.01 wt%, O_2 = 47.97 wt% and Ca^{2+} = 40.08 wt%. Biogenic calcite includes organic components and based on the control shells (380 µatm, ambient temperature) carbon concentrations were ~19.5 wt% ($\pm$ 1.09 SD) whilst calcium concentrations were ~30 wt% ($\pm$ 2.5 SD). These concentrations were used as a guide to indicate spectra that were outside the justifiable range.

2.3.3.2 Inorganic and organic components of shell element concentrations

To investigate differences between individual shells of the same scenario, consideration has been given to the organic and inorganic components. Ca^{2+} is indicative of the inorganic component in $CaCO_3$. Using the equation for $CaCO_3$ allows the ratio of element concentrations together based on pure inorganic $CaCO_3$:

I.e. Ca^{2+} = 40.08 %, C = 12.01 % and O_2 = 47.97 %

The ratio of inorganic to organic components of the element indicates what proportion of the element was attached each. This allows an indication of whether the EDS beam has hit a marginal edge of a polymorph as organic components lie on the edges of

calcite and aragonite. This is important as the organic components of biogenic $CaCO_3$ lie on the cell edges and could be a reason for differences in the EDS element concentration if the beam of EDS hits a margin edge. By deciphering the differences linked between the organic and inorganic parts will allow this to be documented. Any discretions were next compared to the sulphur component to see if any correlation exists as the sulphur component is usually linked with the organic matrix.

2.3.4 Statistical Analysis

Two sample t-tests were applied to the element concentration data obtained from the shells. This allowed testing the data obtained to determine if temperature of pCO_2 had influence on the element concentrations. These statistical analyses were chosen because they allow the difference between two population means to be tested from the two independent samples. One pre-requisite for this testing is that the data followed normal distribution, which the data was checked for before proceeding.

Two null hypothesis were:

1. Increased temperature did not change the concentration of element X.
2. Increased pCO_2 did not change concentrations of element X.

First, the data from both shells per scenario per element were combined. T-tests were carried out using statistical software package *Minitab 17* by comparing the data of a specific element in one scenario with the data of that element in each of the other scenarios. This was done first for increased temperature and secondly for increased pCO_2. The number of observations per sample give a value for Degrees of freedom (DF), this is used to calculate a p-value. P-values were obtained for each test which allow the likelihood that the null hypothesis is true. The p-values derived from the t-tests were said to be significant if $p \leq 0.01$ (99% confident) or ≤ 0.05 (a 95% confident). This allows determining with 95% confidence that the difference in the data sampled lies within these confidence intervals. Any p-value returned $p > 0.05$ was deemed insignificant.

3

Influence of Mg:Ca Ratio, Temperature and Water Movement on Non-biogenic $CaCO_3$ Polymorphs

The aragonite-calcite sea hypothesis depicts homogeneous switches in the Mg:Ca ratio determining whether aragonite or calcite is the dominant non-biogenic calcium carbonate polymorph in the marine environment. Considering temperature differences across the latitudes suggests that shifts in dominant polymorph formation may not be spatially uniform (Morse et al., 1997; Balthasar & Cusack, 2015). This study investigates the influence of Mg:Ca ratio and temperature on the first formed polymorph precipitates in the presence and absence of water movement in order to quantify the influence of these three parameters on polymorph formation.

3.1 Aims of the chapter

This chapter aims to investigate the influence of Mg:Ca ratio and temperature on non-biogenic $CaCO_3$ polymorph formation in artificial seawater. These variables were chosen to investigate how Mg:Ca ratio and temperature influence the non-biogenic $CaCO_3$ polymorphs formed in relation to Phanerozoic seawater composition. The main objectives for this study were threefold:

(i) To quantify the influence of Mg:Ca ratios 1, 2 & 3 on the polymorph formation.

(ii) To quantify the influence of temperature, using 20°C & 30°C, on $CaCO_3$ polymorph formation.

(iii) To determine how water movement influences the effect of Mg:Ca ratio and temperature on polymorph formation.

Phanerozoic Mg:Ca ratios range from 0.9-5.2 (Wilkinson & Algeo, 1989; Hardie, 1996; Lowenstein et al., 2001; Siemann, 2003; Dickson, 2002; Dickson 2004; Demicco et al., 2005). The Mg:Ca ratios of 1, 2 and 3 were therefore chosen in order to constrain the lower range of Mg:Ca ratios from the Phanerozoic. This aspect of the research aims to provide better resolution around the Mg:Ca ratio of 2 which is often considered to be the threshold for the switch between calcite and aragonite fields (Sandberg, 1975; Füchtbauaer & Hardie, 1976; Sandberg, 1985; Hardie, 1996). Constant addition of bicarbonate (220mM delivered over 8 hours) was added to a mother solution of Mg:Ca ratio 1,2 and 3 at 20°C & 30°C, arriving at a final Ca^{2+} concentration of ~10.2mM as described in section 2.1. A constant addition technique was chosen to pin-point the parameters at which the first formed polymorphs appear by the time the end Mg:Ca ratio was reached. It also allows a more constant environment where the pH and alkalinity can be controlled.

Data from Morse et al. (1997) and Balthasar & Cusack (2015) indicate that more aragonite is formed relative to calcite at increased temperature and Mg:Ca ratios. However, as the artificial seawater used within this study was of a lower saturation state than in the degassing experiments (Morse et al., 1997; Balthasar & Cusack, 2015), it was hypothesised that higher proportions of aragonite would form at comparable Mg:Ca ratios and temperature.

Water movement was included as a parameter to mimic the natural environment in which ooid formation occurs to allow the non-biogenic polymorph formation mechanisms be viewed in an environmental context. The continuous addition method used here has not previously been used with shaken conditions (see section 2.1.1.). There are however, some similarities with the experimental conditions used by Bots et al. (2011), who used a more complex artificial seawater solution and used glass beads to provide nucleation surfaces, analogous to ooid formation. Instead, this research used seawater of known Mg:Ca ratio, corrected for salinity of ~35 with the addition of HCO_3^-, and used glass slides for nucleations surfaces which were able to be removed for analysis of precipitates. This chapter investigates the influence of Mg:Ca ratio, temperature and water movement,

as well as the interplay between these three parameters, on the proportion of aragonite and calcite formed and whether the proportion is influenced by nucleation or growth of the crystals grown.

3.2 Results

Results are presented for precipitates formed under Mg:Ca ratios 1,2 and 3, at 20°C and 30°C, in still and shaken conditions, in terms of the mole percentage of aragonite, the average number of nucleations and the average crystal size of both aragonite and calcite. In these experiments, three vaterite crystals were found in one experiment in shaken conditions and therefore insignificant and not included in the data presented here.

The first crystal nucleations for all experiments were achieved within the 6 hour experiment timeframe although higher Mg:Ca ratios and lower temperature took the longest time to nucleate. Co-precipitation of aragonite and calcite occurred in all experimental scenarios. The highest mole percentage of aragonite formed was 99.66% aragonite and the lowest was 2.41%. These results indicate that polymorph precipitation does not shift from one mineralogy to another as a generic switch as previously suggested (Stanley & Hardie, 1998) as there is always a co-precipitation of polymorph forms under these conditions. This co-precipitation of aragonite and calcite over a range of experimental parameters is in agreement with the work of Balthasar & Cusack (2015).

3.2.1 The influence of Mg:Ca ratio on polymorph formation

3.2.1.1 Mg:Ca ratio influence: the percentage of aragonite

Increased Mg:Ca ratio increases the mole percentage of aragonite formed in still conditions at 20°C (***Figure 3-1***). These results are in agreement with previous findings where higher concentrations of magnesium in solution facilitate precipitation of aragonite by the inhibition of calcite (Mucci & Morse, 1983; Falini et al., 1994; Morse et al., 2007; Park et al., 2008; De Choudens-Sanchez & Gonzalez, 2009).

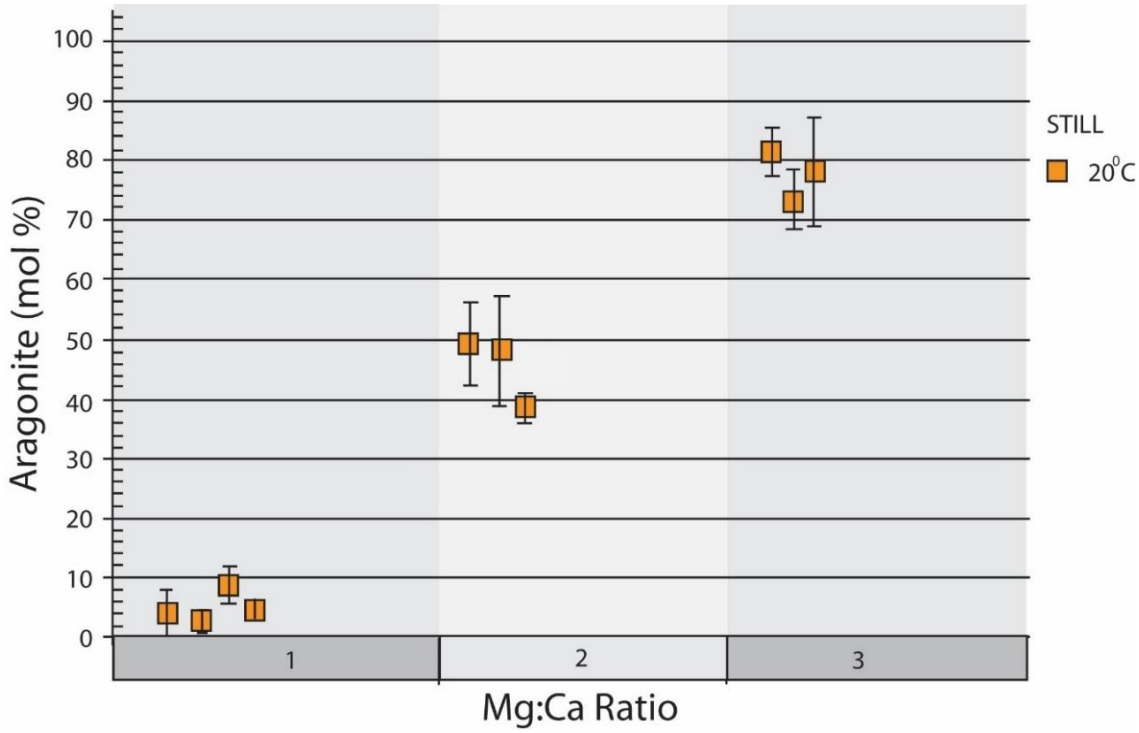

Figure 3-1: Influence of Mg:Ca ratio on the mole percentage of aragonite.
Results are expressed as mean mole percentage of aragonite ± SD per scenario replicate, t = 20°C, still conditions (see section 2.1). Each scenario was replicated four times. Fourth replication for Mg:Ca ratio scenario failed to precipitate fully formed crystals without contamination and therefore not presented here.

3.2.1.2 The influence of Mg:Ca ratio on the number of nucleations and crystal growth

The proportion of aragonite/calcite crystals formed increased at increased Mg:Ca ratio (***Figure 3-2A***). This was due to more nucleations of aragonite occurring at increased Mg:Ca ratio whilst at the same time, fewer nucleations of calcite occurred at increased Mg:Ca ratio. Calcite precipitates forming at increased Mg:Ca ratio, although forming in fewer numbers, find it easier to form attachments to nucleation surfaces from solution than by forming further attachments to nucleations already formed. This was increasingly obvious at Mg:Ca ratio 3, where the highest proportions of aragonite were formed in comparison to calcite giving the largest proportion of aragonite/calcite crystals formed.

In terms of crystals size, the proportion of aragonite/calcite crystal size was observed to have a larger proportional increase with increased Mg:Ca ratio compared to the crystal number formed (***Figure 3-2B***). This was due to the crystals of aragonite forming being of similar sizes whereas the crystal sizes of calcite decreased at increasing Mg:Ca ratio,

allowing for the proportional increase of aragonite/calcite observed (***Figure 3-2B***). This supports the concept that growth of calcite is a function of the magnesium content of solution, and that aragonite will be facilitated at the expense of calcite (Mucci et al., 1983).

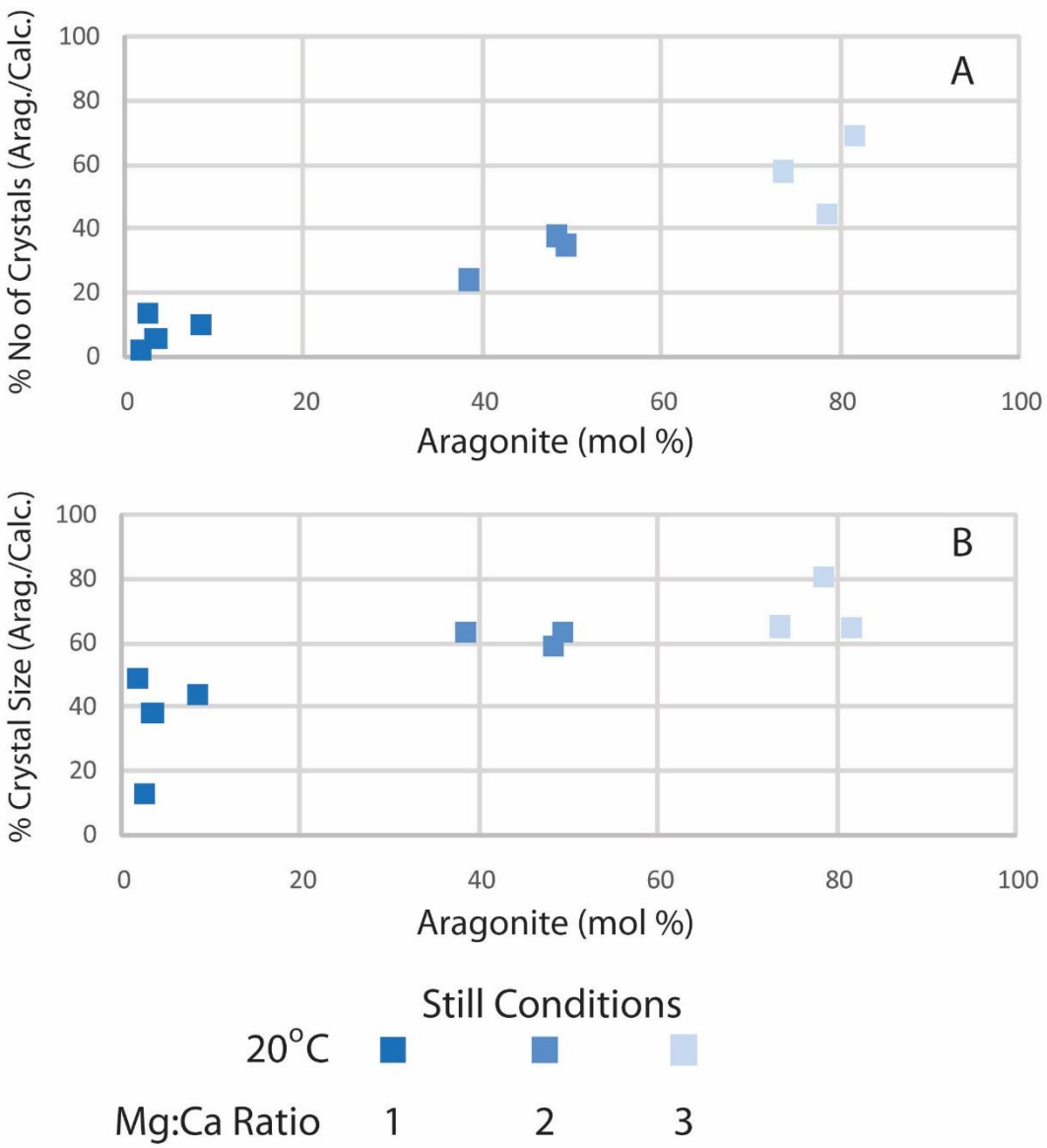

Figure 3-2: **The influence of Mg:Ca ratio on the number and size of aragonite crystals. Results are presented for the aragonite mole percentage against crystal number (A) and crystal size (B) from continuous addition method (section 2.1.) *t*= 20°C in still conditions. Increased Mg:Ca ratio 1-3 is represented by change from dark to light colour Upper graph A presents the average number of crystals of aragonite/calcite as a percentage. Lower graph B presents results the average volume of crystals of aragonite/calcite acquired from bootstraps as a percentage.**

In summary, higher Mg:Ca ratios increase the mole percentage of aragonite formed. This occurs because more nucleations of aragonite occur at increased Mg:Ca ratio whilst increased Mg:Ca ratios resulted in a decreased number of crystals of calcite occurring and these nucleations were also of smaller size than at lower Mg:Ca ratio.

3.2.2 The influence of temperature on polymorph formation

3.2.2.1 Temperature influence on the percentage of aragonite

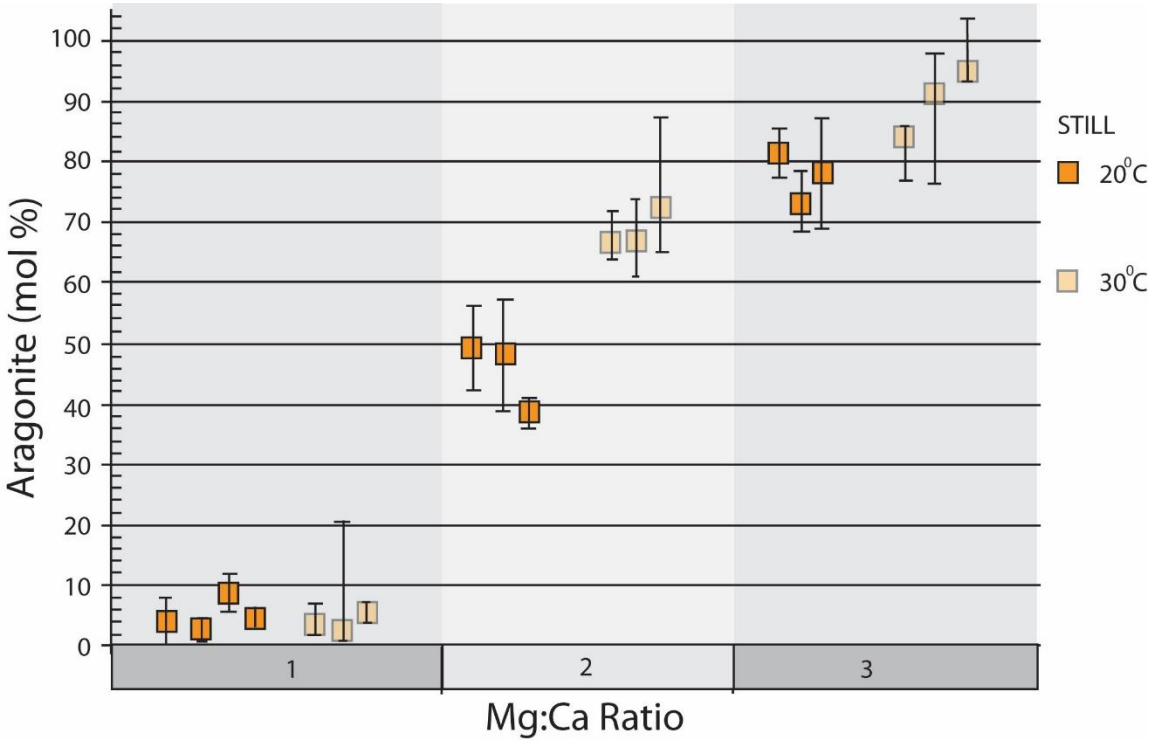

Figure 3-3: **Influence of increased temperature on the mole percentage of aragonite**. Results are expressed as mean mole percentage of aragonite ± SD per scenario replicate, t = 20°C, still conditions (see section 2.1). Each scenario at 20°C was replicated four times, the fourth replication for Mg:Ca ratio 3 scenario failed to precipitate without contamination and is not presented here. Scenarios at 30°C (pale orange) were replicated in triplicate.

The influence of higher temperature was observed to increase the mole percentage of aragonite precipitated, the largest increase occurred at Mg:Ca ratio 2 at 30°C (***Figure 3-3***). This result suggests that a temperature of 30°C increases the mole percentage of aragonite precipitated regardless of the Mg:Ca ratio compared to a temperature of 20°C. These results are in agreement with previous studies which found that increased

temperature increases the proportion of aragonite formed compared to calcite (Morse et al., 1997; Balthasar & Cusack, 2015).

3.2.2.2 Influence of temperature on the number of nucleations and crystal growth

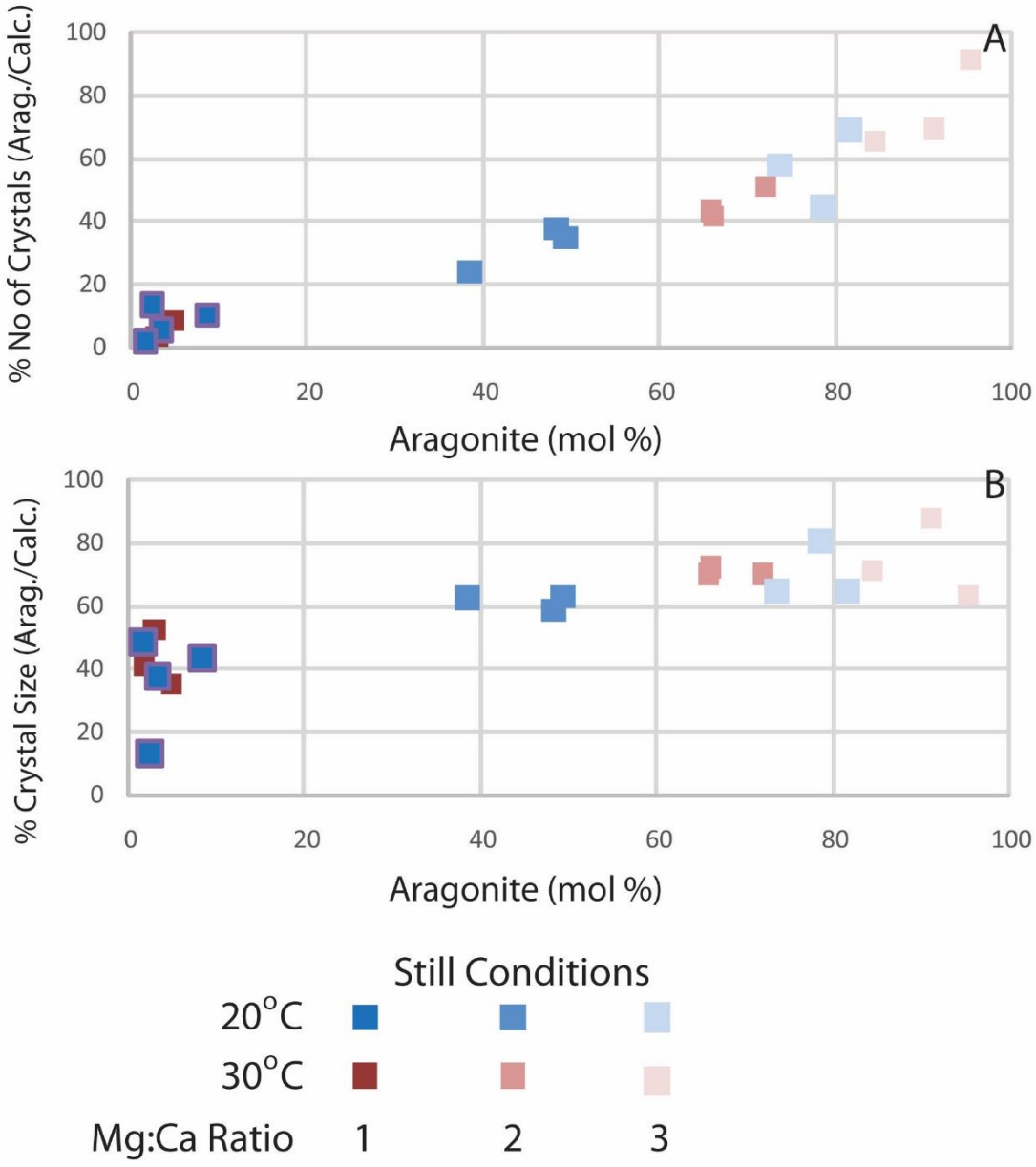

Figure 3-4: The influence of temperature on the number and size of crystals.
Results are presented for the aragonite mole percentage against crystal number (A) and crystal size (B) from continuous addition method (section 2.1.) *t*= 20°C (blue squares) and t=30°C (red squares) in still conditions. Increased Mg:Ca ratio 1-3 is represented by change from dark to light colour Upper graph A presents the average number of crystals of aragonite/calcite as a percentage. Lower graph B presents the average volume of crystals of aragonite/calcite acquired from bootstraps as a percentage.

The proportion of aragonite/calcite formed at higher temperature increases with increased Mg:Ca ratio (***Figure 3-4A***). At Mg:Ca ratio of 1, higher temperature does not influence the proportion of aragonite to calcite crystals formed (***Figure 3-4A***). At Mg:Ca ratios of 2 and 3, the mole percentage of aragonite formed was increased as the proportion of numbers of aragonite/calcite crystals were increased, especially at Mg:Ca ratio of 3 where the crystals formed were almost only of aragonite (***Figure 3-4A***). This suggests that increased temperature does not alter the opportunity to attach to nucleation surfaces at Mg:Ca ratio 1 and 2, but at Mg:Ca ratio of 3, the increased concentration of Mg^{2+} in solution allowed more opportunity for nucleations to occur (***Figure 3-4A***). The increase in the proportion of the number of nucleations of aragonite/calcite at 30°C suggest that higher temperature allows the activity of the ions in solution to increase and this allows more opportunity for them to attach to nucleation surfaces they pass as a result, Mg^{2+} inhibiting nucleation of calcite and facilitating nucleation of aragonite instead.

Temperature is known to increase the rate of precipitation of $CaCO_3$ (Mejri et al., 2014) and decrease the timeframe for induction of precipitation which can increase the precipitation rate (He et al., 1994). As Mg:Ca ratio of 1 has the lowest Mg^{2+} content in solution, calcite will not be affected to the same extent by Mg^{2+} as it is in higher concentration Mg^{2+} solution therefore allowing the proportion of crystals of aragonite/calcite formed to be similar.

In terms of crystal volume the percentage of aragonite/calcite was lowest at Mg:Ca ratio of 1 where temperature does not appear to have an influence over the size of crystals formed compared to lower temperature (***Figure 3-4B***). However, the proportion of aragonite/calcite size is increased at Mg:Ca ratio 2, and is slightly higher at Mg:Ca ratio of 3 than at a lower temperature (***Figure 3-4B***). This suggests that increased temperature facilitates growth of aragonite more than it does that of calcite by allowing more opportunity for ion collisions to increase the growth of aragonite at Mg:Ca ratio 2 and 3, again possibly due to the influence of Mg^{2+} inhibiting the growth of calcite allowing more growth of aragonite. This also suggests that Mg^{2+} in solution was increasingly incorporated into the calcite crystal lattice at a higher temperature of 30°C, inhibiting the calcite growth at higher Mg:Ca ratio. This agrees with other studies that show Mg^{2+} is temperature

sensitive and will increase the proportion of aragonite compared to calcite at a higher temperature (Burton & Walter, 1987; Morse et al., 1997; Balthasar & Cusack, 2015).

The variance in crystal sizes observed at both 20°C and 30°C may be explained by the instantaneous precipitation which was only found to occur at Mg:Ca ratio 1 ***Figure 3-4B***).

In summary, at 30°C there was a greater mole percentage of aragonite formed at Mg:Ca ratios of 2 and 3 compared to those formed at 20°C at the same Mg:Ca ratios (***Figure 3-3; Figure 3-4)***. The increase observed was due to formation of larger crystal sizes of aragonite compared to calcite at increased Mg:Ca ratio with higher temperature.

3.2.3 The influence of water movement on polymorph formation

3.2.3.1 The influence water movement on the percentage of aragonite

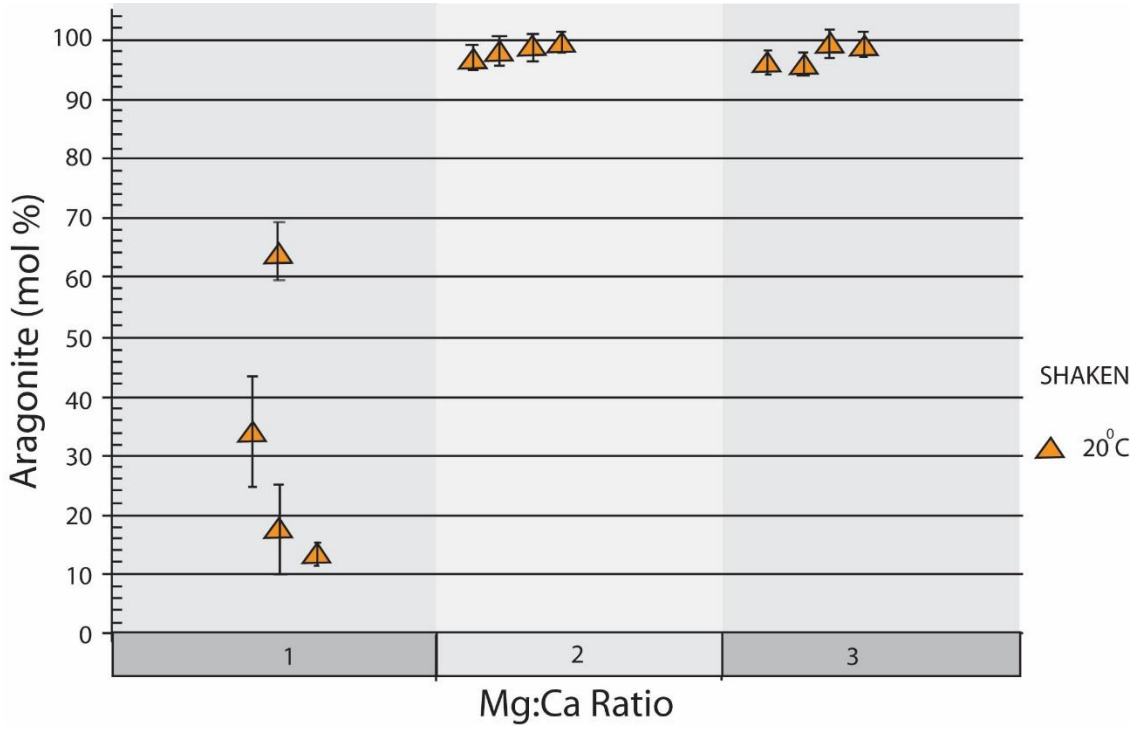

Figure 3-5: The influence of water movement on the mole percentage of aragonite. Results are expressed as mean mole percentage of aragonite ± SD per scenario replicate, t = 20°C, shaken conditions (see section 2.1). Each scenario at 20°C was replicated four times.

Water movement increased the mole percentage of aragonite produced at increased Mg:Ca ratio (***Figure 3-5***). The proportions of aragonite formed under shaken conditions were largest at Mg:Ca ratio 2 and 3 where both these rates were above 95%. The increase observed may be due to increased opportunity for ions to move past each other, passing surfaces they can attach to. Shaken conditions caused large variability in the mole percentage of aragonite formed at Mg:Ca ratio 1.

3.2.3.2 The influence of Mg:Ca ratio with water movement on the number of Nucleations and crystal growth

The influence of water movement increased the proportion of aragonite crystals formed compared to calcite at increased Mg:Ca ratio (***Figure 3-6A***). Shaking of the solution allows more opportunity for particles to move past each other to form attachments to nucleation sites, increasing the numbers of nuclei precipitated. This suggests that in shaking conditions at an increased Mg:Ca ratio, the water movement may allow more opportunity for Mg^{2+} ions to attach to calcite growth surfaces inhibiting nucleation.

However, shaken conditions also increased the variability in the number of nucleations formed. For aragonite in particular, when fewer nucleations occurred, larger crystals formed, but when more aragonite crystals formed these remained small. It could be that larger crystals result from many nucleations forming initially, and due to water movement, the nucleations became dislodged which allows for agglomeration between the nucleated particles and results in larger crystals. Therefore, larger crystals of aragonite were formed in shaken conditions at the expense of the number of crystals formed (***Figure 3-6***). This trend was not observed in calcite, but the calcite crystals formed were of decreasing size at increased Mg:Ca ratio in shaken conditions, most likely due to Mg^{2+} inhibiting calcite growth (***Figure 3-6B***).

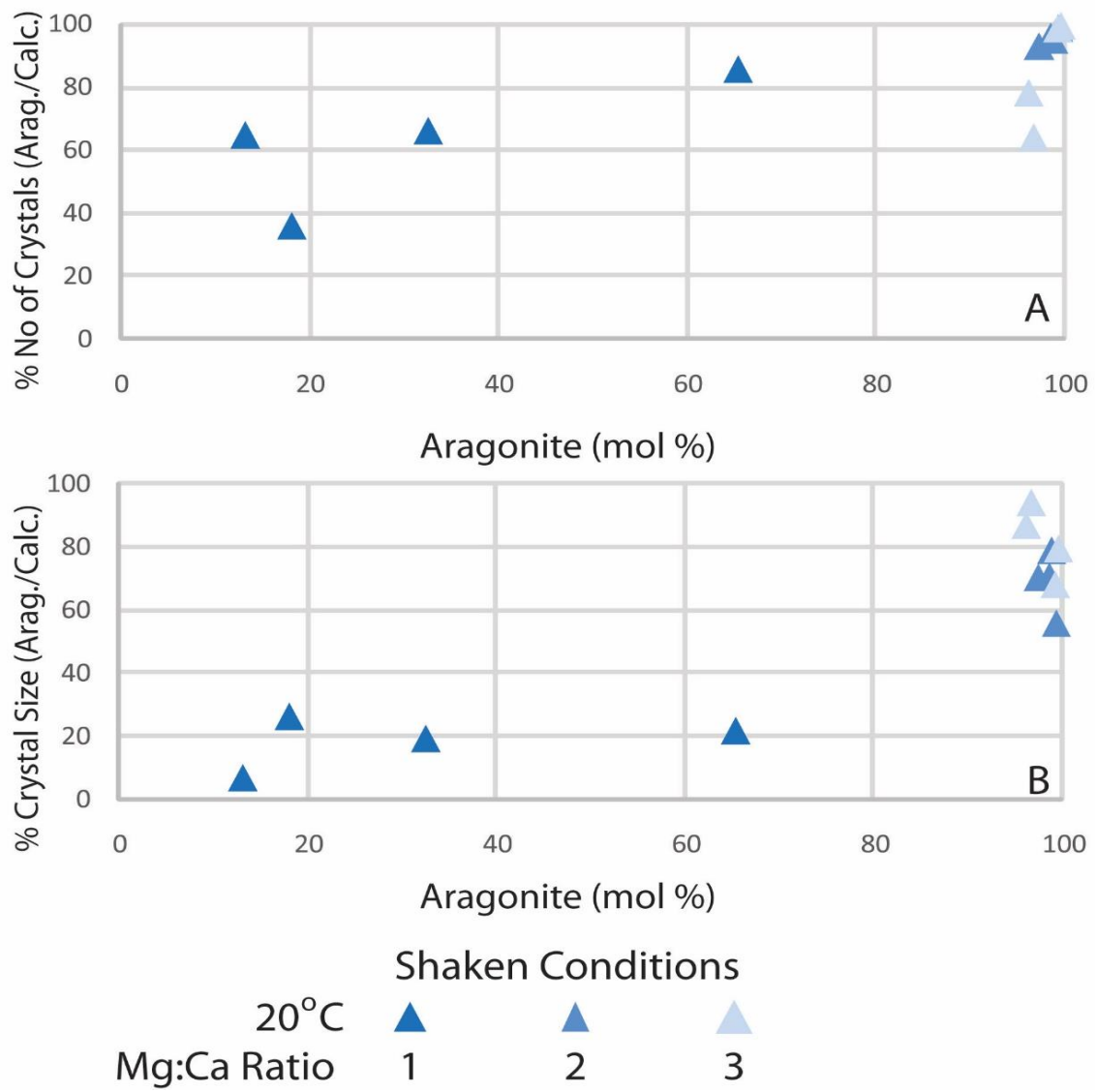

Figure 3-6: The influence of Mg:Ca ratio in water movement on the crystal number and size. Results are presented for the aragonite mole percentage against crystal number (A) and crystal size (B) from continuous addition method (section 2.1.) *t*= 20°C in shaken conditions. Increased Mg:Ca ratio 1-3 is represented by change from dark to light colour. Upper graph A presents the average number of crystals of aragonite/calcite as a percentage. Lower graph B presents results the average volume of crystals of aragonite/calcite acquired from bootstraps as a percentage.

In summary, water movement increased the mole percentage of aragonite precipitated at increased Mg:Ca ratios. The increase was due to an increased number of nucleations occurring at increased Mg:Ca ratio. Shaken conditions increased the size of aragonite/calcite crystals formed due to fewer and smaller crystals of calcite forming.

Water movement increased the variance on the number of nucleations formed between experiments.

3.2.4 The influence of temperature with water movement

3.2.4.1 Mole percentage of aragonite

In shaken conditions at 30°C, the mole percentage of aragonite formed was significantly increased at Mg:Ca ratio 1 (~70% increase) and remained similar (above 96%) at Mg:Ca ratios 2 & 3 compared to percentages of aragonite formed at 20°C (***Figure 3-7***). This result suggests that a higher temperature of 30°C in shaken conditions had a larger influence over the proportion of aragonite precipitated, increasing the proportion to above 80% at all Mg:Ca ratios compared to a lower temperature of 20°C in shaken conditions. The smaller increase in the proportion of aragonite formed at Mg:Ca ratio 2 and 3 compared to Mg:Ca ratio 1 at 30°C is due to the proportion of aragonite formed already being within the highest reaches (90% at Mg:Ca ratio 1, ~98% at Mg;Ca ratios 2 and 3) **(*Figure 3-7*)**.

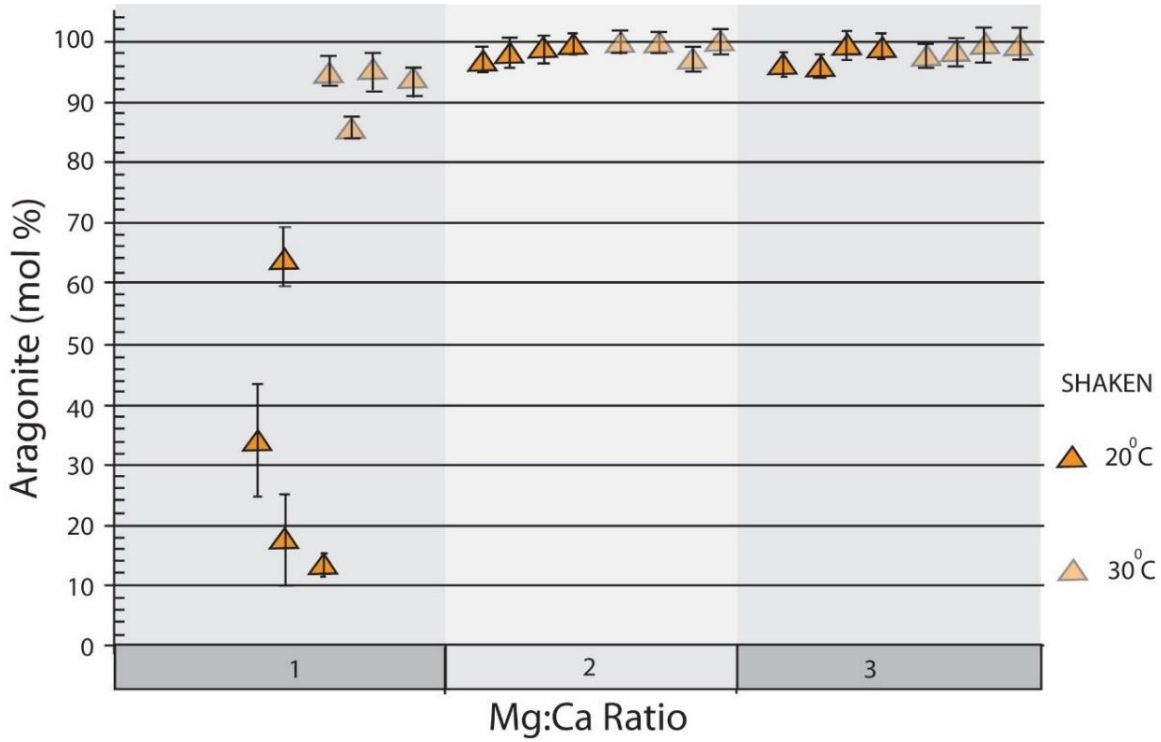

Figure 3-7: **The influence of higher temperature in shaken conditions on the mole percentage**. **Results are expressed as mean mole percentage of aragonite ± SD per scenario replicate, t = 20°C (dark orange), 30°C (pale orange), in shaken conditions (see section 2.1). Each scenario at was replicated four times.**

3.2.4.2 **The influence of temperature with water movement on the number of nucleations and crystal growth**

Shaken conditions at elevated temperature were observed to increase the proportion of aragonite/calcite crystal number compared to lower temperatures at all Mg:Ca ratios (***Figure 3-8A***). The influence of elevated temperature in shaken conditions is most evident at Mg:Ca ratio 1 and 2, but this is because the crystals formed at Mg:Ca ratio 3 at 20°C were already within the higher proportions of aragonite/calcite observed, therefore, increasing the temperature therefore had less impact on these proportions (***Figure 3-8***). The greatest increase in aragonite/calcite number was observed at Mg:Ca ratio of 3 which has the highest Mg^{2+} concentration present in solution. This suggests that calcite formation was inhibited by increasing the opportunity for Mg^{2+} to form attachments and incorporate into the calcite crystal lattice due to the shaken conditions, destabilising the lattice and inhibiting nucleation.

Overall, the number of aragonite crystals increased with either similar sized crystals forming or were larger at increased Mg:Ca ratio, whilst calcite crystals were decreased and of smaller sizes at higher Mg:Ca ratios in shaken conditions increased the proportion size of aragonite/calcite observed (***Figure 3-8B***). These observations suggest that increasing temperature under shaken conditions allows the activity of the ions to be increased to give opportunity for larger aragonite crystals to form by decreasing the energy requirements to attach to growth surfaces.

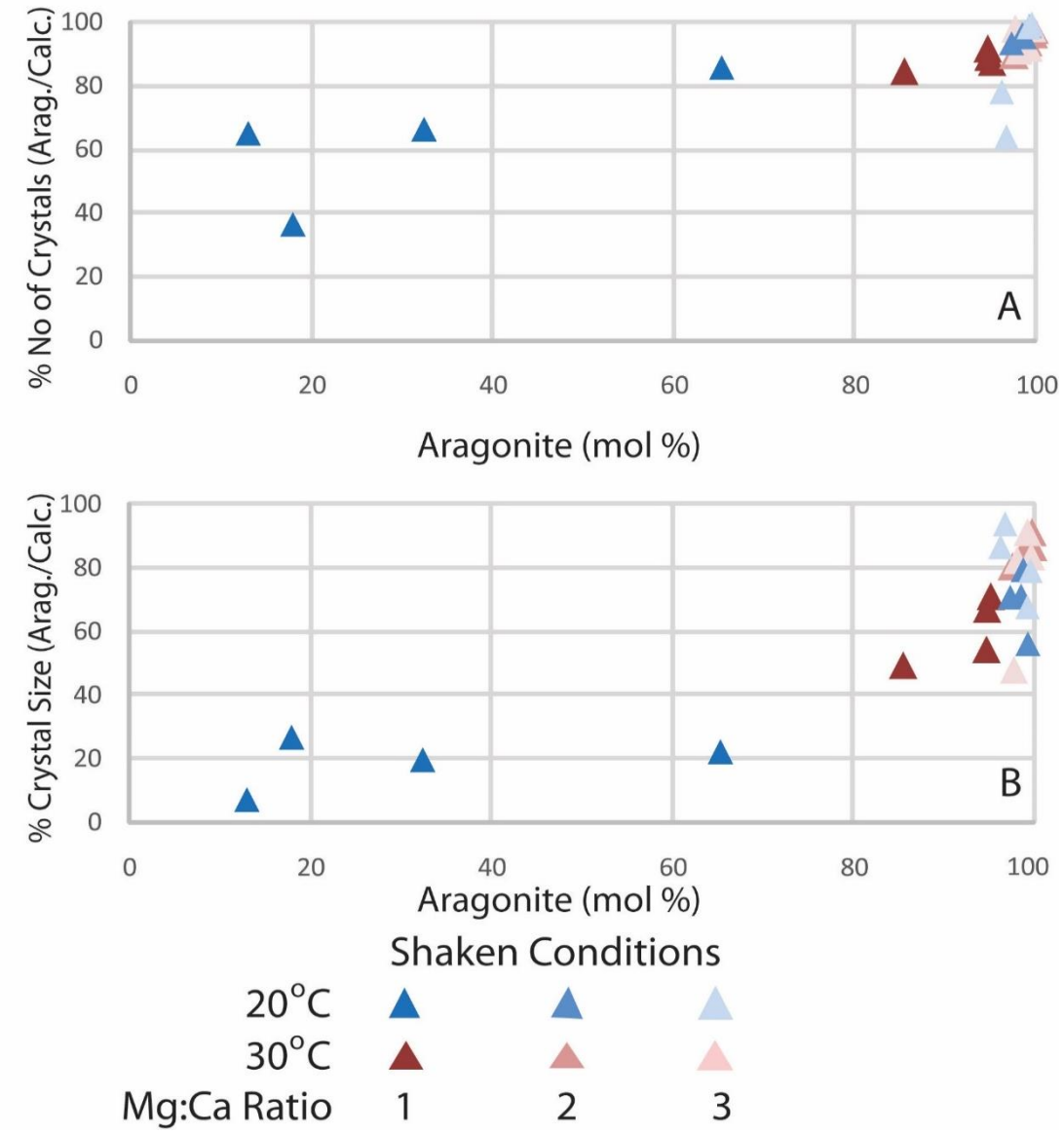

Figure 3-8 : The influence of water movement and temperature on the number and size of crystals.
Results are presented for the aragonite mole percentage against crystal number (A) and crystal size (B) from continuous addition method (section 2.1.) *t*= 20°C (blue squares) and t=30°C (red squares) in shaken conditions. Increased Mg:Ca ratio 1-3 is represented by change from dark to light colour. Upper graph A presents the average number of crystals of aragonite/calcite as a percentage. Lower graph B presents results of the average volume of crystals of aragonite/calcite acquired from bootstraps as a percentage.

In summary, shaken conditions with increased temperature at 30°C increased mole percentage of aragonite. This increase was due to the more crystals of aragonite forming of larger crystal size, whilst fewer crystals of calcite formed and were of smaller crystal size, increasing the proportion of aragonite to calcite compared to those formed at 20°C in shaken conditions.

3.2.5 Combined influences on polymorph precipitates.

3.2.5.1 The influence of Mg:Ca ratio, temperature and water movement on polymorph formation.

Results presented for the percentage of aragonite show that increased Mg:Ca ratio increases the percentage formed at increased Mg:Ca ratio, in still conditions at 20°C (Figure 3-9). This percentage was also further increased at higher temperature of 30°C at Mg:Ca ratio 2 and 3 (***Figure 3-9***). At Mg:Ca ratio 1 at 30°C the results were similar (***Figure 3-9***).

The influence of increased Mg:Ca ratios in shaken conditions at 20°C was to increase the percentage of aragonite compared to the proportion formed in still conditions at increased Mg:Ca ratio, at 20°C (***Figure 3-9***). Again, at increased Mg:Ca ratio in shaken conditions at a higher temperature of 30°C the percentage of aragonite was further increased compared to those formed under increased Mg:Ca ratio in still conditions at 30°C (***Figure 3-9***).

The increased proportion of aragonite formed at increased Mg:Ca ratios is in agreement with previous studies (Morse et al., 1997; Balthasar & Cusack, 2015). However, the results presented (***Figure 3-9***) show that at all Mg:Ca ratios, aragonite was facilitated, even below a Mg:Ca ratio of 2 which was previously thought to be the critical threshold for the switch between aragonite and calcite facilitation. The aragonite-calcite sea hypothesis was based on the concept that there was a global switch in the dominant mineralogy facilitated around the critical threshold of Mg:Ca ratio of 2 (Sandberg, 1975; Füchtbauaer & Hardie, 1976; Sandberg, 1985; Hardie, 1996). The largest increase in aragonite was formed at Mg:Ca ratio 1 in shaken conditions at 30°C. These results indicate that both aragonite and calcite co-precipitate at all Mg:Ca ratios, in agreement with results of Balthasar & Cusack (2015), and therefore that the dominant mineralogy formed may not occur in a spatially uniform pattern as previously hypothesised by Sandberg (1983).

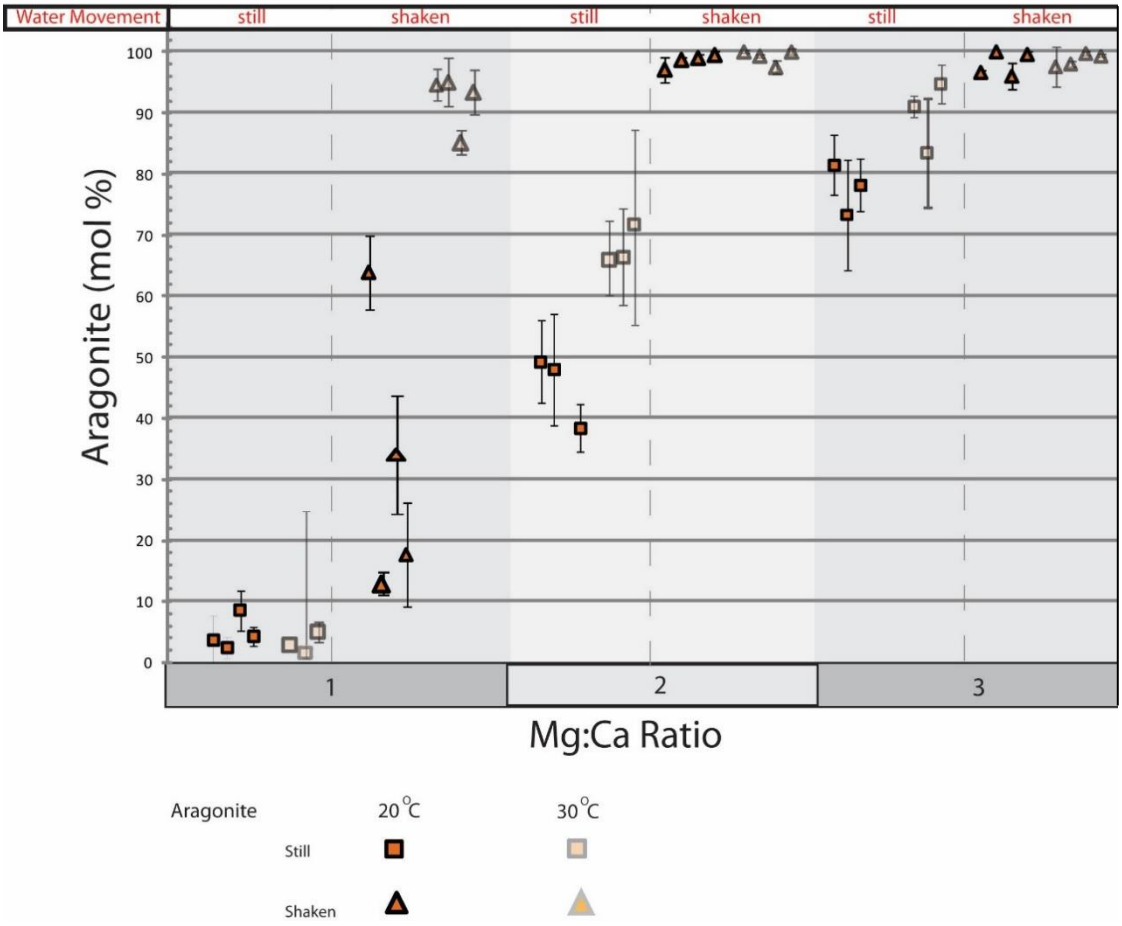

Figure 3-9: The influence of Mg:Ca ratio alongside temperature and water.
Results are expressed as mean mole percentage of aragonite ± 95% ci per scenario replicate at increased Mg:Ca ratio, for t = 20°C (dark orange) and 30°C (pale orange), in still conditions (squares) and shaken conditions (triangles) (see section 2.1).

In summary, an increase in Mg:Ca ratio increased the proportion of aragonite in conditions of still and shaken water movement and temperature of 20°C and 30°C. The influence of increased Mg:Ca ratio at higher temperature amplifies the proportion of aragonite formed.

3.2.5.2 **The influence of temperature, Mg:Ca ratio and water movement on polymorph formation.**

The influence of temperature at 30°C on polymorph formation increased the percentage of aragonite compared to 20°C formed under all parameters except at Mg:Ca ratio 1 in still conditions, where the proportion of aragonite stayed similar (***Figure 3-10***). The influence of temperature was greatest in still conditions where the largest increase of

aragonite was observed between precipitates formed at 20°C and those at 30°C at each Mg:Ca ratio (***Figure 3-10***). However, it must be noted that at higher Mg:Ca ratio the influence of higher temperature was less significant in shaken conditions, but this was because the proportions formed remain similar to these as they are already within the highest percentages possible (***Figure 3-10***).

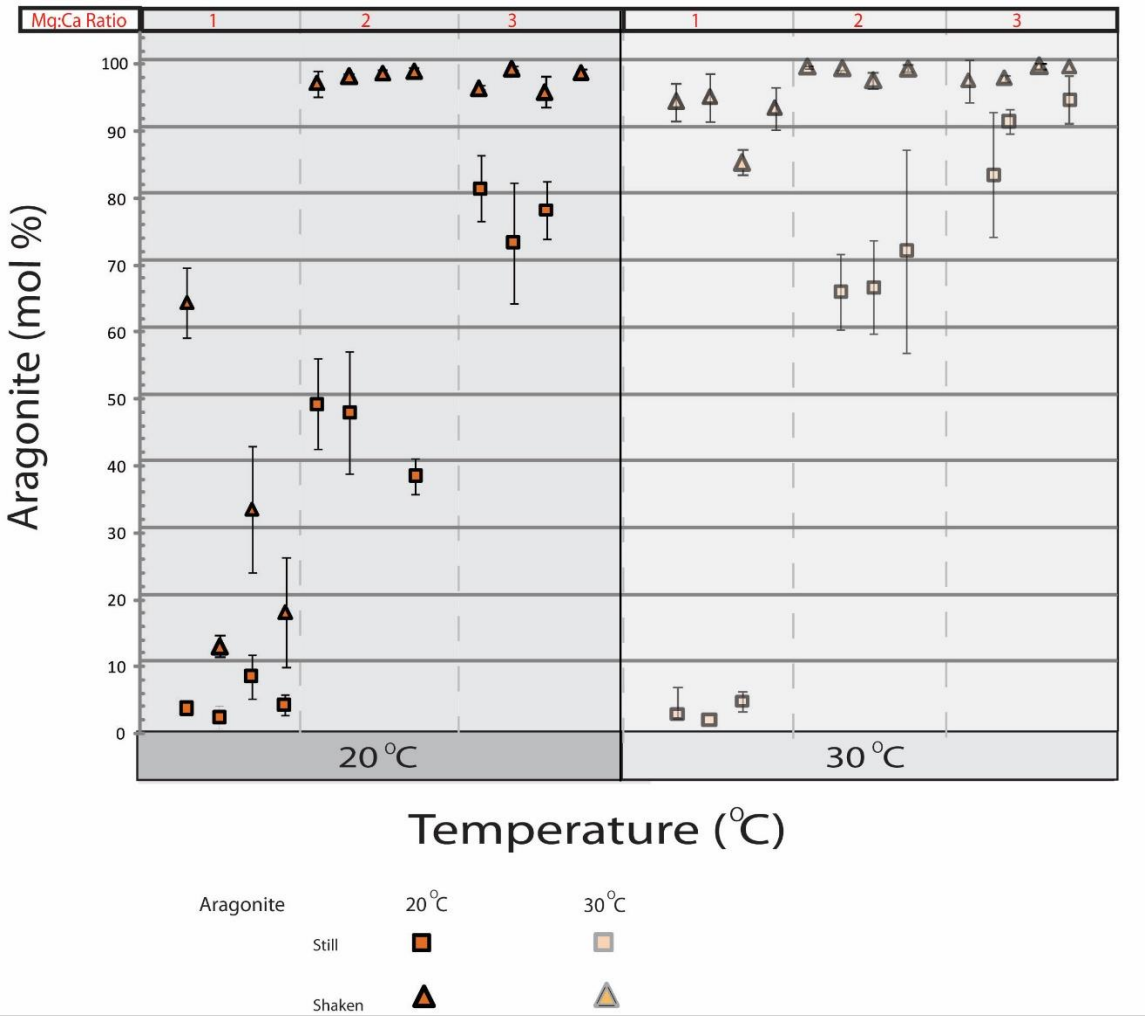

Figure 3-10: The influence of temperature, Mg:Ca ratio and water movement on the mole percentage of aragonite.
Results are expressed as mean mole percentage of aragonite ± 95% ci per scenario replicate for t = 20°C (dark orange) and 30°C (pale orange), in still conditions (squares) and shaken conditions (triangles) at Mg:Ca ratios 1, 2 and 3 (see section 2.1).

These results are in agreement with previous studies that higher temperature aids higher proportions of aragonite to form (Füchbauer & Hardie, 1976; Burton & Walter, 1987; Morse et al., 1997; Balthasar & Cusack, 2015). The incorporation of Mg^{2+} into calcite is

temperature sensitive and is a calcite growth inhibitor due to its incorporation altering the thermodynamic properties of calcite. Increased concentrations of Mg^{2+} in solution with higher temperature therefore facilitate more aragonite compared to calcite (Mucci & Morse, 1983; Sun et al., 2014).

In summary, higher temperature increases the proportion of aragonite formed in still and shaken conditions at higher Mg:Ca ratio 2 and 3 to above 65% (***Figure 3-10***). At Mg:Ca ratio of 1, calcite remains the predominant polymorph formed.

3.2.5.3 The influence of Water movement, Mg:Ca ratio and temperature on polymorph formation.

The influence of water movement on polymorphs formed was to increase the proportion of aragonite formed in all scenarios compared to still conditions (***Figure 3-11***). Water movement facilitates more than 80% aragonite under all parameters except at Mg:Ca ratio 1 at 20°C (***Figure 3-11***). The variance in the mole percentage of aragonite precipitated in shaken conditions at Mg:Ca ratio 1 at 20°C ranges between 12-65% (***Figure 3-11***). This variance can be accounted for due to the rapid and instantaneous precipitation which occurred under shaken conditions at Mg:Ca ratio 1 at 20°C, which may occur due to the lower concentration of Mg^{2+} in solution allowing precipitation to occur more readily of both aragonite and calcite.

The influence of water movement was added to the experimental set-up to assess environmental conditions similar to that of ooid formation. These results suggest that water movement increases the proportion of aragonite precipitated (***Figure 3-11***) and therefore the marine seawater movement would have significant influence of non-biogenic $CaCO_3$ precipitates forming. Further, these results suggest that shaken conditions in higher temperatures such as 30°C further increase the proportion of aragonite formed (***Figure 3-11***). This may be due to temperature increasing the activity of Mg^{2+} in solution and the water movement allowing more opportunity for it to incorporate into the crystal lattice of calcite inhibiting its growth, and facilitating aragonite formation. This suggests that if seawater temperature was to increase then the proportion of aragonite facilitated would be increased at any given Mg:Ca ratio, whereas what would be expected is at lower Mg:Ca ratio, calcite should be dominant.

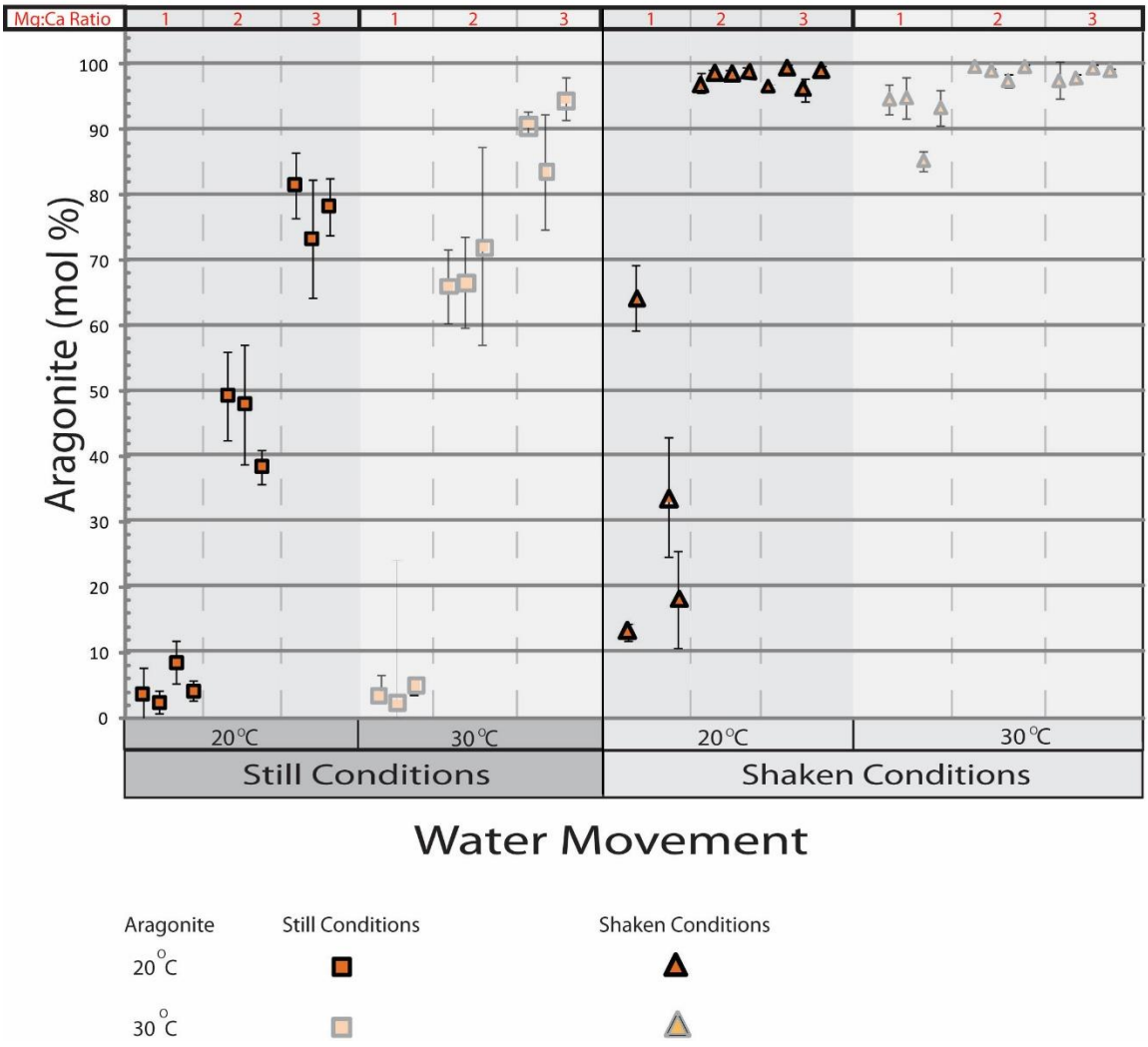

Figure 3-11: The influence of water movement alongside Mg:Ca ratio and temperature. Results are expressed as mean mole percentage of aragonite ± 95% ci per scenario replicate for still (squares) and shaken conditions (triangles) at t = 20°C (dark orange) and 30°C (pale orange), at Mg:Ca ratios 1, 2 and 3 (see section 2.1).

3.3 Discussion

3.3.1 The Influence of Mg:Ca Ratio

The mole percentage of aragonite precipitated was increased at higher Mg:Ca ratio in still conditions at 20°C (***Figure 3-1*).** The main aspect increasing the mole percentage at increased Mg:Ca ratio is the crystal size (***Figure 3-2AB***). Increased concentrations of magnesium present in solution facilitate the precipitation of aragonite by inhibiting the formation of calcite (Mucci & Morse, 1983). The influence of Mg:Ca ratio is likely to be due to the increased concentrations of Mg^{2+} present in solution. Mg^{2+} ions influences calcite

more so than aragonite. Mg^{2+} attaches to crystal surfaces, preventing calcite growth but they can also incorporate into the calcite crystal lattice, but Mg^{2+} is four times less likely to do so in aragonite (Mejri et al., 2014; Sun et al., 2015). The incorporation of Mg^{2+} ions into calcite alters thermodynamic properties increasing calcite solubility (Mejri et al., 2014; Sun et al., 2015). This impacts by decreasing calcite formation which was increasingly obvious at Mg:Ca ratio 3, where the highest proportions of aragonite to calcite nucleations occurred (***Figure 3-2***). Increased aragonite formation occurring at higher Mg:Ca ratio is in agreement with the evidence observed in the primary mineralogy of ooid formations from the Phanerozoic made by Sandberg (1975). From the ooids it was observed that calcite would be the dominant mineralogy facilitated at lower Mg:Ca ratios (Oligocene to Mid-Jurassic (25-175Ma), Late Pennsylvanian (285-305 Ma and Early Mississippian to Mid-Cambrian (335-545 Ma)). Aragonite would be facilitated at higher Mg:Ca ratios (Holocene – Miocene (0-25 Ma), Mid-Jurassic – Early Permian (175-285 Ma), Mid-Pennsylvanian – Late Mississippian (305-335 Ma) and Early Cambrian to late Precambrian (545-600+ Ma) (Gaffin, 1987)) (see Chapter 1, ***Figure 1-2***). The increase in aragonite formed at increased Mg:Ca ratio is also in agreement with the Morse et al. (1997) findings.

The increase in aragonite formation at higher Mg:Ca ratios has been documented in previous studies (Lippman, 1960; Folk, 1974; Füchbauer & Hardie, 1976; Wilkinson, 1979; Hardie, 1996; Stanley & Hardie, 1998; Morse et al., 2010; Bots et al., 2011; Balthasar & Cusack, 2015) and were hypothesised outcomes from these experiments. However, what these results disagree with in terms of the aragonite-calcite sea hypothesis is that at all Mg:Ca ratios the dominant mineralogy was never purely calcite or aragonite, but instead a co-precipitation of both polymorphs, agreeing with the findings of Balthasar & Cusack (2015). The evidence from this study that co-precipitation of aragonite and calcite occurs at all three Mg:Ca ratios, may explain why aragonite relics of gastropods and ammonites have been found within the rock record from the Phanerozoic, because they should have been prone to rapid dissolution in calcite-facilitating sea periods (Stanley & Hardie, 1998). The results presented show that below Mg:Ca ratio 2, calcite was indeed the most dominant polymorph formed in still conditions resulting in the lower mole percentage of aragonite formed (***Figure 3-1***). However, results from this study conclude that although the mole percentage of aragonite was higher at increased Mg:Ca ratio, calcite still remains the most dominant polymorph at Mg:Ca ratio of 2 unless temperature is considered (***Figure***

3-1). At Mg:Ca ratio 3, aragonite was the most dominant polymorph (***Figure 3-1***). Therefore, the dominant polymorph mineralogy, in terms of the influence of Mg:Ca ratio facilitating aragonite at Mg:Ca ratios above 2, does agree with the suggested critical threshold boundary of Mg:Ca ratio of 2 (Sandberg, 1975; Füchbauer & Hardie, 1976; Sandberg, 1985; Hardie, 1996) but only for still conditions at 20°C. The results presented here do not represent exclusivity to one polymorph type below Mg:Ca ratio 2 as previously proposed (Sandberg, 1983). The results also do not match previous studies that a lower Mg:Ca ratio of between 1 & 2 facilitated high Mg-calcite with no aragonite (Folk, 1974; Danberg, 1975; Füchbauer & Hardie, 1980; Lowenstein et al., 2001; Stanley, 2008), as aragonite was co-precipitated with calcite in all scenarios.

Results gained for the influence of Mg:Ca ratio increasing the mole percentage of aragonite at increasing Mg:Ca ratios, adds further evidence that the boundary between calcite and aragonite formation at Mg:Ca ratio of 2 needs reconsidered because aragonite was still precipitated at low Mg:Ca ratio (Lee & Morse, 2010; Bots et al., 2011; Balthasar & Cusack, 2015). This study has also documented that the mole percentage of aragonite increases due to crystal volume increase (***Figure 3-2B***) rather than in terms on numbers of nucelations (***Figure 3-2A***). This suggests there were more opportunities for nucleations of aragonite to occur because increasing concentrations of Mg^{2+} can facilitate the growth of aragonite at the expense of calcite. Mg^{2+} can incorporate into the crystal lattice of calcite by replacing Ca^{2+}, but this is much rarer in aragonite (Mucci & Morse, 1985). Mg^{2+} incorporation into the lattice of calcite will affect the surface processes and inhibit calcite nucleation and at the same time facilitate aragonite (Sun et al., 2015). As Mg^{2+} is 30 times less likely to adsorb to aragonite compared to calcite this will promote the formation of aragonite, increasing the possibility of aragonite growth (Mucci & Morse, 1985). In terms of crystal growth, an increased Mg:Ca ratio does not appear to influence aragonite/calcite growth as crystals formed at increased Mg:Ca ratio were of similar sizes at all Mg:Ca ratios (***Figure 3-2B***). This suggests ion activity was not increased or decreased, maintaining similar growth at all Mg:Ca ratios possibly due to hydrated Mg^{2+} ions being present in solution having slow exchange rates of their water molecules from the hydrated outer shell at 20°C in still conditions (Macguire & Cowan, 2002). The Mg^{2+} ions would therefore find it more difficult to form attachments as in order to free up bonds that can form attachment, they

must first release water molecules which kinetically is difficult preventing further growth (Macguire & Cowan, 2002).

Increased concentrations of Mg^{2+} within the solution allow for attachment of Mg^{2+} ions to the surface processes of calcite nucleations (Mucci & Morse, 1985). The Mg^{2+} blocks the possibility for growth after the initial nucleation making growth more difficult than nucleation (Morse et al., 2010). . This suggests that attachments to nucleation surfaces were easier to form from solution than further attachments to nucleations already formed. This explains why the proportion of aragonite to calcite size increases more than the aragonite to calcite crystal numbers formed (***Figure 3-2***). The initial nuclei is influenced by concentration of Mg^{2+} in solution, however following nucleation the concentration of Mg^{2+} has more influence on the induction time to full nucleation than to inhibit nucleation (Niedermayr et al., 2013). This may explain the calcite crystals formed being fewer in number due to increased Mg^{2+} whereas aragonite crystals forming were not as influenced.

Mg^{2+} incorporation into the calcite crystal lattice also alters thermodynamic properties of the crystal and increases its solubility and stability. Aragonite is more soluble compared to calcite and the lattice is more densely packed (Morse et al., 2007). However, the incorporation of Mg^{2+} into the calcite lattice destabilises the crystal lattice and increases its solubility (Sun et al., 2015). Therefore, the influence of Mg^{2+} on the lattice structures of aragonite and calcite may be pivotal in promoting aragonite over calcite at increased Mg:Ca ratio.

3.3.1 The Influence of Temperature

The facilitation of polymorph formation out of equilibrium with the Mg:Ca ratio they form in may be explained by temperature (Burton & Walter, 1987). The influence of temperature on $CaCO_3$ polymorph formation although documented in the literature to increase aragonite formation at the expense of calcite at higher temperature (Burton & Walter, 1987; Morse & Mackenzie, 1990; Burton, 1993; Morse & He, 1993), was often overlooked in favour of other drivers of carbonate formation such as Mg:Ca ratio or pCO_2. The presented results demonstrate that in still conditions, a higher temperature of 30°C resulted in an increased mole percentage of aragonite precipitated except at Mg:Ca ratio of 1 where the percentage of aragonite formed was similar, compared to 20°C (***Figure 3-3***).

The largest increase in mole percentage compared to 20°C occurred at Mg:Ca ratio 2 (***Figure 3-3***). An explanation for this could be that higher temperature alters the thermodynamics of calcite resulting in calcite crystals becoming less stable, and less predominant, compared to those of aragonite (Sun et al., 2015), and thus increasing the percentage of aragonite formed. Increased aragonite facilitation at higher temperature has been documented previously (Burton & Walter, 1984; Morse et al. 2010; Balthasar & Cusack, 2015) and were expected results as hypothesised for these current experiments. Again, like the influence of Mg:Ca ratio, increasing the aragonite mole percentage is due to increasing crystal volumes (***Figure 3-4B***) rather than crystal number (***Figure 3-4A***).

At increased temperature, the proportion of crystals of aragonite to calcite formed were similar at Mg:Ca ratio 1 and increased at Mg:Ca ratios 2 & 3 (***Figure 3-4A***). This was explained by the number of aragonite crystals formed increasing at increased Mg:Ca ratios and compared to lower temperature, whilst the crystals of calcite formed, decreased at increasing Mg:Ca ratio and increased temperature. It was considered that increased temperature does not alter the number of nucleations formed at Mg:Ca ratio of 1 compared to lower temperature (***Figure 3-4A***), because the opportunity for ions to attach to nucleation surfaces, and the activity of the ions in solution, remained the same compared to results for lower temperatures. However, at Mg:Ca ratios of 2 and 3, the number of nucleations of aragonite were increased compared to lower temperature (***Figure 3-4B***), suggesting increased temperature allows more opportunity for attachments to form by increasing the activity of the ions in solution (Sun et al., 2015). This may be a direct effect of temperature influencing the Mg^{2+} ions in solution as Mg^{2+} incorporation into calcite is temperature sensitive (Mucci & Morse, 1985). Mg^{2+} activity will increase at higher temperature allowing easier incorporation into the crystal lattice of calcite increasing its solubility resulting in more free ions, which can then be free for facilitation of aragonite nucleations at the expense of the change in thermodynamic properties of calcite.

Although the number of nucleations of aragonite was not greatly influenced until at higher Mg:Ca ratio, the proportion of aragonite to calcite volume at Mg:Ca ratios 2 and 3 was increased at higher temperature (***Figure 3-4B***). There was little difference between the ratio of aragonite to calcite size at Mg:Ca ratio of 1, but there was a greater variance on the sizes formed compared to lower temperature **(*Figure 3-4B***). Burton & Walter (1987)

also reported that temperature increased the growth rate of aragonite. This may be explained by the possibility that increased temperature facilitates growth to become easier and allows more opportunity for more ion collisions increasing the growth of aragonite at Mg:Ca ratio 2 & 3. At Mg:Ca ratio 1 increased temperature was not sufficient to increase the growth of aragonite crystals any larger than at cooler temperatures. However, as the number of nucleations of these crystals was increased this may indicate temperature increases the activity of ions so they find it easier to attach to new nucleations surfaces as opposed to allowing attachments to already formed nucleations to increase growth. He et al. (1994) observed that increased numbers of crystals may be due to increased temperature which increased the nucleation rate by decreasing the time of induction of nucleation. The increase in aragonite to calcite size may also be explained by the smaller crystals of calcite forming being due to having less opportunity to form attachments at higher temperature, most likely due to the presence of Mg^{2+} in solution, inhibiting growth sites (Mucci et al., 1983).

The fluctuations in temperature throughout the Phanerozoic are evident from isotopic analysis of carbon from pedogenic minerals in soil (Yapp & Poths, 1992) and phytoplankton within sediment cores (Pagani et al., 1999), C_3 plant stomatal pores (McElwain & Chaloner, 1995) and isotopic analysis of boron in planktonic foraminifera (Pearson & Palmer, 2000). Although these all indicate that the temperature throughout the Phanerozoic did fluctuate, how it evolved and how temperature influenced sea surface temperature are still not agreed upon (Royer et al., 2004; Wallman, 2004; Darrenougue et al., 2014; Hetzinger et al., 2018).

However, $CaCO_3$ formed in the marine environment is also segregated by polymorph type depending on the latitude and depth it formed at (Morse et al., 2007). This finding that increased temperature facilitates increases in aragonite formation compared to lower temperature is very important. Shallow marine pools are of warmer temperatures and form aragonite cements, whereas deeper waters and colder latitudes consist of calcite (Burton & Walter, 1987). Morse et al. (1997) proposed that $CaCO_3$ mineralogy was dependent on both the Mg:Ca ratio and temperature that it formed at. However, further constraint of the polymorph phases grown under parameters of Mg:Ca ratio and temperature show co-precipitation of aragonite and calcite occurs more often than pure

forms of $CaCO_3$ polymorphs at a wide range of Mg:Ca ratios (Balthasar & Cusack, 2015). Both of these studies (Morse et al., 1997; Balthasar & Cusack, 2015) used degassing of artificial seawater solution and therefore could have been influenced by changes in pH through degassing of solution. The constant addition technique used in this present study allowed pH to be held more stable and therefore the Mg:Ca ratio did not change through the timeframe of the experiment, allowing to pin point the exact constraints on polymorph formations.

In this study, higher temperature increased the percentage of aragonite formed at increased Mg:Ca ratio, suggesting that an increase in seawater temperature could facilitate non-biogenic aragonite where previously calcite was predominant by increasing the proportions of high Mg-calcite and aragonite facilitated (Burton & Walter, 1987). The implications of this could result in the formation of $CaCO_3$ out of equilibrium from the seawater Mg:Ca ratio from which it forms and therefore be prone to dissolution, especially as aragonite is less stable than calcite at present day surface conditions (Albright, 1971; Morse et al., 2007; Kawano, 2009). By aragonite being facilitated at increased temperature at the expense of calcite reinforces the importance of the influence of temperature in mineral formation in the natural environment. The aragonite-calcite sea hypothesis is based on the idea that homogeneous seawater chemistry oscillations occur which facilitate the $CaCO_3$ mineralogy formed (Sandberg, 1983). The findings of this study are in agreement with Balthasar & Cusack (2015), suggesting that the aragonite-calcite sea hypothesis must consider temperature as an influencer of aragonite-calcite seas as well as Mg:Ca ratio as latitudinal variations in temperature can influence the $CaCO_3$ polymorph facilitated.

3.3.1 The influence of Mg:Ca ratio & Temperature combined

The Mg:Ca ratio is considered the primary driving force behind the switches in mineralogy in aragonite-calcite seas (Hardie, 1996; Morse et al., 1997; Lowenstein et al., 2003). The substitution of magnesium for calcium in calcite is a function of Mg:Ca ratio and temperature (Burton & Walter, 1991; Morse et al., 2007). This substitution influences the stability of the lattice of calcite which can prevent calcite growth (Davis et al., 2000) but as substitution into the lattice of aragonite is very rare, aragonite stability is not effected in

the same way (Morse et al., 1997). Therefore, increasing the Mg:Ca ratio, increases the concentration of Mg^{2+} present in solution which should impact on calcite growth, but not influence aragonite growth in the same way. This can explain the increase in aragonite formed whilst the proportion of calcite formed decreased at increased Mg:Ca ratio (***Figure 3-3***). The results presented for the influence of temperature show that increased temperature increases the proportion of aragonite further at all Mg:Ca ratios except Mg:Ca ratio 1 where results at both 20°C and 30°C were similar (***Figure 3-3***). The influence of temperature solely can increase the formation of aragonite by allowing a lowering of the energy required to form nucleations (Ogino et al., 1987; Bots et al 2011). The present study's results are in agreement with Morse et al. (1997) and Balthasar & Cusack (2015) that there was a non-linear relationship between Mg:Ca ratio and temperature.

Morse et al. (1997) was the first to propose Mg:Ca ratio and temperature had a non-linear relationship which gave non-overlapping phases of $CaCO_3$ polymorphs precipitated from artificial seawater. However, Balthasar & Cusack (2015) further investigated this relationship and show that polymorphs of aragonite and calcite co-precipitate in varying proportions, aragonite being facilitated over calcite at higher Mg:Ca ratio and temperature. The present study's results are in agreement with the results of Balthasar & Cusack (2015) as co-precipitation occurred at all Mg:Ca ratios. The results of Balthasar & Cusack (2015) differ from Morse et al. (1997) by examination of the experiment precipitates in time slices throughout the run instead of the precipitates formed at the end of the 48hour experiment. This allowed for the first formed precipitates to be quantified giving a more accurate depiction of the constraints on the mineralogy formed, and therefore are more comparable to the results of the current study. The results of Balthasar & Cusack (2015) suggest that temperature has influence over mineralogy at a given Mg:Ca ratio.

The current study's results presented suggest that non-biogenic aragonite was facilitated instead of calcite under parameters of increased Mg:Ca ratio, and even more-so at increased temperature (***Figure 3-12 B***) agreeing with the findings of Balthasar & Cusack (2015) (***Figure 3-12 A***). Mg^{2+} into the calcite crystal lattice substituting for Ca^{2+} occurs as a function of both temperature and increasing Mg:Ca ratio (Burton & Walter, 1991; Bots et al., 2011). The results presented here suggest slightly lower percentages of aragonite form

at a given Mg:Ca ratio and temperature (***Figure 3-12B***) than formed with Balthasar & Cusack (2015) (***Figure 3-12A***). This was likely due to the solution chemistry being of lower saturation state, by use of constant addition methodology, due to the lower pCO_2 in solution (Zhong & Mucci, 1989) rather than degassing of supersaturated solution where saturation state would be higher. Comparison of the results presented with the results of Balthasar & Cusack (2015) (***Figure 3-12A***) show that even at a lower saturation state co-precipitation of aragonite and calcite has occurred, but that the mole percentage of aragonite formed is slightly lowered as hypothesised (***Figure 3-12B***). Further, this study shows that increased temperature increases the proportion of aragonite formed (***Figure 3-12B***) which follows the same trend as depicted by the results of Balthasar & Cusack (2015) (***Figure 3-12A***).

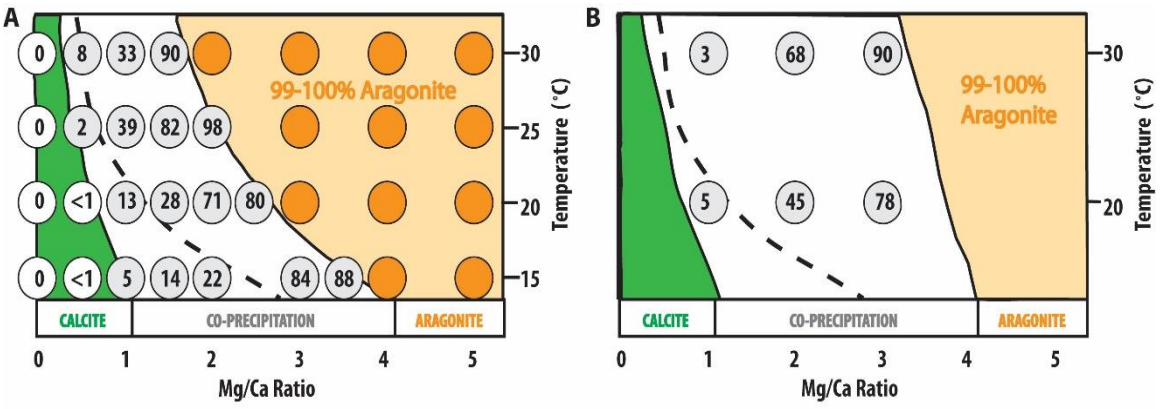

Figure 3-12: Comparison of previous degassing experiments (Balthasar & Cusack, 2015) to the present continuous addition results.
Balthasar & Cusack (2015) results (A) for $CaCO_3$ precipitates yielded from the degassing of artificial seawater solution in still conditions (Chapter 1, Figure 5) compared to (B) $CaCO_3$ precipitates from the presented continuous addition method (method discussed in section 2.1.2) in still conditions. Both A and B are presented as a percentage of aragonite yielded for the first-formed precipitates. The black dashed line in both A and B indicates the proposed boundary for the critical threshold switch in polymorph formation as proposed by Morse et al. (1997).

The findings of Balthasar & Cusack (2015) are important in the context of aragonite-calcite seas, as the aragonite-calcite sea hypothesis proposes a homogenous switch between calcite and aragonite being the dominant polymorph formed from seawater (Sandberg, 1983). Co-precipitation of polymorphs observed suggested that variations in temperature across the latitude could influence the mineralogy formed (Balthasar &

Cusack, 2015). The fastest rates of warming are occurring at the poles, where cooler temperature previously facilitated calcite, the warming the areas are succumbing to may increase the formation of aragonite, which is less stable (Albright, 1971). Higher temperatures facilitate the more incorporation of Mg^{2+} into calcite and therefore facilitate aragonite at the expense of calcite. The present study's results further emphasise the importance of temperature alongside the Mg:Ca ratio on polymorph formation. Here it has been observed that higher temperature increases the volume of the crystals of aragonite formed, without necessarily increasing the number of nucleations formed (***Figure 3-4***). This increases the proportion of crystal size of aragonite to calcite because at the same time fewer crystals of calcite form and these were smaller. This indicates that the crystal growth of aragonite is greatly increased by temperature suggesting a faster growth rate compared to calcite most likely influenced by the activity of Mg^{2+} inhibiting calcite growth and aiding the growth of aragonite (Mucci & Morse, 1985). The method of continuous addition used allowed for the first formed precipitates to be analysed under known seawater chemistry at their time of formation and show higher temperature increases the aragonite at the expense of calcite formed at al Mg:Ca ratios investigated.

3.3.2 The influence of Water Movement

The aragonite-calcite sea hypothesis was based on observations from the original mineralogy of ooids (Sandberg, 1975; Sandberg, 1983) where the mineralogy of ooids is observed to have oscillated between aragonite and calcite throughout the Phanerozoic, matching with oscillations in seawater chemistry (Sandberg, 1983). Constant addition method mimics the way influxes to ocean chemistry would occur. Water movement was added to the experiment set-up in order to mimic the natural environment from which ooids would precipitate from seawater. This allowed the subsequent $CaCO_3$ formation to be studied in a context more realistic to that of the natural marine environment.

Water movement was observed to increase the mole percentage of aragonite produced compared to still conditions (***Figure 3-11***). The largest increase in aragonite mole percentage was observed at Mg:Ca ratio 1 when compared to still conditions (***Figure 3-11***), suggesting that the lowest concentration of Mg^{2+} present in solution was given more opportunity in shaken conditions to influence nucleation and growth, facilitating aragonite

at the expense of calcite. Shaken conditions therefore increase the opportunity for Mg^{2+} to inhibit, and block the surface processes of the calcite crystal lattice, acting as a calcite growth inhibitor, increasing aragonite facilitation (Mucci & Morse, 1985; Morse et al., 2007).

The most interesting finding was that the increase in aragonite compared to calcite in shaking conditions was due to an increase in the percentage of nucleations of aragonite to calcite (***Figure 3-6A***). This was more notable at Mg:Ca ratio 1 and 2 where the percentage number of aragonite to calcite formed increased at Mg:Ca ratio 1 from 7.7% to 63.1% and Mg:Ca ratio 2 from 31.98% to 95.8% on average in still and shaken conditions respectively. This suggests that the addition of water movement allows enough agitation of the solution to allow an increased opportunity for ions to move past each other, and therefore for passing surfaces to which they can attach. At Mg:Ca ratio 3 the percentage of aragonite to calcite nucleations increased similarly to crystals formed at Mg:Ca ratio 2, but there was more variation in the number where increased numbers formed at the expense of crystal size (***Figure 3-6B***). One explanation for this is that the larger crystals formed result from many nucleation sites forming initially, and due to water movement the nucleations become dislodged and allow for agglomeration between the nucleated particles resulting in larger crystals.

The results observed may offer an explanation for aragonite ooid precipitation occurring out of equilibrium with the seawater chemistry, as aragonite is less stable that calcite under atmospheric conditions (Albright, 1971). Evidence from fluid inclusions in evaporite deposits record fluxes in seawater chemistry of the past and support secular changes in seawater chemistry (Lowenstein, et al., 2001; Horita et al., 2002) which support the switch in mineralogy suggested by the aragonite-calcite sea hypothesis (Sandberg, 1983). The evidence presented from this study indicates that co-precipitation occurs in all experiments therefore, there is no generic switch in mineralogy. These results indicate that the influence of water movement increased the proportion of aragonite formed (***Figure 3-5*)** by increasing the number of nucleations of aragonite to calcite rather than increasing crystal volumes (***Figure 3-6; Figure 3-11***). Aragonite is less stable than calcite and is prone to dissolution when formed out of equilibrium with the seawater and therefore less likely to be retained in the rock record (Kiessling, et al., 2008). This study examined the first

formed precipitates and therefore may indicate a more accurate representation of what originally would be facilitated.

Whilst aragonite was increasingly facilitated in shaking conditions as the Mg:Ca ratio was increased, the number of nucleations of calcite in shaken conditions decreased (***Figure 3-6B***). This may be due to water movement inhibiting opportunity for adhesion to nucleation surfaces, making nucleation more difficult than in still conditions. Water movement allows more opportunity for ions to pass nucleations allowing greater possibility for attachments to form. At Mg:Ca ratio 1 the crystal size was increased which could be due to water movement allowing more attachments to be made but the Mg^{2+} ions not being present in high enough concentrations to prevent calcite growth (Macguire & Cowan, 2002). The increase of aragonite to calcite nucleations also suggests that nucleation of aragonite was increasingly facilitated at the expense of calcite nucelations in shaken conditions, and therefore the results should represent a more realistic environmental context.

This could suggest that aragonite has more opportunity to occur as a first formed precipitate. As periods of calcite dominance are preserved in the rock record occur under calcite sea periods but aragonite is less stable, it may be prone to dissolution as out of equilibrium with the seawater chemistry leaving the calcite relics behind as they are found to co-precipitate in all experiments.

At Mg:Ca ratio 2 & 3 calcite growth was similar (***Figure 3-6***) and may be influenced by the water movement allowing more opportunity for Mg^{2+} ions to attach to growth surfaces but because there was a higher concentration of magnesium this acts in a way to prevent further growth and larger crystals from forming at these higher Mg:Ca ratios (Mucci et al., 1983).

3.3.2.1 **The influence of Water Movement and Temperature**

Under conditions of water movement, higher temperature facilitates more aragonite formation compared to calcite compared to sill conditions. Higher temperature increases the activity of the ions in solution and with the added water movement (***Figure 3-11***) this give more opportunity to form attachments to nucleation surfaces. This suggests

that calcite-facilitating conditions therefore were decreased and much rarer and aragonite was facilitated at the expense of calcite. The boundary for 99-100% aragonite was shifted to the left under shaken conditions compared to still conditions due to the increase in aragonite formed at both 20°C and 30°C (***Figure 3-13***). The 'co-precipitation' field under shaken conditions was of higher percentages of aragonite with the highest calcite proportion being 68% compared to 97% under still conditions. These results are similar to the results of Balthasar & Cusack (2015) from degassing experiments in still conditions which were yielded under higher saturation state where their results achieved 99-100% aragonite precipitation in most experiments at Mg:Ca ratio 3 and above (***Figure 3-12A***). Shaken conditions results from this study yield above 98% at Mg:Ca ratio 2 and above (***Figure 3-13B***).

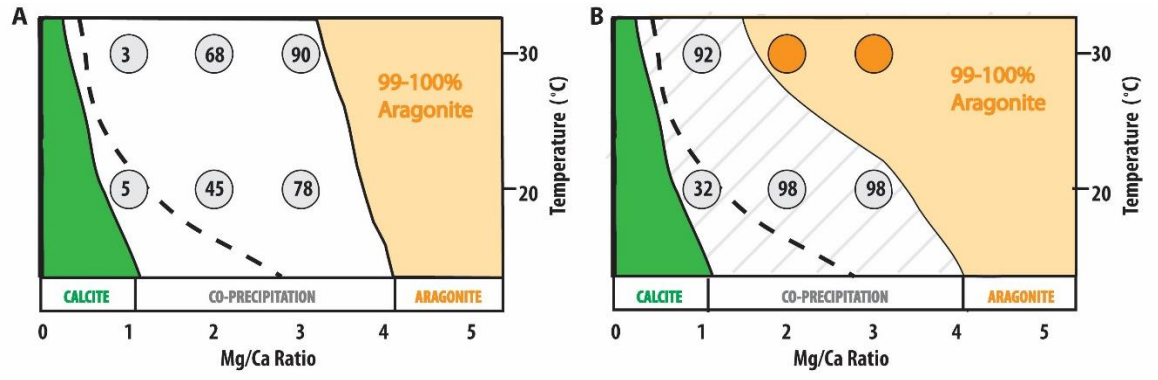

Figure 3-13: Comparison of $CaCO_3$ precipitates under the influence of water movement from the continuous addition method results.
Comparison of results from continuous addition method (section 2.1.2) in still conditions (A) and shaken conditions (B) presented in figure style of Balthasar & Cusack (2015) (Chapter 1, Figure 5). Both A and B are presented as a percentage of aragonite yielded for the first-formed precipitates. The black dashed line in both A and B indicates the proposed boundary for the critical threshold switch in polymorph formation as proposed by Morse et al. (1997).

One difference between this study's results and the Balthasar & Cusack (2015) was that this study presents 'co-precipitation' fields which yield a smaller range results for the percentage of aragonite (32-99%) at Mg:Ca ratios 1-3, which were of higher percentages of aragonite obtained at lower Mg:Ca ratio than in the results of Balthasar & Cusack (2015) (3-90% at Mg:Ca ratios 1-3). Bots et al. (2011) also reported high proportions of aragonite formation in their sulphate-free solutions, also from shaken conditions under constant addition precipitation experiments, at 21 °C (>99.5% from Mg:Ca ratio 0.96 to 5.22) which

are at a similarly high percentage to this study's shaken conditions results. By using constant addition technique and water movement allowed for the current study to be a more accurate representation of the polymorphs that precipitate first. Using this technique could therefore can be viewed as a more accurate representation for application to the marine environment where ooids would form. Temperature increases the growth rate of aragonite faster than calcite (Burton & Walter, 1987) and the results presented observed increased growth of aragonite ***Figure 3-8***). Higher temperature increases the Mg^{2+} content of calcite increasing its solubility (Berner, 1975) allowing aragonite growth which although less stable than calcite at room temperature and pressure, is preferentially facilitated (Kawano et al., 2009). This trend was increasingly facilitated in shaken conditions at higher temperature (***Figure 3-11***). The observed increase in aragonite formed in shaken conditions with higher temperature suggest that in the natural marine environment if temperature increased more aragonite will be facilitated even at a lower Mg:Ca ratio. Lowered Mg:Ca ratios were previously thought to be a calcite-facilitator (Sandberg, 1975; Stanley & Hardie, 1998; Morse et al., 2007). This ultimately could lead to increased solubility of aragonite polymorphs if temperature variations across the latitudes are considered. The seawater chemistry would be influenced to precipitate polymorphs out of equilibrium with the seawater they form from, facilitated by increased temperature and water movement.

3.4 **Conclusions**

Non-biogenic $CaCO_3$ precipitation experiments were carried out to allow the parameters of Mg:Ca ratio, temperature and water movement to be investigated into how they influence $CaCO_3$ polymorph formation. Results presented answer all aims of the chapter to show that not only does increased Mg:Ca ratio of solution increase the percentage of aragonite formed, temperature and shaking conditions also increases the proportion of aragonite formed. These three parameters are important influences that need to be considered when assessing non-biogenic $CaCO_3$ mineralogy under the constraints of the aragonite-calcite sea hypothesis.

The results from precipitation experiments for the first three objectives are summarised in **Table 3-1.** A key finding from this study was that in all experiments aragonite

and calcite were found to co-precipitate, indicating that polymorph precipitation does not shift from one mineralogy to another as previously suggested (Stanley & Hardie, 1998). The present study also differs from the work of Morse et al., (1997) who suggested non-overlapping precipitation fields dependent upon the Mg:Ca ratio and temperature together but further supports the findings of Balthasar & Cusack (2015) who presented 'mixed' fields of co-precipitation of aragonite and calcite from degassing experiments of supersaturated solution. This study shows that at even at a lower saturation state, the proportion of aragonite to calcite was increased at higher Mg:Ca ratio, elevated temperature and in water movement.

In all experiments, aragonite and calcite were found to co-precipitate, supporting evidence that polymorph precipitation does not shift from one mineralogy to another, as previously suggested (Stanley & Hardie, 1998). This differs from the aragonite-calcite sea hypothesis which proposes a generic switch between calcite and aragonite sea conditions, where co-precipitation would only occur above Mg:Ca ratio 2 (Stanley & Hardie, 1996), as my results show co-precipitation at Mg:Ca ratios of 1. This however, is in agreement with recent results of Balthasar & Cusack (2015) who observed $CaCO_3$ crystals formed in distinct polymorph growth fields as a function of temperature and that temperature is key in facilitating polymorph selection at a given Mg:Ca ratio. This study's results also suggests that water movement amplifies the influence of Mg:Ca ratio and temperature to facilitate more aragonite at the expense of calcite. This is important when considering the natural marine environment where non-biogenic $CaCO_3$ forms, such as ooid formations. Mg:Ca ratio is viewed as the driving force behind aragonite-calcite sea periods, however, the results from this study show that both temperature and water movement also influence the mineralogy to increase the proportion of aragonite formed, even at a lower Mg:Ca ratio. This could give an explanation for ooid precipitation of aragonite primary mineralogy out of equilibrium with seawater chemistry of lower Mg:Ca ratio.

	Influence of Mg:Ca ratio (at increased ratios 1-3)			Influence of Temperature (20 & 30°C)			Influence of Water Movement (still vs shaken conditions)			Influence of Water Movement and Elevated Temperature Combined		
KEY + increase - decrease ~ no obvious trend	Av. mole %	% number (arag./calc.)	% size (arag./calc.)	Av. mole %	% number (arag./calc.)	% size (arag./calc.)	Av. mole %	% number (arag./calc.)	% size (arag./calc.)	Av. mole %	% number (arag./calc.)	% size (arag./calc.)
	+	+	+	+	+	+	+	+	+	+	+	+

Table 3-1: Summary of the influences of Mg:Ca ratio, temperature and water movement on non-biogenic $CaCO_3$ polymorphs. The three parameters' influences on $CaCO_3$ polymorph precipitation (Mg:Ca ratio, temperature and still/shaken conditions) are summarised in the table to indicate changes in the mole percentage of aragonite, numbers of crystals precipitated and the average size of crystal precipitated. Each parameter is summarized to show the change to polymorph precipitation as the Mg:Ca ratio increased from 1-3.

This study adds further support that aragonite-calcite sea theory needs to be revaluated as the hypothesis is based on a generic switch between calcite and aragonite sea conditions, where co-precipitation would only occur above Mg:Ca ratio 2 (Stanley & Hardie, 1998). Each of the parameters of increased Mg:Ca ratio (***Figure 3-1***), increased temperature (***Figure 3-3***) and shaken conditions (***Figure 3-5***) influence the mineralogy to increase the percentage of aragonite formed, further these parameters combined together amplify the increase in aragonite observed in formed $CaCO_3$ precipitates (***Figure 3-9, Figure 3-10 and Figure* 3-11**).

4

The influence of sulphate and parameters of Mg:Ca ratio, temperature and water movement on non-biogenic $CaCO_3$ polymorphs

Evidence contained from halite fluid inclusions within abiotic marine deposits reveal that the Mg:Ca molar ratio has co-varied with sulphate (SO_4^{2-}) throughout the Phanerozoic (Lowenstein et al., 2001; Horita et al., 2002; Lowenstein et al., 2003). When magnesium (Mg^{2+}) concentration increases, so does the SO_4^{2-} level, matching with aragonite-facilitating $CaCl_2$ sea periods (Lowenstein et al., 2003) (Chapter 1, ***Figure 1-7***). $CaCO_3$ precipitates forming are influenced by changes in seawater chemistry (Railsback & Anderson, 1987). Changes in chemistry (e.g. SO_4^{2-} presence) therefore may influence the precipitation parameters of the first formed polymorphs of $CaCO_3$. The study presented investigates the influence of sulphate on $CaCO_3$ polymorphs grown under constant addition method as discussed in Chapter 2. This chapter's results allow direct comparison to the polymorphs precipitated in sulphate-free scenarios presented in Chapter 3 precipitated at Mg:Ca ratio 1, at 20°C and 30°C in still and shaken conditions, but with the added influence of sodium sulphate within the mother solution.

4.1 Introduction

Seawater chemistry has been championed as the main driver for the switch between calcite-dominant seas and aragonite-dominant seas (Hardie, 1996). Previous work has shown that polymorph selection is a function of both Mg:Ca ratio and

temperature (Morse et al., 1997; Balthasar & Cusack, 2015) (Chapter 3). 'Calcite seas' were proposed to lie between Mg:Ca ratios of 0.9 to 1.7 (Horita et al., 2002), but the mineralogy formed at these times is noted rarely to be pure calcite (Adabi, 2004; Wilkinson et al., 1985; Zhuravlev & Wood, 2009), matching well with the co-precipitation presented in the results presented in Chapter 3 Balthasar & Cusack (2015).

SO_4^{2-} is ubiquitous to the marine environment of evaporite formation (Schultz & Zabel, 2007 in Fernandez-Diaz et al 2010). Growing $CaCO_3$ crystals incorporate foreign ions present in solution into their lattice structure, the SO_4^{2-} ion is one impurity which can retard the growth of calcite when SO_4^{2-} present in solution (Davis et al., 2000; Fernandez-Diaz et al., 2010). When SO_4^{2-} is present an increase the uptake of Mg^{2+} ion into the crystal lattice of calcite occurs (Busenberg & Plummer, 1985), a known calcite growth inhibitor. However, the presence of SO_4^{2-} alongside the influence of Mg:Ca ratio on polymorph formation has previously been neglected (Lee & Morse, 2010). The critical threshold of Mg:Ca ratio 2, was proposed by Bots et al. (2011) to be lowered in the presence of higher SO_4^{2-} concentrations, lowering the Mg:Ca ratio aragonite would occur. Therefore, if the critical threshold is lowered in the presence of SO_4^{2-} this would suggest calcite-facilitating sea periods would be rare (Bots et al., 2011). Further, when Mg^{2+} and SO_4^{2-} concentrations are increased they will favour the precipitation of aragonite at the expense of calcite (Burton, 1993). This is due to SO_4^{2-} having a greater influence over the calcite stability and rate of calcite precipitation than it does on aragonite (Walter, 1986). Bots et al. (2011) proposed a threshold of 5mM SO_4^{2-} and Mg:Ca ratio >0.3 which is much lower than seawater chemistry composition evidence gained from fluid inclusion data (Hasiuk & Lohmann, 2008; Newton et al., 2011). Therefore, if increased concentrations of SO_4^{2-} increase the proportion of aragonite formed (Busenberg & Plummer, 1985; Kontrec et al., 2004; Bots et al., 2011; Tang et al., 2015), and increased temperature also increases aragonite at the expense of calcite (Morse et al., 1997; Balthasar & Cusack, 2015; also, see Chapter 3), do the effects of SO_4^{2-} and temperature together also increase the proportion of aragonite formed?

4.2 Aims of the chapter

The continuous addition method set-up (section 2.1.2.) was designed to quantify the proportions of $CaCO_3$ polymorphs grown under the constraints of Mg:Ca ratio, temperature and water movement (presented in Chapter 3). As polymorph formation is influenced by ions in solution such as Mg^{2+} uptake into calcite, inhibiting growth and preventing nucleation of crystals, then SO_4^{2-} in solution could also have an influence on $CaCO_3$ precipitation. To place the results in the context of a more realistic natural seawater environment the influence of SO_4^{2-} was added to the continuous addition methodology (section 2.1.2.1.) The main objectives for this study were threefold:

(i) To quantify the influence of SO_4^{2-} on the first-formed $CaCO_3$ polymorphs at a Mg:Ca ratio of 1.

(ii) To quantify the influence of SO_4^{2-} on the first-formed $CaCO_3$ polymorphs at temperatures of 20°C and 30°C at a Mg:Ca ratio of 1.

(iii) To quantify the influence of SO_4^{2-} on the first-formed $CaCO_3$ polymorphs formed in shaken conditions at a Mg:Ca ratio of 1 at 20°C and 30°C.

No work has been done to show how precipitation of the first-formed $CaCO_3$ polymorphs are altered in relation to each other under the constraints of SO_4^{2-}, Mg:Ca ratio and temperature together in still and shaken conditions.

It was hypothesised that the presence of SO_4^{2-} should increase the proportion of aragonite compared to calcite therefore the choice of Mg:Ca ratio to be used was important so that a proportion of aragonite to calcite could be quantified. Sulphate-free scenarios discussed in Chapter 3 presented the lowest formed percentage of aragonite at Mg:Ca ratio 2 yielded 45% aragonite at 20°C, and 68% aragonite at 30°C, therefore already in the upper reaches of possible outcomes, especially at higher temperature. By selecting Mg:Ca ratio of 1 for the SO_4^{2-} comparison aimed to have a proportion of aragonite to calcite for all sulphate-present scenarios, therefore comparable to a 'calcite-dominance' suggested by Bots et al. (2011).

The combination of Mg:Ca ratio 1 and an end-target sulphate concentration of 5mM SO_4^{2-} was selected as this concentration was also the lowest SO_4^{2-} concentration

found within the Phanerozoic as suggested from halite fluid inclusions and basinal brine data modelling (Horita et al., 2002; Lowenstein et al., 2003) and should still influence polymorph formation. Tang et al. (2012) shows that higher concentrations of SO_4^{2-} decrease the nucleation rate and favours aragonite growth, therefore would not allow for quantification of calcite dominance due to dominance of aragonite. By adding SO_4^{2-} to these parameters already investigated will give an idea of the influences from natural influxes to seawater on the $CaCO_3$ polymorphs.

4.3 **Results**

Results are presented in this section for the percentage of aragonite formed, and for the number and the size of crystals of aragonite and calcite formed from continuous addition method (section 2.1.2.1.) of artificial seawater solution Mg:Ca ratio 1 with 5mM SO_4^{2-} (end concentration). In this study, no vaterite crystals were observed. Bots et al. (2011) document having observed vaterite within their continuous addition precipitation study, however they did not look at the first-formed crystals. Vaterite is the least stable of $CaCO_3$ polymorphs and therefore may have occurred but be unstable and re-dissolve into solution. Low concentrations of SO_4^{2-} ions have previously shown to inhibit vaterite but enable calcite formation (Cailleau et al., 1979; Tlili et al., 2006; Paquette et al., 1996; Mejri et al., 2014) and in this study calcite was formed under all scenarios and may be a reason for no evidence of vaterite formation. Previous studies have shown that in order for vaterite to occur, calcite formation would have to be inhibited to a higher degree (Busenberg & Plummer, 1985; Vavouraki et al., 2008; Bots et al., 2011). As calcite was formed in all scenarios this suggests that calcite formation was not inhibited more than vaterite. Results presented were statistically tested by application of bootstrap statistics to test the data to within 95% ci.

The first-formed precipitates for all experiment scenarios were achieved within the 6-hour experiment timeframe with the lower temperature of 20°C and shaken conditions taking the longest time to nucleate (2 hours longer than 20°C in still conditions). The highest percentage of aragonite formed was 92.9% and the lowest was 10.9%, indicating co-precipitation of aragonite and calcite in all scenarios. The co-precipitation results presented here were of a similar finding to the results presented in Chapter 3, and are a

result which is in agreement with Balthasar & Cusack (2015), indicating that polymorph precipitation does not shift from one mineralogy to another as a generic switch as previously suggested (Stanley & Hardie, 1998).

4.3.1 The influence of sulphate

4.3.1.1 The influence of sulphate on the percentage of aragonite

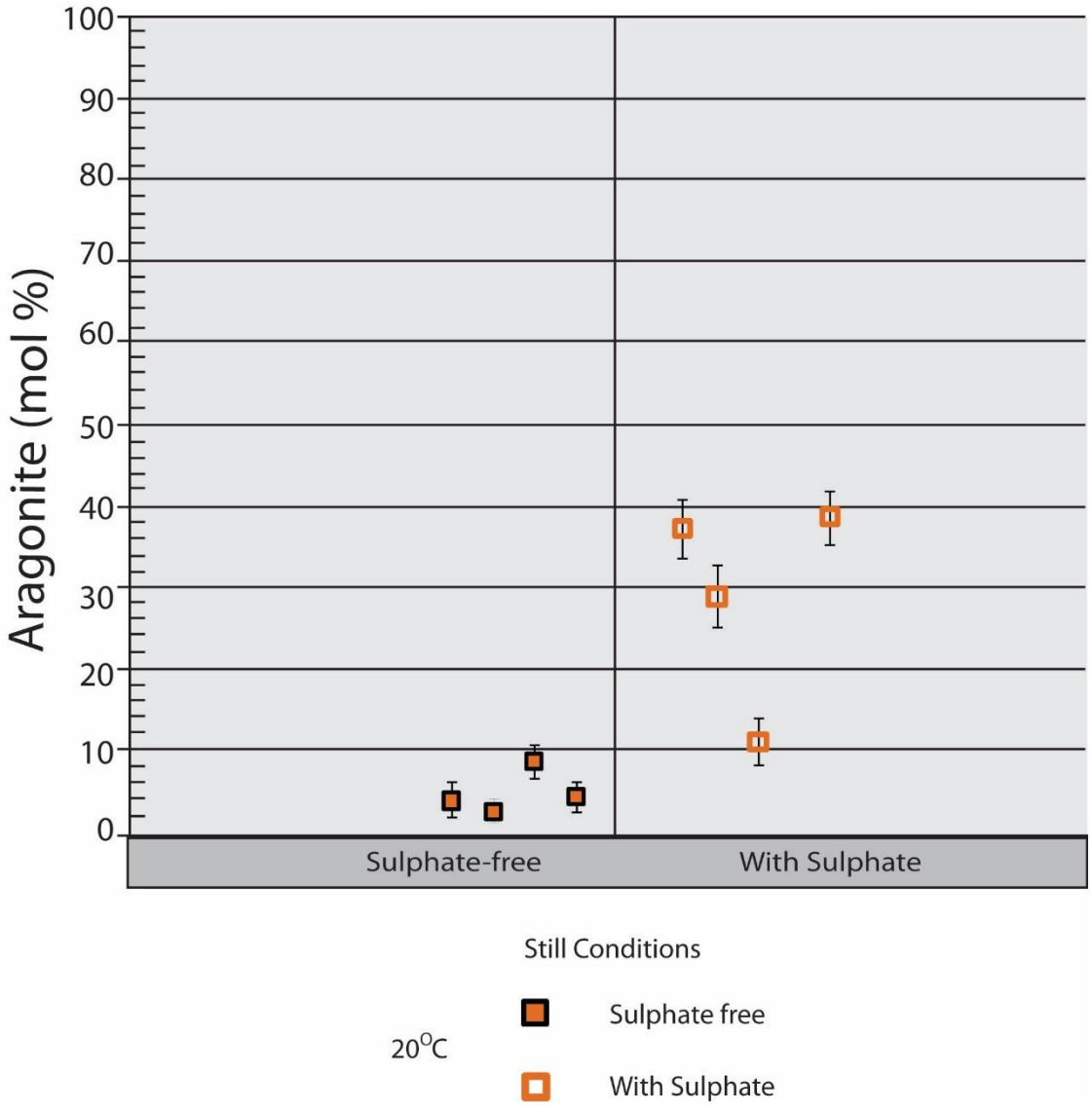

Figure 4-1: Influence of sulphate on the mole percentage of aragonite.
Results are expressed as mean mole percentage of aragonite ± 95% ci per scenario replicate, *t* = 20°C, for still conditions in sulphate-free scenarios (closed datum) (see section 2.1.) and scenarios with (end target) 5mM SO_4^{2-} in solution (open datum).

When SO_4^{2-} was present the mole percentage of aragonite was increased compared to sulphate-free scenarios (***Figure 4-1***). This suggests that the presence of

SO_4^{2-} allows more aragonite to form by inhibiting the formation of calcite, matching previous results (Busenberg & Plummer, 1985; Kontrec et al., 2004; Vavouraki et al, 2008; Bots et al., 2011; Tang et al., 2012). This may be due to the SO_4^{2-} ion substituting for carbonate (CO_3^{2-}) in the lattice of calcite which would allow more Mg^{2+} into the calcite crystal lattice due to stretching of the bonds (Kontrec et al., 2004), altering the thermodynamic properties of calcite and making it more susceptible to dissolution (Busenburg & Plummer, 1985). The increase in the aragonite percentage also agrees with previous investigation, where SO_4^{2-} aids preference to aragonite formation compared to calcite (Bots et al., 2011).

4.3.1.2 **The influence of sulphate on the number of nucleations and crystal growth**

The presence of SO_4^{2-} increases the number of nucleations aragonite/calcite (open squares) in comparison to the number of nucleations produced in sulphate-free scenarios (closed squares) (***Figure 4-2A***). This suggests that the presence of SO_4^{2-} aids the nucleation of aragonite crystals whilst preventing more nucleations of calcite compared to sulphate-free scenarios, maintaining the number of calcite crystals resulting in the increased aragonite mole percentage observed.

The mole percentage of aragonite that was increased (***Figure 4-1***) was due to the number of nucleations of aragonite increasing compared to the number of nucleations of calcite (***Figure 4-2A***), rather than an increase in crystal size (***Figure 4-2B***). The size of the aragonite crystals formed in the presence of SO_4^{2-} were similar to those from sulphate-free conditions, however, the calcite crystals formed were slightly smaller than those from sulphate-free conditions, which resulted in a similar ratio of aragonite to calcite crystal size as in sulphate-free conditions (***Figure 4-2B***). This suggests that the presence of SO_4^{2-} made it easier for attachments to form, resulting in the number of nucleations increasing rather than by increasing crystal growth. As the presence of SO_4^{2-} in still conditions, at 20 °C, does not inhibit or promote the calcite growth of the first-formed precipitates (***Figure 4-2B***). This result agrees with the previous work of Reddy & Nancholas (1976) who noted SO_4^{2-} ions inhibited the dissolution of calcite allowing crystal formation but that the precipitation rate would be supressed, slowing the growth of the crystals. This may be because SO_4^{2-} has less influence on the morphology of aragonite compared

to calcite (Busenberg & Plummer, 1985; Zuddas & Mucci, 1994; Kontrec et al., 2004; Tang et al., 2012), therefore allowing aragonite formation more so than calcite.

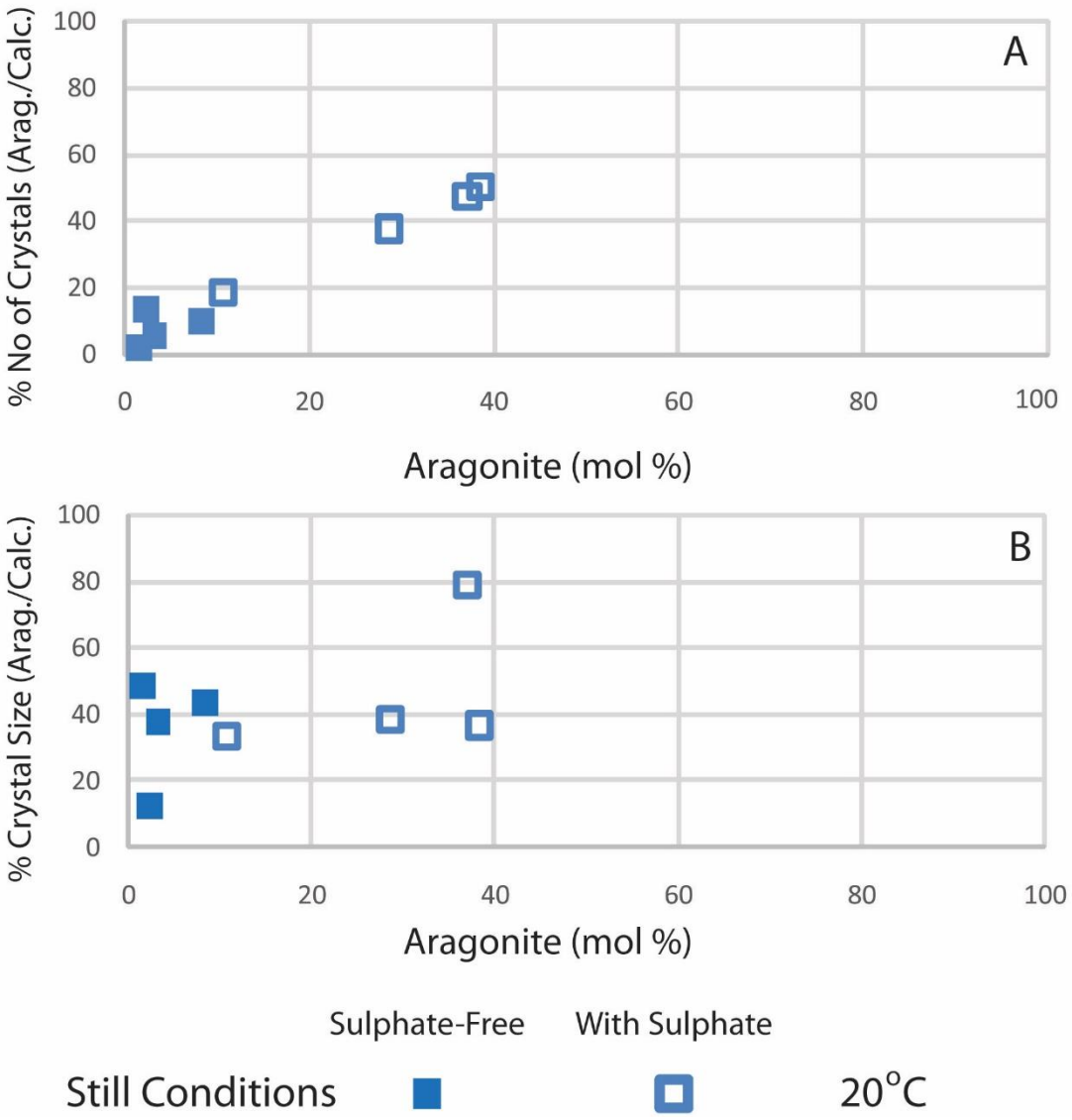

Figure 4-2: The influence of sulphate presence on the number and size of crystals in still conditions at 20°C.
Results are presented for the aragonite mole percentage against crystal number (A) and crystal size (B) from continuous addition method (section 2.1.) *t*= 20°C in still conditions, sulphate-free scenarios (closed datum) and scenarios with (end target) 5mM SO_4^{2-} present (open datum). Upper graph A presents the average number of crystals of aragonite/calcite as a percentage. Lower graph B presents results the average volume of crystals of aragonite/calcite as a percentage.

In summary, the presence of sulphate increases mole percentage of aragonite formed at 20°C in still conditions. The increase in the percentage of aragonite formed

was due to the number of nucleations of aragonite increasing in the presence of SO_4^{2-} compared to sulphate-free scenarios.

4.3.2 The influence of sulphate and temperature

4.3.2.1 The influence of sulphate and increased temperature on the percentage of aragonite

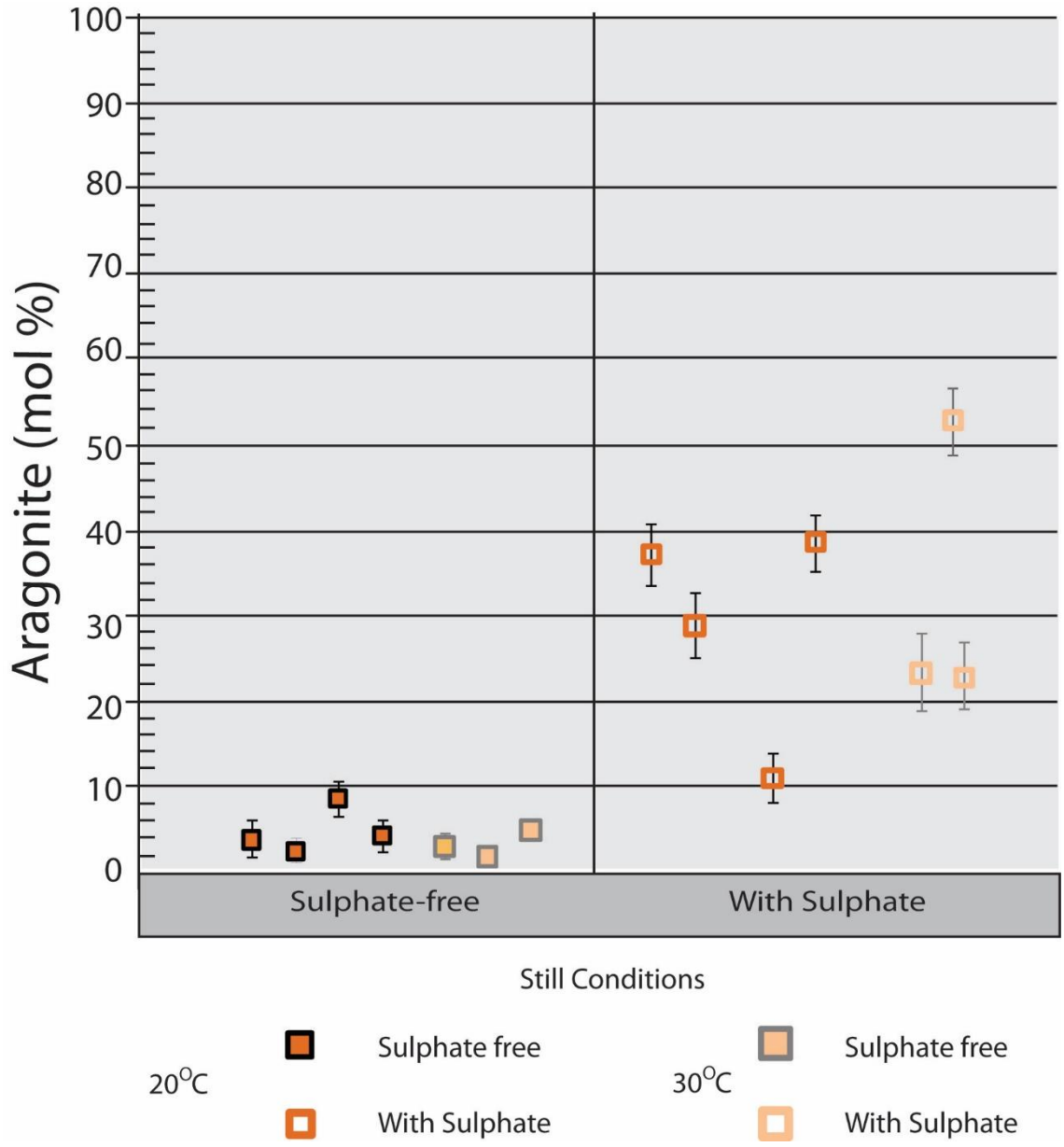

Figure 4-3: The influence of sulphate and higher temperature on the percentage of aragonite. Results are expressed as mean ole percentage of aragonite ± 95% ci per scenario replicate, *t*= 20°C (dark orange) & 30°C (pale orange), still conditions, sulphate-free (closed datum) and scenarios with (end target) 5mM SO_4^{2-} present (open datum).

The influence of SO_4^{2-} increased the percentage of aragonite formed at higher temperature of 30°C (pale orange, open squares) compared the lower temperature of 20°C (dark orange, open squares) ***(Figure 4-3***) and also increased the percentage of aragonite at both 20°C and 30°C compared to that formed in sulphate-free scenarios (closed squares) (***Figure 4-3***). The presence of SO_4^{2-} appears to amplify the influence of temperature and may be due to allowing SO_4^{2-} to increase the percentage of aragonite by aiding Mg^{2+} to fill and incorporate into the calcite crystal lattice due to SO_4^{2-}substitution for CO_3^{2-}, this stretches the bonds of the lattice due to the SO_4^{2-} larger ionic size (Busenberg & Plummer, 1985; Kontrec et al., 2004; Tang et al., 2012). SO_4^{2-} does not incorporate into the lattice of aragonite easily (Walter, 1986; Mucci et al., 1989).

4.3.2.2 **The influence of sulphate with elevated temperature on the number of nucleations and crystal growth**

The number of aragonite/calcite crystals was lowered in the presence of SO_4^{2-} with elevated temperature of 30°C (red open squares) compared to those with SO_4^{2-} with lower temperature of 20°C (blue open squares) (***Figure 4-4A***). This indicates that the influence of SO_4^{2-} with elevated temperature increased number of aragonite crystals forming whilst the number of calcite crystals formed decreased.

However, comparison of the influence of SO_4^{2-} at elevated temperature (red open squares) to sulphate-free scenarios with elevated temperature (red closed squares), indicates the presence of SO_4^{2-} increases the aragonite/calcite crystal number formed those formed in sulphate-free scenarios at 30°C (***Figure 4-4A***).

In the presence of SO_4^{2-}, elevated temperature of 30°C (open red squares) increased the size of aragonite/calcite formed compared to scenarios with SO_4^{2-} at lower temperature of 20°C (open blue squares) and in sulphate-free scenarios at elevated temperature (closed red squares) (***Figure 4-4B***). This result of increased aragonite crystal growth at 30°C when influenced by SO_4^{2-} in solution agrees with results gained by Mejri et al. (2014).

Observed were larger crystals of aragonite compared to the sizes of calcite crystals formed at elevated temperature. However, the highest numbers of aragonite and calcite crystals formed in the presence of SO_4^{2-} at 30°C occurred at the expense of

their crystal size. The SO_4^{2-} incorporation would stretch bonding and allow for more magnesium incorporation into the calcite crystal lattice inhibiting calcite growth.

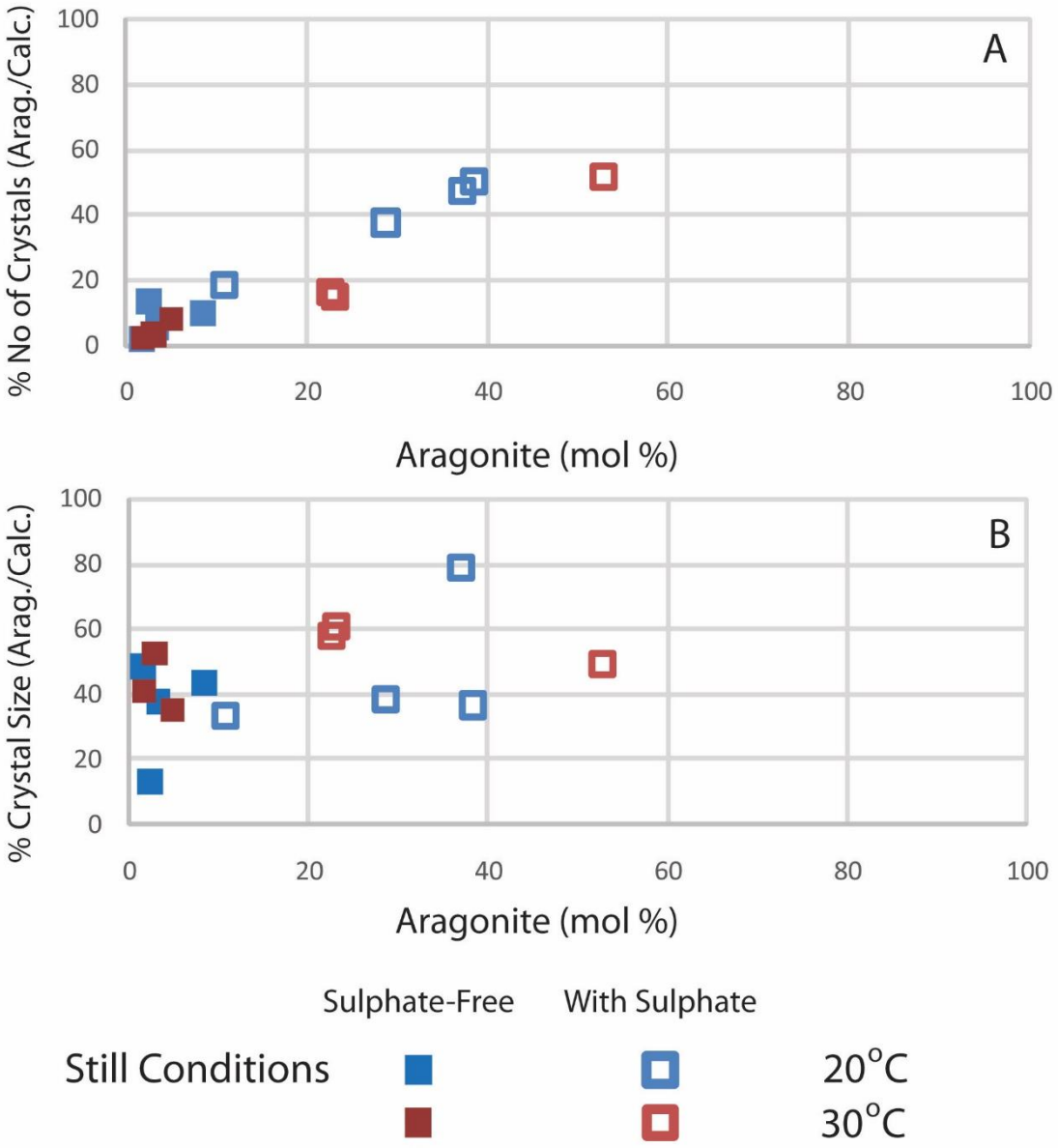

Figure 4-4: The influence of sulphate with elevated temperature on the number and size of crystals.
Results are presented for the aragonite mole percentage against crystal number (A) and crystal size (B) from continuous addition method (section 2.1.) *t*= 20°C (blue) and 30°C (red) in still conditions, sulphate-free scenarios (closed datum) and scenarios with (end target) 5mM SO_4^{2-} present (open datum). Upper graph (A) presents the average number of crystals of aragonite/calcite as a percentage. Lower graph (B) presents results from bootstraps for the average volume of crystals of aragonite/calcite as a percentage.

The increased number and size of aragonite crystals compared to the decreased number and size of calcite crystals formed allowed for the overall increase in the aragonite mole percentage observed (***Figure 4-3; Figure 4-4***).

In summary, the influence of SO_4^{2-} at temperature of 30°C increased the percentage of aragonite formed compared to aragonite formed at 30°C in sulphate-free scenarios. This was due to an increase in aragonite crystal growth. At the same time the number of nucleations and the average growth of calcite crystals were both decreased.

4.3.3 The influence of sulphate with water movement

4.3.3.1 The influence sulphate with water movement on the percentage of aragonite

When sulphate is present with water movement there was an increase the mole percent of aragonite (open datum) compared to sulphate-free conditions (closed datum) (***Figure 4-5***). This suggests that the presence of SO_4^{2-} in shaken conditions increases the opportunity for ions to attach to surfaces making attachment easier for aragonite formation, increasing the proportion of aragonite.

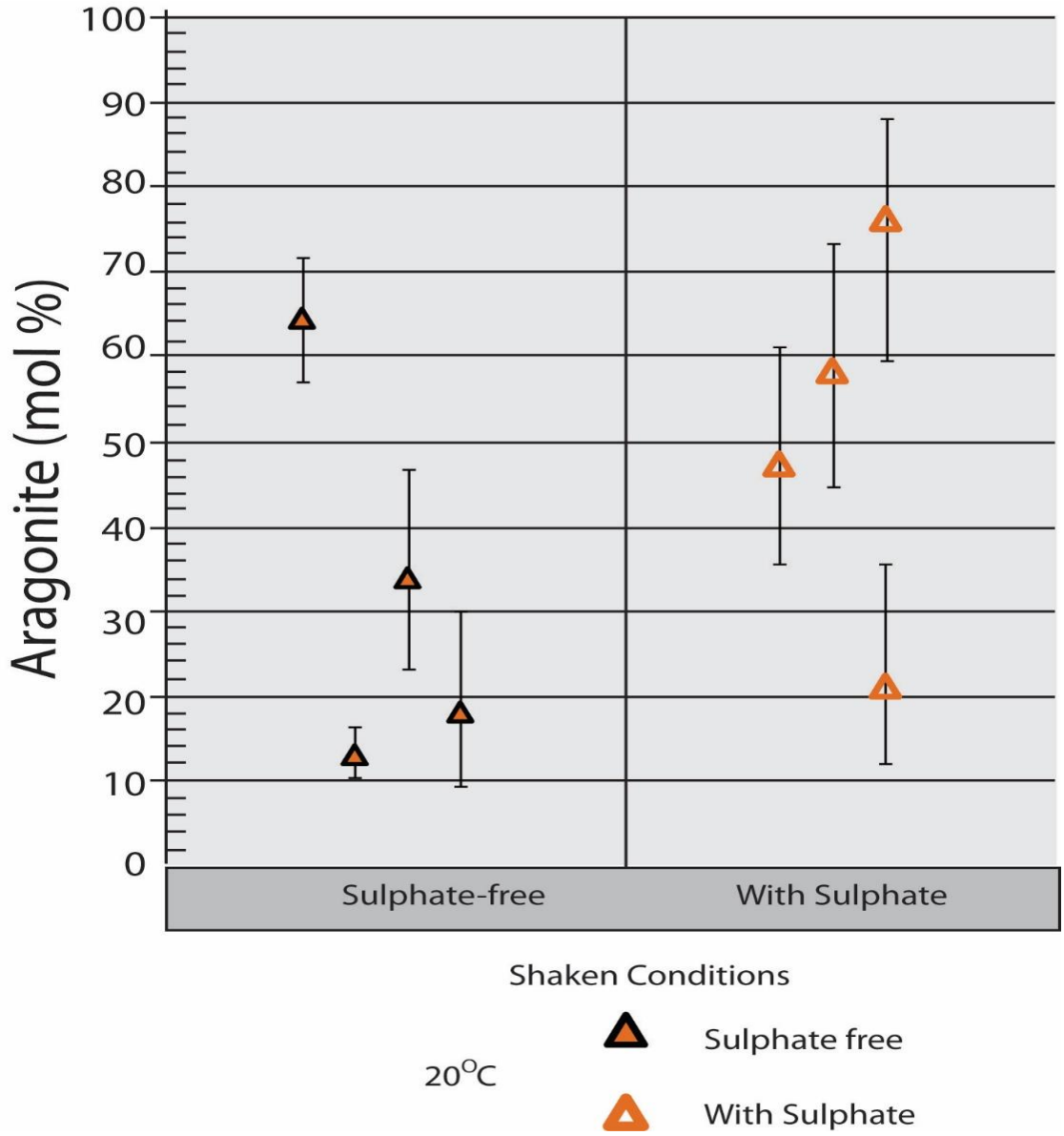

Figure 4-5: The influence of sulphate on the mole percentage of aragonite in shaken conditions.
Results are the average of 10,000 bootstraps (section 2.2.4.) to give mean mole percentage of aragonite ± 95% ci per scenario replicate, *t*=20°C, shaken conditions, sulphate-free scenario (closed datum) and scenarios with (end target) 5mM SO_4^{2-} present (open datum).

4.3.3.2 The influence of sulphate with water movement on the number of nucleations and crystal growth

The presence of SO_4^{2-} in shaken conditions at 20°C does not influence the number of aragonite/calcite crystals formed compared to sulphate-free scenarios (***Figure 4-6A***). This could be due to the SO_4^{2-} ion in solution increasing the energy required for ions to be able to attach to nucleation surfaces making nucleation more difficult. Decreased

opportunity for ions to attach to nucleation surfaces may be due to the size of the SO_4^{2-} ion being larger, when in suspension (Arroyo-de Dompablo et al., 2015. This would also increase the opportunity for SO_4^{2-} to hit off the smaller ions such as Ca^{2+} and Mg^{2+}, repelling the ions preventing them forming attachments to nucleation sites.

However, the influence of SO_4^{2-} in shaken conditions increased the size of aragonite/calcite crystals formed compared to sulphate-free conditions (***Figure 4-6B***). This was attributable to an increase in the size of aragonite, whilst the size of calcite crystals was similar to those formed in sulphate-free scenarios. The size of the crystals may be larger if SO_4^{2-} ions incorporate into the crystal lattice, this is less common in the lattice of aragonite compared to calcite but can still occur, and thus would allow stretching of the bonds between ions (Mejri et al., 2014). The similarity in the size calcite crystals may be due to the water movement preventing the SO_4^{2-} ions from being able to incorporate into the calcite crystal lattice due to the water motion and their large ion size, which would prevent the SO_4^{2-} ion from influencing the thermodynamic properties of the calcite lattice as hypothesised.

Therefore, the increase in the aragonite mole percentage (***Figure 4-5***) can be attributed to an increase in the size of crystals formed (***Figure 4-6B***) rather than by increasing the number of nucleations formed compared to sulphate-free conditions (***Figure 4-6A***).

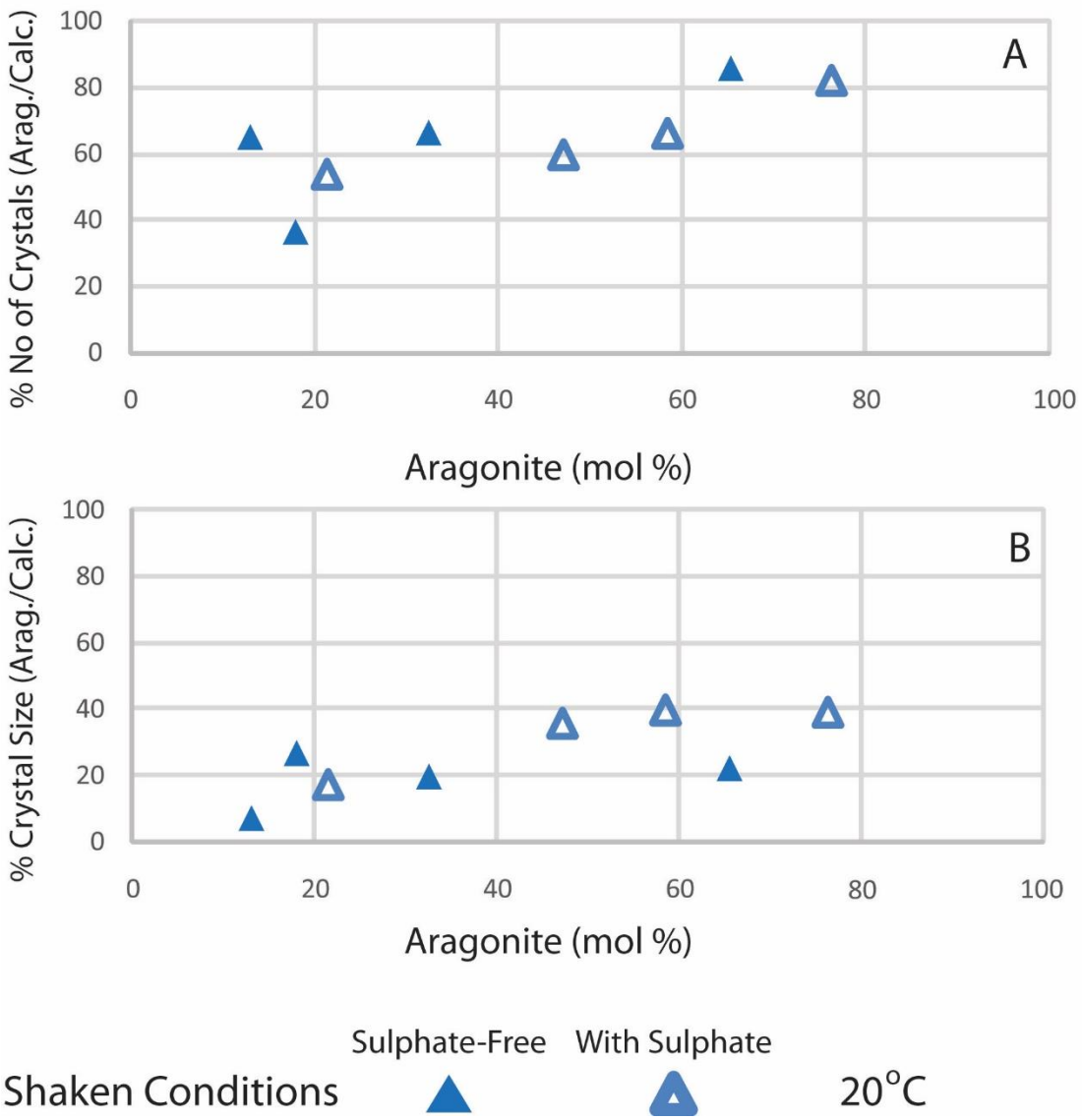

Figure 4-6: The influence of water movement with the presence of sulphate on number and size of aragonite and calcite crystals.
Results are presented for the aragonite mole percentage against crystal number (A) and crystal size (B) from continuous addition method (section 2.1.) *t*= 20°C (blue) in shaken conditions, sulphate-free scenarios (closed datum) and scenarios with (end target) 5mM SO_4^{2-} present (open datum). Upper graph (A) presents the average number of crystals of aragonite/calcite as a percentage. Lower graph (B) presents results from bootstraps for the average volume of crystals of aragonite/calcite as a percentage.

In summary, the presence of SO_4^{2-} with water movement increases the proportion of aragonite formed compared to sulphate-free conditions. This is due to an increase in the size of aragonite crystals with a slight decrease in the number of calcite crystals formed compared to sulphate-free conditions.

4.3.4 The influence of water movement and temperature in the presence of sulphate

4.3.4.1 The influence of water movement and temperature with the presence of sulphate: the percentage of aragonite

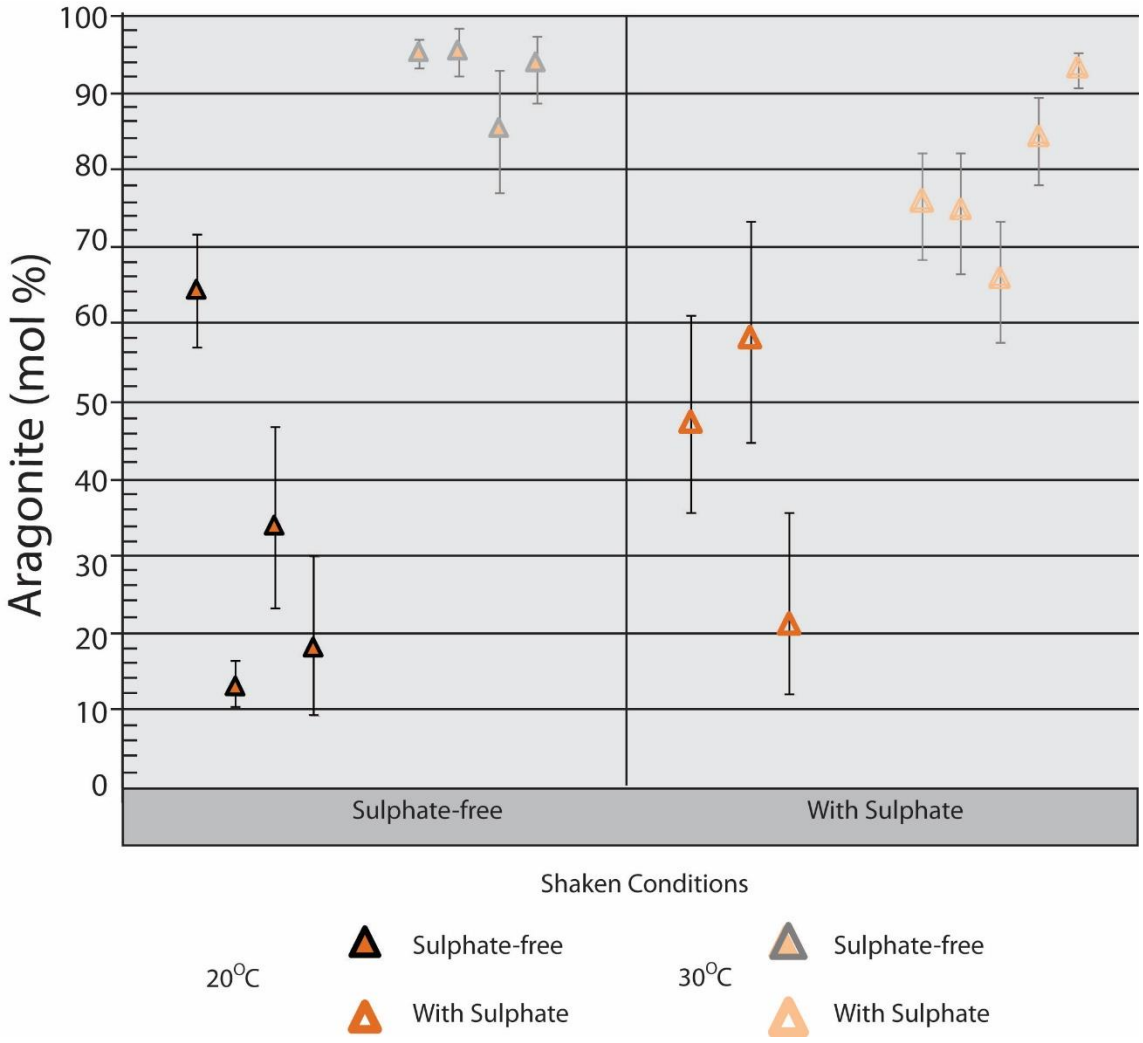

Figure 4-7: The influence of water movement in the presence of sulphate on the percentage of aragonite.
Results are expressed as mean percentage of aragonite ± 95% ci per scenario replicate, t= 20°C (dark orange) and 30°C (pale orange), in shaken conditions, sulphate-free scenarios (closed datum), in the presence of 5mM end target SO_4^{2-} scenarios (open datum).

In the presence of SO_4^{2-} with water movement at higher temperature (pale orange) decreased the mole percentage of aragonite slightly compared to sulphate-free scenarios in shaken conditions at 30°C (***Figure 4-7***). This decrease occurs with more spread in the percentages formed, possibly indicating that the SO_4^{2-} present at higher

temperature was given more opportunity to incorporate into calcite, the variance indicating the water movement and subsequently influencing the proportion of aragonite forming. However, comparing the presence of SO_4^{2-} with water movement at higher temperature to SO_4^{2-} with water movement at 20°C, according to the observed results the percentage of aragonite formed was increased (***Figure 4-7***). This suggests that SO_4^{2-} in shaken conditions when at higher temperature influences polymorph formation by allowing aragonite to be more stable and inhibiting calcite growth compared to lower temperature.

4.3.4.2 The influence of sulphate with water movement at higher temperature on the number of nucleations and crystal growth

The influence of SO_4^{2-} in shaken conditions at elevated temperature of 30°C (red open triangles), induced a similar proportion of aragonite/calcite crystals formed compared to those formed with SO_4^{2-} in shaken conditions at lower temperature of 20°C (blue open triangles) (***Figure 4-8A***). The presence of SO_4^{2-} appears to inhibit nucleations at higher temperature in shaken conditions compared to sulphate-free conditions as observed by lowered proportion of aragonite to calcite crystals forming (***Figure 4-9A).*** SO_4^{2-} ions may be attaching to nucleation surfaces before other ions may have the opportunity to do so and therefore preventing other ions from attaching, decreasing the numbers of nucleations. As the SO_4^{2-} ion is much larger than ions of Mg^{2+} and Ca^{2+}, this makes it more difficult for these smaller ions to force the SO_4^{2-} from nucleation sites to form attachment. As Mg^{2+} is a calcite growth inhibitor and is temperature sensitive this promotes the nucleation of aragonite at the expense of calcite. Therefore, any nucleations of calcite that could have formed may dissolve into solution due to altered thermodynamics (Klepetsanis et al., 1999).

However, the presence of SO_4^{2-} in shaken conditions with elevated temperature (red open triangles) was observed to increase the crystal size of aragonite/calcite compared to the size of those formed with SO_4^{2-} in shaken conditions at lower temperature (blue open triangles) (***Figure 4-8B***). This was due to the aragonite crystals formed being larger at elevated temperature compared to those formed at lower temperature.

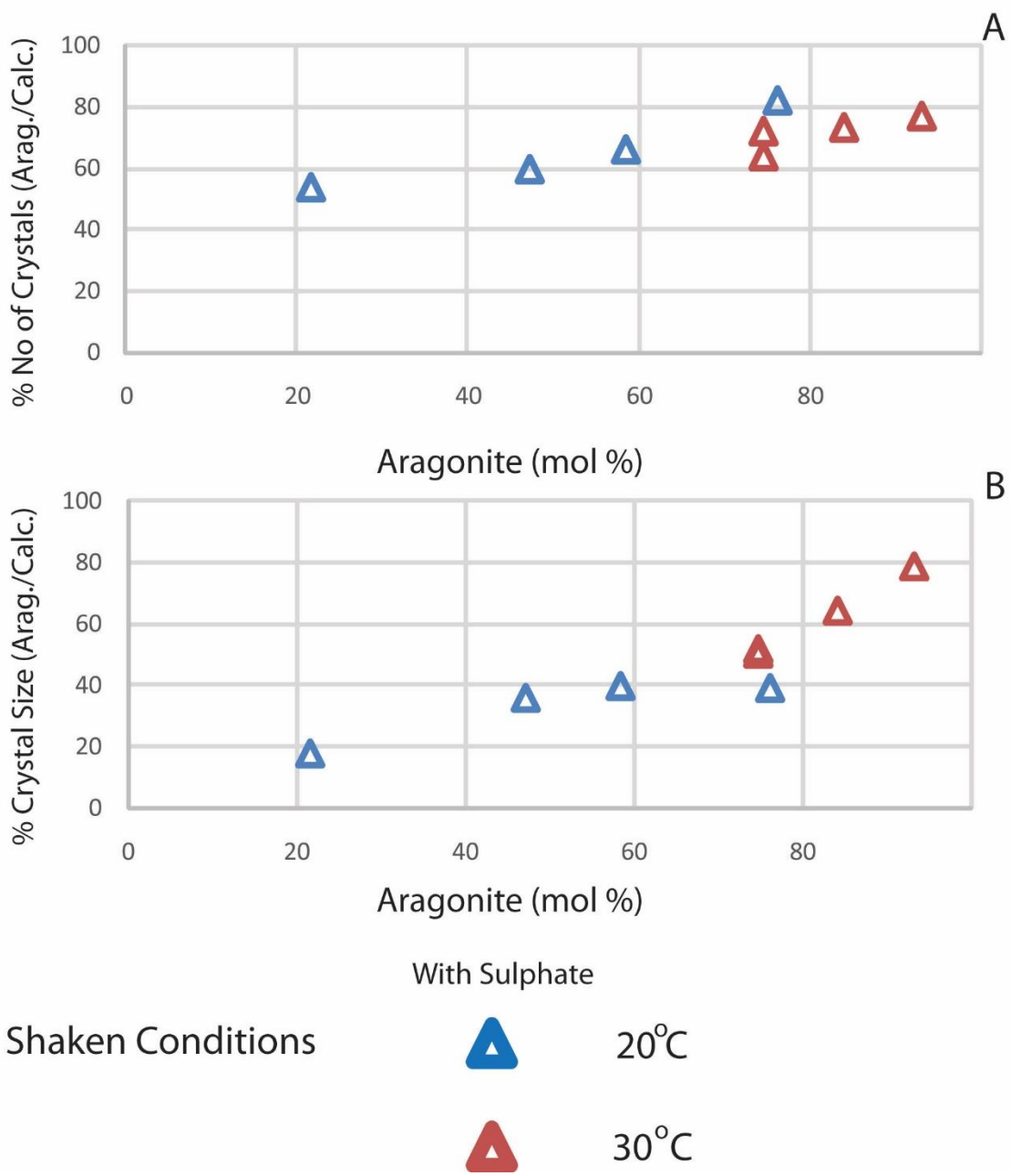

Figure 4-8: The influence of sulphate with elevated temperature on the number and size of crystals.
Results are presented for the aragonite mole percentage against crystal number (A) and crystal size (B) from continuous addition method (section 2.1.) t= 20°C (blue) and 30°C (red) in shaken conditions, all scenarios with (end target) 5mM SO_4^{2-} present. Upper graph (A) presents the average number of crystals of aragonite/calcite as a percentage. Lower graph (B) presents results from bootstraps for the average volume of crystals of aragonite/calcite as a percentage.

SO_4^{2-} in shaken conditions did not influence the calcite crystals formed as these were of similar sizes at both 20°C and 30°C. The influence of SO_4^{2-} in shaken conditions increased the crystal sizes of aragonite/calcite in comparison to those in sulphate-free

scenarios (***Figure 4-9B***). The presence of SO_4^{2-} in solution facilitates the growth of aragonite. At higher temperature, this is amplified allowing the SO_4^{2-} and Mg^{2+} ions to become more active facilitating aragonite growth by making attachment easier (Mejri et al., 2014). This also suggests that it is easier to overcome the energy barrier for attachment to occur allowing more opportunity for ions to attach to surfaces and increasing the crystal size (Arroyo-de Dompablo et al., 2015).

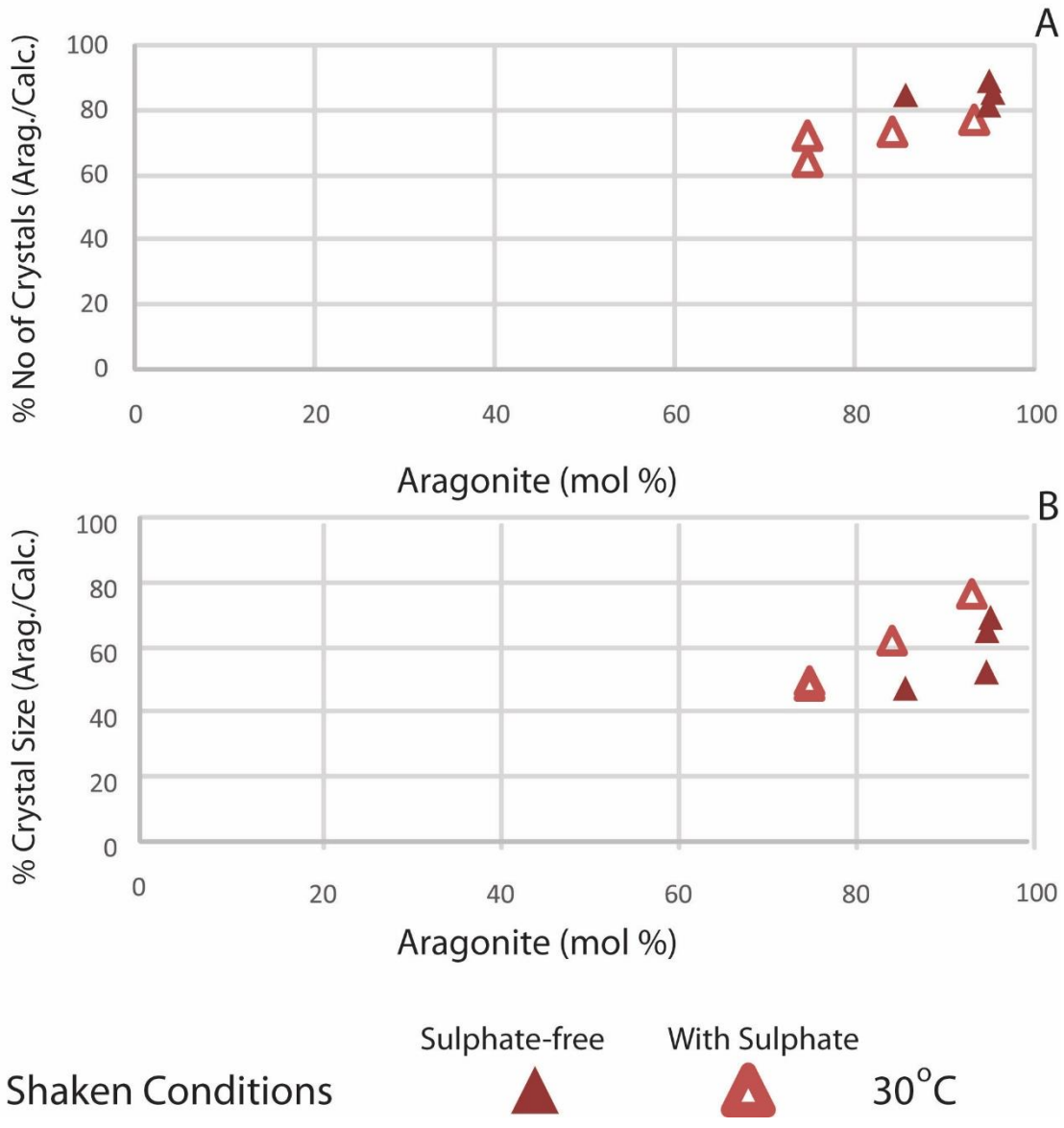

Figure 4-9: The influence of sulphate in shaken conditions with elevated temperature on the number and size crystals.
Results are presented for the aragonite mole percentage against crystal number (A) and crystal size (B) from continuous addition method (section 2.1.) *t*= 30°C (red) in shaken conditions, sulphate-free scenarios (closed datum) and scenarios with (end target) 5mM SO_4^{2-} present (open datum). Upper graph (A) presents the average number of crystals of aragonite/calcite as a percentage. Lower graph (B) presents results from bootstraps for the average volume of crystals of aragonite/calcite as a percentage.

This could be due to both SO_4^{2-} and Mg^{2+} ions in solution being calcite growth inhibitors (Tang et al., 2012), which at increased temperature allows increased incorporation into the calcite crystal lattice resulting in instability of the calcite lattice and more prone to dissolution under these conditions. The decrease in number of calcite crystals and their size agrees with Tang et al. (2012) who showed that calcite growth in inhibited by sulphate reducing the precipitation rate occurring.

Thus, the increase in the aragonite mole percentage observed (***Figure 4-7***) can be attributed to the increased crystal size (***Figure 4-8A; Figure 4-9A***), in particular of aragonite, when sulphate was present in shaken conditions at elevated temperature.

In summary, the influence of SO_4^{2-} under shaken conditions at elevated temperature of 30°C increased the percentage of aragonite formed compared to those with SO_4^{2-} at the lower temperature of 20°C. This was due to fewer crystals of aragonite forming but these were of much larger sizes whilst at the same time the number of calcite crystals was decreased and these crystals formed were much smaller than formed under shaken conditions at 20°C when SO_4^{2-} was present. However, at the same elevated temperature, the influence of sulphate and shaken conditions decreased the percentage of aragonite formed, this was due to fewer crystals nucleating of aragonite but of larger size, whereas the number of calcite crystals was maintained but these were of smaller size.

4.3.5 Combined influences on polymorph precipitates

4.3.5.1 The influence of sulphate and temperature: Comparison of scenarios with sulphate at temperatures of 20°C and 30°C

The influence SO_4^{2-} had on polymorph formation at higher temperature of 30°C was to increase the percentage of aragonite formed compared to cooler temperature of 20°C when SO_4^{2-} was present (***Figure 4-10***). The proportion of aragonite formed was increased when SO_4^{2-} was present under shaken conditions at 30°C compared to when SO_4^{2-} was present in still conditions (***Figure 4-10***). This result demonstrates that the influence of SO_4^{2-} increases the proportion of aragonite formed when there was an increase in temperature under both still and shaken conditions, suggesting that SO_4^{2-} ions at higher temperature favour the formation of aragonite at the expense of calcite. This

may be due to the increased temperature allowing more opportunity for SO_4^{2-} ions to incorporate into the crystal lattice of calcite, they do not affect aragonite crystal lattices to the same degree (He & Thomson, 1994). The stretching of the bonds would allow for more Mg^{2+} to fill and incorporate as Mg^{2+} incorporation is temperature sensitive and resulting in altered thermodynamic properties and calcite lattice growth inhibition and dissolution (Mejri et al., 2014).

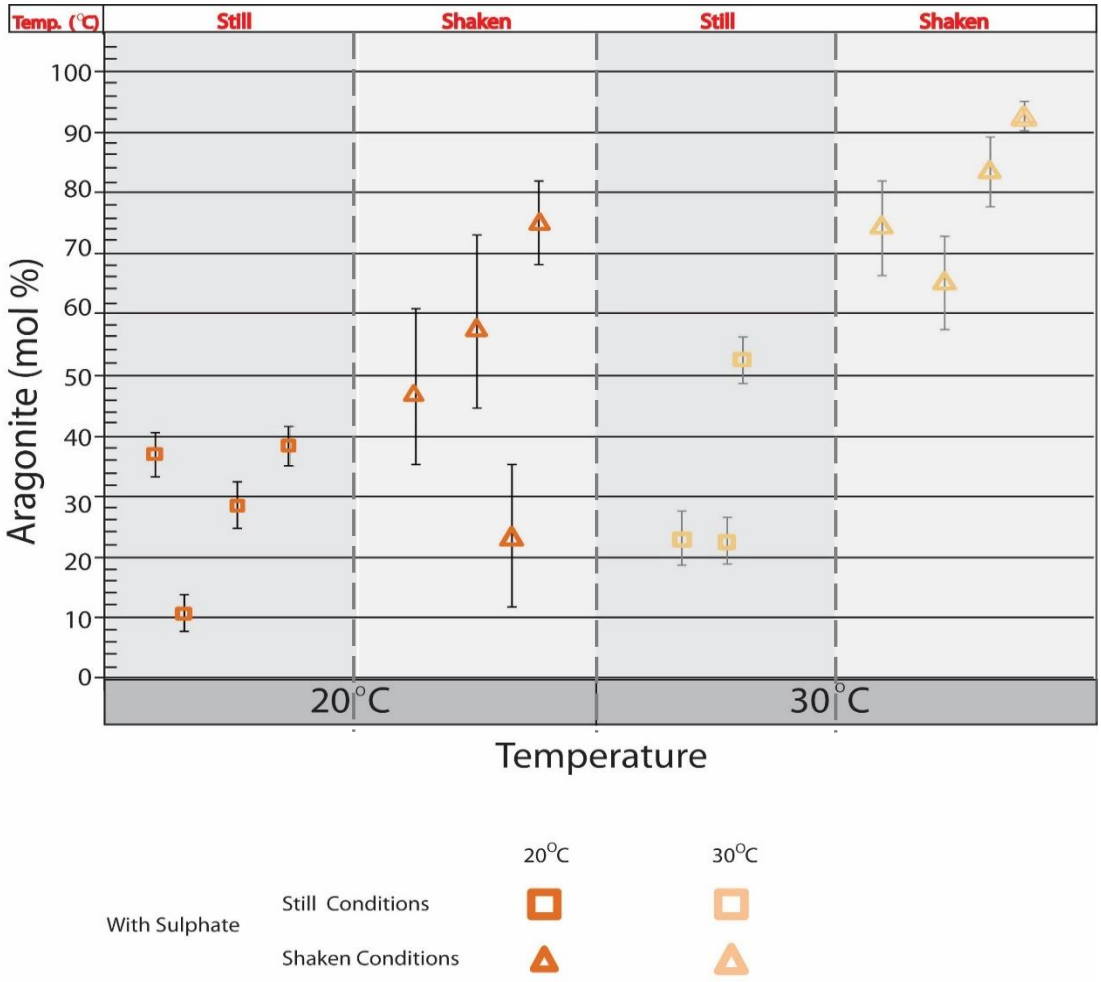

Figure 4-10: $CaCO_3$ precipitates formed when sulphate is present at 20°C and 30°C in still and shaken conditions.
Results are presented for the mean percentage of aragonite ± 95% ci per scenario replicate, *t*= 20°C (dark orange, to the left) and 30°C (pale orange, to the right), in still conditions (squares) and shaken conditions (triangles), all scenarios in the presence of 5mM (end target) SO_4^{2-}.

4.3.5.2 The influence of sulphate in water movement on polymorph formation

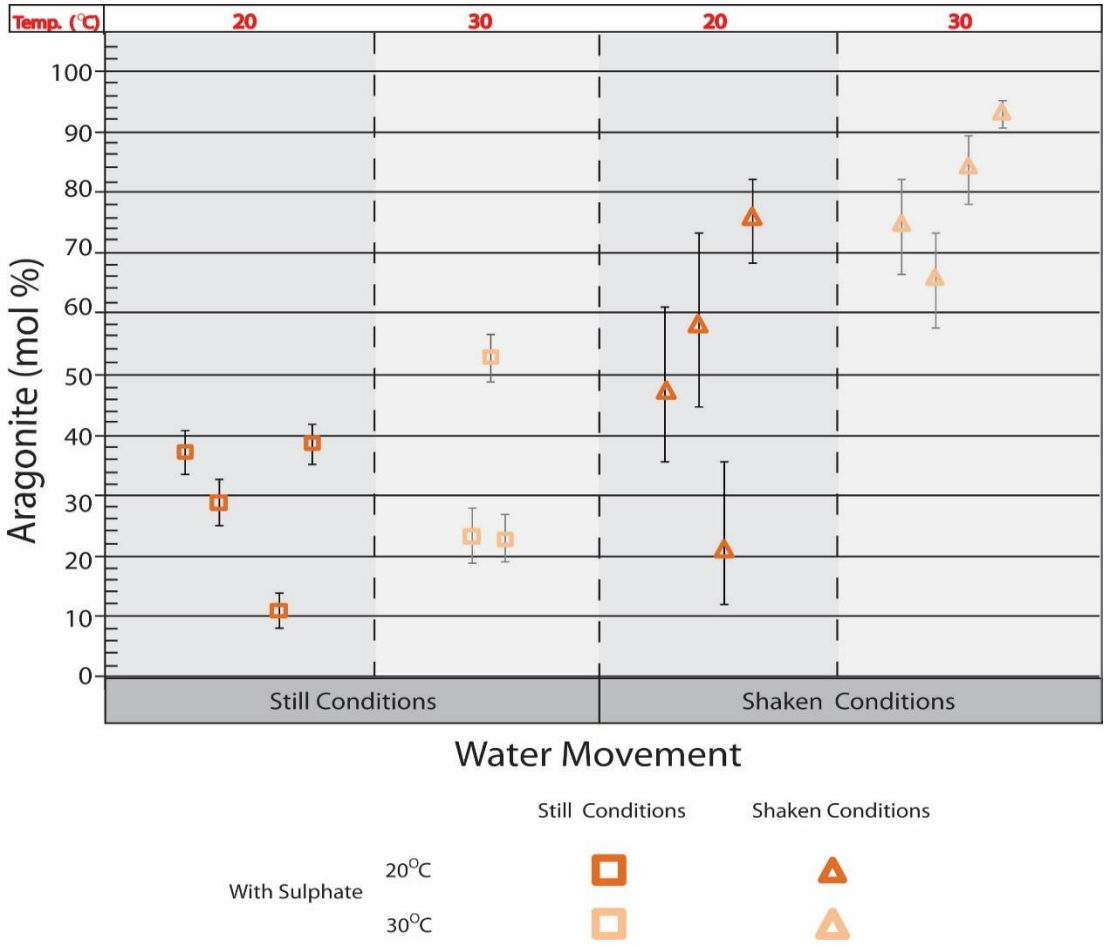

Figure 4-11: $CaCO_3$ precipitates formed in the presence of water movement and the presence of sulphate at 20°C and 30°C.
Results are presented for the mean percentage of aragonite ± 95% ci per scenario replicate, in still conditions (squares, to the left) and shaken conditions (triangles, to the right), *t*= 20°C (dark orange) and 30°C (pale orange), all scenarios in the presence of 5mM (end target) SO_4^{2-}.

SO_4^{2-} in shaken conditions increases the percentage of aragonite formed compared to those formed with SO_4^{2-} in still conditions (***Figure 4-11***). This result is true at both 20°C and 30°C (***Figure 4-11***). Water movement increases the opportunity for ions to form attachments allowing more possible opportunities for crystal growth. This trend is amplified at 30°C compared to 20°C suggesting increased temperature increased the activity of the ions in solution and when the solution is shaken this increases the opportunity for collisions and therefore attachments to be made (***Figure 4-11***). The increase in aragonite percentage formed with SO_4^{2-} under shaken conditions at higher

temperature suggests that Mg^{2+} are increasingly able to incorporate into the crystal lattices of calcite crystals as this is temperature driven, and results in hindered calcite growth and possible calcite dissolution allowing more aragonite to form at the expense of calcite.

4.4 Discussion

4.4.1 The influence of sulphate on polymorph formation

The influence of SO_4^{2-} in solution increased the mole percentage of aragonite formed compared to sulphate-free scenarios under still conditions (***Figure 4-1; Figure 4-3***). SO_4^{2-} ions decrease the calcite precipitation rate compared to aragonite (Busenberg & Plummer, 1985; Kontrec et al., 2004; Vavouraki et al, 2008; Bots et al., 2011; Tang et al., 2012). Mucci & Morse (1989) believed that the presence of SO_4^{2-} and Mg^{2+} ions were the key facilitator for the preference to form aragonite over calcite. SO_4^{2-} and Mg^{2+} ion concentrations favour aragonite precipitation at the expense of calcite due to increased calcite solubility and decreased precipitation rate (Burton, 1993), in turn increasing the mole percentage of aragonite. When SO_4^{2-} and Mg^{2+} are present together in solution Takano (1985) suggested that Mg^{2+} increases the incorporation of SO_4^{2-} into calcite. However, Burton & Walter (1991) contest that it is in fact the presence of SO_4^{2-} which inhibits Mg^{2+} to incorporate into calcite. The results presented here indicate that aragonite was formed at the expense of calcite to a higher degree than it was in sulphate-free conditions (***Figure 4-1***), therefore hinting that it is the SO_4^{2-} ion which influences the proportions of $CaCO_3$ polymorphs formed.

The influence of SO_4^{2-} in shaken conditions also increases the mole percentage formed compared to still conditions (***Figure 4-10***). However, SO_4^{2-} has less influence on the percentage of aragonite in shaken conditions at 30°C compared to the percentage of aragonite formed in the sulphate-free scenario (***Figure 4-7***), but this percentage remains higher than with SO_4^{2-} in shaken conditions at 20°C (***Figure 4-11***).

Previously, calcite was viewed as forming at lower Mg:Ca ratio i.e. less than 2 (Folk, 1974; Danberg, 1975; Füchbauer & Hardie, 1980; Lowenstein, 2001; Stanley, 2008; Mejri et al., 2014). Morse et al. (1997) and Balthasar & Cusack (2015) proposed that the Mg:Ca

ratio for calcite formation had a non-linear relationship with temperature (section 1.3.6, Figure 3) and therefore indicating that polymorph formation was not solely influenced by Mg:Ca ratio. Results presented in Chapter 3 are in agreement that Mg:Ca ratio of 2 as a boundary between calcite and aragonite formation is inaccurate without considering temperature, noting that co-precipitation of calcite and aragonite occurred at all Mg:Ca ratios of 1, 2 and 3 (***Figure 4-12A***). This is in agreement with previous work of Morse et al, (1997) and Balthasar & Cusack, (2015). It was hypothesised that the influence of SO_4^{2-} at Mg:Ca ratio of 1 would increase the percentage of aragonite formed at the expense of calcite compared to those grown in sulphate-free scenarios. The results presented here indeed show that the percentage of aragonite was increased in all sulphate-present scenarios, except when shaken at 30°C, but the percentage in that scenario still remained within the upper reaches of percentage formation.

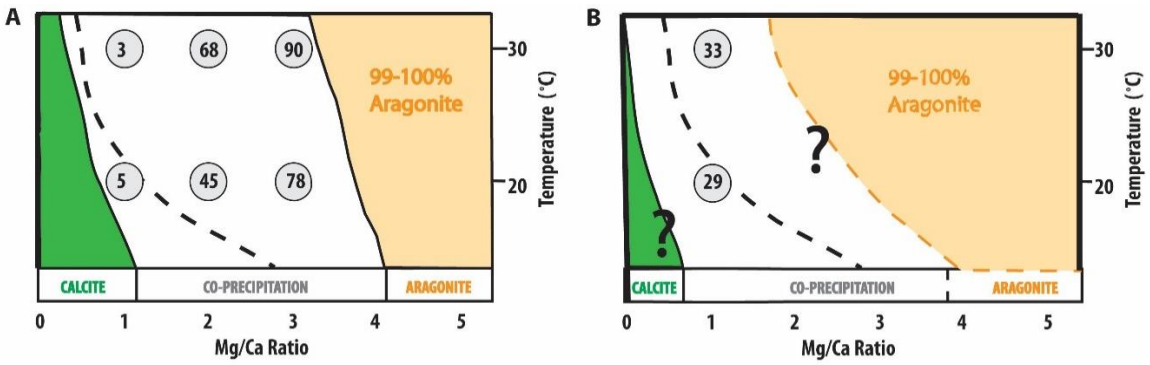

Figure 4-12: Results from continuous addition method from sulphate-free scenarios and scenarios with sulphate.
Comparison of results from continuous addition method (section 2.1.2.) in still conditions from sulphate-free scenarios (A) (Chapter 3) and with sulphate present (B). Both A and B are presented as a percentage of aragonite yielded for the first-formed precipitates. The black dashed line in A and B indicates the proposed boundary for the critical threshold switch in polymorph formation as proposed by Morse et al. (1997). The orange dashed line represents hypothesized shift in boundary of 99-100% aragonite formation to the left under the influence of sulphate compared to sulphate-free scenarios in A.

The percentages of aragonite formed were increased by the influence of SO_4^{2-} by ~25-30% (***Figure 4-12***). Although these percentages were showing calcite was most dominant, they do indicate that the proportion of aragonite has increased under the influence of SO_4^{2-}. This suggests that, in agreement with Bots et al. (2011), the threshold for a calcite-dominant period would be lower when SO_4^{2-} is present in solution. The co-precipitation area gained from sulphate-free scenarios in Chapter 3 under continuous

addition method was wider than results proposed by Balthasar & Cusack (2015) who used degassing of solution. This widening of co-precipitation was due to lower proportions of aragonite to calcite forming at lower Mg/Ca ratios in still conditions when under continuous addition method, most likely due to a lower saturation state compared to the proportion presented via degassing methods by Balthasar & Cusack (2015). The observed influence of SO_4^{2-} on the polymorphs precipitated under continuous addition method was to increase the co-precipitation phase further due to the calcite phase and co-precipitation phases shifting to the left of ***Figure 4-12***. The threshold where calcite would be dominant was lowered compared to sulphate-free scenarios (***Figure 4-12***), and is in agreement with evidence from Bots et al. (2011) experiments, who only observed 100% calcite polymorphs when there was no SO_4^{2-} or Mg^{2+} present in solution. As both SO_4^{2-} and Mg^{2+} were present in solutions in the presented results, a pure calcite was never to be expected. The aragonite phase for 99-100% aragonite formation is predicted to occur at lower Mg:Ca ratio under the influence of sulphate (***Figure 4-12***). The presented results from sulphate-present scenarios suggest that because the polymorph phases in ***Figure 4-12*** have shifted to the left, the possibility of a calcite dominant sea period occurring would be rare as previously proposed by Bots et al. (2011).

The presence of SO_4^{2-} was documented by Bischoff & Fyfe (1968) to inhibit the transformation of aragonite to calcite SO_4^{2-} in solution. The concept of a 'switch' in mineralogy being triggered by solution chemistry was suggested to result from the presence of SO_4^{2-} in solution (Dydo et al., 2003; Tang et al., 2012). The observations presented from this study show that in terms of the first-formed polymorphs, there is a co-precipitation of calcite and aragonite (***Figure 4-12***), this was higher than that formed in sulphate-free scenarios but suggests that polymorphs of $CaCO_3$ do not 'switch' from one type to another.

The concentration of SO_4^{2-} used in this study does sit at the lower range within the Phanerozoic concentrations inferred from marine halite fluid inclusions (SO_4^{2-} fluctuated between 5 & 30mM) (Horita et al., 2002; Lowenstein et al., 2003) and correlates with $\sigma^{34}S$ isotope records within the early Jurassic and Cretaceous of between 5 & 4 mM respectively (Newton et al., 2011). However, the accuracy of the data obtained from halite fluid inclusions remains debated as to whether it is truly representative of

Phanerozoic seawater chemistry (Lowenstein & Timofeeff, 2008; Gill et al., 2011). $\sigma^{34}S$ isotope data suggested that the SO_4^{2-} concentration within Phanerozoic seawater is 2-5mM lower than the concentrations obtained from halite fluid inclusions (Gill et al., 2007; Gill et al., 2011). Other estimates of SO_4^{2-} in the Phanerozoic note the threshold between $MgSO_4$ and $CaCl_2$ evaporites forming were 9mM SO_4^{2-} (Lowenstein et al., 2003). Therefore, having used 5mM SO_4^{2-} in this study this allowed for this error range and allows application to natural seawater investigation into how the growth parameters of $CaCO_3$ polymorphs are altered at this lower SO_4^{2-} concentration representative of both suggestion SO_4^{2-} concentrations. Bots et al. (2011) presented that even low SO_4^{2-} concentrations had influence on the $CaCO_3$ polymorph precipitated facilitating aragonite at the expense of calcite, and the results presented in this study are in agreement (***Figure 4-12***). However, the proposed lower threshold of Bots et al. (2011) where calcite dominance would occur at 5mM SO_4^{2-} and Mg:Ca ratio of 0.3 is not supported by halite fluid inclusion data (Hasiuk & Lohmann, 2008; Newton et al., 2011; Wortmann & Chernyavsky, 2007). As the results presented here support the findings of Bots et al. (2011) this suggests that the forming $CaCO_3$ mineralogy is influenced by other factors other than seawater chemistry such as temperature and water movement.

4.4.2 The influence of sulphate with temperature on polymorph formation

The present study observed that even in the presence of a low SO_4^{2-} (5mM end-target) concentration, that the percentage of aragonite was increased compared to those grown in sulphate-free scenarios (***Figure 4-1)***. This trend was observed when the temperature was higher at 30°C in scenarios with sulphate compared to 20°C with SO_4^{2-}, amplifying the percentage of aragonite formed (***Figure 4-3***). The increase in aragonite formed in sulphate-present scenarios at higher temperature (***Figure 4-3***) suggest the influence of SO_4^{2-} was enhancing the temperature sensitive nature of magnesium ions (Mejri et al., 2014). SO_4^{2-} has more influence over calcite mineralogy than that of aragonite due to the possibility for it substituting into the calcite crystal lattice for carbonate ions (Tang et al., 2012). Even low SO_4^{2-} concentrations, as used within this study would allow the substitution of SO_4^{2-} for CO_3 ions in calcite stretching the calcite crystal lattice allowing more Mg^{2+} to incorporate within the lattice resulting in increased

calcite solubility and hindering calcite growth (Busenberg & Plummer, 1985). Any incorporation of Mg^{2+} or SO_4^{2-} ions into the calcite crystal lattice results in instability and further inhibits any crystal growth by these ions of blocking growth surfaces making bond attachments more difficult (Zarga et al., 2013; Tang et al., 2014). This means nucleations of calcite that could have formed may dissolve into solution due to altered thermodynamics (Tang et al., 2012; Arroyo de-Dompablo et al., 2015).

Previous studies have noted that the influence of SO_4^{2-} diminishes the time taken to form nucleations but increases the precipitation rate and subsequent growth of aragonite crystals (Bots et al., 2011; Bots et al., 2012; Mejri et al., 2014; Arroyo-de Dompablo et al., 2015). The crystals formed in conditions with sulphate did indeed reach quantifiable size quicker than in sulphate-free conditions. The results presented in Chapter 3 observed that increased temperature formed larger proportions of aragonite to calcite which is in agreement with other studies of $CaCO_3$ polymorph formation (Ogino et al., 1987; Morse et al., 1997; Bots et al., 2011; Mejri et al., 2014; Balthasar & Cusack, 2015).

Model predictions have postulated that seawater temperature throughout the Phanerozoic has fluctuated based on evidence from marine sediment cores and isotopic analysis (Schrag et al., 1995). However, the accuracy of the representation for sea surface temperature remains contested today (Royer et al., 2004; Wallman, 2004). Previous studies have observed that SO_4^{2-} lowers the Mg:Ca ratio at which aragonite is favoured to precipitate (Bots et al., 2011) and inhibits calcite formation (Mejri et al., 2014; Petrou & Terzidaki, 2014). Therefore, it is important to investigate the influence higher temperature in seawater would have on polymorph formation when SO_4^{2-} is present, as temperature has been observed to increase aragonite formation at the expense of calcite (Burton & Walter, 1987; Morse et al., 2007; Balthasar & Cusack, 2015).

The influence of Mg:Ca ratio has been shown to be a function of temperature (Morse et al., 1997; Balthasar & Cusack, 2015) and Mg^{2+} incorporation into calcite is also known to be a function of temperature (Burton & Walter, 1987; Burton & Walter, 1991; Mucci & Morse, 1989; Morse et al., 2007). Therefore, more Mg^{2+} incorporating into the lattice due to the stretching of bonds by SO_4^{2-} (Arroyo-de Dompablo et al., 2015) may be

increased at higher temperature, and therefore may explain why there was an increase in the proportion of aragonite formed compared to the aragonite proportion formed in sulphate-free scenarios.

The contested Mg:Ca ratio for the change from aragonite to calcite seas is debated between to range between 1 (Wilkinson & Algeo, 1989) and 2 (Hardie, 1996). The results observed here indicated that the Mg:Ca ratio is lowered in the presence of SO_4^{2-} supporting the work of Bots et al. (2011) that aragonite would be facilitated at lower Mg:Ca ratios in the presence of SO_4^{2-}. The influence of temperature on mineralogy is amplified in the presence of SO_4^{2-} (***Figure 4-3***). This suggests that temperature allows the activity of these ions in solution is increased which may allow more opportunity for the energy barrier allowing attachment to nucleations sites to be reached which would modify the growth and morphology of polymorphs forming (Mejri et al., 2014; Sun et al., 2015).

The influence of SO_4^{2-} with higher temperature on $CaCO_3$ mineralogy formation are important parameters to assess as allow in vitro non-biogenic precipitation experiments to be applied to the natural marine realm. SO_4^{2-} in seawater has been connected to the formation of dolomite (Hardie, 1987). However, other authors disagree proposing that the incorporation of SO_4^{2-} inhibits dolomite production (Baker & Kastner, 1981; Slaughter & Hill, 1998). One possibility for the differences in their studies could be due to the effect of temperature with SO_4^{2-}. An increase in temperature can aid dolomite production (Bots et al., 2011) which in turn impacts on the Mg^{2+} by decreasing it through precipitation (Arvidson et al., 2006; Holland et al., 1996; Mackenzie et al., 2008). Dolomitization has been suggested to be influential in the changes within major ion composition of seawater (Horita et al., 2002). This would also impact on the Mg:Ca ratio due to the removal of Mg^{2+} from solution alongside SO_4^{2-} as they become incorporated into the rock releasing Ca^{2+} (Stanley & Hardie, 1999). This suggests that higher temperature could facilitate a lower Mg:Ca ratio by the production of dolomite which would result in aragonite-facilitating conditions (***Figure 4-12B***). This interpretation could be important when considering latitudinal variations in temperature as this could lead to altered mineralogy due to the influence of SO_4^{2-} and temperature together.

4.4.3 Influence of sulphate with water movement on polymorph formation

The aragonite-calcite sea hypothesis was based on the observation that original mineralogy of ooids oscillated between aragonite and calcite throughout the Phanerozoic (Sandberg, 1983). The continuous addition method was therefore designed to investigate $CaCO_3$ formation in both still and shaken conditions (section 2.1.2.) to be able to replicate water movement in the context of a marine environment more applicable to that where non-biogenic ooids would form. By adding the influence of SO_4^{2-} to the continuous addition set-up allows consideration of the natural ion flux in seawater may in turn influence the mineralogy forming. As $CaCO_3$ precipitates, foreign ions can incorporate into the crystal lattice and this alters both the morphology and the thermodynamic properties of the polymorphs formed (Mejri et al., 2014). Therefore, as SO_4^{2-} is the second most common soluble mineral found after NaCl and is ubiquitous to marine evaporite environments, SO_4^{2-} will have influence on the mineralogy formed as it substitutes for CO_3^{-} in the $CaCO_3$ lattices formed (Takano, 1985; Staudt et al., 1984; Kampschulte & Strauss, 2004). Results presented show that when SO_4^{2-} was present with water movement, an increase in the percentage of aragonite forms compared to sulphate-free scenarios with water movement (***Figure 4-5***). The increase in aragonite formed is also increased compared to still conditions with SO_4^{2-} (***Figure 4-11***). SO_4^{2-} alters calcite stability due to incorporation into the calcite crystal lattice by substituting for CO_3^{-} ions which results in an increased c-axis (height) and in turn alters the thermodynamic properties (Arroyo-de Dompablo et al., 2015).

The increase in aragonite formed suggests that the presence of SO_4^{2-} amplifies the opportunity to precipitate aragonite in shaken conditions, influencing aragonite to become the dominant mineralogy formed (***Figure 4-7***). SO_4^{2-} is known to have more influence on calcite than on aragonite (Busenberg & Plummer, 1985; Walter, 1986; Mejri et al., 2014). By SO_4^{2-} having more influence on calcite when SO_4^{2-} is present, allows more opportunity for aragonite to form at the expense of calcite, this is observed in ***Figure 4-6*** where fewer crystals of calcite, which were of smaller size, formed compared to sulphate-free shaken conditions, whilst at the same time the crystals of aragonite formed were larger. This suggests that the percentage of aragonite occurs due to SO_4^{2-} in shaken

conditions having more influence over the crystal size of $CaCO_3$ polymorphs formed rather than the nucleation rate. This result disagrees with Reddy & Nancholas (1971) who demonstrated that crystallization was independent of the speed of shaking. Klepetsanis et al. (1999) also proposed shaking speeds of 100 – 400 rpm did not influence the precipitation occurrence. Bots et al. (2011) used 270 rpm in their study on the influence of sulphate on polymorph formation, but did not compare to still conditions. The presented results were gained using 80 rpm, because a slower speed was required that allowed movement of the mother solution over the glass slides used as nucleation surfaces (section 2.1.2.), but ensuring that the slides did not move over each other preventing nucleation. This slower speed used may explain the influence on nucleation rate, as this is lower than other studies

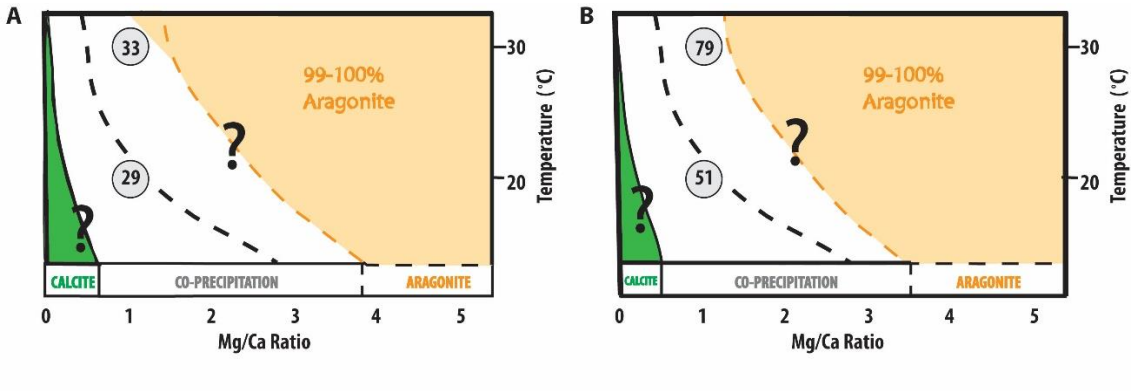

Figure 4-13: Results from continuous addition method of scenarios with sulphate in still and shaken conditions.
Comparison of results from continuous addition method with the influence of sulphate in solution on polymorph formation (section 2.1.2.) in still conditions (A) (Chapter 3) and shaken conditions (B). Both A and B are presented as a percentage of aragonite yielded for the first-formed precipitates. The black dashed line in A and B indicates the proposed boundary for the critical threshold switch in polymorph formation as proposed by Morse et al. (1997). The orange dashed line represents hypothesized shift in boundary of 99-100% aragonite formation moving towards the left, lowering the Mg:Ca ratio at which the switch between calcite and aragonite formation would occur.

One reason that the growth of aragonite was increased but not in terms of the number of nucleations could be due to the saturation state not being high enough to allow the energy barrier to nucleation to be achieved (Petrou & Terzidaki, 2014). The continuous addition method set-up is of lower saturation state than that of previous studies using degassing methodology (Morse et al., 1997; Balthasar & Cusack, 2015), and this can explain why higher percentages of aragonite formed at lower Mg:Ca ratio in

Chapter 3 compared to Balthasar & Cusack (2015). This would result in larger crystals occurring because it was more difficult to form nucleations compared to attaching to nucleations already formed and allowing their growth to continue.

The influence of SO_4^{2-} in a shaking environment was observed to increase the percentage of aragonite formed compared to that formed in the presence of SO_4^{2-} in still conditions (***Figure 4-13***). These observations indicate that the influence of sulphate in shaken conditions increases the proportion of aragonite formed to become the dominant mineralogy at Mg:Ca ratio of 1.

Seawater chemistry has been investigated to determine its influence over mineralogy in the context of aragonite-calcite seas. There remains debate over the timing of the switch between aragonite and calcite facilitating sea periods (Berner, 2004; Arvidson et al., 2013). The presented results disagree with the original aragonite-calcite sea hypothesis that aragonite should be the dominant mineralogy formed at Mg:Ca ratio above 2 (Hardie, 1996) as co-precipitation occurs at Mg:Ca ratio of 1. In agreement with Bots et al. (2011), the presented results do show that the Mg:Ca ratio that calcite dominance occurs is much lower when SO_4^{2-} is present, especially in water movement. The presented results do support this proposal by showing that although Mg:Ca ratio is a strong driver of mineralogy, it was observed that temperature and water movement in the presence of sulphate all amplify the dominance of aragonite at the expense of calcite. The results from the present study indicate that due to other drivers such as temperature and water movement that amplifies the mole percentage of aragonite formed. This scenario is representative of the natural marine realm and therefore suggests that a calcite-facilitating sea condition would be extremely rare and therefore may explain why constraining the timing of oceanic states has been uncertain (Vulpius & Kiessling, 2018).

The observed results from continuous addition method scenarios with sulphate in water movement are particularly interesting in relation to the sedimentary record in terms of fossil ooids. The aragonite-calcite sea hypothesis was developed based on the observation that the original ooid mineralogy were of primary calcitic mineralogy rather than formed from diagenesis of aragonitic ooids (Sandberg, 1975; 1983; Tucker & Bathurst, 2009). The presence of sulphate increased the formation of aragonite at the

expense of calcite, suggesting that sulphate in shaken environments directly amplified the incorporation of Mg^{2+} inhibiting calcite growth. If these results were applied to ooid formation this would suggest that the Mg^{2+} content of forming ooids in more turbulent waters would be higher in Mg^{2+} inhibiting calcite formation. This has implications in the natural environment as aragonite is more prone to dissolution than calcite and therefore more unstable. This could be suggestive that more turbulent waters could facilitate aragonitic ooids. Further, temperature was observed to be a determining factor in the mineralogy formed in the presented work. The original mineralogy of ooids has previously been thought to be primarily controlled by the Mg:Ca ratio of seawater (Stanley & Hardie, 1998). However, based on the results here not when sulphate is present, not only does temperature influence the mineralogy formed, but water movement also amplifies the proportion of aragonite forming. A change in water movement conditions with changes in climate, such as increased temperature could have the possibility to facilitate sudden change in mineralogy facilitated by altering the co-precipitation ratio facilitated. The presented results including water movement as a variable have indicated that it is a factor that must be considered alongside drivers such as Mg:Ca ratio, temperature and SO_4^{2-} in future non-biogenic studies as it has shown direct influence on the mineralogy formed and therefore has far-reaching implications for the natural environment.

4.5 Conclusions

Non-biogenic $CaCO_3$ precipitation experiments were carried out to allow the parameters of Mg:Ca ratio, temperature and water movement to be investigated under the influence of SO_4^{2-} in solution on their polymorph formation. The results presented answer the aims of this chapter to show that when SO_4^{2-} is present the proportion of aragonite formed was increased further from that formed in sulphate-free scenarios at 20°C. At 30°C the proportion is also increased except when water movement is included at 30°C with SO_4^{2-}, but these proportions are already in the highest reaches of aragonite percentage. Results presented in this chapter are in agreement with previous work that the influence of SO_4^{2-} on $CaCO_3$ polymorph formation does not influence aragonite as much as it does calcite (Bots et al., 2011; Mejri et al., 2014; Arroyo-de Dompablo, 2015).

This can be clearly seen by decreased growth and decreases in the number of nucleations formed of calcite under all sulphate experiment scenarios.

The results from precipitation experiments for the first three objectives are summarized in **Table 4-1.** A key finding from this study was that, like the results from Chapter 3, co-precipitation of aragonite and calcite occurred in all scenarios under the influence of sulphate, but the proportion of aragonite formed was much greater. This is in agreement with the proposal that the critical threshold for the switch between aragonite and calcite would be lowered in the presence of SO_4^{2-} (Bots et al., 2011), as previously it was believed at a Mg:Ca ratio of 1 calcite only would form. As can be seen in ***Figure 4-12***, the boundary between calcite formation and the co-precipitation field and the boundary between co-precipitation and 99-100% aragonite have both shifted to the left indicating that calcite dominant sea period occurrence would be much rarer than that of an aragonite sea period.

The present study concludes that SO_4^{2-} influences the parameters of temperature and water movement to facilitate higher proportions of aragonite and therefore suggest the Mg:Ca ratio at where the threshold between calcite and aragonite occurs would be lowered (***Figure 4-13***). This emphasizes that although individually each parameter under the influence of SO_4^{2-} influences the proportion of aragonite formed, combined these parameters have the greatest influence, allowing aragonite to be the dominant mineralogy formed. Therefore, the way in which aragonite-calcite sea hypothesis is viewed should be reviewed with consideration of all parameters together. The results gained in this study are important when applying to a natural marine realm as the results gained may have implications for biogenic $CaCO_3$ mineralogy which forms under these conditions. Although biogenic forms of $CaCO_3$ have some control over their mineralogy, the seawater chemistry remains to be their source for formation and therefore, these results indicate that SO_4^{2-} and temperature allow aragonite to form at Mg:Ca ratio of 1 which was previously perceived as being a calcite-facilitating Mg:Ca ratio. This could lead to mineralogy forming out of equilibrium with the seawater conditions that they form within.

	Influence of SO_4^{2-}			Influence of SO_4^{2-} at increased temperature of 30°C			Influence of SO_4^{2-} with water movement					
	Comparison to sulphate-free scenarios			Comparison to scenarios with SO_4^{2-} at 20°C			Influence of SO_4^{2-} with water movement			Influence of SO_4^{2-} with water movement at increased temperature of 30°C		
							Comparison to sulphate-free scenarios			Comparison to scenarios with SO_4^{2-} at 20°C in shaken conditions		
	Av. mole percentage of aragonite	% crystal N° (aragonite /calcite)	% crystal volume (aragonite /calcite)	Av. mole percentage of aragonite	% crystal N° (aragonite /calcite)	% crystal volume (aragonite/ calcite)	Av. mole percentage of aragonite	% crystal N° (aragonite /calcite)	% crystal volume (aragonite/ calcite)	Av. mole percentage of aragonite	% crystal N° (aragonite /calcite)	% crystal volume (aragonite/ calcite)
+ increase - decrease ~ similar	+	+	~	+	~	+	~	~	+	+	~	+

Table 4-1: Summary of the influence of sulphate on $CaCO_3$ precipitates formed under known parameters of Mg:Ca ratio, temperature and water movement.
Results presented for this study are summarized for the three aims of this chapter: to quantify the influence of sulphate, to quantify the influence of sulphate at elevated temperature and to quantify the influence of sulphate in water movement upon the polymorphs of $CaCO_3$.

5

The influence of temperature and pCO_2 on minor element concentrations in *Mytilus edulis* shells

The aragonite-calcite sea hypothesis was formulated from evidence of non-biogenic $CaCO_3$ formation within the Phanerozoic (Sandberg, 1983). As seawater chemistry has an influence on the subsequent mineralogy, biomineral formation should have similar controls (Dickson, 2002). Secular variation of seawater Mg/Ca ratio within the Phanerozoic influenced the mineralogy of hyper-calcifiers (Ries et al., 2010), linking with aragonite-calcite sea conditions (Sandberg, 1983). However, not all marine organisms found within the rock record match the aragonite-calcite sea hypothesis (Adabi, 2004; Zhuravlev & Wood, 2009; Balthasar et al., 2011) possibly due to localised influences such as temperature, pCO_2 and ion availability. As organisms have variable controls over their mineralogy, direct application of aragonite-calcite sea conditions is complicated. This chapter's research investigates the influence of temperature and pCO_2 on the elemental compositions of the bimineralic shell of *Mytilus edulis* (*M. edulis)*. *M. edulis* has strong biological control over its mineralogy (Lorens & Bender, 1977; 1979; Rosenburg & Hughes, 1991) and a known physiological mechanism for the exclusion of magnesium (Mg) from its shell (Lorens & Bender, 1977). Investigation of the shell elemental concentrations grown under known conditions of temperature and pCO_2 by Fitzer et al (2014a) allows for a comparison to non-biogenic results. Chapters 3 and 4 suggested the influence of seawater chemistry on non-biogenic mineralogy appeared to be constrained by environmental factors. Analysis of the elemental concentrations in *M. edulis* should help understand what influence the environment has on biomineral formation, giving an insight into how aragonite-calcite sea conditions influence biomineralisation.

5.1 Introduction

Evaluation of shell minor element chemistry is important as shell composition can provide information on environmental conditions such as water temperature (Vander Putten et al., 2000). Solution chemistry and environmental conditions influence the non-biogenic $CaCO_3$ mineralogy formed under laboratory conditions (Chapter 3 & 4). Here, the mineralogy of biogenic $CaCO_3$ was investigated to understand the role of the environment on biogenic calcification. A number of studies have indicated that simple calcifying organisms such as hyper-calcifiers are influenced by seawater conditions (Stanley & Hardie, 1998; Stanley et al., 2002) with Porter (2007) noting that mineralogy was influenced only at the time of first evolving, however evidence from more complex organisms remain inconclusive. Kiessling et al., (2008) concluded that mineralogy was influenced more strongly by sudden environmental impacts such as mass extinctions than they were by seawater chemistry evolution over time.

M. edulis was selected for this study specifically because its shell is bi-minerallic, has a tolerance of a wide range of environmental conditions, and is also found over wide geographical areas (Seed & Suchanek, 1992; Gossling, 1992). Much work has been done on bivalves, in particular *M. edulis,* because they are commonly found in coastal zones and subject to a range of environmental conditions throughout their growth (Seed & Suchanek, 1992; Gossling, 1992). Many studies have used *M. edulis* as the subject to test how solution chemistry influences mineralogy (Taylor et al., 1969; Carter, 1990; Harper et al., 1997). *M. edulis* has strong biological control over its mineralogy (Lorens & Bender, 1979; Rosenburg & Hughes, 1991) and calcification occurs in a space that is physically isolated from the external environment and results in an inner aragonite layer and outer calcite layer (Lorens & Bender, 1980). *M. edulis* mussels are found naturally within the sea-lochs of the British Isles, the Atlantic Ocean, and the South American coasts (Dalbeck, 2007). *M. edulis* has a high economical worth commercially to harvesting fisheries being valued at more than £21 million in the UK in August 2014 (Cocker & Green, 2015).

The *M. edulis* shells selected for analysis were grown under known temperature and pCO_2 conditions (see Fitzer et al., 2014a; 2014b). The bi-minerallic properties of the shell allow comparison of the non-biogenic results (Chapter 3 & 4) on aragonite and calcite to investigate the shell elemental concentrations of Mg and sulphur (S) under known temperature and pCO_2 conditions, as well as elements such as sodium (Na) and strontium

(Sr) concentrations which have previously been thought to be indicators of environmental parameters such as temperature and pCO_2 (Zhao et al., 2017a; Lorrain et al., 2010). In cooler waters, bivalves increased their calcite production through physiological controls (Lowenstam, 1954).

Minor element incorporation into biogenic $CaCO_3$ can affect biomineral formation and growth by altering structure and composition. Non-biogenic $CaCO_3$ growth results (Chapter 3) observed increased Mg concentrations in solution facilitated the growth of aragonite at the expense of calcite, the trend further amplified at elevated temperature and in water movement. Similarly the presence of sulphate in solution increased the proportion of aragonite formed at lower Mg:Ca ratios than in sulphate-free solutions and this trend was amplified at elevated temperature and in water movement (Chapter 4).

The first investigation in this work is to assess if Mg and S concentrations increase in the shell layers of aragonite and calcite by an increase in temperature of 2°C. Assessing the impact of temperature on biogenic $CaCO_3$ growth allows a comparison to the non-biogenic results (Chapter 3 & 4). The role of temperature on aragonite-calcite sea conditions has shown to be influential on non-biogenic $CaCO_3$ formation (see Chapter 3; Morse et al., 1997; Balthasar & Cusack, 2015). The influence of sulphate in seawater impacts on non-biogenic mineralogy by lowering the threshold for aragonite formation (Bots et al., 2011) and this trend is amplified at elevated temperature (see Chapter 4). Therefore, investigating the influence of temperature on aragonite-calcite sea conditions on calcifying organisms is a new concept which can provide insights into temperature's influence on biomineralisation. Direct application of geochemical data obtained from non-biogenic growth studies to how well it can be used to interpret biogenic calcification remain debated (Immenhauser et al., 2015).

Aragonite-calcite sea conditions were traditionally seen as a spatially homogeneous switch between aragonite or calcite precipitation, however, non-biogenic studies have indicated that there could be latitudinal variances in mineralogy if temperature is to be considered (Balthasar & Cusack, 2015). If temperature impacts on the Mg intake of biogenic $CaCO_3$ of *Mytilus edulis* you should expect that this could represent a latitudinal gradient with respect to the influence of Mg on the shell. Understanding the mechanisms involved on biogenic calcification are important in our understanding of the evolution of biomineralisation.

The second investigation was to assess if increased pCO_2 representing a projected level under scenarios of ocean acidification (OA) (IPCC, 2013) has impact on the elemental concentrations of Mg and S in the aragonite and calcite shell layers. Observed global CO_2 concentrations have been increased by 40% from anthropogenic sources since industrialisation (~1750AD) (Doney et al., 2009). Of this, 33% has entered the ocean, lowering pH (Raven et al., 2005), accelerating both OA and global climate change (IPCC, 2013) and influencing marine calcification (Fitzer et al., 2014; Bach, 2015; Zhao et al., 2017). pCO_2 is a strong influencer of the $CaCO_3$ system (Lee & Morse, 2010). There have been strong links between the carbon cycle and climate change observed within the rock record giving evidence to environmental changes such as elevated pCO_2, global warming and OA impacts on biota and calcification in the past (Hönisch et al., 2012). To understand if environmental influences impact on the proposed aragonite-calcite sea conditions that influence the mechanisms behind the changes in mineralogy, aids in our understanding of how environmental change impacts on biomineralisation. This is of interest to assess in biogenic mineralogy as there are biological controls over shell formation.

Biogenic $CaCO_3$ formation is influenced by changes in sources of $[CO_3^{2-}]$ and $[Ca^{2+}]$ content in the oceans alongside available inorganic carbon (Weiner & Addadi, 2011). Elevated pCO_2 will lower the carbonate saturation state increasing the possibility for dissolution, especially for aragonite, which is less stable in ambient conditions compared to calcite (Doney et al., 2009). Previous studies have noted that several species of bivalve had lowered rates of calcification in elevated pCO_2 conditions (Ries et al., 2009; Hiebenthal et al., 2013) which could be attributed to changing saturation state. Elevated pCO_2 have also shown to impact on bivalves in terms of their growth and mineralogy (Kroeker et al., 2010; Fitzer et al., 2014a, 2014b, 2014c, 2015; Hendriks et al., 2015; Zhao et al., 2017a) and these changes should show in the concentration of elements within the shells. Elevated temperature and pCO_2 have also shown to impact on the structural integrity of biomineral formation (Fitzer et al., 2014b; 2014c) and therefore could lead to changes in elemental composition due to defects in crystal lattice structures allowing incorporation of foreign ions.

Understanding how changes in temperature and pCO_2 will influence the carbon species in seawater, and in turn, biomineralising mechanisms will aid our understanding on how environmental conditions influence biogenic mineralogy (Gattuso & Hansson,

2011). pCO_2 has been viewed as one of the main drivers of aragonite-calcite sea conditions (Sandberg, 1983). Evidence from investigations into ooid mineralogy suggest that pre-Carboniferous pCO_2 was higher than today and facilitated calcite ooids and calcifying skeletal parts (Mackenzie & Pigott, 1981). However, lower pCO_2 levels occurred post-Carboniferous and the mineralogy facilitated was of aragonitic ooids and high-Mg calcite suggesting pCO_2 had a major influence on mineralogy (Mackenzie & Pigott, 1981). This also suggested that the Mg content of ooid mineralogy fluctuated as a function of pCO_2, facilitating increased Mg incorporation at lower pCO_2 which would inhibit calcite growth at the expense of aragonite (Mackenzie & Pigott, 1981). However, Allison (2011) disagrees showing pCO_2 does not influence Mg content of biominerals.

This chapter focusses on the impacts of elevated temperature and pCO_2 on element concentrations in 1-year old adult mussels grown under known temperature and pCO_2 for four months. The calcification from within the four-month timeframe was assessed under present day and future pCO_2 (380 and 1000 µatm) at ambient temperature and ambient temperature +2°C, to determine what influence these parameters have on the element concentrations within *M. edulis* calcite and aragonite.

5.1.1 Aims of the Chapter

Non-biogenic precipitation experiments demonstrated that Mg and SO_4^{2-}, along with temperature and water movement, influenced $CaCO_3$ crystal formation (Chapter 3 & 4). Adult *M. edulis* shells grown in controlled temperature and pCO_2 environmental conditions (see Fitzer et al., 2014b for full methodology) were made available and enable investigating the influence of temperature and pCO_2 on element composition in biogenic calcite and aragonite. The key aims for this research were 3-fold:

1. To evaluate what influence temperature and pCO_2 have on the element concentrations of Mg and S in *M. edulis* shells.
2. To evaluate if temperature and pCO_2 influence the element concentrations of Mg and S differently across the calcite and aragonite layers of *M. edulis* shells.
3. To evaluate if temperature and pCO_2 influence element concentrations of Na and Sr across the calcite and aragonite layers of *M. edulis* shells.

5.1.2 Origin of samples

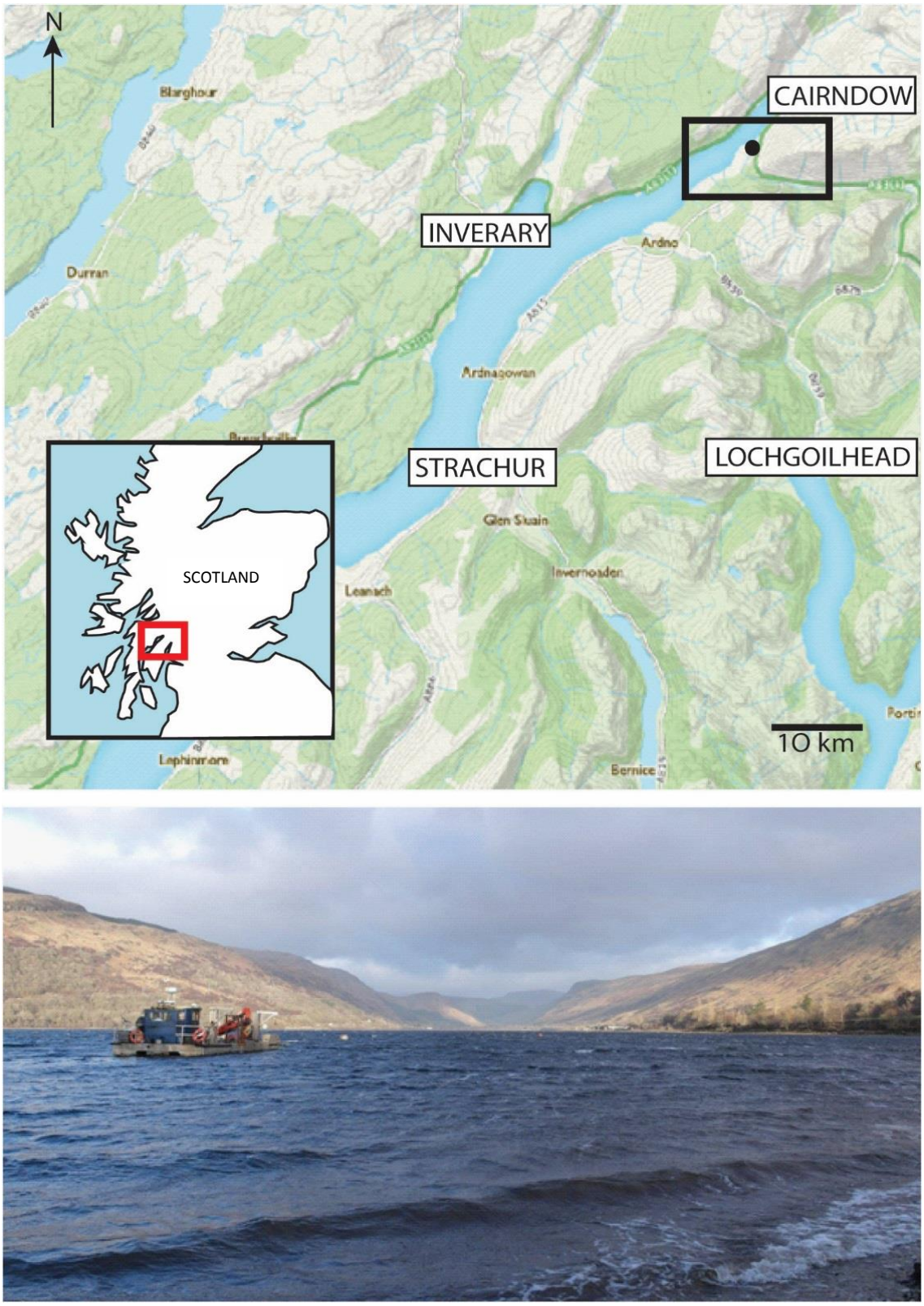

Figure 5-1: Original sample collection site located at Loch Fyne in Western Scotland **Mussels were collected from Loch Fyne prior to placing in laboratory conditions for study by Fitzer et al., (2014a; 2014b; 2015b). Lower photograph views the collection site within Loch Fyne looking to the upper headland. Photo: C.E. Miller.**

The mussels for this study originate from the brackish waters of Loch Fyne, Argyll, UK (56°15'21"N; 4°56'13"W) **(***Figure 5-1***)** from Loch Fyne Oysters Ltd. Loch Fyne is one of the longest and deepest Scottish sea-lochs where the surface waters circulated are influenced by freshwater inflow from hillslope tributaries, as well as tidal influx and wind-blown sediment dust (Tett et al., 1986; Simpson & Rippeth, 1993; Tett et al., 2012). The area is used by both aquaculture and recreational tourism and has a high turnover from forestry on the surrounding hillslopes (Tett et al., 2012) making it an area of high economic value. *M. edulis* specimens were harvested from Loch Fyne during October 2012 at 1-year-old (Fitzer et al., 2014a).

5.1.2.1 **Environmental parameters of multigenerational study**

Fitzer et al. (2014a) transferred the mussels collected from Loch Fyne to four separate 6-litre experimental tanks with natural filtered seawater. Seawater pCO_2 was brought to the required levels for scenarios over a one-month acclimation time. After acclimation, each tank was set to mimic the seasonal changes in temperature of Loch Fyne (*t*). The mussels donated to this chapter's research originated from the adult group of a larger multigenerational study where the scenario temperature and pCO_2 were set to be of ambient temperature (*t*) and pCO_2 of 380 or 1000 µatm, and ambient temperature plus 2°C (*t*+2) and pCO_2 of 380 or 1000 µatm. Mussels were fed 10 ml of cultured microalgae per tank every second day by Fitzer et al. (2014b).

At four months after acclimation the adult mussels for this study were removed from the tanks and shells cleaned and dried (Fitzer et al., 2015). As the mussels were retrieved from the same original collection site at Loch Fyne, and at a similar age prior to placing in laboratory tanks (Fitzer, et al., 2014a, 2014b, 2015) any changes in the element concentrations within new growth will be the result of temperature and pCO_2. A recent study has observed that the $CaCO_3$ mineralogy element content was influenced in part by the size of the shell (Piwoni-Piórewicz et al., 2017). The shell samples used in this work were therefore of similar sizes.

5.1.3 Minor elements in biogenic calcite and aragonite

As shell calcification occurs, ions will replace Ca^{2+} in $CaCO_3$ with the availability of the ions replacing Ca^{2+} being a function of biological and environmental factors (Wright,

1995; Wang & Fisher, 1997). The incorporation of these ions impact on the thermodynamic properties of the mineralogy forming.

5.1.3.1 **Magnesium**

Minor elements are incorporated into the mussel shell as they grow (Weiner & Dove, 2003; Marin, 2012). Variation of uptake of foreign ions influences the mineralisation that occurs by altering crystal lattice structures. The influence of temperature on Mg incorporation into $CaCO_3$ has a long history of research (Dodd, 1967). One reason that Mg content is investigated is because the concentration of marine Mg over the past 1 million years has been fairly consistent in terms of its ratio with calcium (Broeker & Peng, 1982). This allows any variations in Mg/Ca ratio over shorter time periods to be correlated with temperature influence (Rosenthal et al., 1997; Lea et al., 1999; Lear et al., 2002). The shell Mg/Ca ratio of the mollusc has been the focus of studies due to the question over why the Mg/Ca ratio is lower than the seawater chemistry it forms from (Brand et al., 2003; Zhu et al., 2010).

Non-biogenic studies have shown that elevated temperature lowers the Mg/Ca ratio at which aragonite forms at the expense of calcite growth because temperature increases Mg incorporation into the calcite crystal lattice increasing its solubility (Busenberg & Plummer, 1989). Biogenically, much of the research focussing on temperature and Mg incorporation have focussed on foraminifera because they are less complex than other biogenic formers such as bivalves (Rosenthal et al., 1997; Lear et al., 2000; Cléroux et al., 2008). The link between Mg and temperature in biogenic $CaCO_3$ is complex due to a number of influences on the relationship: by salinity (Dodd, 1967), by physiological mechanisms (Lorens & Bender, 1977) or by pH or $[CO_3^{2-}]$ changes (Dissard et al., 2010). The link between temperature and Mg/Ca ratio has also been observed in coccolithophores (Stoll et al., 2001), foraminifera (Nurnberg, 1995; Elderfield & Ganssen, 2000), brachiopods (Lowenstam, 1961; Mill & Grossman, 1994) and echinoderms (Dickson, 2002). It is understood that control of Mg by the Mg/Ca ratio influences the Mg content of calcite (Ries, 2005; Ries, 2006; Stanley et al., 2005; Stanley, 2006). Taylor et al. (2009) investigated Mg incorporation into biominerals and observed that an increase in temperature enriches the Mg incorporation. Attempts have been made to use the Mg/Ca

ratio of the shell as a proxy of temperature environmental conditions in bivalves (Dodd, 1965; Klein et al., 1996; Vihtakari et al., 2016), but this link remains unclear for this group.

Mg incorporation is linked to the organic content which in turn can be influential on the mineralogy formed (Kitamura, 2001; Loste et al., 2003). As Mg and Ca are restricted to the calcified shell, assessing the ratio of Mg to Ca can help to normalise any changes which occurred due to organic content.

Biogenically $CaCO_3$ formed by molluscs is controlled by physiological mechanisms which limit elements taken into the shell such as Mg (Lorens & Bender, 1977; Erez, 2003). Elevated Mg:Ca ratio of seawater increases the proportion of aragonite compared to calcite formed non-biogenically (Chapter 3) with the proportion facilitated to increase under elevated temperature (Chapter 3). Mg incorporation into the crystal lattice of calcite is a known growth inhibitor (Davis et al., 2000). Much work has assessed the role of temperature on the incorporation of Mg into $CaCO_3$ non-biogenically (Morse et al., 2007; Balthasar & Cusack, 2015). These studies document that mineralogy is influenced by seawater Mg/Ca ratio and temperature in a non-linear relationship (Morse et al., 1997). Therefore, biogenically formed $CaCO_3$ should be influenced in the same way. However, due to the physiological mechanisms regulating Mg content, organisms can have control over their own mineralogy (Lorens & Bender, 1977).

Biogenically Mg has shown to substitute for Ca in calcite (Pokroy et al., 2006), however this substitution does not occur in biogenic aragonite formation (Finch & Allison, 2007; 2008; Yoshimura et al, 2015). Any changes to crystal lattice structure may influence the Mg content, not only by its substitution for Ca but by attaching to surfaces of crystals or inter-crystal spaces (Foster et al., 2008; Immenhauser et al., 2015). Studies of biogenic $CaCO_3$ formation investigating elevated temperature scenarios lead to concern because aragonite is less stable than calcite leaving organisms to dissolution and predation (due to softer shells), in modern seawater (Orr et al., 2005; Byrne, 2012; Hiebenthal et al., 2013; Fitzer et al., 2015; Zitter et al., 2015; Zhao et al., 2017b). If increased Mg incorporation into calcite occurs at higher temperature biogenically as it does non-biogenically, investigation of the Mg concentration in bivalve shells, where the organism has control, could help understand how the biomineralisation mechanisms influence mineralogy.

Carbonate mineralogy has been influenced throughout the Phanerozoic by changes in pCO_2 (Wilkinson & Given, 1986; Berner, 2004). Previous work suggested that higher pCO_2 atmospheres in the pre-Carboniferous facilitated calcitic ooids and calcified skeletons, whereas ooids formations forming post-Carboniferous where the pCO_2 was lower and increasingly facilitated aragonite and high Mg-calcite (Mackenzie & Pigott, 1981). This suggested that the Mg content of ooid mineralogy fluctuated as a function of pCO_2, facilitating increased Mg incorporation at lower pCO_2 which would inhibit calcite growth at the expense of aragonite (Mackenzie & Pigott, 1981). However, Allison (2011) disagrees showing pCO_2 does not influence Mg content of biominerals. However, Morse & Lee (2010) found pCO_2 influenced mineralogy in an opposite direction than previously suggested (high pCO_2 facilitating aragonite formation), noting that factors such as pH and alkalinity also have a role to play in the mineralogy forming.

Biogenically, it was suggested that organisms with higher Mg content were more prone to dissolution in elevated pCO_2 than those of low-Mg calcite (Morse et al., 2007). This would be due to the influence of elevated pCO_2 lowering saturation state (Feely et al., 2004). However, Ries et al. (2009) observed that elevated pCO_2 did not directly relate to the mineralogical solubility. To determine how temperature and pCO_2 influence Mg incorporation into *M. edulis* shells will aid in our understanding of how biomineral formation occurs under these parameters.

5.1.3.2 **Sulphur**

Throughout the Phanerozoic, sulphate (SO_4^{2-}) has co-varied with Mg^{2+} (Lowenstein et al., 2001; Horita et al., 2002). Sulphur (S) is present in the marine realm as part of the S cycle, through redox reactions transforming sulphide minerals or calcium sulphate compounds and transferring them from rivers into the ocean. Concentrations of S in biogenic $CaCO_3$ are variable between 100s-1000s parts per million (Busenberg & Plummer, 1985) and is the 4th most common marine ion (Halvey et al., 2012) contributing a large component of the alkalinity budget which influences pH (Morel & Hering, 1993; Halvey et al., 2012). S has been acknowledged to be present within calcite biogenically (Milliman, 1974).

The concentrations of sulphur within bivalve shells have received little attention and remain unclear (Yoshimura et al., 2014). One of the main areas for debate is where

S is found within the $CaCO_3$. A number of authors observe S as reflective of the organic matrix (Lorens & Bender, 1980; Dauphin & Cuif, 1999; Cuif et al., 2003; Dauphin et al., 2003). However, other authors have observed S being incorporated into the $CaCO_3$ mineralogy as S or SO_4^{2-}, by substitution of CO_3^{2-} ions in calcite (Takano et al., 1980; Busenberg & Plummer, 1985; Takano et al., 1985; Kampschulte & Strauss, 2004; Kontrec et al., 2004; Nguyen et al., 2014). Substitution in turn can influence mineralogy by deformation of the crystal lattice (Fernandez-Diaz et al., 2010; Arroyo-de Dompablo et al., 2015; Perrin et al., 2017). Crystal lattice defects are suggested to occur more frequently with faster growth rates and in turn more substitution of both Ca^{2+} and CO_3^{2-} by other ions in general (Yoshimura et al., 2017).

Incorporation of S has been linked to representing environmental conditions influencing growth (Yoshimura et al., 2013). Lorens & Bender (1980) suggested S could be used as a proxy for organic content within *M. edulis* shells. However, this remains contested as organic content and S measurements don't always reflect this (Dalbeck et al., 2006). Inorganic S is correlated with the Mg content in the calcite layer of *M. edulis* (Kontrec et al., 2004) and in turn linked to temperature. S is thought to be representative of the organic matrix (Dauphin et al., 2003; Yoshimura et al., 2014).

Previous work has discussed that S is incorporated easier into calcite than aragonite (Kontrec, et al., 2004), mostly allied to the calcitic organic matrix (Vander Putten et al., 2000; Dauphin et al., 2003). However, England (2005) observed that *M. edulis* calcite contains less organic content compared to aragonite. Incorporation of sulphur into $CaCO_3$ influences the lattice structure in the same way all foreign ions can (Kontrec et al., 2004) causing distortion by substituting for CO_3^{2-} ions (Kontrec et al., 2004). Such defects to the crystal lattice can allow for increased Mg concentrations incorporating with the lattice structure in the spaces left by sulphur incorporation (Kralj et al., 2004). By analysing the concentrations of both Mg and S in *M. edulis* shells, may suggest a link between the organic content as represented by the connection S has to the organic matrix. High growth rate is also correlated with low S concentrations within the aragonite layer of clams but only in summer months, this therefore suggests that lower S concentrations could represent link with elevated temperature (Yoshimura et al., 2014).

The presence of SO_4^{2-} on non-biogenic $CaCO_3$ growth increases aragonite formation at the expense of calcite at increased Mg/Ca ratio and at elevated temperature (Chapter 4). Recent laboratory work suggests that the Mg/Ca ratio at which aragonite forms at was decreased in the presence of sulphate (Bots et al., 2011). As *M. edulis* has a physiological mechanism which controls uptake of Mg into the shell (Lorens & Bender, 1977) it is of interest to analyse other elements such as S which have shown to correlate with changes in temperature and individual variability in growth (Yoshimura et al., 2014) to see if the concentrations of these are also influenced like Mg uptake is.

5.1.3.3 **Sodium and Strontium**

Elements other than Mg and S incorporate into *M. edulis* shells and some have links to environmental parameters such as sodium (Na) and strontium (Sr) both being influenced by temperature and pCO_2 (Zhao et al., 2017a; Lorrain et al., 2010).

Sodium sulphate is the second most common water-soluble mineral in nature after NaCl and therefore is present in natural seawater influencing salinity and ion availability for subsequent $CaCO_3$ polymorphs precipitated from seawater (Garett, 2011; Vavouraki et al., 2008). Although Na is known to actively substitute for Ca in $CaCO_3$ both non-biogenically and biogenically (Billings & Ragland, 1968) the mechanisms for sodium incorporation is still ambiguous. However, the influence Na has on $CaCO_3$ mineralogy has been suggested to influence polymorph formation (Perrin et al., 2017). Although Na^+ and SO_4^{2-} ions can incorporate into the calcite lattice (Busenberg & Plummer 1985; 1989; Takano 1985), they are more easily incorporated into the aragonite crystal lattice (Kitano et al., 1962; Okumura & Kitano, 1986; Morse & Mackenzie, 1990). This substitution is possible because the ionic radius of Na is similar to that of Ca, therefore substitution should not defect the crystal lattice structure (Yoshimura et al., 2017). Despite this, Busenberg & Plummer (1985) noted a dependency on the defects to influence Na incorporation. Furthermore, laboratory experiments investigate the influence of salinity noted that although Na incorporation is preferential in aragonite, if higher concentrations of Na are present in seawater, this can have an inhibiting influence on Na incorporation (Kitano et al., 1962; Okumura & Kitano, 1986). Investigation of the incorporation of elements within $CaCO_3$ formation can be used as a ratio against Ca content to give an insight into the environmental conditions at the time of formation (Dissard et al., 2010).

Zhao et al. (2017) observed that Na incorporation increased non-linearly when pH decreased, unaided by the influence of temperature. With pH and pCO_2 being linked, the pCO_2 level may influence Na incorporation into mussel shells. Although ion substitution and incorporation has shown to be of common occurrence in $CaCO_3$ formation, White et al., (1978) suggested that the Na ion in corals did not appear be influenced by environmental parameters that did effect Mg, S or Sr.

Alongside ratios of Mg/Ca, the ratio of Sr/ Ca has previously been investigated as a possible indicator of temperature and salinity in the past (Beck et al., 1992; Nürnberg, 1996). Sr incorporation is documented on many occasions to be influenced by temperature as observed in bivalves (Dodd, 1965), coccolithophores (Stoll et al., 2002) and foraminifera (Lea et al., 2002). However, the mechanisms of Sr incorporation in bivalve shells remain poorly understood compared to other organisms due to complexities in the underlying mechanisms for calcification. Some factors making Sr incorporation complex are metabolism, salinity (Klein et al., 1996) and kinetics (Vander Putten et al., 2000), but these don't match with studies investigating Sr incorporation non-biogenically or in foraminifera (Klein et al., 1996; Vander Putten et al., 2000; Lorrain et al., 2010). Sr incorporation into biogenic $CaCO_3$ has been correlated with accelerated rates of calcite growth (Lorens, 1981). The Sr incorporation into foraminifera is thought to be influenced by the CO_3^{2-} concentration of seawater, and in turn calcite saturation state (Lea et al., 1999; Mortyn et al., 2005; Rosenthal et al., 2006; Dissard et al., 2010). De Leeuw (2002) documented that the incorporation of Sr into calcite would influence the growth kinetics, this was later thought to be dependent on the actual Sr concentration present at the time of formation (Wasylenki et al., 2005). Lowered concentrations of Sr have been shown to promote calcite growth (Wasylenki et al., 2005).

5.2 **Methodology**

Donated adult mussel shells grown under known temperature and pCO_2 conditions (see Fitzer et al., 2014a) were removed after 4 months, cleaned and then air-dried before mounting in resin. Each shell in resin was cut down their length, 8-10mm from the centre. A second cut was made cutting precisely through centre of each shell to give the required cross-section per shell. Each cross section was polished before gold coating ready for analysis (for all steps see section 2.3.2.).

Analysis of the shell elemental concentrations were carried out using scanning electron microscopy with Energy Dispersive Spectroscopy (EDS). Each shell specimen had three transects of spot analysis completed on the calcite and aragonite layers grown under known laboratory conditions, from the outer shell edge (calcite) to inner shell (aragonite). This technique was repeated on 2 shell specimens per scenario of ambient temperature (*t*) at a pCO_2 of 380 or 1000 µatm, and ambient temperature plus 2°C (*t*+2) at a pCO_2 of 380 or 1000 µatm. Spot analyses in both calcite and aragonite measured concentrations of the elements of C, O, Ca, Mg, S, Na and Sr (see section 2.3.2.).

	Scenario	% of points measuring Mg below EDS detection limits	% of points measuring S below EDS detection limits	% of points measuring Na below EDS detection limits	% of points measuring Sr below EDS detection limits
Calcite	*t*, 380	33.79	0	13.08	15.26
	t+2, 380	6.49	0	1.18	18.88
	t, 1000	3.08	0	0.88	20.51
	t+2, 1000	0.74	0	0	18.5
Aragonite	*t*, 380	58.88	0.92	0.92	42.32
	t+2, 380	6.84	0	0	13.92
	t, 1000	3.9	0	0	4.16
	t+2, 1000	29.52	2.88	0	5.76

Table 5-1: The proportion of the spot analysis omitted as below limits of detection by EDS. The number of spot analysis points removed from the total analyses for each element presented as a percentage (%) of total number measured.

The minimum spacing between spot analyses is 1 µm in EDS. When taking spot analyses across the aragonite thickness, some shells were observed to have aragonite either less than 2µm thick at the tip, or that the aragonite layer had not tapered completely up to the tip edge like the calcite layer did. Therefore, as shell growth occurs both in length and thickness, this allowed for the aragonite layer to be measured separately on the interior shell surface instead of the tip edge. This technique allowed the new growth of aragonite, calculated based on a proportion of the growth that occurred in the calcite layer, to be measured where the aragonite layer would be thick enough to give enough analysis points for EDS (see section 2.3.2.1.). Alongside Mg, Na and Sr measurements had the highest proportion of concentrations falling below detection limits (***Table 5-1***).

Variability in element concentrations between individual shells from the same growth conditions were present. Examination of organic vs. inorganic element concentrations of both C and O can be used as one possible explanation for the variability noted. Using the concentration of Ca measured as an indication of the inorganic components the inorganic and organic components of C and O can be calculated by showing the change in concentration from pure inorganic $CaCO_3$ using the equation for $CaCO_3$ formation (see section 2.3.3.2.). The ratio of inorganic to organic components of the element indicates what proportion was attached to each. This allows an indication of whether the EDS beam has hit a marginal edge of a polymorph as organic components lie on the edges of calcite and aragonite. EDS does not differentiate between inorganic and organic components of the elements measured, therefore calculating what proportion of the elements were linked to the organic content of the shell was assessed as a possible method to account for differences between individual shells.

5.2.1 Statistical Analysis

Investigation of the differences between the element concentrations were carried out using 2-sample t-tests considering all conditions for normality were met. T-tests were possible because the dataset met normal distribution. Single element concentrations of Mg, S, Na and Sr were tested, as were Mg/Ca ratios. These were used to show differences between ambient conditions (*t*, 380) and elevated temperature (*t*+2, 380), elevated pCO_2 (*t*, 1000) or combined temperature and pCO_2 (*t*+2, 1000). The first null hypothesis being assessed was test that an increase in temperature did not change the concentration of the element or the element/element ratio being assessed. The second null hypothesis was to test that an increase in pCO_2 did not increase the concentration of the element or element/element ratio being assessed. Statistically significant differences were considered to reject the null hypothesis when $p \leq 0.05$. All analysis was carried out using statistics package *Minitab 17* (See section 2.3.4. for more detail).

5.3 **Results**

EDS spot analysis results yielded minor element concentrations of Mg, S, Na and Sr in both the calcite and aragonite layers of each shell sample and are presented in *Table **5-2*** for those above detection limits. Any spot analysis results that were below detection limits were removed from further analyses.

Scenario, (shell sample)	Layer	Mg Conc. Range (wt. %)	S Conc. Range (wt. %)	Na Conc. Range (wt. %)	Sr Conc. Range (wt. %)	Average Transect Length µm (SD)
***t*, 380 (1)**	Calcite	0.04- 0.09	0.10- 0.48	0.10- 0.22	0.03- 0.15	119.00 (1.73)
	Aragonite	0.02- 0.08	0.02- 0.11	0.16- 0.47	0.02- 0.23	24.00 (3.00)
***t*, 380 (2)**	Calcite	0.03- 0.15	0.09- 0.57	0.08- 0.18	0.02- 0.20	296.00 (21.28)
	Aragonite	0.01- 0.11	0.02- 0.08	0.12- 0.37	0.02- 0.25	10.00 (0.57)
***t*+2, 380 (1)**	Calcite	0.05- 0.18	0.14- 0.31	0.07- 0.22	0.02- 0.18	117.66 (14.01)
	Aragonite	0.02- 0.10	0.03- 0.35	0.11- 0.35	0.02- 0.17	3.33 (0.57)
***t*+2, 380 (2)**	Calcite	0.04- 0.18	0.09- 0.49	0.04- 0.20	0.04- 0.10	127.33 (6.42)
	Aragonite	0.02- 0.10	0.05- 0.14	0.11- 0.24	0.16- 0.16	11.30 (1.52)
***t*, 1000 (1)**	Calcite	0.05- 0.13	0.39- 0.75	0.06- 0.16	0.02- 0.18	50.00 (10.00)
	Aragonite	0.02- 0.07	0.04- 0.09	0.12- 0.28	0.02- 0.11	2.60 (0.57)
***t*, 1000 (2)**	Calcite	0.02- 0.12	0.07- 0.41	0.07- 0.20	0.03- 0.18	157.00 (19.05)
	Aragonite	0.02- 0.08	0.02- 0.11	0.06- 0.25	0.02- 0.21	4.30 (0.57)
***t*+2, 1000 (1)**	Calcite	0.04- 0.15	0.12- 0.43	0.10- 0.24	0.02- 0.13	130.00 (0.00)
	Aragonite	0.03- 0.07	0.02- 0.10	0.21- 0.46	0.01- 0.16	10.33 (0.57)
***t*+2, 1000 (2)**	Calcite	0.02- 0.12	0.06- 0.41	0.10- 0.29	0.03- 0.12	108.00 (9.00)
	Aragonite	0.01- 0.06	0.02- 0.15	0.25- 0.51	0.02- 0.27	17.66 (0.57)

Table 5-2: Summary of EDS results from *M. edulis* calcite and aragonite layers.
Summary of the range of concentrations (minimum to maximum) of Mg, S, Na and Sr measured within the calcite and aragonite layers of *M. edulis* shells. Data are expressed as wt. % for each element. Average transect length is expressed as the average distance analysed of 3 transects per layer ±SD.

The new growth area of each shell grown in the 4-month laboratory conditions was very small (~0.24-0.99mm), most growth occurred in the shortest shells (*t*+2, 1000). The aragonite layer was much thinner than the calcite layer in all shells, and not always present at the tip end ***(Figure 5-2)***. Two-way t-tests were carried out to compare the data combined from both shells in one scenario to each of the other scenarios, again combining the data from both shells.

A

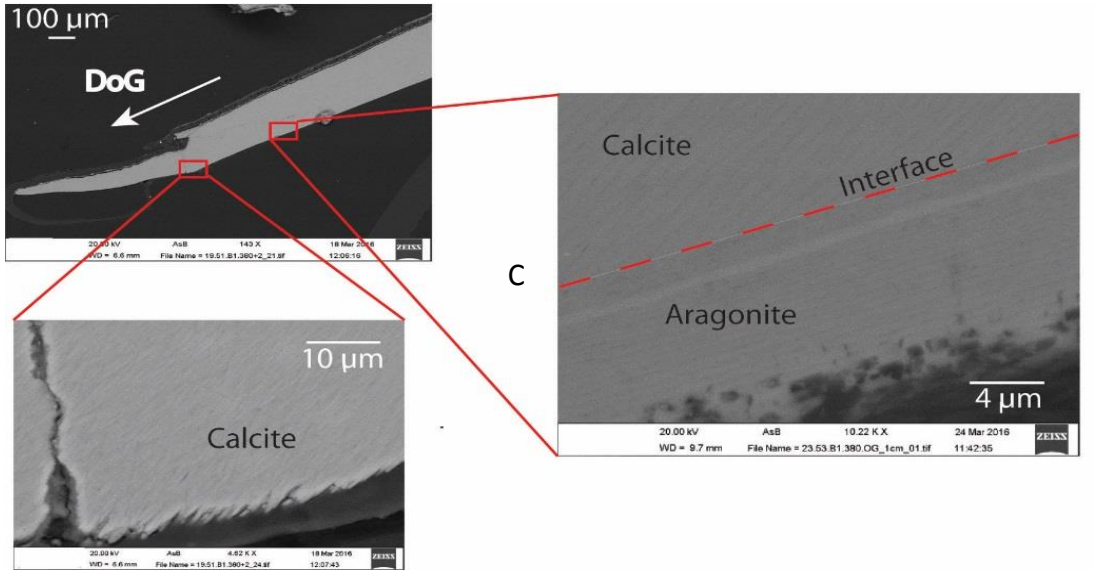

B

Figure 5-2: Angle Selective Backscatter Electron image (AsB) of *Mytilus edulis* shell polished section.
AsB image captured as described in section 2.3.2.3. A- The shell tip of *Mytilus edulis* grown in elevated temperature at 380 µatm pCO_2 (*t*+2, 380), DoG = direction of growth. Inset B - Calcite layer extending to the interior edge. Inset C - Aragonite and calcite interface (red dashed line). Aragonite was present in a very thin layer on the interior edge.

Where bias between individual shells cannot be ruled out, differences in organic content could offer an explanation. 2-sample t-tests were carried out on ratios of inorganic/organic carbon and inorganic/organic oxygen of the calcite and aragonite layers (for method see section 2.3.3.2) For each experiment scenario of temperature and pCO_2, the inorganic/organic ratios of either carbon or oxygen from both shells were compared to each other for the aragonite and calcite layers to determine if there were significant differences in the ratio between shell datasets. Boxplot summaries for all inorganic/organic ratios of carbon or oxygen are given in ***Figure 5-3*** separated for the layers of calcite and aragonite.

For calcite, the inorganic/organic ratio of carbon was significantly different between shells in all scenarios ($p < 0.01$) indicating a variation in the organic content of the shells. The ratio of inorganic/organic oxygen in calcite for most scenarios was also found to be significantly different ($p < 0.01$), except for elevated temperature at ambient pCO_2 (t+2, 380) where the results were not significantly different ($p > 0.05$).

In aragonite, the inorganic/organic ratio of carbon was significant in all scenarios of elevated temperature ($p < 0.01$) and for elevated pCO_2 ($p < 0.05$). However, although there were large differences calculated between shells in the ratios of inorganic/organic oxygen in aragonite (i.e. *t*+2, 1000) (***Figure 5-3***), the data was found to be similar between shells under all scenarios of temperature and pCO_2 ($p > 0.05$).

The differences in organic content observed may help account for variances between shells in elemental concentration and will be discussed in relation to concentrations of Mg, S, Na and Sr in later sections.

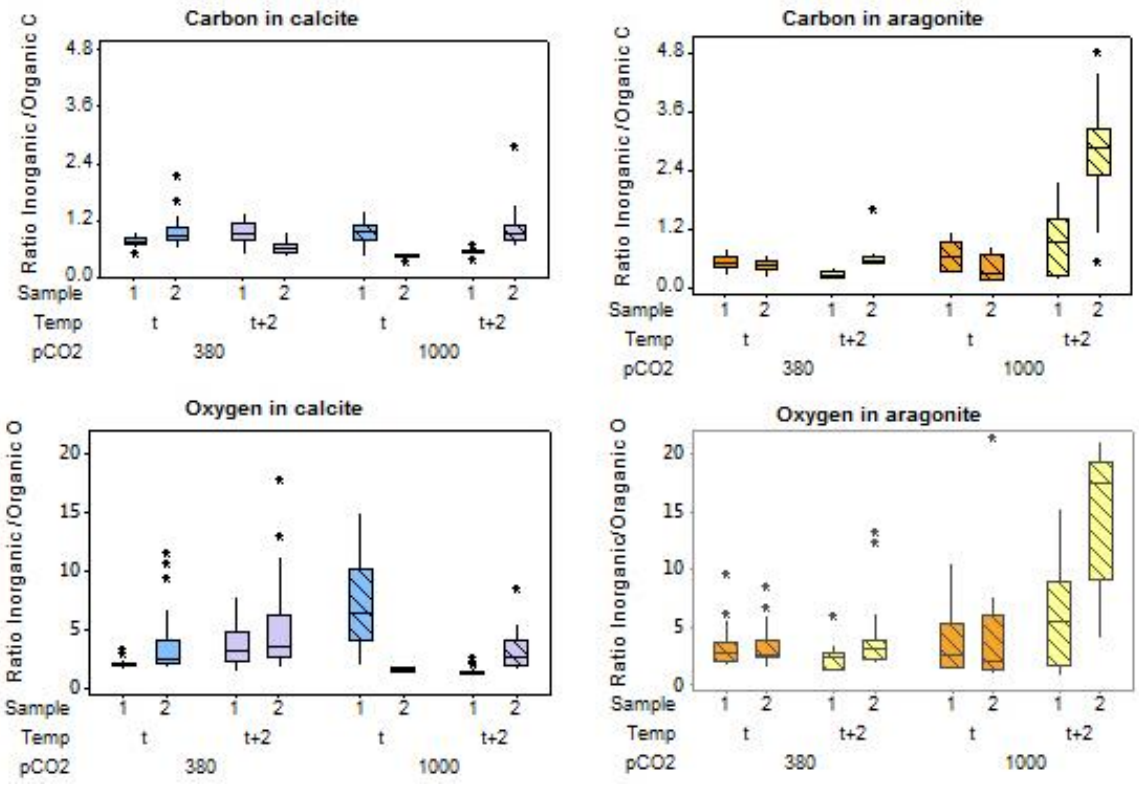

Figure 5-3: Inorganic/organic ratios for carbon and oxygen in calcite and aragonite. Average inorganic/organic ratio from calculations as explained in section 2.3.3.2. for the calcite layer are presented on the left, blue box plots representing ambient *t* (°C) and purple representing ambient *t*+2 (°C) and on the right presented for the aragonite layer, orange boxplots representing ambient *t* (°C) and yellow representing ambient *t*+2 (°C). Slanted lines in both graphs represent elevated pCO_2. Each box represents the interquartile range of each data set and separated by the median. Whiskers represent the lowest values Q1-1.5 (Q3-Q1) or highest values Q3 + 1.5 (Q3 - Q1) from the box. Outliers are represented by asterisk (*).

5.3.1 Influence of temperature (*t*) and pCO_2 on elemental concentrations in *M. edulis* calcite and aragonite layers

5.3.1.1 Magnesium concentration

Scatter plots of Mg concentrations in calcite and aragonite from the exterior edge towards the interior edge of the shell are presented in Figure 5-4***.*** Each graph indicates the three transects of spot analyses per shell for Mg normalised to a percentage of the original length measured so that individual shell layers of different thicknesses can be compared.

There were notable differences between the elemental concentrations in the calcite and aragonite of *M. edulis* shells. Mg concentrations were higher in calcite than aragonite. The variability of Mg concentration in aragonite was more consistent in all shells and Mg levels were 0.02- 0.09 wt. % under all scenarios of *t* and pCO_2 and thus lower than in calcite (Figure 5-4), most notably at the exterior edge next to the periostracum (0.07-0.18 wt. %) under all scenarios of *t* and pCO_2 (Figure 5-4).

Elevated temperature (*t*+2, 380) significantly increases the Mg concentrations compared to the range at ambient temperature (*t*, 380) present in calcite ($p < 0.01$, $T = -5.14$, $df = 83$, $n = 92, 55$) **(*Figure 5-5*).** At ambient temperature and elevated pCO_2 the concentration of Mg in calcite is increased (*t*, 380 compared to *t*, 1000), but results were not significantly different ($p > 0.05$). However, the combined treatment of elevated temperature and pCO_2 significantly decreased the Mg concentration (*t*+2, 380 compared to *t+2*, 1000) ($p < 0.01$, $T = 2.51$, $df = 99$, $n = 55, 71$). The distribution of Mg across the calcite layer was variable between individual shells of the same scenario, the largest variability notable between shells at ambient temperature and pCO_2 where the concentration varied in calcite 0.02-0.16 wt. % (*t*, 380) (***Figure 5-5***).

Concentrations of Mg in aragonite did not yield significant results under elevated temperature or elevated pCO_2 ($p > 0.05$ in all scenarios). However, the aragonite layer of *M. edulis* has been noted in a previous study to have a higher organic content than calcite (England, 2005). As the concentration of Mg varies between scenarios in aragonite, to rule out any bias in changes in concentration observed which may come from any organic compounds which make up the shell parts the Mg/Ca ratio can be investigated.

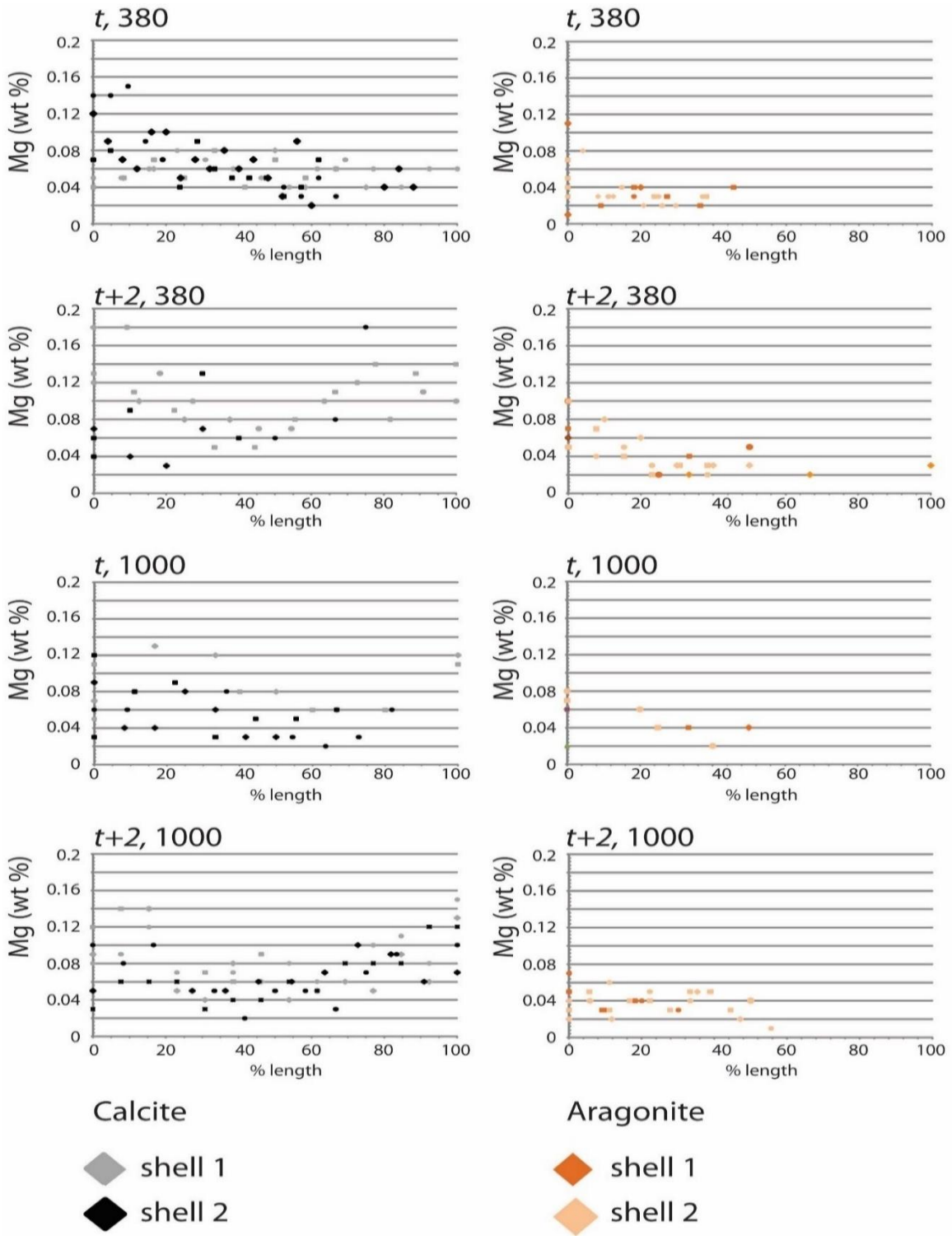

***Figure 5-4*: Scatter plots of Mg element concentration within the calcite and aragonite layers of *M. edulis*.**

The concentration of Mg within the calcite (left black & grey) and aragonite (right orange & peach) layers of *M. edulis* shells. Transects read from outer shell at 0% length towards inner shell at 100%. Each data point equals one analysis point in one transect. For each shell, all spot analysis from 3 transects per layer are plotted to determine any relationships. The distance analysed across the shell is normalised to a percentage distance to allow comparison between shells where layers were different sizes (distances of transects as given in *Table 5-2*). In aragonite, most analyses for Mg from 60% length to 100% (innermost shell edge) fell below detection limits and therefore are not indicated.

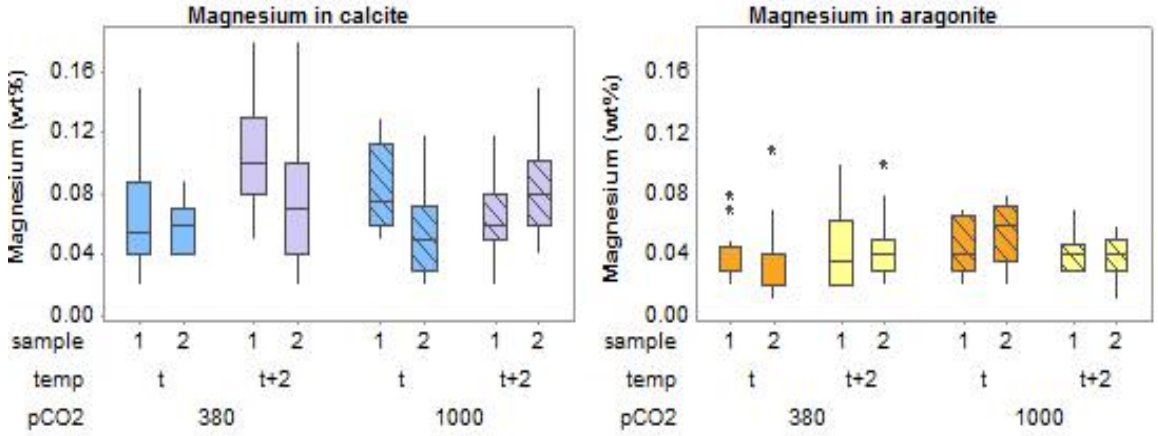

Figure 5-5: Magnesium in *M. edulis* calcite and aragonite.
Average concentrations for Mg measurements by EDS of the calcite layer are presented on the left, blue box plots representing ambient *t* (°C) and purple representing ambient *t*+2 (°C) and on the right presented for the aragonite layer, orange boxplots representing ambient *t* (°C) and yellow representing ambient *t*+2 (°C). Slanted lines in both graphs represent elevated pCO_2. Each box represents the interquartile range of each data set and separated by the median. Whiskers represent the lowest values Q1-1.5 (Q3-Q1) or highest values Q3 + 1.5 (Q3 - Q1) from the box. Outliers are represented by asterisk (*).

The Mg/Ca ratio of the shell layers was investigated to rule out any bias in changes observed which may come from any organic compounds which make up the shell parts. Mg and Ca are restricted to the calcified shell, therefore assessing the ratio of Mg to Ca normalises any changes which occurred due to organic content. The Mg/Ca ratio of the shells also allowed the Mg content to be assessed in the context of the environmental conditions the shell grew within as it is an indicator of water temperature (Ullman et al., 2013). As temperature was controlled in the laboratory, which could influence Mg uptake, the Mg/Ca ratio content of the shells should be relatively constant unless biological factors from the organism itself are involved (Poulain et al., 2015).

In calcite, the Mg/Ca increased significantly ($p < 0.01$, $T = -4.71$, $df = 83$, $n = 93; 55$) with elevated temperature at pCO_2 380 (*t*+2, 380) compared to ambient conditions (*t*, 380). However, a decrease in the Mg/Ca ratio observed with elevated pCO_2 (*t*, 380 and *t*, 1000) at ambient temperature was not statistical significant ($p > 0.05$). The Mg/Ca ratio was also observed to increase significantly with combined elevated temperature and pCO_2 compared to the other 3 scenarios (*t*, 380 ($p < 0.05$, $T= 0.33$, $df = 69$, $n = 93, 39$); *t*+2, 380 ($p < 0.05$, $T= -2.59$, $df = 130$, $n = 93, 72$); *t*, 1000 ($p < 0.05$, $T = -2.42$, $df = 93$, $n = 39, 72$)). (***Figure 5-6***). These results suggest a positive link between elevated temperature and the

Mg/Ca ratio matching with previous studies (Klein et al., 1996). The results presented here demonstrate that elevated temperature significantly increased the concentration of Mg, and more so than elevated pCO_2 in calcite. This suggests extreme conditions of elevated temperature and pCO_2 can significantly influence the Mg/Ca ratio in *M. edulis* calcite suggesting elevated temperature facilitates more substitution of Mg for Ca in calcite at elevated temperatures, matching with previous studies (Taylor et al., 2009).

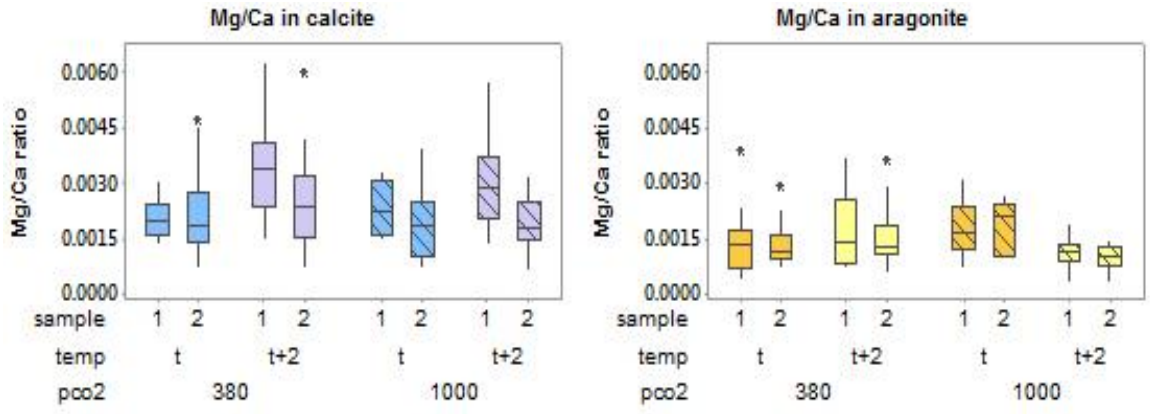

Figure 5-6 : Mg/Ca ratio trends in M. edulis calcite and aragonite layers.
Average Mg/Ca ratio from EDS measurements of the calcite layer are presented on the left, blue box plots representing ambient *t* (°C) and purple representing ambient *t*+2 (°C) and on the right presented for the aragonite layer, orange boxplots representing ambient *t* (°C) and yellow representing ambient *t*+2 (°C). Slanted lines in both graphs represent elevated pCO_2. Each box represents the interquartile range of each data set and separated by the median. Whiskers represent the lowest values Q1-1.5 (Q3-Q1) or highest values Q3 + 1.5 (Q3 - Q1) from the box. Outliers are represented by asterisk (*).

However, in aragonite the only significant results for Mg/Ca ratio were observed at combined elevated temperature and pCO_2 (*t*+2, 1000) which when compared to the other 3 scenarios showed combined elevated temperature and pCO_2 significantly decreased the Mg/Ca ratio in aragonite (*t*, 380 ($p < 0.05$, $T = 2.3$, $df = 35$, $n = 27, 32$); *t*+2, 380 ($p < 0.01$, $T = 3.45$, $df = 38$, $n = 30, 32$); *t*, 1000 ($p < 0.01$, $T = 3.27$, $df = 11$, $n = 11, 32$)) (***Figure 5-6***). All other 2-sample t-tests were found to be not statistically significant when comparing scenarios of elevated temperature at ambient pCO_2 (*t*+2, 380; $p > 0.05$) or at ambient temperature and raised pCO_2 (*t*, 1000; $p > 0.05$).

These results for Mg/Ca ratio in aragonite suggest that increases in both temperature and pCO_2 together alters the ratio of Mg/Ca in aragonite. These results are most likely due to the fact Mg is less likely to substitute for Ca in the lattice of pure

aragonite than it does in calcite and this is due to the size of the Mg ion not being able to fit into the aragonite crystal lattice spaces, decreasing the concentration of Mg/Ca. Due to these reasons, Mg content could be questioned to be adsorbed to defects of the crystal lattice or possibly from incorporated organic content (Foster et al., 2008). Normally Mg will not substitute for Ca in the crystal lattice of aragonite biogenically (Finch & Allison, 2007; 2008; Yoshimura, 2015). Under extreme environmental conditions of elevated temperature and pCO_2 that the Mg content is significantly different to the other scenarios. This suggests that these resultant changes to the crystal lattice structure of aragonite may influence the uptake of Mg to the mineralised shell. The results presented here would fit with previous suggestions which observed the structural integrity of *M. edulis* shells under extreme conditions would be significantly impacted upon causing changes to material properties (Fitzer et al., 2014a; Fitzer et al., 2015b) as this would influence the ion uptake mechanisms by the crystal lattice. The results presented also suggest that the organism's physiological mechanisms to exclude Mg from the shell have to increase under extreme environmental conditions, therefore altering the composition of the mineralisation.

5.3.1.2 **Sulphur Concentration**

Scatter plots of S concentrations in calcite and aragonite from the exterior edge towards the interior edge of the shell are presented in ***Figure 5-7***. Each graph indicates the three transects per shell of spot analyses for S normalised to a percentage of the original length measured so that individual shell layers of different thicknesses can be compared. Sulphur concentrations in calcite were lowest at the exterior edge and increase towards the inner edge aragonite-calcite interface boundary in all scenarios (***Figure 5-7***).

The concentrations of sulphur measured in calcite were relatively consistent between all shells, excluding *t*, 1000 (shell 1) where the concentrations were raised in comparisons to all other shells examined **(*Figure 5-7***). Polished section for shell 1 (t, 1000) was checked for possible polishing defects in case of artefact as suggested by Perrin et al. (2017), but no issues were found. S concentrations between shell 1 and 2 in elevated pCO_2 conditions (t, 1000) were significantly different to each other ($p < 0.01$, $T = 10.19$, $df = 21$, $n = 15, 26$). However, other element concentrations from shell 1 (*t*, 1000) spectra were retained, and all 3 transect data were of similar S concentration therefore, a possible

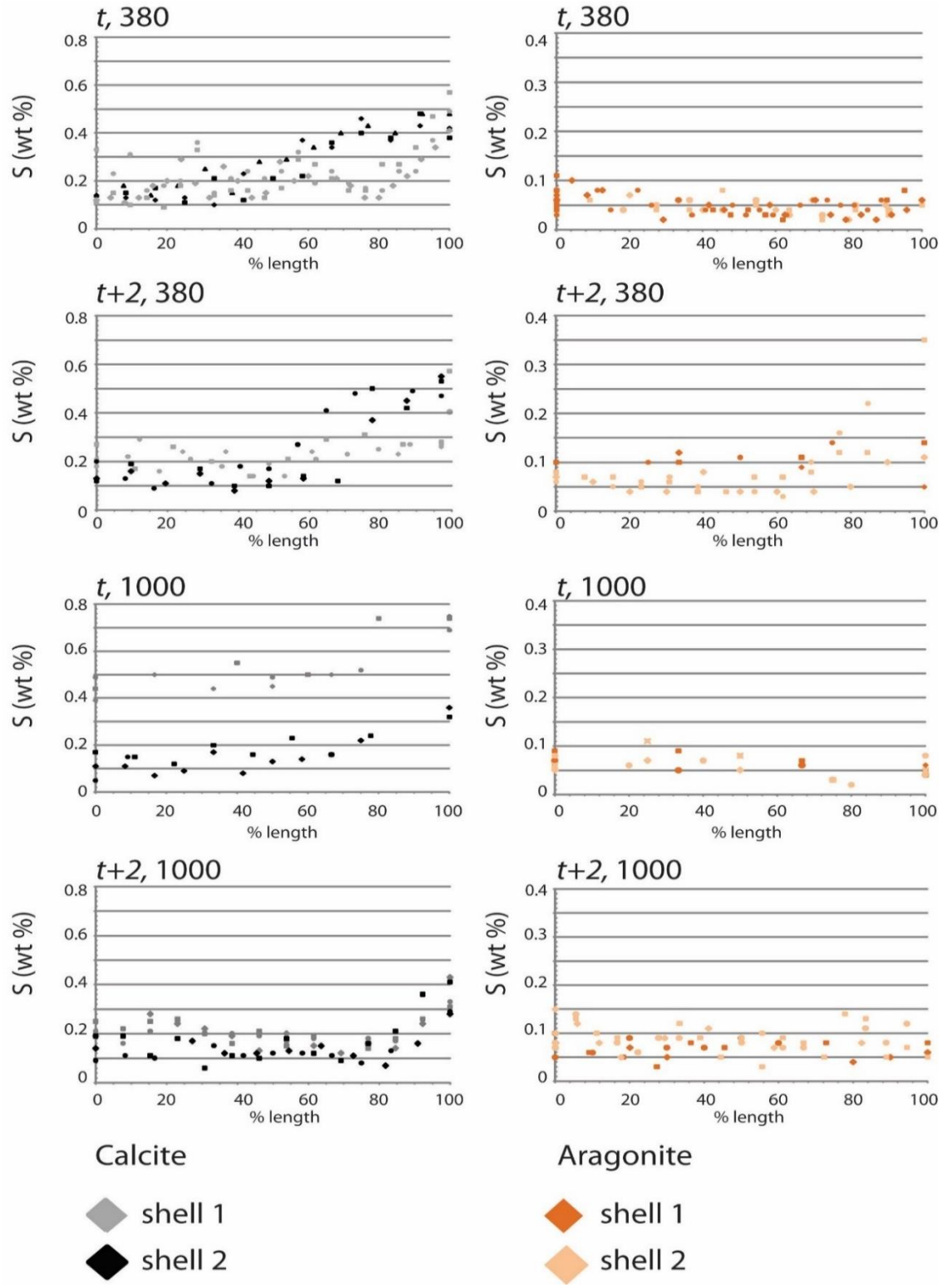

Figure 5-7: **Scatter plots of S element concentration within the calcite and aragonite layers of *M. edulis*.**

The concentration of S within the calcite (left black and grey) and aragonite (right orange and peach) layers of *M. edulis* shells. Transects read from outer shell at 0% length towards inner shell at 100%. Each data point equals one analysis point in one transect. For each shell, all spot analysis from 3 transects per layer are plotted to determine any relationships. The distance analysed across the shell is normalised to a percentage distance to allow comparison between shells where layers were different sizes (distances of transects as given in Table 5-2). (Note the y-axis maximum scale for aragonite extends to half that of calcite).

explanation for the higher concentrations could be due to crystal orientations resulting from the direction of the cut of the section and the placement of the S in the layer (Perrin et al., 2017). At ambient temperature and pCO_2 (*t*, 380) the concentration across the calcite layer increased from 0.2 wt.% at the exterior edge and continued to increase peaking at 0.57 wt.% at the aragonite-calcite interface (***Figure 5-7***). The maximum sulphur concentration overall was higher in calcite than in aragonite (***Figure 5-7***) consistent with previous work (Kontrec, et al., 2004). Variation was also noticed between individual shell aragonite layers for S concentrations at elevated temperature at both ambient and elevated pCO_2 (*t*+2, 380 and *t*+2, 1000). S concentrations have previously been correlated with the organic matrix of calcite (Vander Putten et al., 2000; Dauphin et al., 2003) and therefore may explain the higher inorganic/organic ratio in aragonite (***Figure 5-3***).

The sulphur concentrations in new aragonite were relatively consistent in all scenarios (***Figure 5-7***). In the aragonite layer, the S concentration decreases from the aragonite-calcite boundary towards the interior edge at ambient temperature and pCO_2 but this trend was not observed at elevated temperature (*t*+2, 380) where the concentration increases (***Figure 5-7***). At elevated pCO_2 (t, 1000) the concentration of S in aragonite decreases before increasing towards the interior edge (***Figure 5-7***). There was no observed difference in the S concentrations between shells for the aragonite layer as there were between shells in the calcite layer of elevated pCO_2 (*t*, 1000). Combined elevated temperature and pCO_2 (*t*+2, 1000) show the S concentration was fairly steady (***Figure 5-7***).

In calcite, the S concentration was not significantly different at elevated temperature (*t*+2, 380) compared to ambient temperature and pCO_2 (*t*, 380), $p > 0.05$ (***Figure 5-8***). The increase in S concentration in calcite measured at elevated pCO_2 at ambient temperature (*t*, 1000) was found to be significant when compared to ambient temperature and pCO_2 (*t*, 380) ($p < 0.01$, $T = -2.33$, $df = 49$, $n = 109, 41$). However, as shell 1 appeared to be greatly higher in S content compared to all other shells (***Figure 5-8***), the paired t-test was repeated using only shell 2 (*t*, 1000) data and this concluded elevated pCO_2 was not significant on comparison to ambient pCO_2 (*t*, 380) ($p > 0.05$). Elevated pCO_2 did indicate a significant decrease in the S concentration when shell 2 (*t*, 1000) was compared to elevated temperature at ambient conditions ($p < 0.05$, $T = -2.33$, $df = 59$, $n = 61, 41$) (***Figure 5-8***). Combined elevated temperature and pCO_2 (*t*+2, 1000) showed

significant results in comparison to elevated temperature and ambient pCO_2 (*t*+2, 380) ($p < 0.01$, T = 2.96, df = 97, n = 61, 72) (***Figure 5-8***). These results indicate that the concentration of S in calcite were influenced by increases in pCO_2 (***Figure 5-8***), which significantly decreased the absolute S concentrations measured (***Figure 5-7***).

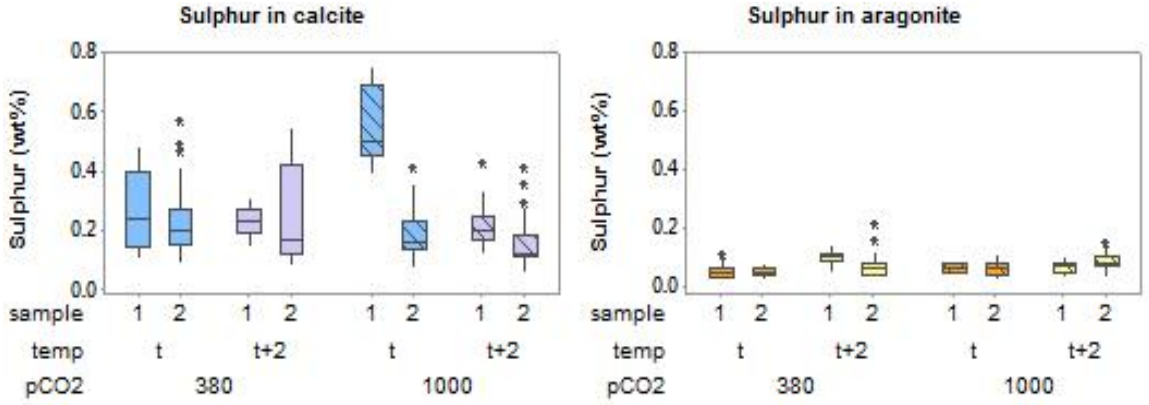

***Figure 5-8*: Sulphur in *M. edulis* calcite and aragonite.**
Concentrations for S measurements by EDS of the calcite layer are presented on the left, blue box plots representing ambient *t* (°C) and purple representing ambient *t*+2 (°C) and on the right presented for the aragonite layer, orange boxplots representing ambient *t* (°C) and yellow representing ambient *t*+2 (°C). Slanted lines in both graphs represent elevated pCO_2. Each box represents the interquartile range of each data set and separated by the median. Whiskers represent the lowest values Q1-1.5 (Q3-Q1) or highest values Q3 + 1.5 (Q3 - Q1) from the box. Outliers are represented by asterisk (*).

Although results for absolute concentrations of S were fairly similar in the aragonite layer across all scenarios and much lower than in calcite (***Figure 5-7***), results gained for aragonite yielded more significant results than for calcite. The concentration of S in aragonite was observed to be significantly different under conditions of elevated temperature (*t*+2, 380) compared to ambient conditions (*t*, 380) ($p < 0.01$, T = -5.23, df = 59, n = 85, 47) (***Figure 5-8***). The decrease in S concentration observed when comparing shell 2 of elevated pCO_2 (*t*, 1000) to elevated temperature at ambient pCO_2 conditions (*t*+2, 380) (***Figure 5-8***) was less significant ($p < 0.05$, T =-2.73, df = 38, n = 85, 26). The increase in S concentration occurring at a combination of elevated temperature and pCO_2 (*t*+2, 1000) compared to ambient temperature and pCO_2 (*t*, 380) (***Figure 5-8***) was found to be statistically significant ($p < 0.01$, T = -8.36, df = 115, n = 85, 67) as it also was when compared to ambient temperature and elevated pCO_2 ($p < 0.01$, T= -3.67, df = 56, n = 26, 67). These results suggest with 99% confidence that elevated temperature had a direct impact on the concentration of S in aragonite, reducing the S concentration (***Figure 5-8***). The impact of

pCO_2 on S was also significant, but to a lesser degree than temperature (95% confidence), unless at elevated temperature in extreme combined scenarios (99% confidence).

5.3.1.3 **Sodium and strontium concentration**

Na and Sr were analysed to determine if there are any relationships representing the elevated temperature or pCO_2 conditions that the shells were grown within.

5.3.1.3.1 Sodium Concentrations

Salinity of the laboratory conditions was closely monitored by Fitzer (see for example Fitzer et al., 2014a) therefore any observed differences within the Na concentrations will be linked to biological responses of the mussel. Na concentrations in calcite were highest at the exterior edge (~0.2 – 0.24 wt. %) decreasing towards the aragonite-calcite boundary. However, the average concentrations of Na were fairly consistent in all scenarios despite variance in concentration across the calcite layer (***Figure 5-9***). In aragonite, the concentrations were more consistent across the layer undulating around the median, and overall the Na concentrations were higher in aragonite than in calcite with a maximum 0.2 wt.% in calcite and 0.47 wt.% in aragonite. (***Figure 5-9***).

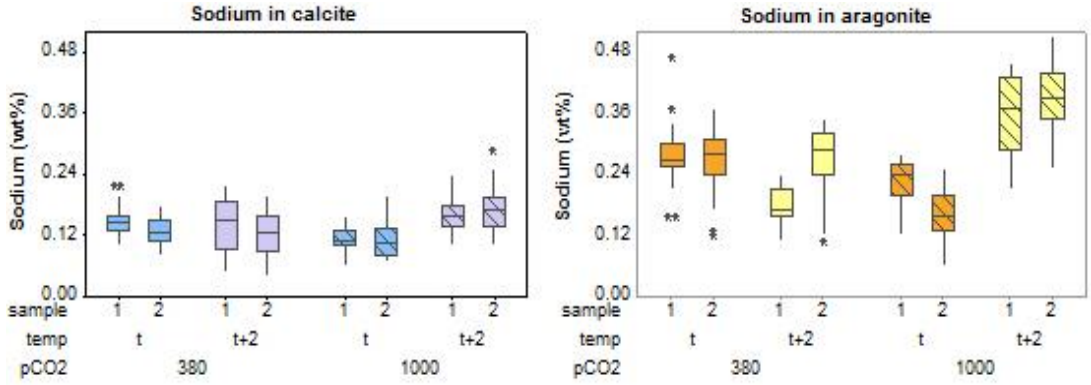

***Figure 5-9*: Sodium in *M. edulis* calcite and aragonite.**
Average concentrations for Na measurements by EDS of the calcite layer are presented on the left, blue box plots representing ambient *t* (°C) and purple representing ambient *t*+2 (°C) and on the right presented for the aragonite layer, orange boxplots representing ambient *t* (°C) and yellow representing ambient *t*+2 (°C). Slanted lines in both graphs represent elevated pCO_2. Each box represents the interquartile range of each data set and separated by the median. Whiskers represent the lowest values Q1-1.5 (Q3-Q1) or highest values Q3 + 1.5 (Q3 - Q1) from the box. Outliers are represented by asterisk (*).

In calcite, elevated temperature (*t*+2, 380) does not significantly influence the Na concentration at ambient pCO_2 (t, 380) compared to ambient conditions ($p > 0.05$). However, elevated pCO_2 significantly increases the Na concentration at ambient

temperature (*t*, 1000) compared to ambient conditions (*t*, 380) ($p < 0.01$, $T = 4.0$, $df = 63$, $n = 108, 41$) (***Figure 5-9***). Combined elevated temperature and pCO_2 (*t*+2, 1000) significantly increases the Na concentration compared to ambient conditions *t*, 380 ($p < 0.01$, $T = -6.31$, $df = 122$, $n = 108, 72$) and combined conditions (*t*+2, 1000) also increase the Na concentration significantly compared to elevated pCO_2 at ambient temperature (*t*, 1000) ($p < 0.01$, $T = -8.25$, $df = 92$, $n = 41, 72$) **(*Figure 5-9*)**.

In aragonite, the Na concentration was significantly different between all scenarios. Na concentrations under elevated temperature and ambient pCO_2 were significantly decreased (*t*+2, 380) compared to ambient conditions (*t*, 380) ($p < 0.05$, $T = 2.46$, $df = 75$, $n = 90, 48$). Conditions of elevated pCO_2 and ambient temperature (*t*, 1000) had significantly decreased the Na concentration compared to ambient condition's (*t*, 380) ($p < 0.01$, $T = 6.86$, $df = 37$, $n = 90, 26$). A combination of elevated temperature and pCO_2 (*t*+2, 1000; $p < 0.01$) compared to elevated pCO_2 and ambient temperature (*t*, 1000) significantly increased the Na concentration ($p < 0.01$, $T = -13.87$, $df = 49$ $n = 26, 72$).

5.3.1.3.2 Strontium Concentrations

The concentrations of Sr were higher in the aragonite than in calcite (***Figure 5-10***) as predicted, which will be due to structural differences in the crystal lattices as the aragonite lattice is more open allowing larger ions to substitute for Ca, like that of Sr (Busenberg & Plummer, 1985; Morse & Mackenzie, 1990).

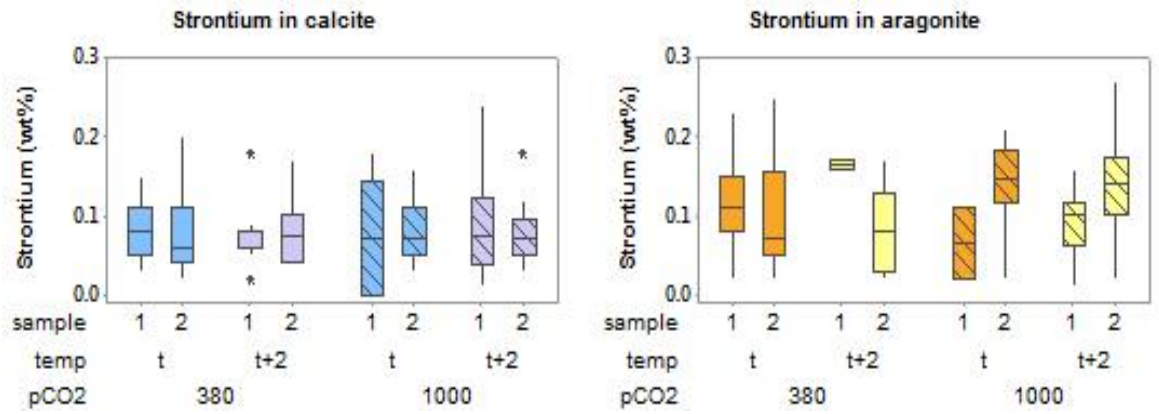

Figure 5-10*: S*trontium concentrations in *M. edulis* calcite and aragonite.
Average concentrations for Sr measurements by EDS of the calcite layer are presented on the left, blue box plots representing ambient *t* (°C) and purple representing ambient *t*+2 (°C) and on the right presented for the aragonite layer, orange boxplots representing ambient *t* (°C) and yellow representing ambient *t*+2 (°C). Slanted lines in both graphs represent elevated pCO_2. Each box represents the interquartile range of each data set and separated by the median. Whiskers represent the lowest values Q1-1.5 (Q3-Q1) or highest values Q3 + 1.5 (Q3 - Q1) from the box. Outliers are represented by asterisk (*).

However, of the 2-sample t-tests ran, p-values obtained for both aragonite and calcite did not indicate any statistical significance in the results ($p > 0.05$). Therefore, both null hypothesis' were accepted, that elevated temperature does not change the Sr concentration and elevated pCO_2 does not change the Sr concentration.

Sr/Ca ratios previously have been investigated as indicators to seawater temperature and salinity in the past (Beck et al., 1992; Nurnberg, 1996). One possible explanation for the results yielded here showing no statistical significance under conditions of either elevated temperature or pCO_2, may be due to having a small sample size, with many of the Sr concentrations measured being below EDS detections limits (***Table 5-1***), leading to inconclusive patterns.

5.4 **Discussion**

Foreign ion incorporation alters the thermodynamic properties of $CaCO_3$ by causing structural changes within the crystal lattice (Morse et al., 2007). The ions used for $CaCO_3$ secretion in organisms are removed from the environment through metabolism (Tynan et al., 2005). Therefore, controlling the environmental parameters under which the organisms calcify allows assessment into how biological control by the organism influences

the mineralogy formed. Many previous studies investigated internal tissue element concentrations because they are more highly concentrated than in the shell (Szefer et al., 2002; Szefer et al., 2006). Studies by Yasoshima & Takano (2001) and Ponnurangam et al. (2016) have suggested that elemental analysis of the shell may be less variable and therefore be a more precise record of the organism's entire lifespan. The results presented here show that there was variability when comparing individual shells (*Table **5-2***).

5.4.1 Influence of temperature (*t*) and pCO_2 on minor element concentrations

5.4.1.1 The influence of elevated temperature (*t*)

Non-biogenic results (Chapter 3; Chapter 4) suggested that elevated temperature would promote aragonite at the expense of calcite, and linked temperature to the mineralogy forming. To try and understand how the non-biogenic results relate to that of biogenic $CaCO_3$ growth under elevated temperature conditions, *M. edulis* shells were grown in constant known temperature (Fitzer et al, 2014a). Lorens & Bender (1977) documented *M. edulis* has a physiological mechanism for controlling Mg content, limiting how much Mg is up taken from the surrounding environment. Therefore, comparing different environmental conditions allows investigation into how elevated temperature may change the organisms control over elements such as Mg, and influence mineralogy. Many previous studies have tried to constrain the influence of elevated temperature on Mg incorporation and uptake into biogenic calcite (Dwyer et al., 1995; Nürnberg et al., 1996; Stoll et al., 2001) to attempt to constrain how non-biogenic $CaCO_3$ mechanisms are applicable to biogenic ones.

Investigation of the Mg/Ca ratio in the aragonite and calcite layers allows trends in Mg content be observed without bias from organic content comprising the components of the shells. Previous studies have indicated *M. edulis* has a number of physiological and biological controls over its calcification (Rosenberg and Hughes, 1991; Klein et al., 1996). Assessing how environmental influences impact on these processes is important to try to understand the mechanisms involved in biomineralisation.

The Mg/Ca ratio at elevated temperature was statistically significant in calcite indicating that temperature increases the Mg content (***Figure 5-5***) (t+2, 380 ($p < 0.01$); t+2, 1000 ($p < 0.05$)). This suggests that the physiological process to exclude Mg (Lorens &

Bender, 1977) was over-ridden at elevated temperature, most significantly in the calcite layer, but that elevated temperature alone does not influence the Mg concentration in aragonite. This indicates that the biomineralisation processes are influenced by higher temperature. The Mg concentration increase in calcite at elevated temperature is likely due to the molecular size of Mg ions being easily substituted into calcite, but less so into aragonite. This explanation could therefore explain why Mg concentrations did not significantly change in the aragonite layer at elevated temperature, overall the concentrations observed were much lower than in calcite (***Figure 5-6***). This link between temperature and Mg substitution of Ca in the calcite crystal lattice has also been discussed in previous studies (Berner, 1975; Reeder, 1983; Mucci & Morse, 1983; Morse et al., 2007). The smaller ionic radius of Mg compared to Ca causes distortion of the crystal lattice of calcite which may make the incorporation of increased concentrations of Mg easier, and in turn increase calcite solubility.

Previous studies have suggested that the biogenic Mg content in calcite is influenced by Mg/Ca ratio (Ries, 2005; Ries, 2006; Stanley et al., 2005; Stanley, 2006). Klein et al. (1996) also reported that elevated temperature could influence the mechanism for Mg regulation based on Mg/Ca ratio concentration in specimens of *Mytilus trossulus*, a close cousin of *M. edulis*. The results of this study suggest a direct influence on Mg concentration by elevated temperature matching the work of Taylor et al. (2009), as Mg/Ca ratio is maintained. Previous work indicated that the regulation of Mg uptake by *M. edulis* was reported to decrease with increasing Mg/Ca ratio (Lorens & Bender, 1980). The results presented here show that at maintained Mg/Ca ratio elevated temperature has further influence than Mg/Ca ratio alone, as this was held constant, on the Mg content of calcite. Investigation of the influence of temperature alone on the elemental composition of *M. edulis* is important as global temperatures are predicted to increase, even if the pCO_2 level is held constant (Meehl et al., 2007). As the Mg concentration in *M. edulis* calcite has shown to increase with elevated temperature, this is significant when considering both global temperature increases as well as smaller scale latitudinal variations. The results in this study differ from those of Vander Putten (2000) who suggested that temperature alone could not account for changes in the Mg incorporation of *M. edulis* shells as in their study they could not account for a correlation between Mg and temperature. Elevated temperature has been reported to influence the thickness of the calcite layer, cooler

temperatures increasing the thickness, warmer temperatures thinning the layer (Lowenstam, 1964). The new growth data was on too short a timeframe of 4 months to determine any trends on the layer thickness.

Changes to physiological processes like ion transport, alter the properties of $CaCO_3$ formed (Gattuso et al., 1999) and therefore altering the uptake of ions into the crystal lattice. Ion transport should be represented in the concentrations within the shell and aid representation of the environmental conditions formed from. Although Mg is less likely to incorporate into aragonite, any Mg measured in aragonite could represent crystal defects where the Mg ion would sit within. The results presented observed that the Mg/Ca ratio in aragonite was also raised under elevated temperature at 380 µatm pCO_2 (*t*+2, 380), however, comparison of results to ambient temperature conditions (*t*, 380) indicated the increase was not significant. Therefore, the increase in Mg measured could indicate crystal defects rather than direct Mg concentration changes facilitated by elevated temperature.

M. edulis has been investigated as an indicator of environmental conditions such as temperature, salinity and latitude (Lowenstam, 1954; Dodd, 1966). Sr/Ca ratios have previously been suggested to indicate temperature in biomineralising organisms (Weber et al., 1973; Smith et al., 1979; Beck et al., 1992; Klein et al., 1996; Stoll et al., 2002; Wannamaker et al., 2008). However, its use as a proxy for palaeo-temperature is debated due to conflicting results (Szefer et al., 2006; Sorte et al., 2013) due to the complex mechanisms involved within the bivalve calcification leaving the relationship of temperature and Sr/Ca ratio in bivalves unclear. Previous studies have observed Sr incorporation as being facilitated by elevated temperature (Dodd, 1965) in bivalves and also with both elevated temperature and pCO_2 in foraminifera (Elderfield et al., 1996).

The results presented here showed Sr incorporation at elevated temperature were not statistically significant in *M. edulis* in either aragonite or calcite, with concentrations measured being fairly steady in both layers (***Figure 5-10***). Overall, Sr concentrations were lower in the calcite layer than the aragonite layer (***Figure 5-10***) and this is likely due to the fact Sr has a larger ionic radius which will fit into the larger spaces available in the aragonite crystal lattice substituting for Ca, whereas in calcite the Mg is more readily substituted for Ca (Busenberg & Plummer, 1985). Many measured concentrations from EDS analysis were below detection limits and therefore removed from further analysis. Poor Sr retainment of Sr measurements may be a possible explanation for no correlation of Sr with

temperature in this research. However, Vander Putten (2000) also found no correlation between Sr/Ca and elevated temperature, and the results from this present study also have been unable to correlate any trend between Sr and Ca concentration with elevated temperature (*t*+2, 380) in calcite or aragonite compared to ambient temperature (*t*, 380) ($p > 0.05$). One suggestion for this was that *M. edulis* may control the Sr/Ca ratio by metabolic activity at the shell mantle which may be subject to physiological control in the same way as it controls Mg (Vander Putten, 2000; England, 2005). Another suggestion was that a salinity above 10 allows the surrounding water to hold the concentration of Sr constant around the shell which could help maintain a steady Sr presence as the mussel forms its calcified parts (Dodd & Crisp, 1982). Salinity was closely controlled within the laboratory conditions.

The Na concentrations in *M. edulis* of aragonite were significantly decreased with elevated temperature ($p < 0.05$) and not significant in calcite ($p > 0.05$). Incorporation of Na into aragonite is more easily achieved in aragonite than calcite (Kitano et al., 1962; Okmura & Kitano, 19986; Morse & Mackenzie, 1990) because Na substitutes for Ca and are of similar size radius (Yoshimura et al., 2017). Although results gained for Na were significant, this disagrees with a previous study where environmental influences such as temperature were found to only have minimal influence over the Na concentration within biogenic skeletal structures (Yoshimura et al., 2017).

S is thought to be representative of the organic matrix of calcite (Vander Putten et al., 2003). S concentrations overall were higher in calcite than aragonite which agrees with previous studies that S is more associated with the organic matrix (Dauphin et al., 2003; Kontrec et al., 2004). However, S concentrations not significantly different with elevated temperature (*t*+2, 380) compared to ambient conditions (*t*, 380) in the calcite layer ($p > 0.05$) (***Figure 5-7***). Inorganic S has been correlated with Mg content in previous studies and suggested to indicate elevated temperature (Kontrec et al., 2003) therefore as S concentrations were not significant this may indicate that there is a low inorganic S concentration. Calculated inorganic/ organic carbon and oxygen ratios (***Figure 5-3***) remain inconclusive for this aspect. The concentration of S was significantly different in aragonite with elevated temperature (< 0.01). However, this result is similar to the Na concentration therefore possibly suggesting a link between S and Na incorporation.

5.4.1.2 **The influence of elevated pCO_2**

Increasing levels of pCO_2 are of concern to calcifying marine life as it reduces the saturation state of seawater (Doney et al., 2009). Elevated pCO_2 without the influence of elevated temperature did not yield statistically significant results ($p > 0.05$) in Mg concentration or the Mg/Ca ratio of both calcite and aragonite. Elevated pCO_2 (*t*, 1000) increased the concentration of Mg in calcite compared to ambient pCO_2 (*t*, 380), but this increase was found to be statistically insignificant ($p > 0.05$) (***Figure 5-5***). Mg is a calcite growth inhibitor and therefore may have slowed calcite growth allowing aragonite growth to increase as observed by the aragonite/calcite ratio. This could indicate that elevated temperature is more influential on the Mg concentration within *M. edulis* calcite than elevated pCO_2 is.

However, on average, the growth of the shells in this study, in terms of aragonite/calcite ratio calculated from the layer thicknesses, was largest at pCO_2 of 380 ((*t*, 380) = 1.69: 5.50; (*t*+2, 380) = 3.00:8.33), as elevated pCO_2 decreased the ratio to a more even ratio ((*t*, 1000) = 3.06:3.11; (*t*+2, 1000) = 2.16:3.07) (as measured by Fitzer et al., 2014a). These results suggest that elevated pCO_2 increased the growth of aragonite compared to calcite more than that by temperature. Vander Putten et al., (2000) argued that temperature is only one factor in a multitude of influencers for Mg incorporation into *M. edulis* shells. These results match with the suggestion from Lee & Morse (2011) on non-biogenic $CaCO_3$ formation that aragonite would be facilitated instead of calcite at raised pCO_2, therefore showing that biological control does not have great influence over this. However, the pCO_2 used for Lee & Morse (2010) was much higher than the controlled pCO_2 levels used within the environmental conditions Fitzer et al. grew the mussels within. As the present study is based on ambient and future pCO_2 predicted concentrations (IPCC, 2013), this allows a realistic environmental context for which to assess the influence pCO_2 has upon the elemental composition of the mineralised shell components.

To counteract higher Mg entering the shell the organism increases the organic matrix component of calcite (Lorens & Bender, 1980). It was suggested that *M. edulis* shells may be influenced by their organic matrix to whether aragonite or calcite would be produced (Kennedy et al., 1969). This would be represented by S content of the shell as S is thought to be representative of the calcite organic matrix (Vander Putten et al., 2000;

Dauphin et al., 2003) and less likely to incorporate into aragonite (Kontrec et all., 2004). However, the link of S concentration to the organic matrix remains debated and some authors have suggested that S substitutes for CO_3^{2-} ions in mineralised shell calcite (Takano et al., 980; Busenberg & Plummer, 1985; Takano et al., 1985; Kontrec et al., 2004; Nguyen et al., 2004). By doing so this would cause distortion of the crystal lattice (Fernandez-Diaz et al., 2010; Arroyo-Dompablo et al., 205; Perrin et al., 2017). However, these distortions on lattice structure would allow for increased Mg incorporation (Kralj et al., 2004) therefore the results here rule out this substitution to the mineralised shell and support the S content being of the organic matrix. Another possible route for crystal defects allowing S incorporation could be explained by the decrease in Mg/Ca ratio measured in calcite. This suggested calcite growth could be faster under these conditions and previous studies have indicated that increased growth rate increased the frequency of crystal lattice defects (Yoshimura et al., 2017). England (2005) observed that S could be positively correlated with strontium and sodium concentrations in the calcite layer of *M. edulis* shells. The present study shows no distinct trend linking Sr and S concentrations.

Sr incorporation has been correlated with accelerated rates of calcite growth (Lorens, 1981; De Leeuw, 2002). Sr incorporation was also thought to be influenced by elevated temperature or pCO_2 in foraminifera (Elderfield et al., 1996). At elevated pCO_2 the Sr concentration in calcite was higher than at 380 µatm (*t*, 380) (***Figure 5-10***), but this rise was not statistically significant therefore findings of this study do not show an influence of pCO_2 on Sr.

5.4.1.3 **The influence of combined elevated temperature and pCO_2**

Other studies have also investigated elevated temperature and pCO_2 impacts on calcification (Orr et al., 2005; Hendricks et al., 2010; Bach, 2015; Fitzer et al., 2014a; 2014b; 2015b). Elevated temperature and pCO_2 is known to increase dissolution of the $CaCO_3$ system by decreasing oceanic pH. The geographical distribution of the mussel has also moved pole-wards in recent years and therefore will be influenced by cooler temperatures (Bergström et al., 2013). Elevation of temperature and pCO_2 added to the environmental influences are projected to increase stress on the calcification of mussels by influencing the energy requirements to do so (Zhao et al., 2017). Therefore, this study should represent

elemental concentration changes in the calcite and aragonite layers of *M. edulis* which match with these findings.

At the time of commencing the multigenerational study of these mussels (October, 2012) scientific research guidance on pCO_2 proposed 380 µatm to be of modern day pCO_2 levels (IPCC, 2007). However, since this time the pCO_2 level in marine waters has risen, measuring 407 µatm in February 2017 (McGee, 2017). To have this rise evident in present day oceans in pCO_2 indicates that marine organisms will already be the subject of increasing acidification scenarios (Fitzer et al., 2014b). Similarly, recent increases in temperature have been recorded to be almost +1°C (Met Office, 2017) from pre-industrial levels. This suggests that organisms will already be adapting to changing environmental conditions and therefore this will be evident in their elemental composition.

A combination of elevated temperature and pCO_2 (*t*+2, 1000) increased the Mg/Ca ratio in calcite significantly more than elevated pCO_2 (*t*, 1000) alone ($p < 0.05$) (***Figure 5-6***). Fitzer et al. (2015b) suggested that elevated temperature alongside elevated pCO_2 may help buffer the effect of rising pCO_2 alone as it appeared that shell calcite properties became more fragile. This suggests that combining the influence of elevated temperature and pCO_2 together has a larger impact on the Mg content of calcite which in turn may impact on the solubility and growth of the layer. Results from Fitzer et al. (2015b) indicated that in elevated temperature and pCO_2 conditions the calcite layer can thin showing the combined influence of temperature and pCO_2 impacted upon the calcite layer growth and stability, in turn this could be indicated by changes in Mg content of calcite increasing (***Figure 5-6***) and inhibiting the calcite growth.

In aragonite, the combined influence of elevated temperature and pCO_2 (*t*+2, 1000) significantly decreased the Mg/Ca ratio compared to elevated pCO_2 alone (*t*, 1000) ($p < 0.01$), and also decreased the Mg/Ca ratio compared to elevated temperature with ambient pCO_2 (*t*+2, 380) (***Figure 5-6***). Elevated temperature and pCO_2 conditions have been shown to influence aragonite more so than calcite because of the direct influence decreasing saturation state (Doney et al., 2009). Mg is less likely to substitute into the crystal lattice of aragonite (Morse et al., 2007) and therefore a decrease in Mg concentration could suggest crystallographic changes which prevent Mg incorporation. Elevated temperature and pCO_2 conditions impact on aragonite crystal structures (Melzner

et al., 2011). The material properties of aragonite were observed to be softer under combined treatments of elevated temperature and pCO_2 which would leave the shell more prone to breakage (Dickinson et al., 2012; Fitzer et al., 2015b). Fitzer et al., 2015b). Therefore, the results presented here could suggest that elevated temperature and pCO_2 conditions facilitating lowered Mg concentrations may be one reason for the aragonite layer to become softer due to changes in crystallography, and this in turn could alter the shell structure through the biomineralising processes (Fitzer et al., 2016).

S concentrations at combined elevated temperature and pCO_2 (*t*+2, 1000) were lower in the calcite layer, but remained similar in the aragonite layer than concentrations measured at elevated pCO_2 alone (*t*, 1000) (***Figure 5-7***). Therefore, elevated temperature and pCO_2 conditions have more influence of S in calcite than in aragonite, indicating that combined elevated temperature and pCO_2 implicates calcite formation as S incorporation should be easier into calcite (Kontrec et al., 2004). One suggestion may be as S is allied to the organic matrix of calcite, this could indicate that the organic matrix is lessened and therefore leave the mussel shell with less protection to the outer calcite layer from environmental elevated temperature and pCO_2 conditions.

The concentrations of Na could also support this theory as the concentration of Na was shown to decrease from outer shell to inner boundary in calcite in all scenarios. This trend was also recorded in results of *M. edulis* analysis by England (2005). This may suggest that the lattice structure of calcite could be deformed allowing Na into the interstitial spaces or that there was a decrease in organic matrix from calcite to aragonite (as indicated by the S concentration). On average, the Na concentration with elevated temperature and pCO_2 were raised in both calcite and aragonite significantly ($p < 0.01$ in both layers) (***Figure 5-9***). Other studies have observed that Na concentrations in *M. edulis* appear to increase with decreasing pH in a non-linear relationship (Zhao et al., 2017). It was suggested that elevated temperature at the lowered pH significantly decreased the Na/Ca ratio (Zhao et al., 2017), therefore the results presented in this study reflect this.

5.4.2 Can environmental changes such as elevated temperature and pCO_2 provide an insight for aragonite-calcite sea influence on biomineralisation?

The findings of this research conclude that the observed concentrations of Mg, S and Na were determined by the layers of calcite and aragonite, but further influenced by temperature and pCO_2 conditions. Concentrations of Sr remained inconclusive in this study. This leads to suggestion that the direct application of aragonite-calcite sea conditions to biogenic $CaCO_3$ formation are complex. The results do suggest that the external environmental influences of temperature and pCO_2 allow the physiological mechanisms held by organisms to overprint the original mineralogy constraints such as seawater chemistry conditions. Temperature in particular influenced the incorporation of Mg into calcite more so than into aragonite, indicating that crystallographic differences allow for different concentrations of minor elements to incorporate, however, temperature enhances this. Changes to the concentrations incorporated suggest material properties are influenced which has been observed in other studies indicating a direct impact on the hardness of aragonite and calcite (Fitzer et al., 2015b). These results link to the non-biogenic studies presented in Chapter 3 and 4. Both these chapters suggested temperature influenced aragonite formation at the expense of calcite as a result of accelerated Mg activity.

The results from this chapter set out to determine is biogenic $CaCO_3$ mineralogy may be constrained by similar mechanisms to non-biogenic $CaCO_3$ when the organism has some control. Elevated pCO_2 or combined elevated temperature and pCO_2 conditions were more influential on the element concentrations of S and Na. Again, both element concentrations initially were determined by the mineralogy. S concentrations decreased whilst Na was increased in calcite, indicating possible links to the mechanisms behind how ions incorporates into the mineralogy. The concentrations of S and Na were shown to decrease in aragonite in elevated pCO_2 conditions of combined temperature and pCO_2 conditions. pCO_2 previously has been proposed as a main driver of aragonite-calcite sea conditions. The results presented here suggest that concentrations of minor elements are influenced by possible changes in the carbonate chemistry of seawater, which could suggest the possibility that S in calcite is present in SO_4^{2-} form and substituting for CO_3^{2-} ions. Further, elevated Na concentrations in aragonite have previously correlated with

decreased in pH (Zhao et al., 2017), likely facilitated by increased pCO_2 but in turn could be representative of the aragonite layer softening and allowing more ion incorporation.

5.5 Conclusions

This research has observed that environmental change has influence on the elemental concentrations within the calcite and aragonite layers of *M. edulis* shells. Individually conditions of elevated temperature were found to have significant influence on the concentrations of Mg but did not alter S, Na or Sr concentrations. However, elevated pCO_2 has more influence of S and Na in calcite. In aragonite, elevated temperature is most influential on the S concentrations, but elevated pCO_2 and combined elevated temperature and pCO_2 significantly increased the concentrations of S and Na. This is due to chemical level organisation of the crystal lattice influencing how the ions incorporate into $CaCO_3$ and altering the thermodynamic properties that calcite and aragonite have.

Element ratios are problematic for palaeo-temperature proxy reconstructions (Graniero et al., 2017). Factors that control elemental ratios in molluscs appear to vary among studies (Carre et al., 2006; Klein et al., 1996; Takesue & van Geen, 2004; Freitas et al., 2006; Sosidan et al., 2006; Poulain et al., 2015). These kinetic and metabolic controls appear to be unpredictable among different genera or even within the same species from the same locality (Lorrain et al., 2005). This research has indicated that element concentrations were influenced by changing environments. However, there remain some differences between individual shells which cannot be fully accounted for without further investigation. Future studies could be enhanced by the use of empirical standards to build upon the data achieved which would allow assessment of the data against fixed aragonite/calcite ratios.

This research adds to our knowledge on the possible impacts of elevated temperature and pCO_2 conditions on *M. edulis* element concentrations which can be used as a guide to how such climate changes will influence shell formation and allow prediction into how calcification under such scenarios may be impacted on, even when the organism has some control over its one formation. The four scenarios (*t*, 380; *t*+2, 380; *t*, 1000; *t*+2, 1000) investigated allow for examination of how each impact on the element concentrations. The scenario with the most impact on elemental concentrations was at

combined elevated temperature and pCO_2 influence (*t*+2, 1000). This research has indicated that the concept of aragonite-calcite seas should be reassessed to include multiple influences on mineralogy alongside the main drivers of Mg/Ca ratio and pCO_2. The elemental concentrations assessed were influenced differently dependent upon the mineralogy. Here the influences of temperature and pCO_2 act as a proxy for potential biomineral alteration. These results have potential implications for calcification in future changing climates. Understanding the mechanisms altering calcification mechanism is therefore important considering projected environmental changes in the near future (IPCC, 2013). Assessing the influence of aragonite-calcite sea conditions on $CaCO_3$ mineralogy of both non-biogenic and biogenic origin require all drivers to be viewed together to allow a full understanding the underlying mechanisms impacting on the evolution of biomineralisation.

6

Discussion and Future Work

This thesis investigated the suggested drivers of aragonite-calcite sea conditions on both non-biogenic, and biogenic $CaCO_3$ formation. This chapter summarises the main findings of this research and discusses the mechanisms influencing non-biogenic aragonite and calcite formation and what relationships these may have with biogenic $CaCO_3$ elemental compositions in relation to aragonite-calcite sea conditions (Sandberg, 1983). This research provides new insights into the constraints on non-biogenic $CaCO_3$ precipitation and aims to apply them to a biogenic $CaCO_3$ study under known parameters to give an insight to $CaCO_3$ mineralogy in the context of aragonite-calcite sea conditions. Detailed results and discussions for each section have been given in more detail in Chapter 3, 4 and 5. Continuous addition technique allowed assessing the influence of (1) Mg:Ca ratio, temperature and water movement on $CaCO_3$ phases under steady pH (Chapter 3) and (2) how sulphate influences non-biogenic $CaCO_3$ precipitation (Chapter 4). The concluding research chapter presents an investigation into how the $CaCO_3$ elemental composition of mussel shells was influenced under controlled temperature and pCO_2 conditions, representing two of the main drivers of aragonite-calcite sea conditions.

The aragonite-calcite sea hypothesis was formulated based on the observations that the primary mineralogy of ooids has switched, facilitated by fluctuations in the seawater chemistry. Evidence supporting this hypothesis comes from a range of sources including marine evaporite deposition (Hardie, 1996), fluid inclusions in marine deposits (Horita et al., 2002; Lowenstein et al. 2001; 2003; Timofeeff et al., 2006; Coggon et al., 2010), and echinoderm skeletons (Dickson, 2002; 2004). The primary driver is the Mg:Ca ratio of seawater, facilitating aragonite and high-Mg calcite formation above a ratio of 2, and below 2 only facilitating calcite. However, the critical threshold for this switch is debated. This has led to other influencing factors on $CaCO_3$ mineralogy to be investigated such as pCO_2,

SO_4^{2-} and temperature, all of which have individually indicated links to $CaCO_3$ mineralogy formation. Links of aragonite-calcite sea conditions matching tectonic-eustatic-climatic cycles (Engel & Engel, 1958; Vail et al., 1977; Fischer, 1981, 1983) further emphasising global scale influences on non-biogenic $CaCO_3$ mineralogy. Evidence from an increase in metazoan trace fossils matching with an increase in Ca^{2+} (Knoll & Carroll, 1999) lead to suggestions of a link between MOR, composition of seawater and bio-calcification all occurring within the same timeframe (Brennan et al., 2002). This hints that aragonite-calcite sea conditions will in turn also influence the evolution of biogenic $CaCO_3$ (Harper et al., 1997; Stanley & Hardie, 1998; Porter, 2010), although direct application of non-biogenic studies to biogenic $CaCO_3$ suggest this does not appear to work as a general rule (Kiessling et al., 2008; Zhuravlev & Wood, 2009; Porter, 2010).

The research presented in this thesis commenced by investigating the first-formed $CaCO_3$ precipitates using continuous addition technique, allowing quantification of the parameters surrounding the precipitation. This allowed expansion on quantifying the volumetric proportion of aragonite, to include components of crystal size and number of crystals to determine which aspect impacted more on the $CaCO_3$ mole percentage. Laboratory studies are important in advancing our understanding of the constraints to non-biogenic $CaCO_3$ formation.

Key aims from this research were: to provide an insight into the impact of Mg:Ca ratio, temperature and water movement influences on aragonite-calcite sea conditions; next, to further this knowledge by assessing the non-biogenic influence of sulphate on $CaCO_3$ mineralogy under the same constraints.

Next this research aimed to investigate how incorporation of Mg, S, Na and Sr into biogenic $CaCO_3$ is influenced under the constraints of known temperature and pCO_2. This allowed application of how CaCO3 mineralogy is influenced non-biogenically in Chapter 3 and 4 and compared to biogenic $CaCO_3$ growth where the organism has some control over its mineralogy. As the research progressed, this allowed a better understanding of the following issues:

1. The influence of Mg on $CaCO_3$ mineralogy: the role of Mg:Ca ratio, the primary driver of aragonite-calcite seas, on the first formed precipitates of $CaCO_3$ and to

investigate the influence of Mg^{2+} on crystal size and the number of crystals formed (Chapter 3).

2. Provide an insight into how latitudinal variation in seawater temperature potentially influences marine $CaCO_3$ mineralogy at differing Mg:Ca ratios constraining those found within the Phanerozoic (Chapter 3): $CaCO_3$ in the marine environment is segregated by polymorph, dependent on latitude and depth (Morse et al., 2007). Aragonite-calcite sea conditions originally were viewed as spatially homogeneous, but temperature impacts on the mineralogy non-linearly alongside the Mg:Ca ratio (Morse et al., 1997; Balthasar & Cusack, 2015). Insight to first-formed precipitates under continuous addition technique (Chapter 3); provide insight into the influence of Mg^{2+} in biogenic aragonite and calcite at elevated temperature (Chapter 7).
3. Water movement: allow for an insight to the natural marine environment, similar to that where ooid formation would occur, and compare to still conditions at 20°C and 30°C (Chapter 3).
4. Presence of sulphate: determine what role the natural environment fluxes of sulphate may impact on $CaCO_3$ mineralogy alongside temperature and water movement (Chapter 4), and by using the same technique as the sulphate-free scenarios of Chapter 3 allow for comparison to sulphate-free conditions. This projects a framework for which to assess environmental influences on non-biogenic marine calcification. Provide insight into how biogenic aragonite and calcite are influenced at ambient and elevated temperature (Chapter 7).
5. Consider whether elemental concentrations of sodium and strontium depict any correlation with elevated temperature or pCO_2 which may results from natural environmental conditions in the marine realm (Chapter 7).
6. Assess if the consensus that seawater chemistry is likely to influence biomineralisation is an oversimplification and whether the influence of seawater chemistry can be by environmental conditions.

6.1 Non-biogenic $CaCO_3$ from Continuous Addition Technique

Results presented in Chapter 3 indicated that the proportion of aragonite to calcite was increased as a function of Mg:Ca ratio and temperature together, and was further amplified by water movement. Under all scenarios, co-precipitation of aragonite and calcite occurred. This finding suggests that firstly that there is no generic switch in $CaCO_3$ mineralogy formed at the proposed critical threshold of Mg:Ca ratio of 2, represented by the presence of aragonite at all Mg:Ca ratios. These results disagrees with Hardie (1996) as no exclusivity to one polymorph type below 2 exists when specifically looking at the first-formed precipitates. Further, the results observed do show that calcite remains the most dominant polymorph at a Mg:Ca ratio of 2 unless temperature or water movement are considered, but none of the investigated Mg:Ca ratios resulted in the exclusive precipitation of only one polymorph. Therefore, the assumption that Mg:Ca ratios of 1-2 do not facilitate aragonite (Folk, 1974; Sandberg, 1975; Füchtbauer & Hardie, 1980; Lowenstein et al., 2001; Stanley, 2008) can be abandoned. This is especially true at elevated temperature or in shaken environments (see Chapter 3).

Results observed are particularly important in the context of pin-pointing the exact constraints on polymorph growth as the continuous addition technique allowed for quantification of first-formed precipitates. This differed to other studies, such as Morse et al. (1997), where the investigated precipitates combined first-formed precipitates with much later precipitates that were formed under altered experimental conditions. Balthasar & Cusack (2015), used the degassing experiments of supersaturated solutions as detailed by Morse et al. (1997) but analysed the first-formed precipitates by alteration of the original method. The results presented here, although in agreement with Balthasar & Cusack (2015), yield lower proportions of aragonite than gained via degassing experiments. The continuous addition technique successfully prevented rapid changes in pCO_2 that would occur in degassing experiments, and therefore allow the pH to be held more constant. The seawater solution as a result will have been of lower saturation state than that of Balthasar & Cusack (2015), which can account for lower proportions of aragonite. Interestingly, lower saturation state makes nucleation more difficult, possibly suggesting aragonite formation is less costly to achieve than calcite. Further, these results are of

interest because the co-precipitation field range observed is much larger than presented by Balthasar & Cusack (2015). This research therefore indicates that calcite dominant sea conditions would be even less likely than predicted by Balthasar & Cusack (2015), even at low Mg:Ca ratio, as the co-precipitation of aragonite and calcite remains to occur.

Increase in temperature influences $CaCO_3$ mineralogy such that proportions of aragonite to calcite were increased. This reinforces previous studies suggesting the Mg:Ca ratio and temperature have a non-linear relationship on $CaCO_3$ mineralogy. The non-linear connection between Mg:Ca ratio and temperature had been documented in previous studies (Morse et al., 1997; Balthasar & Cusack, 2015). However, what was apparent from the research presented in Chapter 3 was that elevated temperature the aragonite mole percentage was mainly increased through larger aragonite crystal size rather than increasing the number of crystals whilst fewer crystals of calcite formed and were of smaller size. Mg^{2+} incorporation into calcite has previously been documented as being decreased at lower Mg:Ca ratio (Stanley et al., 2005) preventing destabilisation of the calcite crystal lattice and therefore allowing calcite to be dominant. However, the research presented here indicates that at lower Mg:Ca ratio and higher temperature the aragonite proportion increases, due to increases in the aragonite crystal size. The findings suggest that the barrier to nucleation is stronger than crystal growth, indicating that when assessing the mechanisms for $CaCO_3$ precipitation, including temperature will influence the mineralogy via the Mg^{2+} concentration inhibiting calcite and facilitate aragonite.

Thus far, laboratory experiment studies on $CaCO_3$ precipitation often use seeding of $CaCO_3$ with glass beads and shaking of solutions to form a nucleation surface to allow further analyses of the precipitates (Tesoriero & Pankow, 1996; Bots et al., 2011). This research differs in that water movement was addressed as a variable to compare still to shaking environments on the $CaCO_3$ mineralogy. Results indicated that shaking environments amplified the results yielded under all parameters of Mg:Ca ratio and temperature to increase the aragonite to calcite proportion. Water movement increases the proportion of aragonite to calcite by increasing the number of crystals of aragonite whilst forming fewer and smaller crystals of calcite. However, adding the influence of temperature to shaking conditions amplifies the number and size of aragonite crystals formed whilst forming fewer smaller crystals of calcite. This finding could have implications

for marine calcification as shallow marine waters where aragonite formation is predominant. These waters also tend to be warmer, therefore results gained could be indicative of such an environment. The insight that water movement and temperature increase the aragonite proportion explain why aragonite formation is more common in more turbulent and warmer shallow marine waters, whereas calcite is more common in quieter, cooler and deep waters (Burton & Walter, 1987). Further investigation of water movement would be required to include natural ion fluxes from river inputs and terrestrial weathering to the present set-up to determine a natural environmental framework of $CaCO_3$ mineralogy.

6.2 The Influence of Sulphate

To replicate a more real-life scenario, the influence of sulphate was added because it is ubiquitous to all marine settings and is known to influence the $CaCO_3$ polymorph phase formed (Bots et al., 2011; Tang et al., 2012). The results of Chapter 4 can be directly compared to the results of Chapter 3 because the continuous addition technique used is identical in set-up, with the exception of the presence of sulphate. Sulphate has previously been discussed as being one of the triggers for a 'switch' in $CaCO_3$ mineralogy (Dydo et al., 2003; Tang et al., 2003). However, like in sulphate-free conditions presented in Chapter 3, a co-precipitation of aragonite and calcite was observed in all scenarios in the presence of sulphate in Chapter 4, which at Mg:Ca ratio of 1 varies from what has previously been expected (Folk, 1974; Sandberg, 1975; Füchtbauer & Hardie, 1980; Lowenstein et al., 2001; Stanley, 2008). This adds further support to the idea that in the presence of sulphate the critical threshold for aragonite formation is lowered, supporting previous suggestions (Bots et al., 2011). Further, contrary to previous observations by Bots et al. (2011), no vaterite was observed to form. Therefore, this research suggests that the influence of sulphate inhibits vaterite formation more so than calcite formation. This observation could be due to the lower saturation state of the presented research.

However, the calcite that formed was of smaller size than in sulphate-free conditions, but there was no decrease in aragonite crystal size. Compared to sulphate-free conditions the presence of sulphate was more influential on the number of nucleations of aragonite to calcite proportion forming than the proportion of crystal size. However, with added parameters of temperature and water movement it was the aragonite crystal size that was

increased whilst calcite crystals were precipitated in fewer numbers of smaller sizes. The influence of lower saturation state may make nucleation more difficult under the investigated conditions, thus resulting in larger but fewer crystals forming. These results also suggest that the sulphate increases the energy barrier to nucleation of crystals of calcite leading to the conclusion that it directly influences Mg^{2+} to impact on calcite. This has significant implications for marine calcification. Mg^{2+} and SO_4^{2-} have been shown to co-vary throughout the Phanerozoic where high Mg:Ca ratio matches with high concentrations of SO_4^{2-} (Lowenstein et al., 2003). Aragonite-calcite sea conditions have been matched with episodes of eustatic-climatic-tectonic change which in turn alter seawater Mg:Ca ratio, pCO_2 and therefore saturation state (Sandberg, 1983; Morse & Mackenzie, 1990; Stanley & Hardie, 1998; Guidry et al., 2007; Andersson et al., 2008). The results presented here are of lower saturation state than those presented by Bots et al. (2011) but remain to show that the Mg:Ca ratio threshold for the facilitation of aragonite was lowered in the presence of sulphate.

To assess the impact of water movement rotation speeds of 80 rpm were used to prevent the nucleation surface on the glass slides from passing over each other. Previous studies showed that crystallization was independent of the speed of shaking (Reddy & Nancholas, 1971) and speeds of 100-400 rpm were observed to not influence precipitation (Klepetsanis et al., 1999). However, here the 80 rpm speed has clearly shown to increase the proportion of aragonite to calcite occurring by an increase at 20°C and 30°C when compared to still conditions with sulphate. This suggests that further investigation into water movement could yield an insight into influences in the mechanisms to form nucleations and crystal growth, possibly indicating water turbulence could impact on the dominant $CaCO_3$ mineralogy forming. In both sulphate-free and with sulphate scenarios, the influence of water movement appears to significantly increase the proportion of aragonite compared to calcite.

Bots et al. (2011) suggested a lower Mg:Ca ratio threshold of 0.3 below which calcite dominance would occur at 5mM SO_4^{2-} although this was not supported by halite fluid inclusion data (Wortmann & Chernyavsky, 2007; Hasik & Lohmann, 2008; Newton et al., 2011). However, the results of this research support the findings of Bots et al. (2011).

6.3 *Mytilus edulis* Shell Elemental Concentrations

The *Mytilus edulis* (*M. edulis*) mussel shells used for elemental analysis were grown in the laboratory under controlled temperature and pCO_2 for four months (Fitzer et al., 2014a). The range of temperature the mussel shells were subjected to is small but within the temperature range that is projected to occur by 2100 (IPCC, 2013). This is an important consideration, especially with observations to date showing recent increases in temperature have been recorded to be almost +1°C (Met Office, 2017) from pre-industrial levels. These aspects are of particular importance in the context of projected climate changes that can impact on marine organisms. This work improves our understanding of how environmental influences can impact marine calcifiers. Identifying patterns of how variation in elemental composition and possible changes in mineralogy are linked to temperature and/or pCO_2 is important for predicting how calcification adapts to changing environments and, last but not least, to improve our understanding of the Phanerozoic evolution of biomineralisation. Further, understanding how the organisms respond under the selected scenarios can be used to understand past evolutionary mechanisms in the context of aragonite-calcite sea conditions.

This research found that the concentrations of Mg, S and Na were determined by the layers of calcite and aragonite, but were further influenced by temperature and pCO_2 conditions. Sr concentrations in this study were inconclusive for both aragonite and calcite. This indicates that direct application of aragonite-calcite sea conditions are complex and that the physiological mechanisms can overprint these conditions facilitated by environmental conditions. Elevated temperature increased Mg concentrations in calcite, but did not influence aragonite unless under extreme conditions of elevated temperature and pCO_2 combined. This matches with results in Chapter 3 & 4 that indicated a direct influence of temperature on non-biogenic aragonite and calcite formation. In the non-biogenic studies aragonite was facilitated at the expense of calcite and this proportion of aragonite to calcite was increased with temperature in both sulphate–free scenarios and those with sulphate. The non-biogenic studies also suggested that higher temperature increased Mg^{2+} activity which results in the increased suppression of calcite but not aragonite. This research on *M. edulis* shells Mg concentrations were higher in calcite than aragonite. This indicates that the two layers of *M. edulis* were influenced differently under

the same environmental conditions, suggesting crystallographic differences allow for different concentrations of minor elements to incorporate. This result can be directly related to results for material properties being influenced by changes in temperature and pCO_2 observed by Fitzer et al (2014b). The combined influence of increased temperature and pCO_2 conditions on *M. edulis* impacted on the aragonite layer to become softer and less stiff (Fitzer et al., 2014b). Correlating the elemental concentration of Mg to the observations of Fitzer et al. (2014b) could suggest future impacts of ocean acidification significantly decrease in the Mg/Ca ratio in aragonite due to the softening effect and changes in the crystal lattice structure. Softer shells could lead to increased morbidity and predation impacts. Aragonite is more susceptible to changes in saturation state (Doney et al., 2009), and this may be due to the influence of pCO_2. The significant finding of elevated temperature influencing Mg concentration in calcite but not aragonite could also help answer why the study of Porter (2010) noted the possibility for clades of calcifying organisms to evolve aragonite whilst in a calcite sea but never observing calcite forming in an aragonite sea.

In calcite, elevated pCO_2 or combined elevated pCO_2 and temperature decreased S concentrations, whereas Na was increased. This may suggest the possibility of S being present in the form of SO_4^{2-} substituting for CO_3^{2-} ions (Takano et al., 1980; Busenberg & Plummer, 1985; Kontrec et al., 2004) as this could be influenced by changes in the carbonate chemistry of the seawater. It may also suggest that combined elevated temperature and pCO_2 have more influence on S concentrations in calcite if related to the organic matrix. This could indicate a thinner organic matrix which would leave the shell with less protection to the outer calcite layer. Elevated temperature also showed significant influence on concentrations of S and Na in aragonite where both concentrations decreased. However, these element concentrations were also shown to be increased significantly under elevated pCO_2 and also combined elevated temperature and pCO_2. Increased Na concentrations in aragonite have previously been correlated with decreases in pH and could be representative of a softening aragonite layer (Fitzer et al., 2014b) allowing more incorporation of minor elements into the crystal lattice.

This research shows that variation in temperature and pCO_2 significantly impacts the elemental composition of *M. edulis* shells. This has provided an insight into the potential

of aragonite-calcite sea conditions to influence shell formation. Although in this study the seawater Mg:Ca ratio associated with aragonite-calcite sea conditions has not been varied, particularly the described patterns of Mg concentrations are consistent with those expected for inorganic calcite in an aragonite-calcite sea scenario.

6.4 Wider Implications and Future Work

$CaCO_3$ minerals account for some of the most widely distributed deposits in the marine environment of both non-biogenic and biogenic origins throughout geological history (Sandberg, 1975; Lowenstam & Weiner, 1989). This abundance and wide distribution is of great importance to the Earth system as it links the biosphere, geosphere and atmosphere. Aragonite and calcite sea conditions as defined by the Sandberg (1983) hypothesis, propose that fluctuations in seawater chemistry drove switches in the dominant $CaCO_3$ mineralogy. However, this hypothesis does not appear to have a direct application to all $CaCO_3$ mineralogy found within the rock record or in complex calcifying organisms. The research presented here proposes that the primary driver of seawater chemistry does indeed influence mineralogy. However, consideration of multiple drivers together with must be taken into consideration to fully understand the mechanisms facilitating $CaCO_3$ mineralogy formation.

The non-biogenic studies presented in Chapter 3 and 4 indicated successful technique in demonstrating how the influences of Mg:Ca ratio, temperature, water movement and sulphate influence all have impact on the $CaCO_3$ polymorph precipitated under a lower saturation state than of previous degassing experiments. Further assessment of the full range of Mg:Ca ratios representative of the Phanerozoic would allow higher resolution results to show how the proportions of aragonite to calcite are influenced. The knowledge of the non-linear relationship with temperature also indicates that further assessment of a wider temperature range, especially into cooler temperatures where calcite should be more dominant, would be of interest. Possible investigation into the changes that occur in mineralogy under different rates of water movement would allow assessment of $CaCO_3$ growth under scenarios of extreme weather conditions such as high turbulence. This would allow further understanding into $CaCO_3$ growth in environmental conditions which are becoming more common due to global climate change and resulting changes to weather systems. Assessing the rate of water movement with the presence of

sulphate in this scenario would also add strength to its application to the natural marine environment.

The 'new' growth of the *M. edulis* shells (Chapter 5) was found to be quite small due to only having spent four months in laboratory conditions. The shells used for this study were unique due to their growth constraints, however, there is a possibility that having a longer growth period in controlled conditions may allow more analysis to be assessed on the elemental control of the mussel allowing for larger new growth areas. This would particularly be of interest for assessing Sr incorporation. Sr has previously been used to assess correlation of the Sr/Ca ratio to be used as an indicator of temperature and salinity (Beck et al., 1992; Klein et al., 1996). In the present research Sr did not yield significant results to allow correlation with temperature. Such links may be evident in a larger area over a longer timeframe. Due to the constraints of EDS, many concentrations (particularly of Sr) fell below detection limits, therefore constraining any relationship between Sr and Ca was not possible, a ratio previously thought to be influenced by temperature (Rosenthal et al., 1997; Lea et al., 1999). Further investigation by finer resolution analysis via wavelength dispersive x-ray spectroscopy (WDS) microprobe analysis may allow more detailed measurements to aid in determining if Sr/Ca ratios can be related to changes in temperature. The need for future replication of these scenarios could also be enhanced by using empirical standards to build upon the data achieved allowing for assessment of the data against fixed aragonite/calcite ratios.

Non-biogenic studies of $CaCO_3$ precipitation presented here indicated that the proportion of aragonite facilitated was increased with increased Mg:Ca ratio, further increased by elevated temperature and that water movement also increased the aragonite proportion. Results from this thesis appear to be directly influenced by the mechanisms of how ions influence mineralogy. This research has indicated that the concept of aragonite-calcite seas should be reassessed to include multiple parameters shown to influence $CaCO_3$ mineralogy alongside the main drivers of Mg:Ca ratio and pCO_2; temperature, water movement and sulphate. The results contribute to our knowledge of how non-biogenic and biogenic $CaCO_3$ growth is related under certain parameters. This allows for a possible insight into how aragonite-calcite sea conditions influence biomineralisation. Both non-biogenic and biogenic $CaCO_3$ investigations indicate that temperature plays an important

role in $CaCO_3$ formation. This also suggests that in both systems there are underlying similarities in the mechanisms facilitating crystal growth. However, what is uncertain is how non-biogenic studies can be applied across organisms where the physiological mechanisms controlling calcification vary.

In conclusion, each non-biogenic scenario assessed has indicated that every added variable promoted aragonite was facilitated at the expense of calcite and more so than compared to individual variables. Any future studies should consider influences on mineralogy in conjunction with other possible influencers together. It was discussed that biogenically the elemental composition of aragonite and calcite matched with the underlying theory of how ion incorporation from seawater chemistry can be influenced by environmental parameters. This has implications for calcification in future changing climates.

Review and Conclusions

This thesis investigated the suggested drivers of aragonite-calcite sea conditions on both non-biogenic (Chapter 3 & 4), and biogenic $CaCO_3$ formation (Chapter 5). Here the main findings of this research are summarised to conclude the observed mechanisms influencing non-biogenic aragonite and calcite formation and what relationships these may have with biogenic $CaCO_3$ elemental compositions in relation to aragonite-calcite sea conditions (Sandberg, 1983).

Sulphate-free experiments showed the proportion of aragonite relative to the calcite increased as a function of Mg:Ca ratio and temperature non-linearly. The co-precipitation of aragonite and calcite at all Mg:Ca ratios indicates that there is no generic switch in $CaCO_3$ mineralogy formed at the proposed critical threshold of Mg:Ca ratio of 2, represented by the presence of aragonite at all Mg:Ca ratios. Elevated temperature increased the mole percentage of aragonite mainly through the precipitation of larger crystals of aragonite whilst forming fewer crystals of calcite which were smaller in size. This work was achieved under lower saturation state than other studies and yielded a larger co-precipitation field range indicating that calcite dominant sea conditions would be even less likely than previously suggested. This is important for application to the natural environment as increased levels of pCO_2 are of concern to calcifying marine life as this reduces the saturation state of seawater. The addition of water movement further amplified of the proportion of aragonite formed. The insight that water movement and temperature increases the aragonite proportion explains why aragonite formation is more common in more turbulent and warmer shallow marine waters, whereas calcite is more common in quieter, cooler and deep waters.

Co-precipitation of aragonite and calcite occurs in the presence of sulphate at Mg:Ca ratio 1, a lower Mg:Ca ratio that previously expected to facilitate aragonite, adding support to the critical threshold for aragonite formation being lowered in the presence of sulphate (Bots et al., 2011). However, no vaterite was observed to form, suggesting that the influence of sulphate inhibits vaterite formation more-so than calcite formation. The presences of sulphate formed smaller crystals of calcite whilst having no influence on the

size of aragonite crystals formed. The presence of sulphate increased the mole percentage of aragonite formed compared to sulphate-free conditions, and further amplified in elevated temperature and with water movement. These results suggest that sulphate directly influences Mg^{2+} incorporation into crystal formation, resulting in calcite inhibition and the growth of aragonite.

Investigation of shell elemental concentrations grown under known conditions of temperature and pCO_2 allowed for comparison to non–biogenic results to constrain if environmental factors influence calcification. Mg/Ca ratio was statistically significant in calcite at elevated temperature suggesting the physiological processes controlling Mg uptake were overridden at elevated temperature, but elevated temperature alone does not influence Mg concentrations in aragonite.

Elevated temperature was observed to have significant influence on the concentrations of Mg but did not alter S, Na or Sr concentrations in aragonite and calcite. Elevated pCO_2 had more influence on S and Na in calcite than aragonite. S in aragonite was more influenced by elevated temperature whereas calcite was observed to have decreased S concentrations and increased Na concentrations under elevated pCO_2 or combined elevated pCO_2 and temperature. This suggests the possibility of S being present in the form of SO_4^{2-} substituting for CO_3^{2-} ions and the mineralogy therefore being directly influenced by changes in carbonate chemistry of the seawater. Elevated temperature increased Mg concentrations in calcite, but did not influence aragonite unless under extreme conditions of elevated temperature and pCO_2 combined. These results indicate that as the two layers of M. edulis were influenced differently under the same environmental conditions that this was due to crystallographic differences allowing minor elements to incorporate. This in turn will influence the material properties of the shell. As the Mg/Ca ratio was indicated to decrease under scenarios of OA this could lead to softer shells, increasing morbidity and predation impacts.

Work on non-biogenic precipitation provides fundamental data which shows influences on $CaCO_3$ mineralogy are complex and require the influence of drivers of aragonite-calcite sea conditions to be viewed together to fully understand the underlying mechanisms impacting on the evolution of biomineralisation.

References

Adabi, M.H. (2004) A re-evaluation of aragonite versus calcite seas. *Carbonates and Evaporites*. 19, 133-141.

Addadi, L. & Weiner, S. (1992) Control and design principles in biological mineralization. *Angewandte Chemie International Edition in English*, *31*(2), pp.153-169.

Addadi, L., Raz, S. & Weiner, S. (2003) Taking advantage of disorder: Amorphous Calcium Carbonate and its roles in biomineralization. *Advanced Materials*. 15(12), 959-970.

Albright, J.N. (1971) *Vaterite stability*. American Mineralogist. 56, 620-624.

Allaby, M. (2013) *A dictionary of Geology and Earth Sciences (4th Ed).* Oxford University Press: Oxford.

Allemand, D., Ferrier-Pagès, C., Furla, P., Houlbrèque, F., Puverel, S., Reynaud, S., Tambutté, É., Tambutté, S. and Zoccola, D. (2004) Biomineralisation in reef-building corals: from molecular mechanisms to environmental control. *Comptes Rendus Palevol*, *3*(6), pp.453-467.

Andersson, A.J., Mackenzie, F.T. & Bates, N.R. (2008) Life on the margin: implications of ocean acidification on Mg-calcite, high latitude and cold-water marine calcifiers. *Marine Ecology Progress Series. 373*, pp.265-273.

Appelo, C.A.J. & Postma, D. (2005) *Geochemistry, Groundwater and Pollution*. A.A. Balkema Publishers: London.

Archer, D., Kheshgi, H. and Maier-Reimer, E. (1997) Multiple timescales for neutralization of fossil fuel CO2. *Geophysical Research Letters*, *24*(4), pp.405-408.

Archer, D., Martin, P., Buffett, B., Brovkin, V., Rahmstorf, S & Ganopolski, A. (2004) The importance of ocean temperature to global biogeochemistry. *Earth and Planetary Science Letters. 222. 333-348.*

Arroyo-de Dompablo, M.E., Fernández-González, M.A. & Fernández-Díaz, L. (2015) Computational investigation of the influence of tetrahedral oxoanions (sulphate, selenate and chromate) on the stability of calcium carbonate polymorphs. *RSC Advances*. 5(74), pp.59845-59852.

Arvidson, R.S., Guidry, M. & Mackenzie, F.T. (2006) The control of Phanerozoic atmosphere and seawater composition by basalt-seawater exchange reactions. Journal of Geochemical Exploration. 88, 412-415.

B&W Tek (2016) *Introduction to Raman Spectroscopy*. B&W Tek: Newark, USA. [Online] Available from: http://bwtek.com/raman-introduction-to-raman-spectroscopy/ [Accessed 14/08/2016].

Bach, L.T. (2015) Reconsidering the role of carbonate ion concentration in calcification by marine organisms. *Biogeoscience*. 12, 4939-4951.

Baker, P.A. & Kastner, M. (1981) Constraints on the formation of sedimentary dolomite. *Science*. 213, 214–216.

Baker, E.T., German, C.R. and Elderfield, H. (1995) Hydrothermal plumes over spreading-center axes: Global distributions and geological inferences. *Seafloor hydrothermal systems: Physical, chemical, biological, and geological interactions*, pp.47-71.

Balthasar, U., Cusack, M., Faryma, L. & Popov, L.E. (2011) Relic aragonite from Ordovician-Silurian brachiopods: Implications for the evolution of calcification. *Geology*. 39, 967-970.

Balthasar, U. & Cusack, M. (2015) Aragonite-calcite seas – Quantifying the gray area. *Geology.* 43, 99-102.

Barange, M., King, J., Valdes, L. & Turra, A. (2016) The evolving and increasing need for climate change research on the oceans. *ICES Journal of Marine Science*. Doi: 10.1093/icesjms/fsw052

Beck, J.W., Edwards, R.L., Ito, E., Taylor, F.W., Recy, J., Rougerie, F., Joannot, P. & Henin, C., (1992) Sea-surface temperature from coral skeletal strontium/calcium ratios. *Science*, *257*(5070), pp.644-648.

Berelson, W.M., Balch, W.M., Najjar, R., Feely, R.A., Sabine, C., Lee, K. (2007) Relating estimates of $CaCO_3$ production, export, and dissolution in the water column to measurements of $CaCO_3$ rain into sediment traps and dissolution on the sea floor: A revised global carbonate budget. *Global Biogeochem Cycles. 2*1, GB1024. doi:10.1029/2006GB002803

Berger, W.H., Smetacek, V.S. & Wefer, G. (1989) Ocean productivity and paleoproductivity—an overview. *Productivity of the ocean: present and past*. (44), pp.1-34.

Berner, R.A (1975) The role of magnesium in the crystal growth of calcite and aragonite from water. *Geochimica et Cosmichimica Acta.* 39, 489-504.

Berner, R.A. (1994) GEOCARB II: A revised model of atmospheric CO_2 over Phanerozoic time. *American Journal of Science*. 294, 56-91.

Berner, R.A. (1997) The rise of land plants and their effect on weathering and atmospheric CO2 over Phanerozoic time. *American Journal of Science*. 291, 339-376.

Berner, R.A. (2006) GEOCARBSULF: a combined model for Phanerozoic atmospheric O 2 and CO 2. *Geochimica et Cosmochimica Acta*. *70*(23), pp.5653-5664.

Berner, R.A. & Raiswell, R. (1983) Burial of organic carbon and pyrite sulfur in sediments over Phanerozoic time: a new theory. *Geochimica et Cosmochimica Acta*. *47*(5), pp.855-862.

Bilings, G.K. & Ragland, P.C. (1968) Geochemistry and mineralogy of the recent reef and lagoonal sediments south of Belize (British Honduras). *Chemical Geology. 3*(2), pp.135-153.

Bijma, J., Pörtner, H-O., Yesson, C. & Rogers, A.D. (2013) Climate changes and the oceans-What does the future hold? *Marine Pollution Bulletin*. 74, 495-505.

Blackford, J.C. (2010) Predicting he impacts of ocean acidification: Challenges from an ecosystem perspective. *Journal of Marine Systems*. 81, 12-18.

Block, A., von Bloh, W., Klenke, T. & Schellnhuber, H.J. (1991) Multifractal analysis of the micro-distribution of elements in sedimentary structures using images from scanning electron microscopy and energy dispersive x-ray spectrometry. *Journal of Geophysical Research*. 96(B10), 16,233 - 16,230.

Bonatti, E. (1976) Serpentinite protrusions in the oceanic crust. *Earth and Planetary Science Letters*, *32*(2), pp.107-113.

Bradshaw, A.L., Brewer, P.G., Shafer, D.K. & Williams, R.T. (1981) Measurements of total carbon dioxide and alkalinity by potentiometric titration in the GEOSECS program. *Earth Planet Science Letter.* 55, 99-115.

Brand, U., Logan, A., Hiller, N. & Richardson, J. (2003) Geochemistry of modern brachiopods: applications and implications for oceanography and paleoceanography. *Chemical Geology*. *198*(3), pp.305-334.

Breland, J.B. & Byrne, R.H. (1993) Spectrophotometric procedures for determination of sea water alkalinity using bromocresol green. *Deep-Sea Research*. 40, 629—641.

Brennan, S.T. & Lowenstein, T.K. (2002) The major-ion composition of Silurian seawater. *Geochimica et Cosmochimica Acta*. *66*(15), pp.2683-2700.

Brennan, S.T., Lowenstein, T.K. & Horita, J. (2004) Seawater chemistry and the advent of biocalcification. *Geology*. *32*(6), pp.473-476.

Bumbrah, G.S. & Sharma, R.M. (2016) Raman spectroscopy–Basic principle, instrumentation and selected applications for the characterization of drugs of abuse. *Egyptian Journal of Forensic Sciences. 6*(3), pp.209-215.

Brownlee, C., Wheeler, G.L. & Taylor, A.R. (2015) Coccolithophore biomineralisation: New questions, new answers. *Seminars in Cell & Developmental Biology*. 46, 11-16.

Bots, P. (2011) *Experimental investigation of calcium carbonate mineralogy in past and future oceans.* [Online] Available from: http://etheses.whiterose.ac.uk/2393/1/Bots_Thesis.pdf. [Accessed 20/03/2013].

Bots, P., Benning, L.G., Rickaby, R.E.M. & Shaw, S. (2011) The role of SO_4 in the switch from calcite to aragonite seas. *Geology.* **39**, 331-334.

Burns, S.J., Mckenzie, J.A. and Vasconcelos, C., 2000. Dolomite formation and biogeochemical cycles in the Phanerozoic. *Sedimentology*, *47*(s1), pp.49-61.

Burton, E.A. (1993) Controls on marine cement mineralogy: review and assessment. *Chemical Geology*. 105, 163-179.

Burton, E.A. & Walter, L.M. (1987) Relative precipitation rates of aragonite and Mg calcite from seawater: Temperature or carbonate ion control? *Geology*. **15**, 111-114.

Burton, E.A. & Walter, L.M. (1991) The effects of P_{CO2} and temperature on magnesium incorporation in calcite in seawater and $MgCl_2$-$CaCl_2$ solutions. *Geochimica et Cosmichimica Acta*. 55, 777-785.

Busenberg, E. & Plummer, L.N. (1985) Kinetic and thermodynamic factors controlling the distribution of SO_4^{2-} and Na^+ in calcites and selected aragonites. *Geochimica et Cosmichimica Acta. 49, 713-725.*

Byrne, M. (2012) Global change ecotoxicology: identification of early life history bottlenecks in marine invertebrates, variable species responses and variable experimental approaches*. Marine Environmental Research.* 76, pp.3-15.

Caldiera, K. & Wickett, M (2003) Oceanography: anthropogenic carbon and ocean pH. *Nature.* 425-365.

Cailleau, P., Jaquin, C., Dragone, D., Girou, A., Roques, H., Humbert, L. (1979) Influence of foreign ions and of organic matter on the crystallization of calcium carbonates. *Oil Gas Science and Technology*. 34, 83-112.

Capstick, S.B., Pidgeon, N.F., Corner, A.J., Spence, E.M. & Pearson, P.N. (2016) Public understanding in Great Britain of Ocean Acidification. *Nature Climate Change*. DOI: 10.1038/NCLIMATE3005.

Carpenter, S.J. & Lohmann, K.C. (1992) Sr/Mg ratios of modern marine calcite: Empirical indicators of ocean chemistry and precipitation rate. *Geochimica et Cosmochimica Acta*. 56, 1837-1849.

Carter, J.G. (1990) (Ed.), Skeletal Biomineralization: Patterns, Processes and Evolutionary Trends (Van Nostrand Reinhold: New York): i-vii, 1–832 [183]

Catlos, E. (2017) *Zeiss Sigma vaccum field emission SEM* [Online] Available from: http://www.jsg.utexas.edu/microbeam/zeiss/[Accessed on 01/04/17] Jackson School of Geosciences: The University of Texas at Austin.

Chave, K.E. (1954) Aspects of the biogeochemistry of magnesium 1. Calcareous marine organisms. *The Journal of Geology. 62*(3), pp.266-283.

Checa, A.G., Jiménez-López, C., Rodríguez-Navarro, A. & Machado, J.P. (2007) Precipitation of aragonite by calcitic bivalves in Mg-enriched marine waters. *Marine Biology*. *150*(5), pp.819-827.

Chierici, M. and Fransson, A. (2009) Calcium carbonate saturation in the surface water of the Arctic Ocean: undersaturation in freshwater influenced shelves. *Biogeosciences*. *6*(11), pp.2421-2431.

Cléroux, C., Cortijo, E., Anand, P., Labeyrie, L., Bassinot, F., Caillon, N. & Duplessy, J.C. (2008) Mg/Ca and Sr/Ca ratios in planktonic foraminifera: Proxies for upper water column temperature reconstruction. *Paleoceanography*, *23*(3).

Clow, D.W. & Mast, M.A. (2010) Mechanisms for chemostatic behaviour in catchments: Implications for CO_2 consumption by mineral weathering. *Chemical Geology*. 269, 40-51.

Cocker, L. & Green, K. (2015) *Responsible sourcing guide: Farmed mussels.* [Online] Available from http://www.seafish.org/media/1403306/ 2 mussels rsg-cocker 04-15kg.pdf [Accessed on 31/12/2017].

Coggon, R.M., Teagle, D.A., Smith-Duque, C.E., Alt, J.C. & Cooper, M.J. (2010) Reconstructing past seawater Mg/Ca and Sr/Ca from mid-ocean ridge flank calcium carbonate veins. *Science*. *327*(5969), pp.1114-1117.

Cuif, J.P., Dauphin, Y., Doucet, J., Salome, M. and Susini, J. (2003) XANES mapping of organic sulfate in three scleractinian coral skeletons. *Geochimica et Cosmochimica Acta*, *67*(1), pp.75-83.

Culberson, C.H., Pytkowicz, R.M. & Hawley, J.E. (1970) Seawater alkalinity determination by the pH method. *Journal of Marine Research*. 28, 15-21.

Dalbeck, P.C. (2007) *Crystallography, stable isotope and trace element analysis of Mytilus edulis shells in the context of ontogeny* (Doctoral dissertation, University of Glasgow).

Dalbeck, P., England, J., Cusack, M. & Fallick, A.E. (2006) Crystallography and chemistry of the calcium carbonate polymorph switch in M. edulis shells. *European journal of mineralogy*. *18*(5), pp.601-609.

Danberg, V. (1975) *Solid waste chopper of rotary type*. U.S. Patent 3,910,510.

Danburg, J.S. & Yuhas, D.E. (1978) Acoustic microscope images of rock samples. *Geophysical Research Letters*. *5*(10), pp.885-888.

Darrenougue N., De Deckker P., Eggins S. & Payri C. (2014) Sea-surface temperature reconstruction from trace elements variations of tropical coralline red algae. *Quaternary Science Reviews*. 93, 34–46.

Dauphin, Y. & Cuif, J.P. (1999) Relationship between mineralogy and microstructural patterns of calcareous biominerals and their sulfur contents. In *Annales des Sciences Naturelles Zoologie et Biologie Animale.* 2(20), pp. 73-85.

Dauphin, Y., Cuif, J., Doucet, J., Salomé, M., Susini, J. & Williams, C. (2003) In situ mapping of growth lines in the calcitic prismatic layers of mollusc shells using X-ray absorption near-edge structure (XANES) spectroscopy at the sulphur K-edge. *Marine Biology*, *142*(2), pp.299-304.

Davis, K. J., Dove, P.M. & De Yoreo, J.J. (2000) The role of Mg^{2+} as an impurity in calcite growth. *Science*. Vol. **290**, 1134-1137. www.sciencemag.org

De Choudens-Sanchez, V. & Gonzalez, L.A. (2009) Calcite and aragonite precipitation under controlled instantaneous supersaturation: elucidating the role of CaCO3 saturation state and Mg/Ca ratio on calcium carbonate polymorphism. *Journal of Sedimentary Research*. *79*(6), pp.363-376.

Demicco, R.V. & Hardie, L.A. (1994) Sedimentary structures and early diagenetic features of shallow marine carbonates. *SEPM Atlas Series 1.* Society of Sedimentary Geology: Tulsa, OK. pp 265.

Demicco, R.V., Lowenstein, T.K., Hardie, L.A. & Spencer, R.J. (2005) Model of seawater composition for the Phanerozoic. *Geology*. 33(11), 877-880.

De Yoreo, J.J. & Dove, P.M. (2004) Shaping crystals with biomolecules. *Science*. *306*(5700), pp.1301-1302.

De Yoreo, J.J., Zepeda-Ruiz, L.A., Friddle, R.W., Qiu, S.R., Wasylenki, L.E., Chernov,A.A., Gilmer, G.H. & Dove, P.M. (2009) Rethinking Classical Crystal Growth Models through Molecular Scale Insights: Consequences of Kink-Limited Kinetics. *Cryustal Growth & Design*. 9, 5135–5144

Dickson, A.G., Sabine, C.L. & Christian, J.R. (2007) *Guide to best practices for ocean CO_2 measurements*. Vol 3, 1-191. (PICES Special Publication.)

Dickson, A.G. (1981) Instruments & Methods: An exact definition of total alkalinity and a procedure for the estimation of alkalinity and total inorganic carbon titration data. *Deep-Sea Research*. 28A (6), 609-623.

Dickson, J.A.D. (2002) Fossil echinoderms as a monitor of the Mg/Ca ratio of Phanerozoic Oceans. *Science.* 298, 1222. DOI: 10.1126/science.1075882.

Dickson, J.A.D.0 (2004) Echinoderm skeletal preservation: Calcite-aragonite seas and the Mg/Ca ratio of Phanerozoic oceans. *Journal of Sedimentary Research*. 74(30, 355-365.

Dodd, J. (1965) Environmental control of strontium and magnesium in *Mytilus*. *Geochimica et Cosmochimica Acta.* 29, 385–398.

Dodd, J.R. & Crisp, E.L. (1982) Non-linear variation with salinity of Sr/Ca and Mg/Ca ratios in water and aragonitic bivalve shells and implications for paleosalinity studies. *Palaeogeography, Palaeoclimatology, Palaeoecology*, *38*(1-2), pp.45-56.

DOE (1994) *Handbook for methods for the analysis of the various parameters of the carbon dioxide system in seawater (version 2*). Dickson, A.G. & Goyet, C. (eds)., ORNL/CDIA-74.

Doney, S.C., Balch, W.M., Fabry, V.J. & Feely, R.A. (2009) Ocean acidification: a critical emerging problem for the ocean sciences. *Oceanography.* 22, 16.

Doubilet, D. (2016) Picture Credit: Great Barrier Reef. National Geographic In Howard, B.C. (2016) Corals are dying on the Great Barrier Reef. National Geographic [Online] Available from: http://news.nationalgeographic.com/2016/03/160321-coral-bleaching-great-barrier-reef-climate-change/ [Accessed on 01/08/2016].

Dwyer, G.S., Cronin, T.M., Baker, P.A., Raymo, M.E., Buzas, J.S. & Corrège, T. (1995) North Atlantic deepwater temperature change during late Pliocene and late Quaternary climatic cycles. *Science*. 95, 270 (5340), pp 1347 – 1351.

Dydo, P., Turek, M. & Ciba, J. (2003) Scaling analysis of nanofiltration systems fed with saturated calcium sulfate solutions in the presence of carbonate ions. *Desalination*, *159*(3), pp.245-251.

Dyrssen, D. & Sillen, L.G. (1967) Alkalinity and total carbonate in seawater: a plea for P-T-independent data. *Tellus*. 19, 113-121.

Elderfield, H. & Ganssen, G. (2000) Past temperature and δ18O of surface ocean waters inferred from foraminiferal Mg/Ca ratios. *Nature*. *405*(6785), pp.442-445.

England, J., Cusack, M., Dalbeck, P. and Pérez-Huerta, A. (2007) Comparison of the crystallographic structure of semi nacre and nacre by electron backscatter diffraction. *Crystal growth & design*. *7*(2), pp.307-310.

Engel, F.L. & Engel, M.G. (1958) The ketogenic activity of corticotropin, a presumed extra-adrenal action. *Endocrinology. 62*(2), pp.150-158.

Engel, A., Zondervan, I., Aerts, K., Beaufort, L., Benthien, A., Chous, L., Delille, B., Gattuso J-P., Harly, J., Heeman, C., Hoffman, L., Jacquet, S., Nejstgaard, J., Pizay, M-D., Rochelle-Newall, E.S., Schneider, U., Terbrueggen, A. & Riebesell, U. (2005) Testing the direct effect of CO_2 concentration on marine phytoplankton: a mesocosm experiment with the coccolithophorid Emiliania huxleyi. *Limnology and Oceanography*. 50(2), 493-507.

Falini, G., Gazzano, M. & Ripamonti, A. (1994) Crystallization of calcium carbonate in presence of magnesium and polyelectrolytes. *Journal of Crystal Growth*. *137*(3-4), pp.577-584.

FAO (2012) *The State of World Fisheries and Aquaculture 2012.* Rome, pp 209 [Online] Available from: http://www.fao.org/docrep/016/i2727e/i2727e.pdf [Accessed on 15/01/17]

Feely, R.A., Doney, S.C. & Cooley, S.R. (2009) Ocean acidification: Present conditions and future changes in a high CO_2 world. *Oceanography*. 22, 36-47.

Feely, R.A., Sabine, C.L., Lee, K., Berelson, W., Kleypas, J., Fabry, V.J. & Millero, F.J. (2004) Impact of anthropogenic CO_2 on the $CaCO_3$ system in the oceans. *Science*. 305 (5682), pp.362-366.

Fermani, S., Džakula, B.N., Reggi, M., Falini, G. & Kralj, D. (2017) Effects of magnesium and temperature control on aragonite crystal aggregation and morphology. *CrystEngComm. 19*(18), pp.2451-2455.

Fernandez-Diaz, L., Fernandez-Gonzalez, A. & Prieto, M. (2010) The role of sulphate groups in controlling $CaCO_3$ polymorphism. *Geochimica et Cosmochimica Acta*. **74**, 6064-6076.

Finch, A.A. & Allison, N. (2007) Coordination of Sr and Mg in calcite and aragonite. *Mineralogical Magazine*. *71*(5), pp.539-552.

Finch, A.A. & Allison, N. (2008) Mg structural state in coral aragonite and implications for the paleoenvironmental proxy. *Geophysical Research Letters*. *35*(8).

Fischer, A.G. (1981) in Biotic Crisis in Ecological and Evolutionary Time. (ed Nitecki, M.) 103-331 (Academic, New York).

Fischer, A.G. (1982) Long-term climatic oscillations recorded in stratigraphy. *Climate in Earth History*, pp.97-104.

Fischer, A.G. (1983) in Climate in Earth History (ed Berger, W.) 97-104. (National Academy of Sciences, Washinton DC).

Fitzer, S.C., Phoenix, V.R., Cusack, M. & Kamenos, N.A. (2014a) Ocean acidification impacts mussel control on biomineralisation. *Scientific Reports*. 4, 6218.

Fitzer, S.C., Cusack, M., Phoenix, V.R. & Kamenos, N.A. (2014b) Ocean acidification reduces the crystallographic control in juvenile mussel shells. *Journal of Structural Biology*. 188, 39-45.

Fitzer, S.C, Zhu, W., Tanner, K.E., Phoenix, V.R., Kamenos, N.A. & Cusack, M. (2015b) Ocean acidification alters the material properties of *Mytilus edulis* shells. *Journal of the Royal Society Interface*. 12, 20141227.

Fitzer, S.C., Vittert, L., Bowman, A., Kamenos, N.A., Phoenix, V.R & Cusack, M. (2015a) Ocean acidification and temperature increase impact mussel shell shape and thickness: problematic for protection? *Ecology & Evolution.* 5(21), 4875-4884.

Fitzer, S.C., Chung, p., Maccherozzi, F., Dhesi, S.S., Kamenos, N.A., Phoenix, V.R. & Cusack, M. (2016) Biomineral shell formation under ocean acidification: a shift from order to chaos. *Scientific Reports.* 6: 21076. DOI: 10.1038/srep21076.

Forster, P., Ramaswamy, V., Artaxo, P., Bernsten, T., Betts, R., Fahey, D.W., Haywood, J., Lean, J., Lowe, D.C., Myhre, G., Nganga, J., Prinn, R., Raga, G. & Van Dorland, M.R.S. (2007) Changes in atmospheric constituents and in radiative forcing. In

Climate Change 2007: The physical science basis. Contribution of Working Group 1 to the Fourth Assessment Report of the Intergovernmental Panel on Climate Change. Cambridge, United Kingdom and New York, NY, USA: Cambridge University Press.

Folk, R.L. (1974) The natural history of crystalline calcium carbonate: Effect of magnesium content and salinity. *Journal of Sedimentary Petrology*. **44**(1), 40-53.

Freitas, P.S., Clarke, L.J., Kennedy, H., Richardson, C.A. & Abrantes, F. (2005) Mg/Ca, Sr/Ca and stable-isotope ($\delta^{18}O$ and $\delta^{13}C$) ratio profiles from the fan mussel *Pinna nobilis:* seasonal records and temperature relationships. *Geochemical &Geophysical Geosystems*. 6(4). Q04D14. doi:10.1029/2004GC000872.

Freitas, P.S., Clarke, L.J., Kennedy, H., Richardson, C.A. & Abrantes, F. (2006) Environmental and biological controls on elemental (Mg/Ca, Sr/Ca and Mn/Ca) ratios in shells of the king scallop *Pecten maximus*. *Geochimica et Cosmochimica Acta.* 70, 5119-5153.

Füchtbauer, H. & Hardie, L.A. (1976) Experimentally determined homogeneous distribution coefficients for precipitated magnesian calcites: Application to marine carbonate cements. *Geological Society of America Abstracts with Programs*. 8, 877.

Füchtbauer, H. & Hardie, L.A. (1980) Comparison of experimental and natural magnesian calcites: International. *Association of Sedimentologists.* Abstracts. p. 167–169

Gaffin, S. (1987) Ridge volume dependence on seafloor generation rate and inversion using long term sealevel change. *American Journal of Science*. *287*(6), pp.596-611.

Garrett, D.E. (2001) *Sodium sulphate. Handbook of deposits, processing, properties and use*. Harcourt Science and Technology Company: London.

Gattuso, J-P., Allemand, D. & Frankignoule, M. (1999) Photosynthesis and calcification at cellular, organismal and community levels in coral reefs: A review on interactions and control by carbonate chemistry. *American Zoologist*. 39, 160-183.

Gattuso, J-P. & Hansson, L. (2011) *Ocean Acidification* (Eds). Oxford: Oxford University Press.

Gibbs, S.J., Stoll., H.M., Bown, P.R. & Bralower, T.J. (2010) Ocean acidification and surface water carbonate production across the Paleocene-Eocene thermal maximum. *Earth and Planetary Science Letters*. 295, 583-592.

Given, R.K. & Wilkinson, B.H. (1985) Kinetic control of morphology, composition, and mineralogy of abiotic sedimentary carbonates. *Journal of Sedimentary Petrology.* 55, 109-119.

Gill, B.C., Lyons, T.W. and Saltzman, M.R. (2007) Parallel, high-resolution carbon and sulfur isotope records of the evolving Paleozoic marine sulfur reservoir. *Palaeogeography, Palaeoclimatology, Palaeoecology*. *256* (3), pp.156-173.

Gill, B.C., Lyons, T.W., Young, S.A., Kump, L.R., Knoll, A.H. & Saltzman, M.R. (2011) Geochemical evidence for widespread euxinia in the Later Cambrian ocean. *Nature*. *469* (7328), pp.80-83.

Gillikin, D.P., Lorrain, A., Navez, J., Taylor, J.W., André, L., Keppens, E., Baeyens, W. & Dehairs, F. (2005) Strong biological controls on Sr/Ca ratios in aragonitic marine bivalve shells. *Geochemistry, Geophysics, Geosystems*. 6 (5).

Gong, Y.U.T., Killian, C.E., Olson, I.C., Appathurai, N.P., Amasino, A.L., Martin, M.C., Holt, L.J., Wilt, F.H. & Gilbert, P.U.P.A. (2012) Phase transitions in biogenic amorphous calcium carbonate. *PNAS.* 109, 6088-6093.

Gossling, E.M. (1992) Systematics and geographic distribution of *Mytilus*. In The mussel *Mytillus*: Ecology, Physiology, Genetics and Culture (ed. E.M. Gossling); *Developments in Aquaculture and Fisheries Science*. Vol 25, Ch 1, pp 1-20, Elsevier.

Guidry, M.W., Arvidson, R.S. & Mackenzie, F.T. (2007) Biological and geochemical forcings to Phanerozoic change in seawater, atmosphere, and carbonate precipitate composition. *Evolution of Primary Producers in the Sea*. *15*, pp.377-403.

Hach (2010) *What is pH and how is it measured?* [Online] Available from: https://www.hach.com/asset-get.download.jsa?id=7639984488 [Accessed on 12/05/2016]

Halevy, I., Peters, S.E. & Fischer, W.W. (2012) Sulfate burial constraints on the Phanerozoic sulfur cycle. *Science*. *337*(6092), pp.331-334.

Hanor, J.S. (2004) A model for the origin of large carbonate- and evaporite-hosted Celestine ($SrSO_4$) deposits. *Journal of Sedimentary Research*. 74, 168-175.

Hansson, I. & Jagner, D. (1973) Evaluation of the accuracy of Grans Plots by means of computer calculations: Application to the potentiometric titration of the total alkalinity and carbonate content in sea water. *Analytica Chimica Acta.* 65, 363-373.

Hardie, L.A. (1987) Dolomitization: A critical view of some current views: PERSPECTIVES. *Journal of Sedimentary Research*. *57* (1).

Hardie, L. A. (1996) Secular variation in seawater chemistry: An explanation for the coupled secular variation in the mineralogies of marine limestones and potash evaporites over the past 600 m.y. *Geology*. **24**, 279–283.

Hardie, L.A. (1998) On the secular variations in the composition of Phanerozoic marine potash evaporates: Comment and reply. *Geology*. 26(1), 91-96.

Harper, E.M., Palmer, T.J. & Alphey, J.R. (1997) Rapid Communication Evolutionary response by bivalves to changing Phanerozoic sea-water chemistry. *Geological Magazine*, *134*(03), pp.403-407.

Harvey, L.D.D. (2001) A quasi-one-dimensional coupled climate-carbon cycle model 2. The carbon cycle component. *Journal of Geophysical Research*. 106, No C10, 22,355-22,372.

Hasiuk, F.J. and Lohmann, K.C. (2008) Mississippian paleocean chemistry from biotic and abiotic carbonate, Muleshoe Mound, Lake Valley formation, New Mexico, USA. *Journal of Sedimentary Research*. *78* (2), pp.147-164.

Hansson, I. & Jagner, D. (1973) Evaluation of the accuracy of Gran plots by means of computer content in seawater. *Analytica Chimica Acta*. 75, 363-373.

He, S., Oddo, J.E., & Thomson, M.B. (1994) The nucleation kinetics of calcium sulfate dehydrate in NaCl solutions up to 6m and 90°C. *Journal of Colloid Interface Science*. 162, 297-303.

Hendriks, I.E., Duarte, C.M. & Álvarez, M. (2010) Vulnerability of marine biodiversity to ocean acidification: a meta-analysis. *Estuarine, Coastal and Shelf Science*. *86* (2), pp.157-164.

Hendriks, I.E., Duarte, C.M., Olsen, Y.S., Steckbauer, A., Ramajo, L., Moore, T.S., Trotter, J.A. & McCulloch, M. (2015) Biological mechanisms supporting adaptation to ocean acidification in coastal ecosystems. *Estuarine, Coastal and Shelf Science*. *152*, pp.A1-A8.

Hetzinger, S., Halfar, J., Kronz, A., Simon, K., Adey, W.H. & Steneck, R.S. (2018) Reproducibility of Clathromorphum compactum coralline algal Mg/Ca ratios and comparison to high-resolution sea surface temperature data. *Geochimica et Cosmochimica Acta.* 220, pp.96-109.

Hiebenthal, C., Phillipp, E.E.R., Eisenhauer, A. & Wahl, M. (2013) Effects of seawater pCO_2 and temperature on shell growth, shell stability, condition and cellular stress of

Western Baltic Sea *Mytilus edulis* (L.) and *Arctica islandica* (L.). *Mar Biol.* 160, 2073-2087.

Higuchi, T., Fujimura, H., Yuyama, I., Harii, S., Agostini, S. & Oomori, T. (2014) Biotic control of skeletal growth by scleractinian corals in aragonite–calcite seas. *PloS one*. *9*(3), p.e91021.

Hoegh-Guldberg, O., Mumby, P.J., Hooten, A.J., Steneck, R.S., Greenfield, P., Gomez, E., Harvell, C.D., Sale, P.F., Edwards, A.J., Caldeira, K. & Knowlton, N. (2007) Coral reefs under rapid climate change and ocean acidification. *Science*. *318*(5857), pp.1737-1742.

Holland, H.D., Holland, H.J. & Munoz, J.L. (1964) The co-precipitation of cations with CaCO3—II. the co-precipitation of Sr^{2+} with calcite between 90 and 100°C. *Geochimica et Cosmochimica Acta*. *28*(8), pp.1287-1301.

Holland, H.D., Horita, J., Seyfried Jr., W.E. (1996) On the secular variations in the composition of Phanerozoic marine potash evaporates. *Geology*. 24 (11), 993-996.

Hönisch, B., Ridgwell, A., Schmidt, D.N., Thomas, E., Gibbs, S.J., Sluijs, A., Zeebe, R., Kump, L., Martindale, R.C., Greene, S.E. & Kiessling, W. (2012) The geological record of ocean acidification. *Science*. *335* (6072), pp.1058-1063.

Hope, G.A., Woods, R. & Munce, C.G. (2001) Raman microprobe mineral identification. *Minerals Engineering*. 14 (12), 1565-1577.

Horita, J., Friedman, T.J., Lazar, B. & Holland, H.D. (1991) The composition of Permian seawater. *Geochimica et Cosmochimica Acta*. 55, 417-432.

Horita, J., Weinberg, A., Das, N. & Holland, H.D. (1996) Brine inclusions in halite and the origin of the Middle Devonian Prairie Evaporites of Western Canada. Journal of Sediment Research. 66, 956, 964.

Horita, J., Zimmermann, H. & Holland, H.D. (2002) Chemical evolution of seawater during the Phanerozoic: Implications from the record of marine evaporates. *Geochimica et Cosmochimica Acta*. **66**, 3733-3756.

Houston, S., Smalley, C., Laycock, A. & Yardley, B.W.D. (2011) The relative importance of buffering and brine inputs in controlling the abundance of Na and Ca in sedimentary formation waters. *Marine and Petroleum Geology*. 28, 1242-1251.

Hudson, J.D. & Anderson, T.F. (1989) Ocean temperatures and isotopic compositions through time. *Transactions of the Royal Society of Edinburgh: Earth Sciences*. *80*(3-4), pp.183-192.

Ilyina, T., Wolf-Gladrow, D., Munhoven, G. & Heinze, C. (2013) Assessing the potential of calcium-based artificial ocean alkalinization to mitigate rising atmospheric CO_2 and ocean acidification. *Geophysical Research Letters.* 40, 1–6. doi:10.1002/2013GL057981.

Immenhauser, A., Schöne, B.R., Hoffmann, R. & Niedermayr, A. (2016) Mollusc and brachiopod skeletal hard parts: Intricate archives of their marine environment. *Sedimentology*. *63*(1), pp.1-59.

IPCC (2013) *Climate Change 2013: The Physical Science Basis. Contribution of Working Group 1 to the Fifth Assessment Report of the Intergovernmental Panel on Climate Change.* Stoker, T.F., Qin, D., Plattner, G-K., Tignor, M., Allen, S.K., Boschung, J., Nauels, A., Xia, Y., Bex, V. & Midgleey, P.M. Cambridge: Cambridge University Press. DOI 10.1017/CBO9781107415324.

Jahnen-Dechent, W. & Ketteler, M. (2012) Magnesium basics. *Clinical Kidney Journal*. *5*(Suppl 1). pp.i3-i14.

Janiszewska, K., Mazur, M., Escrig, S., Meibom, A. & Stolarski, J. (2017) Aragonitic scleractinian corals in the Cretaceous calcitic sea. *Geology*, *45*(4), pp.319-322.

Jiménez-López, C., Romanek, C.S., Huertas, F.J., Ohmoto, H.& Caballero, E. (2004) Oxygen isotope fractionation in synthetic magnesian calcite. *Geochimica et Cosmochimica Acta*. 68 (16), pp.3367-3377.

Jones, S.J., Lima, F.P. & Wethey, D.S. (2010) Rising environmental temperatures and biogeography: poleward range contraction of the blue mussel, Mytilus edulis L., in the western Atlantic. *Journal of Biogeography*, *37* (12), pp.2243-2259.

Kabalah-Amitai, L., Mayzel,B., Kauffmann, Y., Fitch, A.N., Bloch, L., Gilbert, P.U., & Pokrov, B. (2013) Vaterite crystals contain two interspersed crystal structures. *Science.* 340 (6131), 454- 457. doi: 10.1126/science.1232139.

Kah, L.C., Thompson, C.K., Henderson, M.A. & Zhan, R. (2016) Behavior of marine sulfur in the Ordovician. *Palaeogeography, Palaeoclimatology, Palaeoecology.* 458, pp.133-153.

Kampschulte, A. & Strauss, H. (2004) The sulfur isotopic evolution of Phanerozoic seawater based on the analysis of structurally substituted sulfate in carbonates. *Chemical Geology*. 204 (3), pp.255-286.

Katz, A. (1973) The interaction of magnesium with calcite during crystal growth at 25–90 C and one atmosphere. *Geochimica et Cosmochimica Acta.* 37 (6), pp.1563IN31579-15781586.

Kawano, J., Maeda, S. & Nagai, T. (2016) The effect of Mg^{2+} incorporation on the structure of calcium carbonate clusters: investigation by the anharmonic downward distortion following method. *Physical Chemistry Chemical Physics*. *18*(4), pp.2690-2698.

Kawano, J., Shimobayashi, N., Miyake, A. & Kitamura, M. (2009) Precipitation diagram of calcium carbonate polymorphs: its construction and significance. *Journal of Physics: Condensed Matter*. 21, 425102 (6pp) doi:10.1088/0953-8984/21/42/425102.

Kennedy, W.J., Taylor, J.D. & Hall, A. (1969) Environmental and biological controls on bivalve shell mineralogy. *Biological Reviews*. 44 (4), pp.499-530.

Kentucky Geology Society (2012) *Entelophyllum* rugose coral in Silurian Limestone University of Kentucky. [Online] Available from: https://www.uky.edu/KGS/fossils/rugosecolonial2.htm [Accessed on 18/08/2016].

Kester, D.R., Duedall, I.W., Connors, D.N., & Pytkowicz, R.M. (1967) Preparation of artificial seawater. *Limnology & Oceanography*. 12 (1), 176-179.

Kiessling, W., Abergan, M. & Villier, L. (2008) Phanerozoic trends in skeletal mineralogy driven by mass extinctions. *Nature Geoscience*. **1**, 527-530.

Kimmig, S.R. & Holmden, C. (2017) Multi-proxy geochemical evidence for primary aragonite precipitation in a tropical-shelf 'calcite sea'during the Hirnantian glaciation. *Geochimica et Cosmochimica Acta*, *206*, pp.254-272.

Kitano, Y. & Hood, D.W.(1962) Calcium carbonate crystal forms formed from sea water by inorganic processes. *Journal of the Oceanographical Society of Japan*. *18*(3), pp.141-145.

Klein, R.T., Lohmann, K.C. & Thayer, C.W. (1996) Bivalve skeletons record sea-surface temperature and δ18O via Mg/Ca and 18O/16O ratios. *Geology*. *24*(5), pp.415-418.

Klepetsanis, P.G., & Koutsoukos, P.G (1991) Spontaneous precipitation of calcium sulfate at conditions of sustained supersaturation. *Journal of Colloid Interface Science*. 143 (2), 299-308.

Klepetsanis, P.G., Dalas, E., & Koutsoukos, P.G. (1999) Role of temperature in the spontaneous precipitation of calcium sulfate dehydrate. *Langmuir*. 15, 1534-1540.

Kleypas, J.A., Buddemeier, R.W., Archer, D., Gattuso, J.P., Langdon, C. & Opdyke, B.N. (1999) Geochemical consequences of increased atmospheric carbon dioxide on coral reefs. *Science*. *284*(5411), pp.118-120.

Kleypas, J.A., Feely, R.A., Fabry, V.J., Langdon, C., Sabine, C.L. & Robbins, L.L. (2005) Impacts of ocean acidification on coral reefs and other marine calcifiers: a guide for future research. *Report of a workshop held 18-20 April 2005*, *sponsored by NSF, NOAA, and the US Geological Survey.* St Petersburg, Florida. (Vol. 18, p. 20).

Kominz, M.A.(2004) November. Plate reconstructions require high Cretaceous spreading rates and ridge volumes. In *2004 Denver Annual Meeting*.

Kominz, M.A. & Scotese, C.R. (2005) December. Thermal Cooling of Ocean Lithosphere-New Data-New Insights. In *AGU Fall Meeting Abstracts*.

Kontrec, J., Kralj, D., Brečevic, L., Falini, G., Fermani, S., Noethig-Laslo, V. & Mirosavljević, K. (2004) Incorporation of inorganic anions in calcite. *European Journal of Inorganic Chemistry*. 4579-4585.

Kroeker, K.J., Kordas, R.L., Crim, R.N. & Singh, G.G. (2010) Meta-analysis reveals negative yet variable effects of ocean acidification on marine organisms. *Ecology letters*, *13*(11), pp.1419-1434.

Kuffner, I.B., Andersson, A.J. Jokiel, P.L., Rodgers, K.U.S. & Mackenzie, F.T. (2008) Decreased abundance of crustose coralline algae due to ocean acidification. *Nature Geoscience*. 1, 114-117.

Kuroyanagi, A., Kawahata, H., Suzuki, A., Fujita, K. & Irie, T. (2009) Impacts of ocean acidification on large benthic foraminifers: Results from laboratory experiments. *Marine Micropaleontology*. 73, 190-195.

Lea, D.W., Mashiotta, T.A. & Spero, H.J. (1999) Controls on magnesium and strontium uptake in planktonic foraminifera determined by live culturing. *Geochimica et Cosmochimica Acta*. *63*(16), pp.2369-2379.

Lear, C.H., Elderfield, H. & Wilson, P.A. (2000) Cenozoic deep-sea temperatures and global ice volumes from Mg/Ca in benthic foraminiferal calcite. *Science*. **287**, 269-272.

Lear, C.H., Rosenthal, Y. & Slowey, N. (2002) Benthic foraminiferal Mg/Ca-paleothermometry: A revised core-top calibration. *Geochimica et Cosmochimica Acta*. *66*(19), pp.3375-3387.

Leclercq, N.C., Gattuso, J.P. & Jaubert, J.E.A.N. (2000) CO2 partial pressure controls the calcification rate of a coral community. *Global Change Biology*, *6*(3), pp.329-334.

Lécuyer, C. (2016) Seawater residence times of some elements of geochemical interest and the salinity of the oceans. *Bulletin de la Société Géologique de France*. *187*(6), pp.245-260.

Lee, J. & Morse, J.W. (2010) Influences of alkalinity and pCO2 on CaCO3 nucleation from estimated Cretaceous composition seawater representative of "calcite seas". *Geology.* **38**, pp 115-118.

Levitus, S. Antonov, J.I., Boyer, T.P., Locarnini, R.A., Garcia. H.E. & Mishonov, A. V. (2009) Global ocean heat content 1955-2008 in light of recently revealed instrumentation problems. *Geophysical Research Letters*. 36.

Li, Q., Wang, F., Wang, Z.A., Yuan, D., Dai, M., Chen, J., Dai, J. & Hoering, K.A. (2013) Automated spectrophotometric analyser for rapid single-point titration of seawater total alkalinity. *Environmental Science & Technology*, American Chemical Society. 47, 11139-11146.

Liu, S-T., & Nanchollas, G.H. (1970) The kinetics of crystal growth of calcium sulfate dehydrate. *Journal of Crystal Growth*. 6, 281-289.

Lorens, R.B. & Bender, M.L. (1977) Physiological exclusion of magnesium from *Mytilus edulis* calcite. *Nature*. 269, 793-794.

Lorens, R.B. & Bender, M.L. (1980) The impact of solution chemistry on Mytilus edulis calcite and aragonite. *Geochimica et Cosmochimica Acta*, *44*(9), pp.1265-1278.

Lorens, R.B. (1981) Sr, Cd, Mn and Co distribution coefficients in calcite as a function of calcite precipitation rate. *Geochimica et Cosmochimica Acta*. *45*(4), pp.553-561.

Loste, E., Wilson, R.M., Seshadri, R. & Meldrum, F.C. (2003) The role of magnesium in stabilising amorphous calcium carbonate and controlling calcite morphologies. *Journal of crystal growth.* 254, 206-218.

Lowenstam, H.A. (1954) Factors affecting the aragonite: calcite ratios in carbonate-secreting marine organisms. *The Journal of Geology*. *62*(3), pp.284-322.

Lowenstam, H.A. (1964) Coexisting calcites and aragonites from skeletal carbonates of marine organisms and their strontium and magnesium contents. *Recent researches in the fields of hydrosphere, atmosphere and nuclear geochemistry*. pp.373-404.

Lowenstam, H.A. & Weiner, S. (1989) *On Biomineralization*. Oxford University Press, New York.

Lowenstein, T.K., Hardie, L.A., Timofeeff, M.N. & Demicco, R.V. (2003) Secular variation in seawater chemistry and the origin of calcium chloride brines. *Geology*. 31, 857-860.

Lowenstein, T.K. & Timofeeff, M.N. (2008) Secular variations in seawater chemistry as a control on the chemistry of basinal brines: test of hypothesis. *Geofluids*. 8, 77-92.

Lowenstein, T.K., Timofeeff, M.N., Brennan, S.T., Hardie, L. A. & Demicco, R.V. (2001) Oscillations in Phanerozoic seawater chemistry: Evidence from fluid inclusions. *Science*. 294, 1086- 1088.

Lowenstein, T.K., Timofeeff, M.N., Kovalevych, V.M. & Horita, J. (2005) The major-ion composition of Permian seawater. *Geochimica et Cosmochimica Acta. 69*(7), pp.1701-1719.

Mackenzie, F.T. (2005) *Sediments, Diagenesis, and Sedimentary Rocks. Treatise on Geochemistry* (2nd Ed). Vol 7. Elsevier: London.

MacKenzie, F.T., Arvidson, R.S. & Guidry, M. (2008) Chemostatic modes of the ocean-atmosphere-sediment system through the Phanerozoic time. *Mineralogical Magazine*. 72(1), 329-332.

MacKenzie, F.T. & Morse, J.W. (1992) Sedimentary carbonates through Phanerozoic time. *Geochimica et Cosmichimica Acta*. **56**, 3281-3295.

MacKenzie, F.T. & Pigott, J.D. (1981) Tectonic controls of Phanerozoic sedimentary rock cycling. *Journal of the Geological Society London*. 138, 183-196.

MacGuire, M.E. & Cowan, J.A. (2002) Magnesium chemistry and biochemistry and biochemistry. *Biometals*. 15, 203-210.

Madshus, I.H (1988) Regulation of intracellular pH in eukaryotic cells. *Biochemistry Journal*. 250, 1-8.

Markgraf, S.A. & Reeder, R.J. (1985) High-temperature structure refinements of calcite and magnesite. *American Mineralogist*. *70*(5-6), pp.590-600.

Martin, W. R., & Sayles, F. L. (1994) Seafloor diagenetic fluxes, *in* Material fluxes on the surface of the Earth: Washington, D.C., National Academy Press, p. 143–164.

Martin, S., Rodolfo-Metalpa, R., Ransome, E., Rowley, S., Buia, M.C., Gattuso, J. P. & Hall-Spencer, J. (2008) Effects of naturally acidified seawater on seagrass calcareous epibionts. *Biology Letters*. 4, 689-692.

Marubini, F., Ferrier–Pages, C. & Cuif, J.P. (2003) Suppression of skeletal growth in scleractinian corals by decreasing ambient carbonate-ion concentration: a cross-

family comparison. *Proceedings of the Royal Society of London B: Biological Sciences. 270*(1511), pp.179-184.

Manahan, S.E. (2004) *Environmental Chemistry (8th Ed).* CRC Press: London.

McElwain, J.C. & Chaloner, W.G. (1995) Stomatal density and index of fossil plants track atmospheric carbon dioxide in the Palaeozoic. *Annals of Botany. 76*(4), pp.389-395.

McGhee, M. (2017) *Year 2100 projections*. [Online] Available from: https://www.co2.earth/2100-projections. [Accessed on 02/03/2017]

Meehl, G.A., Stocker, T.F., Collins, W.D., Friedlingstein, P., Gaye, A.T., Gregory, J.M., Kitoh, A., Knutti, R., Murphy, J.M., Noda, A., Raper, S.C.B., Watterson, I.G., Weaver, A.J. & Zhao, Z.C. (2007) *Global climate projections. Climate change 2007: the physical science basis*. Contribution of Working Group 1 to the Fourth Assessment Report of the Intergovernmental Panel on Climate Change (ed. by S. Solomon, D. Qin, M. Manning, Z. Chen, M. Marquis, K.B. Averyt, M. Tignor and H.L. Miller), pp. 747–845. Cambridge University Press: Cambridge.

Mejri, W., Korchef, A., Tlili, M. & Ben Amor, M. (2014) Effects of temperature on precipitation kinetics and microstructure of calcium carbonate in the presence of magnesium and sulphate ions. *Desalination and Water Treatment*. *52*(25-27), pp.4863-4870.

Met Office (2017) *Global Forecast 2017*. [Online] Available from: http://www.metoffice.gov.uk/news/releases/2016/global-forecast-2017 [Accessed 02/03/2017]

Mii, H.S. & Grossman, E.L. (1994) Late Pennsylvanian seasonality reflected in the 18O and elemental composition of a brachiopod shell. *Geology*. *22*(7), pp.661-664.

Millero, F.J., Zhang, J-Z., Lee, K. & Campbell, D.M. (1993) Titration alkalinity of seawater. *Marine Chamistry.* 44, 153-165.

Milliman, J.D. (1974) *Marine Carbonates*. Springer-Verlag: Heidelberg, pp375.

Milliman, J.D. (1993) Production and accumulation of calcium carbonate in the ocean: Budget of a non-steady state. *Global Biogeochemical Cycles*. 7(4), 927-957.

Mitsuguchi, T., Matsumoto, E., Abe, O., Uchida, T. & Isdale, P.J. (1996) Mg/Ca thermometry in coral skeletons. *Science*. *274*(5289), p.961.

Morse, J.W., Arvidson, R.S. & Luttge, A. (2007) Calcium carbonate formation and dissolution. *Chemical Reviews*. **107**, 342-381.

Morse, J.W. & He, S. (1993) Influences of *T*, *S* and P_{CO2} on pseudo-homogeneous precipitation of $CaCO_3$ from seawater: implications for whiting formation. *Marine Chemistry*. 41, 291-297.

Morse, J.W. & Mackenzie, F.T. (1990) *Geochemistry of Sedimentary Carbonates*. Elsevier: Amsterdam.

Morse, J.W., Mucci, A. & Millero, F.J. (1980) The solubility of calcite and aragonite in seawater of 35%. Salinity at 25°C and atmospheric pressure. *Geochimica et Cosmochimica Acta*. 44, 85-94.

Morse, J.W., Wang, Q. & Tsio, M. Y. (1997) Influences of temperature and Mg:Ca ratio on $CaCO_3$ precipitates from seawater. *Geology*. 25, 85-87.

Mortyn, P.G., Elderfield, H., Anand, P. & Greaves, M. (2005) An evaluation of controls on planktonic foraminiferal Sr/Ca: Comparison of water column and core-top data from a North Atlantic transect. *Geochemistry, Geophysics, Geosystems*. *6*(12).

Mucci, A. (1981) The solubility of calcite and aragonite and the composition of calcite overgrowths in seawater and related solutions. [Online] Available from: http://access.library.miami.edu/login?url=http://gateway.proquest.com/openurl?url_ver=Z39.882004&rft_val_fmt=info:ofi/fmt:kev:mtx:dissertation&res_dat=xri:pqdiss&rft_dat=xri:pqdiss:8211812 [Accessed on 23/10/2015]

Mucci, A., 1987. Influence of temperature on the composition of magnesian calcite overgrowths precipitated from seawater. *Geochimica et Cosmochimica Acta*, *51*(7), pp.1977-1984.

Mucci, A., Canuel, R. & Zhong, S. (1989) The solubility of calcite and aragonite in sulfate-free seawater and the seeded growth kinetics and composition of the precipitates at 25°C. *Chemical Geology*. **74**, 309-320.

Mucci, A. & Morse, J.W. (1983) The incorporation of Mg^{2+} and Sr^{2+} into calcite overgrowths: influences of growth rate and solution composition. *Geochimica et Cosmochimica Acta*. **47**, 217-233.

Mucci, A., Morse, J.W. & Kaminsky, M.S. (1985) Auger spectroscopy analysis of magnesian calcite overgrowths precipitated from seawater and solutions of similar composition. *American Journal of Science*. 285(4), DOI 10.2475/ajs.285.4.289.

Nanophoton (2016) *What is Raman Spectroscopy?* [Online] Available from: http://www.nanophoton.net/raman/raman-spectroscopy.html [Accessed n 01/04/2017].

Neilson, J.E., Brasier, A.T. & North, C.P. (2016) Primary aragonite and high-Mg calcite in the late Cambrian (Furongian). Potential evidence from marine carbonates in Oman. *Terra Nova*, *28*(5), pp.306-315.

Newton, R.J., Reeves, E.P., Kafousia, N., Wignall, P.B., Bottrell, S.H. & Sha, J.G. (2011) Low marine sulfate concentrations and the isolation of the European epicontinental sea during the Early Jurassic. *Geology*. *39* (1), pp.7-10.

Nguyen, L.T., Rahman, M.A., Maki, T., Tamenori, Y., Yoshimura, T., Suzuki, A., Iwasaki, N. & Hasegawa, H. (2014) Distribution of trace element in Japanese red coral Paracorallium japonicum by μ-XRF and sulfur speciation by XANES: linkage between trace element distribution and growth ring formation. *Geochimica et Cosmochimica Acta*. *127*, pp.1-9.

Niedermayer, T., Jégou, A., Carlier, M.F., Romet-Lemonne, G. & Lipowsky, R. (2013) Interplay of Stochastic Processes during Actin Depolymerization. *Biophysical Journal*. *104*(2), p.645a.

Nichols, G. (2009) *Sedimentology and stratigraphy*. John Wiley & Sons.

Nikinmaa, M. (2013) Climate change and ocean acidification – Interactions with aquatic toxicology. *Aquatic Toxicology*. 126, 365-372.

Nürnberg, D. (1995) Magnesium in tests of *Neogloboquadrina pachyderma* sinistral from high northern and southern latitudes. *Journal of Foraminiferal Research*. *25*, pp.350-368.

Okumura, M. & Kitano, Y. (1986) Co-precipitation of alkali metal ions with calcium carbonate. *Geochimica et Cosmochimica Acta*. *50*(1), pp.49-58.

Orr, J.C., Fabry, V.J., Aumont, O., Bopp, L., Doney, S.C., Feely, R.A., Gnanadesikan, A., Gruber, N., Ishida, A., Joos, F. & Key, R.M. (2005) Anthropogenic ocean acidification over the twenty-first century and its impact on calcifying organisms. *Nature*, *437*(7059), pp.681-686.

Oxford Labs (2009) Xray Fluorescence. The Oxford Science Park, Oxford X-ray Fluorescence Ltd. [Online] Available from: http://oxford-labs.com/x-ray-fluorescence/the-basic-process/ {Accessed 17/05/2016].

Park, W.K., Ko, S.J., Lee, S.W., Cho, K.H., Ahn, J.W. & Han, C. (2008) Effects of magnesium chloride and organic additives on the synthesis of aragonite precipitated calcium carbonate. *Journal of Crystal Growth*, *310*(10), pp.2593-2601.

Pagani, M., Arthur, M.A. & Freeman, K.H. (1999) Miocene evolution of atmospheric carbon dioxide. *Paleoceanography*. *14*(3), pp.273-292.

Paquette, J., Vali, H., Mucci, A. (1996) TEM study of Pt-C replicas of calcite overgrowths precipitated from electrolyte solutions. *Geochimica et Cosmichimica Acta.* 60, 4689-4701.

Pearson, P.N. & Palmer, M.R. (2000) Atmospheric carbon dioxide concentrations over the past 60 million years. *Nature. 406* (6797), pp.695-699.

Pelejero, C., Calvo, E. & Hoegh-Guldberg, O. (2010) Paleo-perspectives on ocean acidification. *Trends in Ecology & Evolution*. 25(6), 332-344.

Perrin, J., Rivard, C., Vielzeuf, D., Laporte, D., Fonquernie, C., Ricolleau, A., Cotte, M. & Floquet, N. (2017) The coordination of sulfur in synthetic and biogenic Mg calcites: The red coral case. *Geochimica et Cosmochimica Acta*. *197*, pp.226-244.

Petrou, A.L. & Terzidaki, A. (2014) Calcium carbonate and calcium sulfate precipitation, crystallization and dissolution: Evidence for the activated steps and the mechanisms from the enthalpy and entropy of activation values. *Chemical Geology*. 381, 144-153.

Pingitore Jr, N.E. (1978) The behavior of Zn2+ and Mn2+ during carbonate diagenesis: theory and applications. *Journal of Sedimentary Research*. *48*(3).

Piwoni-Piórewicz, A., Kukliński, P., Strekopytov, S., Humphreys-Williams, E., Najorka, J. & Iglikowska, A. (2017) Size effect on the mineralogy and chemistry of Mytilus trossulus shells from the southern Baltic Sea: implications for environmental monitoring. *Environmental Monitoring and Assessment*, *189*(4), p.197.

Pokroy, B., Fitch, A.N., Marin, F., Kapon, M., Adir, N. & Zolotoyabko, E. (2006) Anisotropic lattice distortions in biogenic calcite induced by intra-crystalline organic molecules. *Journal of structural biology*. *155*(1), pp.96-103.

Pokrovsky, O.S. (1998). Precipitation of calcium and magnesium carbonates from homogeneous supersaturated solutions. *Journal of Crystal Growth.* 186, 233-239.

Ponnurangam, A., Bau, M., Brenner, M. & Koschinsky, A. (2016) Mussel shells of Mytilus edulis as bioarchives of the distribution of rare earth elements and yttrium in seawater and the potential impact of pH and temperature on their partitioning behavior. *Biogeosciences*, *13* (3), pp.751-760.

Porter, S.M. (2007) Seawater chemistry and early carbonate biomineralization. *Science. 316*(5829), pp.1302-1302.

Porter, S.M. (2010) Calcite and aragonite seas and the *de novo* acquisition of carbonate skeletons. *Geobiology*. **8**, 256-277.

Prenant, M., Biology Reviews. 2, 365. In Addadi, L., Raz, S. & Weiner, S. (2003) Taking advantage of disorder: Amorphous Calcium Carbonate and its roles in biomineralization. *Advanced Materials*. 15(12), 959-970.

Pytkowicz, R.M. (1965) Rates of inorganic calcium carbonate nucleation. *The Journal of Geology*. *73* (1), pp.196-199.

Radha, A.V., Forbes, T.Z., Killian, C.E., Gilbert, P.U.P.A. & Navrotsky, A. (2010) Transformation and crystallization energetics of synthetic and biogenic amorphous calcium carbonate. *Proceedings of the National Academy of Sciences. 107*(38), pp.16438-16443.

Railsback, L.B. & Anderson, T.F. (1987) Control of Triassic seawater chemistry and temperature on the evolution of post-Paleozoic aragonite-secreting faunas. *Geology*. *15*(11), pp.1002-1005.

Ramsden, E.N. (1996) *Chemistry of the environment*. Nelson Thornes Ltd.: London.

Rasband, W.S., (1997-2012) ImageJ Software. U. S. National Institutes of Health, Bethesda, Maryland, USA. [Online] Download available from: http://imagej.nih.gov/ij/ [Accessed 20/04/2013].

Rathburn, A.E. & De Deckker, P. (1997) Magnesium and strontium compositions of recent benthic foraminifera from the Coral Sea, Australia and Prydz Bay, Antarctica. *Marine micropaleontology*. *32*(3-4), pp.231-248.

Raven, J.A., Caldeira, K., Elderfield, H., Hoegh-Guldberg, O., Liss, P., Riesbesell, U., Shepherd, J., Turley, C., Watson, A., Heap, R., Banes, R. & Quinn, R. (2005*) Ocean Acidification due to increasing Atmospheric Carbon Dioxide. The Royal Society [*Online] available from: *www.royalsoc.ac.uk*. [Accessed on 20/06/2016]. Policy document 12/05 ISBN 0 85403 617 2. pp 68.

Reddy, M.M. & Nancholas, G.H. (1971) The crystallization of calcium carbonate: I.isotopic exchange and kinetics. *Journal of Colloid Interface Science*. 36, 166.

Reddy, M.M. & Nancholas, G.H. (1976) The crystallization of calcium carbonate IV. The effect of magnesium, strontium and sulfate ions. *Journal of Crystal Growth*. 35, 33-38.

Renishaw (2016) *Raman spectroscopy explained* (L9836-9033-01-B) Renishaw plc.: Gloucestershire, UK. [online] Available from: www.renishaw.com/raman [Accessed 17/06/2016].

Reynaud, S., Ferrier-Pagès, C., Meibom, A., Mostefaoui, S., Mortlock, R., Fairbanks, R. & Allemand, D. (2007) Light and temperature effects on Sr/Ca and Mg/Ca ratios in

the scleractinian coral Acropora sp. *Geochimica et Cosmochimica Acta*. *71*(2), pp.354-362.

Richardson, C.A. (1989) An analysis of the microgrowth bands in the shell of the common mussel *Mytilus edulis*. *Journal of the Marine Biological Association of the United Kingdom*. *69* (02), pp.477-491.

Riebesell, U., Fabry, V.J., Hansson, L. & Gattuso, J-P. (2010) (Eds) *Guide to best practices for ocean acidification research and data reporting.* Publications Office of the European Union: Luxembourg.

Ries, J.B. (2005) Aragonite production in calcite seas: effect of seawater Mg/Ca ratio on the calcification and growth of the calcareous alga *Penicillus capitatus*. *Paleobiology*. 31(3), 445-458.

Ries, J.B. (2010) Review: geological and experimental evidence for secular variation in seawater Mg/Ca (calcite-aragonite seas) and its effects on marine biological calcification. *Biogeosciences.* 7, 2795-2849.

Ries, J.B., Cohen, A.L. & McCorkle, D.C. (2009) Marine calcifiers exhibit mixed responses to CO_2-induced ocean acidification. *Geology*, *37*(12), pp.1131-1134.

Ries, J.B., Ghazaleh, M.N., Connolly, B., Westfield, I. & Castillo, K.D. (2016) Impacts of seawater saturation state (Ω A= 0.4–4.6) and temperature (10, 25° C) on the dissolution kinetics of whole-shell biogenic carbonates. *Geochimica et Cosmochimica Acta*. *192*, pp.318-337.

Ries, J.B., Stanley, S.M. & Hardie, L.A. (2006) Scleractinian corals produce calcite, and grow more slowly, in artificial Cretaceous seawater. *Geology*, *34*(7), pp.525-528.

Rosenberg, G.D. & Hughes, W.W. (1991) A metabolic model for the determination of shell composition in the bivalve mollusc, *Mytilus edulis*. *Lethaia*. *24*(1), pp.83-96.

Rosenthal, Y., Boyle, E.A. & Slowey, N. (1997) Temperature control on the incorporation of magnesium, strontium, fluorine, and cadmium into benthic foraminiferal shells from Little Bahama Bank: Prospects for thermocline paleoceanography. *Geochimica et Cosmochimica Acta*. *61*(17), pp.3633-3643.

Rowley, D.B. (2002) Rate of plate creation and destruction: 180 Ma to present. *Geological Society of America Bulletin*, 114(8), pp.927-933.

Royer, D.L., Berner, R.A., Montañez, I.P., Tabor, N.J. & Beerling, D.J. (2004) CO_2 as a primary driver of phanerozoic climate. *GSA today*, *14*(3), pp.4-10.

Sayles, F.L. (1980) The solubility of $CaCO_3$ in seawater at 2°C based upon in-situ sampled pore water composition. *Marine Chemistry*. 9, 223-235.

Sandberg, P.A. (1975) New interpretations of Great Salt Lake ooids and of ancient non-skeletal carbonate mineralogy. *Sedimentology*. **22**, 497-537.

Sandberg, P.A. (1983) An oscillating trend in Phanerozoic non-skeletal carbonate mineralogy. *Nature*. **305** (1), 19-22.

Sandberg, P. A. (1985) Nonskeletal Aragonite and pCO_2 in the Phanerozoic and Proterozoic, in The Carbon Cycle and Atmospheric CO: Natural Variations Archean to Present (eds E.T. Sundquist and W.S. Broecker), American Geophysical Union: Washington, D. C. . doi: 10.1029/GM032p0585

Schacht, U., Wallmann, K., Kutterolf, S., Schmidt, M. (2008) Volcanogenic sediment-seawater interactions and the geochemistry of pore waters. Chemical Geology. 249, 3321-338.

Schöne, B.R., Zhang, Z., Radermacher, P., Thébault, J., Jacob, D.E., Nunn, E.V. & Maurer, A.F. (2011) Sr/Ca and Mg/Ca ratios of ontogenetically old, long-lived bivalve shells (Arctica islandica) and their function as paleotemperature proxies. *Palaeogeography, Palaeoclimatology, Palaeoecology*, *302*(1), pp.52-64.

Schrag, D.P., DePaolo, D.J. & Richter, F.M. (1995) Reconstructing past sea surface temperatures: Correcting for diagenesis of bulk marine carbonate. *Geochimica et Cosmochimica Acta*. *59*(11), pp.2265-2278.

Schultz, H.D. & Zabel, M. (2007) *Marine Geochemistry*. Springer: London.

SEPA (2010) Argyll and Lochaber area management plan catchment summaries. Loch Fyne coastal catchment. [Online] Available from: http://www.sepa.org.uk/media/74764/doc-27-loch-fyne-coastal-catchment-summary.pdf. [Accessed 20/01/2017].

Sepkoski, J.J. (2002) A compendium of fossil marine animal genera. *Bulletins of American Paleontology* 363: 1-560.

Settle, F.A. (1997) *Handbook of instrumental techniques for analytical chemistry*. Prentice Hall PTR.

Siemann, M.G. (2003) Extensive and rapid changes in seawater chemistry during the Phanerozoic: evidence from Br contents in basal halite. *Terra Nova*, *15*(4), pp.243-248.

Simkiss, K. (1965) The organic matrix of the oyster shell. *Comp. Biochem. Physiol*. 16, 427-435.

Simpson, J.H. & Rippeth, T.P. (1993) The Clyde Sea: a model of the seasonal cycle of stratification and mixing. *Estuarine, Coastal and Shelf Science*. 37, 129-144. Http://dx.doi.org/10.1006/ecss.1993.1047.

Slaughter, M., Hill, R.J., 1991. The influence of organic matter in organogenic dolomitization. *Journal of Sedimentary Research*. 61, 296–303.

Soetaert, K., Hofmann, A.F., Middelburg, J.J., Meysman, F.J.R. & Greenwood, J. (2007) Reprint of "The effect of biogeochemical processes on pH". *Marine Chemistry*. 106, 380-401.

Sorte, C.J., Etter, R.J., Spackman, R., Boyle, E.E. & Hannigan, R.E. (2013) Elemental fingerprinting of mussel shells to predict population sources and redistribution potential in the Gulf of Maine. *PloS one*. *8* (11), p.e80868.

Spencer, R.J. & Hardie, L.A. (1990) Control of seawater composition by mixing of river waters and mid-ocean ridge hydrothermal brines: Geochemical Society Special Publication 2.Spalding, M. D., Ravilious, C. & Green. E. P. (2001) *World atlas of coral reefs.* Berkley: University of California Press.

Stanley, S.M., Ries, J.B. & Hardie, L.A. (2002) Low-magnesium calcite produced by coralline algae in seawater of Late Cretaceous composition. *Proceedings of the National Academy of Sciences*. *99*(24), pp.15323-15326.

Stanley, S.M. (2008) Effects of global seawater chemistry on biomineralisation: Past, present and future*. Chemical Reviews*. **108**, 4483-4498.

Stanley, S.M. & Hardie, L.A. (1998) Secular oscillations in the carbonate mineralogy of reef-building and sediment-producing organisms driven by tectonically forced shifts in sediment-producing organisms driven by tectonically forced shifts in seawater chemistry. *Palaeogeography, Palaeoclimatology, palaeoecology*. **144**, 3-19.

Stanley, S.M. & Hardie, L.A. (1999) Hypercalcification: paleontology links plate tectonics and geochemistry to sedimentology. *gSa Today*, *9*(2), pp.1-7.

Stanley, S.M., Ries, J.B. & Hardie, L.A. (2005) Seawater chemistry, coccolithophore population growth, and the origin of Cretaceou chalk. *Geology*. 33. 593-596.

Stanley, S.M., Ries, J.B. & Hardie, L.A. (2010) Increased production of calcite and slower growth for the major sediment producing Alga *Halimeda* as the Mg/Ca ratio of

seawater is lowered to a 'calcite sea' level. *Journal of Sedimentary Research*. 80,6-16.

Staudt, W.J. & Schoonen, M.A. (1995) Sulfate incorporation into sedimentary carbonates. ACS Publications. 612. 342-345.

Steinacher, M., Joos, F., Frölicher, T.L., Plattner, G-K. & Doney, S.C. (2009) Imminent ocean acidification in the Arctic projected with the NCAR global coupled carbon cycle-climate model. *Biogeosciences*. 6, 515-533.

Stoll, H.M., Ruiz Encinar, J., Ignacio Garcia Alonso, J., Rosenthal, Y., Probert, I. & Klaas, C., (2001) A first look at paleotemperature prospects from Mg in coccolith carbonate: Cleaning techniques and culture measurements. *Geochemistry, Geophysics, Geosystems*. *2*(5). Paper number 2000GC000144.

Stoll, H.M., Rosenthal, Y. & Falkowski, P. (2002) Climate proxies from Sr/Ca of coccolith calcite: calibrations from continuous culture of Emiliania huxleyi. *Geochimica et Cosmochimica Acta*. *66*(6), pp.927-936.

Stoll, H.M., Skimizu, N., Archer, D. & Ziveri, P. (2007) Coccolithophore productivity response to greenhouse event of the Paleocene-Eocene Thermal Maximum. *Earth and Planetary Science Letters*. 258, 192-206.

Suess, E. & Fütterer, D. (1972) Aragonitic ooids: experimental precipitation from seawater in the presence of humic acid. *Sedimentology*. 19, 129-139.

Sun, W., Jayaraman, S., Chen, W., Persson, K.A. & Ceder, G. (2015) Nucleation of metastable aragonite $CaCO_3$ in seawater. *PNAS.* 112(11), 3199-3204.

Swart, P.K. (2015) The geochemistry of carbonate diagenesis: The past, present and future. *Sedimentology*. *62*(5), pp.1233-1304.

Takano, B., Asano, Y. & Watanuki, K. (1980) Characterization of sulfate ion in travertine. *Contributions to Mineralogy and Petrology*. *72*(2), pp.197-203.

Tang, Y., Zhang, F., Cao, Z., Jing, W. & Chen, Y. (2012) Crystallization of $CaCO_3$ in the presence of sulfate and additives: Experimental and molecular dynamics simulation studies. *Journal of Colloid and Interface Science*. 377, 430-437.

Tao, J., Zhou, D., Zhang, Z., Xu, X. & Tang, R. (2009) Magnesium-aspartate-based crystallization switch inspired from shell molt of crustacean. *Proceedings of the National Academy of Sciences*. *106*(52), pp.22096-22101.

Taylor, J.D. (1969) The shell structure and mineralogy of the Bivalvia. Introduction. Nuculacea-Trigonacea. *Bull. Br. Mus. Nat. Hist.(Zool.)*. *3*, pp.1-125.

Taylor, J.D. (1973) The structural evolution of the bivalve shell. *Palaeontology*. *16*(3), pp.519-534.

Takano, B. (1985) Geochemical implications of sulfate in sedimentary carbonates. *Chemical Geology*. *49*(4), pp.393-403.

Tett, P., Gowen, R., Grantham, B., Jones, K. & Miller, B.S. (1986) The phytoplankton ecology of the Firth of Clyde sealochs Striven and Fyne. *Proceedings of the Royal Society of Edinburgh*. 90B: 223-238.

Tett, P., Valcic, B., Potts, T., Whyte, C., Culhane, F. & Fernandes, T. (2012) Mussels and Yachts in Loch Fyne, Scotland: a Case Study of the Science-Policy Interface. *Ecology and Society*. 17(3): 16. Http://dx.doi.org/10.5751/ES-04995-170316.

Tesoriero, A.J. & Pankow, J.F. (1996) Solid solution partitioning of Sr^{2+}, Ba^{2+}, and Cd^{2+} to calcite. *Geochimica et Cosmochimica Acta*, 60, 1053– 1063. doi:10.1016/0016-7037(95)00449-1.

Timofeeff, M.N., Lowenstein, T.K., Da Silva, M.A.M. & Harris, N.B. (2006) Secular variation in the major-ion chemistry of seawater: Evidence from fluid inclusions in Cretaceous halites. *Geochimica et Cosmochimica Acta*. *70*(8), pp.1977-1994.

Thompson, T.G. & Bonnar, R.U. (1931) The buffer capacity of seawater. *Industrial and Engineering Chemistry-Analytical Edition*. 3, 371-390.

Tlili, M.M., Ben Amor, M., Garbrielli, C., Joiret, S., & Maurin, G. (2006) On the initial stages of calcium carbonate precipitation. *European Journal of Water Quality*. 37, 89-108.

Tostevin, R., He, T., Turchyn, A.V., Wood, R.A., Penny, A.M., Bowyer, F., Antler, G. & Shields, G.A. (2017) Constraints on the late Ediacaran sulfur cycle from carbonate associated sulfate. *Precambrian Research*. *290*, pp.113-125.

Tucker, M.E. & Bathurst, R.G.C. (2009) *Carbonate Diagenesis (Eds)*. The international Association of Sedimentologists. Doi: 10.1002/9781444304510.

Tynan, S., Eggins, S., Kinsley, L., Welch, S.A. & Kirste, D. (2005) Mussel shells as environmental tracers: An example from the Loveday Basin. In Roach, I.C. (ed) (2005) Regolith 2005 – Ten Years of CRC LEME. CRC LEME, 314-317.

Tyrell, T & Zeebe, R.E. (2004) History of carbonate ion concentration over the last 100 million years. *Geochimica et Cosmochimica Acta*. 68 (17), 3521-3530.

Ullman, C.V., Bohm, F., Rickaby, R.E.M. & Korte, C., (2013) The Giant Pacific Oyster (Crassostrea gigas) as a modern analog for fossil ostreoids: Isotopic (Ca, O, C) and

elemental (Mg/Ca, Sr/Ca, Mn/Ca) proxies. *Geochemistry, Geophysics & Geosystems*. 14(10), pp.4109-4120.

Vail, P.R., Mitchum, R.M. & Thompson, S. (1977) Seismic stratigraphy and global changes of sea level. *American Association of Petroleum Geologists Memoir*. 26, 83-97.

Vander Putten, E., Dehairs, F., Keppens, E. & Baeyens, W. (2000) High resolution of trace elements in the calcite shell layer of modern Mytilus edulis: Environmnetal and biological controls. *Geochimica et Cosmichimica Acta.* 64 (6), 997-1011.

Valsami-Jones, E., Baltatzis, E., Bailey, E.H., Boyce, A.J., Alexander, J.L., Magganas, A., Anderson, L., Waldron, S. & Ragnarsdottir, K.V. (2005) The geochemistry of fluids from an active shallow submarine hydrothermal system: Milos Island, Hellanic Volcanic Arc. *Journal of Volcanology and Geothermal Research*. 148, 130-151.

Vavouraki, A.I., Putnis, C.V., Putnis, A. & Koutsoukos, P.G. (2008) An atomic force microscopy study of the growth of calcite in the presence of sodium sulphate. *Chemical Geology*. **253**, 243-251.

Verkaaik, M.F.C., Hooijschuur, J-H., Davies, G.R. & Ariese, F. (2015) Raman spectroscopic techniques for Planetary exploration: Detecting microorganisms through minerals. *Astrobiology*, 15(8), pp 1-11, DOI: 10.1089/ast.2015.1329.

Vermeij, G.J. (1983) Traces and trends of predation, with special reference to bivalved animals. *Palaeontology*, *26*(3), pp.455-465.

Vihtakari, M., Ambrose, W.G., Renaud, P.E., Locke, W.L., Carroll, M.L., Berge, J., Clarke, L.J., Cottier, F. & Hop, H. (2017) A key to the past? Element ratios as environmental proxies in two Arctic bivalves. *Palaeogeography, Palaeoclimatology, Palaeoecology*, *465*, pp.316-332.

Volk, T. (1989) Sensitivity of climate and atmosphere CO_2 to deep-ocean and shallow-ocean carbonate burial. *Nature*. 337 (16), 637-640.

Von Davier, M. (1997) Bootstrapping goodness-of-fit statistics for sparse categorical data-Results of a Monte Carlo Study. *Methods of Psychological Research Online*. 2(2), 29-48.

Vulpius, S. & Kiessling, W. (2018) New constraints on the last aragonite-calicte sea transition from early Jurassic ooids. *Facies*. 64(3). http://doi.org/10.1007/s10347-017-0516-x.

Wallmann, K. (2004) Impact of atmospheric CO2 and galactic cosmic radiation on Phanerozoic climate change and the marine δ18O record. *Geochemistry, Geophysics, Geosystems*. *5*(6).

Wallmann, K. (2001) The geological water cycle and the evolution of marine δ18O. *Geochimica et Cosmochimica Acta* 65: 2469-2485.

Walter, L. M. (1986) Relative efficiency of carbonate dissolution and precipitation during diagenesis: A progress report on the role of solution chemistry. In Gautier, D.L. (Ed) *Roles of organic matter in sediment diagenesis*. Society of Economic Palaeontologists and Mineralogists Special Publication.

Warren, J.K. (2016) *Evaporites: A geological compendium*. Springer.

Wang, W.X. & Fisher, N.S. (1997) Modelling the influence of body size on trace element accumulation in the mussel Mytilus edulis. *Marine Ecology Progress Series*, *161*, pp.103-115.

Wang, D., Hamm, L.M., Giuffre, A.J., Echigo, T., Rimstidt, J.D., De Yoreo, J.J., Grotzinger, J. & Dove, P.M. (2012) Revisiting geochemical controls on patterns of carbonate deposition through the lens of multiple pathways to mineralization. *Faraday Discuss. 159, 371-386.*

Wanamaker Jr, A.D., Kreutz, K.J., Wilson, T., Borns Jr, H.W., Introne, D.S. & Feindel, S., (2008) Experimentally determined Mg/Ca and Sr/Ca ratios in juvenile bivalve calcite for Mytilus edulis: implications for paleotemperature reconstructions. Geo-Marine Letters, 28(5), pp.359-368.

Wasylenki, L.E., Dove, P.M. & DeYoreo, J.J. (2005) Effects of temperature and transport conditions on calcite growth in the presence of Mg^{2+}: Implications for paleothermometry. *Geochimica et Cosmochimica Acta*. **69**, 4227-4236.

Weber, J.N., 1973. Temperature dependence of magnesium in echinoid and asteroid skeletal calcite: a reinterpretation of its significance. *The Journal of Geology*, *81*(5), pp.543-556.

Weiner, S., Sagi, L. & Addadi, L. (2005) Choosing the path less travelled. *Science*. 309, 1027-1028.

Weiner, S. & Dove, P.M. (2003) An overview of biomineralisation processes and the problem of the vital effect. In Dove, P.M., De Yoreo, J.J. & Weiner, S (eds) *Biomineralization.* Washington D.C., Minerlogical Society of America Reviews in Mineralogy and Geochemistry. 54, 1-29.

Weiss, I.M., Tuross, N., Addadi, L. & Weiner, S. (2002) Mollusc larval shell formation: amorphous calcium carbonate is a precursor phase for aragonite. *Journal of Experimental Zoology Part A: Ecological Genetics and Physiology*. 293 (5), pp.478-491.

Wilbur, K.M. (1972) Shell formation in mollusks. *Chemical Zoology*, *7*, 103-145.

Wilkinson, B.H. (1979) Biomineralisation, palaeoceanography and the evolution of calcareous marine organisms. *Geology*. **7**, 524-527.

Wilkinson, B.H. & Algeo, T.J. (1989) Sedimentary carbonate record of calcium-magnesium cycling. *American Journal of Science*, *289*(10), pp.1158-1194.

Wilkinson, B.H. & Given, R.K. (1986) Secular variation in abiotic marine carbonates: Constraints on Phanerozoic atmospheric carbon dioxide contents and oceanic Mg/Ca ratios. *The Journal of Geology*. 94 (3), 321-333.

Willett, K.M., Hurst, D.F., Dunn, R.J.H., Dolman, A.J. Eds. (2016): Global Climate [in "State of the Climate in 2015"]. *Bulletin of the American Meteorological Society*, 97 (8), S7–S62.

Willmott, C.J., Ackleson, S.G., Davis, R.E., Feddema, J.J., Klink, K.M., Legates, D.R., O'Donnell, J. & Rowe, C.M. (1985) Statistics for the evaluation and comparison of models. *Journal of Geophysical Research.* 90, (C5), 8995-9005.

Wolf-Gladrow, D.A., Zeebe, R.E., Klaas, C., Körtzinger, A. & Dickson, A.G. (2007) Total alkalinity: The explicit conservative expression and its application to biogeochemical processes. *Marine Chemistry*. *106*(1), pp.287-300.

Wood, R. A. (2011) Paleoecology of the earliest skeletal metazoan communities: Implications for early biomineralization. *Earth-Science Reviews*. 184-190.

Wortmann, U.G., Chernyavsky, B., Bernasconi, S.M., Brunner, B., Böttcher, M.E. & Swart, P.K. (2007) Oxygen isotope biogeochemistry of pore water sulfate in the deep biosphere: dominance of isotope exchange reactions with ambient water during microbial sulfate reduction (ODP Site 1130). *Geochimica et Cosmochimica Acta. 71*(17), pp.4221-4232.

Wright, D.A. (1995) Trace metal and major ion interactions in aquatic animals. *Marine Pollution Bulletin*, *31*(1), pp.8-18.

Yao, W. & Byrne, R.H. (1998) Instruments and methods Simplified seawater alkalinity analysis: Use of linear array spectrometers. *Deep-Sea Research I*. 45, 1383—1392.

Yapp, C.J. & Poths, H. (1992) Ancient Atmospheric CO_2 Pressures Inferred from Natural Goethites. *Nature*. *355*(6358), p.342.

Yasoshima, M. & Takano, B. (2001) Bradybaena similaris (Ferrusac) shell as a biomonitor of copper, cadmium and zinc. *Bulletin of Environmental Contamination and Toxicology*. 66(2), 239-248.

Yoshimura, T., Tamenori, Y., Kawahata, H. & Suzuki, A. (2014) Fluctuations of sulfate, S-bearing amino acids and magnesium in a giant clam shell. *Biogeosciences*. *11*(14), pp.3881-3886.

Yoshimura, T., Tamenori, Y., Iwasaki, N., Hasegawa, H., Suzuki, A. & Kawahata, H. (2013) Magnesium K-edge XANES spectroscopy of geological standards. *Journal of synchrotron radiation*. *20*(5), pp.734-740.

Zeebe, R.E. & Wolf-Gladrow, D.A. (2001) *CO2 in seawater: equilibrium, kinetics, isotopes* (No. 65). Gulf Professional Publishing.

Zittier, Z.M.C., Bock, C., Lannig, G. & Pörtner, H.O. (2015) Impact of ocean acidification on thermal tolerance and acid-base regulation of *Mytilus edulis* (L.) from the North Sea. *Journal of Experimental Marine Biology and Ecology*. 473, 16-25.

Zhang, Z., Falter, J., Lowe, R. & Ivey, G. (2012) The combined influence of hydrodynamic forcing and calcification on the spatial distribution of alkalinity in a coral reef system. *Journal of Geophysical Research: Oceans*. *117*(C4).

Zhao, L., Schöne, B.R., Mertz-Kraus, R. & Yang, F. (2017) Sodium provides unique insights into transgenerational effects of ocean acidification on bivalve shell formation. *Science of the Total Environment*. 577, 360-366.

Zhao, L., Schöne, B.R. and Mertz-Kraus, R., 2017b. Controls on strontium and barium incorporation into freshwater bivalve shells (Corbicula fluminea). *Palaeogeography, Palaeoclimatology, Palaeoecology*, *465*, pp.386-394.

Zhu, F., Kong, Y., Liang, J., Li, C., Hu, Y., Zhou, Y., Liu, X., Xie, L. & Zhang, R. (2010) Tuning calcite magnesium content by soluble shell matrices: Insights into biomineral impurity control. *Materials Science and Engineering: C*. *30*(7), pp.963-969.

Zhuravlev, A.Y. & Wood, R.A. (2009) Controls on carbonate skeletal mineralogy: Global CO_2 evolution and mass extinctions. *Geology.* **37**, 1123-1126.

Appendix I

Sulphate-free (still)		Artificial seawater precipitation experiment results										
					Polymorph distribution	Number of nucleations		Surface area precipitated			Total Alkalinity of mother solution	
Mg:Ca ratio aim	Experiment ID	Mg:Ca ratio & [Ca^{2+}] at beginning (B) and end (E) (mM)	T (°C)	Env. Condition-water movement	Arag mole%	Ave.no of aragonite crystals	Ave. No of calcite crystals	Ave.size of arag crystals (µm²)	Ave. size of calcite crystals (µm²)	Time 1st crystals observed (mins)	Predicted TA at time of 1st crystals	TA at end of experiment
1	J1.1.n K1.1.n L1.1.n M1.1.n	1.001 Ca^{2+} B- 11.20, E- 10.40	20	still	3.731 2.414 8.512 4.165	3.00 8.33 13.67 2.00	50.67 53.33 122.67 107.33	2.493 2.010 1.319 1.337	3.6252 6.7517 1.7619 1.6028	120 150 210 180	6.10 6.59 4.66 5.36	11.79* - 8.33* -
1	P1.2.n XL1.2.n XP1.2.n	1.001 Ca^{2+} B- 11.20, E- 10.40	30	still	3.024 1.814 4.873	4.67 18.33 85.00	141.00 741.00 979.33	1.787 17.914 2.030	2.0977 18.1634 2.9547	150 120 120	2.83 2.25 2.25	6.90* 7.73 6.90*
2	J2.1.n K2.1.n L2.1.n M2.1.n	1.996 Ca^{2+} B- 11.24, E- 10.41	20	still	49.300 48.05 29.319 38.458	52.33 37.00 39.00 78.00	99.00 61.667 171.67 249.00	2.441 3.115 2.243 2.276	1.9182 2.7273 1.8107 1.7592	210 180 180 240	4.66 5.36 5.36 4.94	10.97* - 10.30* -
2	K2.2.n L2.2.n M2.2.n	2.003 Ca^{2+} B- 11.20, E-10.40	30	still	66.067 66.730 72.195	35.67 18.67 14.67	47.00 26.33 14.33	4.813 5.757 4.119	3.0111 3.2426 2.5451	270 270 300	5.15 5.15 5.73	7.89 - 6.29
3	L3.1.n M3.1.n O3.1.n P3.1.n	3.001 Ca^{2+} B - 11.22, E-10.41	20	still	81.587 73.464 78.353 62.736	131.00 81.67 33.33 65.00	59.00 59.33 41.33 81.33	1.618 2.884 2.924 2.911	1.2578 2.2002 1.3959 2.1683	270 240 210 180	5.28 - 5.00 -	8.01 - 7.86 -
3	K3.2.n L3.2.n M3.2.n	2.998 Ca^{2+} = 11.200	30	still	39.979 83.622 94.862	272.67 37.33 340.00	120.00 19.67 31.67	3.812 3.028 1.946	1.8020 1.7098 1.3625	270 210 240	5.60 4.36 4.98	7.75* - 7.18*

Appendix I: Summary of sulphate-free experiments in still conditions.

Summary of solution composition and experiment parameters in terms of Mg:Ca ratio and [Ca2+] at the end of each experiment, aimed temperature in still conditions. Results are given for each experiment in terms of the mole percentage of aragonite precipitated, number of nucleations and the size of crystals formed for both aragonite and calcite as an average of crystal precipitates quantified from 3 images per experiment. The predicted TA st the time of first crystals and at the end of each experiment, asterix represents TA based on an average of TA results for that scenario as not measured with that particular experiment run. Dashed line represents where TA equipment unavailable for calculation.

Appendix II

Sulphate-free (shaken)		Artificial seawater precipitation experiment results										
					Polymorph distribution	Number of nucleations		Surface area precipitated			Total Alkalinity of mother solution	
Mg:Ca ratio aim	Experiment ID	Mg:Ca ratio & [Ca^{2+}] at beginning (B) and end (E) (mM)	T (°C)	Env. Condition-water movement	Arag mole%	No of aragonite crystals	No of calcite crystals	Size of arag crystals	Size of calcite crystals	Time 1st crystals observed (mins)	Predicted TA at time of 1st crystals	TA at end of experiment
1	J1.1.a	1.001 Ca^{2+} B- 11.20, E- 10.41	20	shaken	64.3	106.00	18.00	2.6	6.4	210	8.37	12.24
	K1.1.a				13.1	126.33	68.67	1.3	7.0	240	8.79	11.74
	L1.1.a				33.8	39.00	20.00	3.3	8.7	270	10.5	13.04
	M1.1.a				18.1	11.33	20.00	4.4	8.4	270	10.1	12.8
1	J1.2.a	1.001 Ca^{2+} E- 11.20, E-10.41	30	shaken	94.7	140.67	17.33	4.4	2.9	210	5.88	8.28
	K1.2.a				94.9	70.00	10.00	2.9	1.7	210	7.12	9.54
	L1.2.a				85.2	56.67	10.33	5.4	5.1	210	6.78	9.00
	M1.2.a				93.4	33.00	3.00	5.0	4.9	180	6.17	8.44
2	J2.1.a	2.003 Ca^{2+} B- 11.20, E-10.41	20	shaken	97.2	94.67	7.00	1.6	1.1	210	7.40	11.8
	K2.1.a				98.7	117.33	4.67	3.5	2.3	210	9.01	14.88
	L2.1.a				98.7	97.33	5.00	3.7	1.9	210	7.15	11.38
	M2.1.a				99.1	84.67	1.00	2.3	2.4	180	6.46	11.33
2	J2.2.a	2.003 Ca^{2+} B- 11.20, E-10.39	30	shaken	99.6	100.33	2.33	5.6	1.9	180	3.99	7.88
	k				99.0	112.00	7.33	5.1	1.8	150	3.43	8.08
	l				97.5	70.67	8.00	6.2	2.8	180	4.12	8.18
	m				99.6	122.67	4.67	8.0	1.9	240	5.40	8.07
3	J3.1.a	3.001 Ca^{2+} B- 11.22, E – 10.40	20	shaken	96.6	97.00	54.33	6.8	1.4	240	5.38	7.99
	K				99.5	288.67	2.67	2.2	1.7	270	-	-
	L				96.1	40.33	11.33	13.4	4.1	300	-	-
	m				99.2	240.67	4.33	1.8	1.3	270	5.50	8.02
3	J3.2.a	2.998 Ca^{2+}B - 11.20, E- 10.38	30	shaken	97.6	84.33	2.00	5.0	4.0	180	4.53	7.34
	K				98.0	54.33	5.33	2.9	1.3	150	2.61	6.27
	L				99.5	149.67	3.33	3.6	1.5	150	3.77	8.02
	M				99.1	113.00	10.00	7.0	1.9	180	3.712	6.96

Appendix II: Summary of sulphate-free experiments in shaken conditions.
Summary of solution composition and experiment parameters in terms of Mg:Ca ratio and [Ca^{2+}] at the end of each experiment, aimed temperature in shaken conditions. Results are given for each experiment in terms of the mole percentage of aragonite precipitated, number of nucleations and the size of crystals formed for both aragonite and calcite as an average of crystal precipitates quantified from 3 images per experiment. The predicted TA st the time of first crystals and at the end of each experiment, dashed line represents where TA equipment unavailable for calculation.

Sulphate Experiments			Artificial seawater precipitation experiment results											
							Polymorph Distribution	Number of nucleations		Surface area precipitated			Total Alkalinity of mother solution	
Mg:Ca ratio aim	Experiment ID	Mg:Ca ratio	Mg:Ca ratio & [Ca^{2+}] at beginning (B) and end (E) (mM)	Na_2SO_4 Concentration at beginning (B) and end (E) (mM)	T (°C)	Env. Condition - water movement	Arag. Mole %	Ave. no of aragonite crystals	Ave. no of calcite crystals	Ave. size of arag. crystals (μm^2)	Ave. size of calcite crystals (μm^2)	Time 1st crystals observed (mins)	Predicted TA at time of 1st crystals	TA at end of experiment
1	J1.1.b K1.1.b L1.1.b M1.1.b	1.001	B = 11.23, E =10.45	B- 5.5, E - 5.116	20	still	37.06 28.68 10.93 38.43	146.00 88.67 35.00 240.00	162.00 148.00 155.67 240.33	5.697479 0.315673 0.28949 0.352415	1.54 0.511308 0.577008 0.613234	210 180 180 210	7.485 6.396 6.38 7.347	12.95 12.73 12.76 12.69
1	J1.2.b K1.2.b L1.2.b	1.001	B = 11.23, E =10.45	B- 5.5, E - 5.116	30	still	23.26 22.81 52.61	34.33 40.00 275.67	192.67 203.00 262.33	0.877339 0.782465 0.368287	0.560874 0.567394 0.379091	150 150 150	3.8 3.55 3.218	9.29 8.66 7.73
1	J1.1.c K1.1.c L1.1.c M1.1.c	0.999	B = 11.19, E =10.43	B- 5.5, E - 5.116	20	shaken	47.22 58.14 21.17 75.76	61.67 70.67 30.33 78.00	41.67 36.33 26.00 17.33	2.246937 2.523952 0.704996 1.576935	4.042383 3.844181 3.33133 2.47	240 240 210 240	7.226 7.28 6.422 7.254	10.92 10.92 10.94 10.87
1	J1.2.c K1.2.c L1.2.c M1.2.c	0.999	B = 11.19, E =10.43	B- 5.5, E - 5.116	30	shaken	74.77 65.92 84.16 92.99	49.67 51.67 43.67 58.33	19.33 29.00 16.00 17.67	1.067614 1.051239 3.937108 5.70	1.006587 1.052979 2.199106 1.542867	150 150 180 180	3.796 3.53 3.863 3.896	9.29 8.65 7.72 7.83

Appendix III: Summary of experiments in the presence of sulphate.
Summary of solution composition and experiment parameters in terms of Mg:Ca ratio and [Ca^{2+}] at the end of each experiment, aimed temperature in shaken conditions. Results are given for each experiment in terms of the mole percentage of aragonite precipitated, number of nucleations and the size of crystals formed for both aragonite and calcite as an average of crystal precipitates quantified from 3 images per experiment. The predicted TA st the time of first crystals and at the end of each experiment.